MICRORNAS AS BIOMARKERS FOR DETERMINING RESPIRATORY SYNCYTIAL VIRUS DISEASE PATHOGENESIS AND VACCINE EFFICACY

by

LYDIA JANE ANDERSON

(Under the Direction of Ralph Tripp)

ABSTRACT

Respiratory syncytial virus (RSV) is a respiratory tract virus that causes significant morbidity and mortality in children less than 5 years of age, and is a major global public health burden. RSV infection does not confer long-lasting protection, as reinfections occur throughout life, which poses a substantial disease risk on immunocompromised patients and the elderly population. Currently, there is no licensed vaccine to prevent RSV infection. RSV vaccine development has been hampered by the need for a strong and robust protective immune response as well as risk of inducing vaccine enhanced disease. Therefore, the establishment of precise measures of protection and disease severity to evaluate a wide range of RSV vaccine platforms early in development is necessary in order to avoid costly and time-intensive trials.

Host microRNAs (miRNAs) implicated in chronic inflammatory diseases of the lung were screened in vaccinated and RSV-infected BALB/c mice, and their pattern and tempo of expression was evaluate during vaccination and RSV-challenge. Unique miRNA profiles may then be utilized as biomarkers for vaccine efficacy and disease severity upon RSV infection. Our studies indicate that the pattern and tempo of

differentially expressed miRNA differ in a vaccine- and adjuvant-specific manner. In addition, these unique miRNA profiles correlate with known immune correlates and markers of disease severity for the RSV vaccines and vaccine adjuvants. Using an *in vitro* model of lung epithelial cells, we also identified key differences in cellular and exosomal miRNA-associated expression patterns; in addition, these studies demonstrate that exosomes preferentially incorporate specific miRNAs as their cargo during RSV infection.

Lastly, RNA interference (RNAi) technology was used for *in vivo* delivery of exogenous miR-467f to both rescue and further exacerbate the formalin-inactivated RSV (FI-RSV) vaccine enhanced disease phenotype produced upon RSV infection. By inducing gain- and loss- of-function, these studies indicate a biologically relevant role for miR-467f in linking the innate and adaptive immune response to vaccine enhanced disease. Taken together, this work establishes that miRNAs are intimately involved in the immune response and intracellular mechanisms controlling RSV replication and disease pathogenesis, and can be measured as parameters of disease severity and manipulated for therapeutic purposes.

INDEX WORDS: Respiratory syncytial virus, microRNA, vaccines, biomarkers

MICRORNAS AS BIOMARKERS FOR DETERMINING RESPIRATORY SYNCYTIAL VIRUS DISEASE PATHOGENESIS AND VACCINE EFFICACY

by

LYDIA JANE ANDERSON

BS, Emory University, 2011

A Dissertation Submitted to the Graduate Faculty of the University of Georgia in Partial Fulfillment of the Requirements for the Degree

DOCTOR OF PHILOSOPHY

ATHENS, GEORGIA

2016

MICRORNAS AS BIOMARKERS FOR DETERMINING RESPIRATORY SYNCYTIAL VIRUS DISEASE PATHOGENESIS AND VACCINE EFFICACY

by

LYDIA JANE ANDERSON

Major Professor:	Ralph Tripp
Committee:	Harry Dickerson
	Elizabeth Howerth
	John Peroni
	Balázs Rada

Electronic Version Approved:

Suzanne Barbour
Dean of the Graduate School
The University of Georgia
December 2016

DEDICATION

This work is dedicated to my better half, William McDowell Atherton Esq. This journey is not for the faint of heart, but you have stuck by my side through it all. I love you.

ACKNOWLEDGEMENTS

I would like to thank my advisor, Dr. Ralph Tripp, for providing continued guidance and facilitating the development of my professional career for the duration of my PhD. Additionally, I would like to extend my thanks to my committee members, Dr. Harry Dickerson, Dr. Elizabeth Howerth, Dr. John Peroni, and Dr. Balázs Rada, for your valuable input in my research and dedication to my success. Your advice has guided my research as well as my career, and I look forward to continuing to work with each of you in the coming years during my DVM training.

The work presented here would not have been possible without the guidance and encouragement of Dr. Patricia Jorquera Astudillo. I am forever indebted to you, and I want to thank you for your unwavering support and friendship. You have been such a positive influence on me both in and out of the lab, and I cannot express enough gratitude for all of the scientific training and knowledge you have bestowed upon me. I also need to thank Dr. Felipe Sarmiento for sharing Patty with me. You both have become family to me. Additionally, I would like to thank Colin Williams for his dedication and support as both a colleague and a friend; the mouse room would not have been nearly as enjoyable without you. I would also like to express my thanks to Dr. Jarod Hanson, I am grateful for our friendship and endless life discussions. I would also like to thank our wonderful administrator, Leslie Sitz. You have managed every crisis with kindness and patience, and strive to keep us all afloat. I would also like to acknowledge my extended lab family:

Dr. Constantinos Kyriakis, Dr. Maria Naskou, Dr. Patricia Jorquera Astudillo, Dr. Felipe Sarmiento, Colin Williams, Caitlin Reeves, Dr. Miriã Criado, and Dr. Jasmina Luczo for their friendship and support. You all have filled my graduate career with endless memories and many laughs. Finally, I would like to thank all of the Tripp lab members and the UGA Animal Health and Research Center animal care staff and administration.

I would also like to thank Dr. Duncan MacCannell and Angie Thompson at the Centers for Disease Control and Prevention (CDC). You all took a chance on a young woman with a passion for research, and zero skills to back it up. I would not be where I am today without your training and mentorship. A special thank you to Dr. Duncan MacCannell, it is through your guidance that I found my scientific curiosity and I could not have asked for a better person to help me launch my research career. A special thanks to my first and only lab mom, Sigrid McAllister, you have a wonderful way of making people feel special. I am thankful for your kind heart and continued support as I navigate graduate school. To all of the current and former members of DHQP at the CDC, from the bottom of my heart, thank you for your guidance.

Lastly, I would like to thank my family. To my dad, thank you for giving me the strength, passion, and tenacity to dream big in life. To my mom, thank you for your unconditional love. I am also thankful to both of you for encouraging me to be an independent thinker, and for giving me the confidence to succeed in life. Without the two of you, I would not be where I am today and I strive to make you proud every day. To my wonderful boyfriend, William McDowell Atherton Esq. I am thankful for your love, support, and wicked sense of humor. I am fortunate to have a partner in life that not only sees my potential, but also helps me achieve it. To our puppy, Luna you have brought so

much joy to our lives. I am thankful for your constant affection, and beautiful ears that have provided much stress relief. To Jim and Connie Atherton, thank you for being my family. I am so fortunate to have you both in my life, and this journey would not have been possible without each of your support. To my stepmom, Sherry Loyack Stein, thank you for always teaching me to believe in myself, and that wonder woman shoes are always an appropriate choice of footwear. To my stepsiblings, Hunter and Kate Stein, thank you for your laughter and friendship. To the entire Loyack clan: Elaine, Gerald, Sofia, Jerry, Yanni, Melina, Karen, Josh, and Malani, thank you for all of your support and always being my cheerleaders. To my extended family in England, thank you for teaching me that love can travel thousands of miles. Our paths may change as life goes on, but our bond remains strong. And for that, I am grateful.

It is each and every one of you that have made the biggest impact on my life and professional career. I could not have reached this milestone without each of you. They say the best things in life are free. Beyond a shadow of a doubt, this list proves that statement to be true.

TABLE OF CONTENTS

CHAPTER 1

INTRODUCTION

Respiratory syncytial virus (RSV) is the leading cause of serious lower respiratory tract disease in young children and the elderly and is as a common cause of bronchiolitis [1]. RSV generally causes a localized lung infection resulting in a host inflammatory response that recruits immune cells required for viral clearance [2]. Although the host inflammatory response is necessary for viral clearance, accumulating evidence strongly suggests that the response is linked to pulmonary disease pathogenesis [2]. It has been shown that RSV can modulate the host innate immune response by manipulating host cell gene expression and via regulation of expression of microRNAs (miRNAs) that appear to regulate the anti-viral host response, and modifying the robustness of the memory immune response to RSV [3]. Despite RSV being a major healthcare burden, there is currently no safe and effective vaccine available, and there is a lack of effective prophylactic and therapeutic interventions [4]. The first vaccine candidate, formalin-inactivated RSV (FI-RSV), was associated with enhanced disease and also caused two deaths with subsequent natural RSV infection [5]. The lack of success in developing RSV vaccines to date, and the fact that natural RSV infection provides limited protection from re-infection and disease, indicate that the task of developing a safe and efficacious live virus vaccine will be difficult [5]. Therefore, a better understanding of both the host-virus interface and vaccine-enhanced disease is necessary to overcome these hurdles.

This highlights that multiple aspects affect RSV vaccine efficacy and safety, as well as indicate potential solutions to overcoming the obstacles related to RSV vaccine development using miRNA biomarkers and corresponding immune correlates. The long-term goal of this research project is to evaluate miRNA expression profiles as biomarkers for determining protection and disease outcomes for RSV infection. The specific hypothesis of this work is that an alteration in the expression of cellular miRNAs implicated in chronic inflammatory diseases of the lung can be utilized as a biomarker for disease outcome and vaccine-enhanced disease with RSV infection. This hypothesis is based on the observation that specific miRNAs have been found to have critical roles in regulating key pathogenic mechanisms in asthma and in airway hyperresponsiveness, such as the polarization of the adaptive immune response, the activation of T cells, the regulation of eosinophil development, and the modulation of cytokine-driven responses [6,7]. The rationale for these studies is that the discovery of miRNA profiles that can be used as biomarkers can be applied across species to evaluate vaccine efficacy and disease pathogenesis, and that this insight is needed to better understand protective or disease-associated host responses. In addition, a better understanding of miRNA regulation can provide a valuable target for new approaches to prevent and treat inflammatory diseases of the lung, which are urgently needed.

Specific Aim 1: To determine the pattern and tempo of miRNA expression profiles in an *in vivo* BALB/c mouse model post-vaccination/pre-RSV challenge and post-vaccination/post-RSV challenge. Mice are immunized with a set of vaccines chosen by their capability of inducing either a protective immune response (GA2 microparticle and

RSV CP52) or vaccine-enhanced disease (FI-RSV). A group of mice will also receive live RSV A2 prior to challenge to control for natural infection. It is understood that different delivery methods may affect biomarker expression, but we wish to evaluate the vaccines and methods typically used to deliver them. At different time-points after vaccination, and before and after RSV challenge, the lungs, bronchoalveolar lavage (BAL), and sera will be collected and evaluated for patterns of miRNA expression and compared to mock controls. The working hypothesis is that vaccination and RSV infection alters the host miRNA expression profile modulating the host immune response and disease outcome. We believe that miRNAs previously implicated in asthma and airway hyper-responsiveness will be down-regulated in mice who develop a protective immune response, and upregulated in vaccine-enhanced conditions – similar to these models, i.e. mucus hypersecretion, lung inflammation, airway hyperresponsiveness. The rationale is that characterization of host miRNA expression profiles in a mouse model induced by vaccination and RSV infection will allow for an improved understanding of how alterations in the host miRNA expression profile may affect the host immune response and disease outcome.

Specific Aim 2: To develop an *in vitro* model to characterize miRNAs expressed by lung epithelial cells in response to RSV antigens and vaccines. We will use mouse lung epithelial (MLE-15) cells and human airway epithelial (CALU3) cells to study alterations in the expression of miRNAs implicated in the innate immune response. We will infect MLE-15 cells and CALU3 cells with live RSV A2 (RSV) and expose the cells to UV-inactivated RSV A2 (uvRSV). The miRNA expression pattern of these cells will then be

evaluated to define the miRNAs profiles that are RSV- and uvRSV –specific. The working hypothesis is that these alterations in miRNA profiles will be vaccine or RSV protein-specific, allowing for the development of miRNA biomarkers that can determine disease outcomes. The rationale is that by utilizing *in vitro* stimulation of MLE-15 cells and CALU3 cells, we will be able to determine alterations in the expression of miRNAs implicated in the innate immune response to RSV infection. MLE-15 cells are an immortalized type II pneumocyte cell line representing the distal bronchiolar and alveolar epithelium that maintain their differentiated phenotypes and functional characteristics for up to 30–40 cell culture passages [8]. CALU3 cells are an immortalized, well-differentiated and characterized cell line, which is derived from human submucosal glands [9]. In the human lung, the submucosal glands are a major source of airway surface liquid, mucins, and other immunologically active substances [9]. In addition, CALU3 cells show high transepithelial electrical resistance (TEER) and similar expression of differentiation and tight junction/adhesion markers compared to primary cells [10].

Specific Aim 3: To utilize bioinformatic tools to identify functionally relevant gene targets of particular miRNAs. Upon completion of Aims 1 and 2, we will have identified miRNA profiles linked to vaccine efficacy and RSV disease. We will use bioinformatic tools such as TarBase v7.0 (DIANA Tools) and Ingenuity IPA (Qiagen) to elucidate and validate the host genes that are being targeted by the different sets of miRNAs. The working hypothesis is that utilizing these tools we will be able to elucidate the signaling pathways and gene mechanisms by which these miRNAs are modulating RSV disease outcomes. The rationale is that by utilizing bioinformatic tools, we will be able to

elucidate the signaling pathways and gene mechanisms by which these miRNAs are modulating RSV disease outcomes. Then we will translate these findings into disease interventions at the host-virus interface using RNAi technology.

Specific Aim 4: To develop RNA interference (RNAi) approaches to target the expression of miRNA biomarkers of interest. Upon completion of Aims 1, 2, and 3 we will have identified a set of host genes and miRNAs linked to protective immune response against RSV as well as miRNAs involved in vaccine-enhanced disease and airway hyperresponsiveness. Based on these findings, we will select the best candidates and miRIDIAN microRNA Hairpin Inhibitors (GE Dharmacon) will be used to inhibit endogenous microRNAs and miRIDIAN microRNA Mimics (GE Dharmacon) will be used to mimic the function of endogenous miRNAs. By suppressing or enhancing miRNA activity we will be able to further elucidate and validate the functional roles of individual miRNAs *in vitro* (MLE-15 cells) or *in vivo* (BALB/c mice). Our main goal will be inhibiting miRNAs that promote inflammation and disease pathogenesis and promoting those miRNAs involved in protective immune response. The working hypothesis is that RNAi can be used to modulate the miRNAs of interest and thereby improve the immune response to RSV vaccines as well as provide protection against RSV infection and disease pathogenesis. The rationale is that RNAi is a powerful experimental tool for the functional annotation of mammalian genomes. Therefore, RNAi technology can be utilized to modulate the miRNAs of interest and thereby improve the immune response to RSV vaccines as well as provide protection against RSV infection and disease pathogenesis. In addition, it is important to experimentally assess the

functional relevance of the predicted miRNA targeting site(s) in order to understand the roles of miRNA in complex biological processes.

References

1 Knudson, C. J. & Varga, S. M. The Relationship Between Respiratory Syncytial Virus and Asthma. *Vet Pathol*, doi:10.1177/0300985814520639 (2014).

2 Christiaansen, A. F., Knudson, C. J., Weiss, K. A. & Varga, S. M. The CD4 T cell response to respiratory syncytial virus infection. *Immunologic research*, doi:10.1007/s12026-014-8540-1 (2014).

3 Thornburg, N. J., Hayward, S. L. & Crowe, J. E., Jr. Respiratory syncytial virus regulates human microRNAs by using mechanisms involving beta interferon and NF-kappaB. *MBio* **3**, doi:10.1128/mBio.00220-12 (2012).

4 Bakre, A. *et al.* Respiratory syncytial virus modifies microRNAs regulating host genes that affect virus replication. *J Gen Virol* **93**, 2346-2356, doi:10.1099/vir.0.044255-0 (2012).

5 Rey, G. U. *et al.* Decrease in formalin-inactivated respiratory syncytial virus (FI-RSV) enhanced disease with RSV G glycoprotein peptide immunization in BALB/c mice. *PloS one* **8**, e83075, doi:10.1371/journal.pone.0083075 (2013).

6 Lu, T. X. MicroRNA in the Pathogenesis of Allergic Inflammation. (2012).

7 Lu, T. X. & Rothenberg, M. E. Diagnostic, functional, and therapeutic roles of microRNA in allergic diseases. *The Journal of allergy and clinical immunology* **132**, 3-13; quiz 14, doi:10.1016/j.jaci.2013.04.039 (2013).

8 Moore, E. C., Barber, J. & Tripp, R. A. Respiratory syncytial virus (RSV) attachment and nonstructural proteins modify the type I interferon response associated with suppressor of cytokine signaling (SOCS) proteins and IFN-

stimulated gene-15 (ISG15). *Virology journal* **5**, 116, doi:10.1186/1743-422x-5-116 (2008).

9 Zhu, Y., Chidekel, A. & Shaffer, T. H. Cultured human airway epithelial cells (calu-3): a model of human respiratory function, structure, and inflammatory responses. *Crit Care Res Pract* **2010**, doi:10.1155/2010/394578 (2010).

10 Stewart, C. E., Torr, E. E., Mohd Jamili, N. H., Bosquillon, C. & Sayers, I. Evaluation of differentiated human bronchial epithelial cell culture systems for asthma research. *J Allergy (Cairo)* **2012**, 943982, doi:10.1155/2012/943982 (2012).

CHAPTER 2

LITERATURE REVIEW [1,2,3]

[1] Understanding respiratory syncytial virus (RSV) vaccine development and aspects of disease pathogenesis. Jorquera PA*, Anderson L*, Tripp RA. 2015. *Expert Rev Vaccines*. 15(2):173-87. Reprinted here with permission of the publisher.

[2] MicroRNA Profiling from RSV infected biofluids, whole blood and tissue samples. Anderson L, Jorquera PA, Tripp RA. 2016. *Methods Mol Biol*.1442:195-208. Reprinted here with permission of the publisher.

[3] Human Respiratory Syncytial Virus: An Introduction. Jorquera PA, Anderson L, Tripp RA. 2016. *Methods Mol Biol*. 1442: 1-12. Reprinted here with permission of the publisher.

1. RSV Genome and Replication Cycle

Respiratory syncytial virus (RSV) is a pathogenic member of the *Paramyxoviridae* family that can cause severe lower respiratory infections [1]. RSV is in the *Pneumovirinae* subfamily and type species member of the *Pneumovirus.* RSV infection is associated with bronchiolitis and pneumonia in young infants [2] and is the leading cause of lower respiratory tract disease in children in the United States resulting in over 100,000 hospitalizations and ~1,000 deaths per year [3-5]. RSV is the primary cause of hospitalization for respiratory tract illness in young children with infection rates approaching 70% in the first year of life [5]. In addition to young children, studies demonstrate that the elderly and immune compromised are also at an increased risk for severe disease with RSV [4]. Despite substantial efforts, there are no available vaccines and few treatments except for passive immunoprophylaxis [1].

RSV is an enveloped, nonsegmented, negative-sense, single-strand RNA virus [6-8]. The viral genome consists of 10 open reading frames (ORFs) that encode 9 structural and 2 nonstructural proteins [8]. The nucleoprotein (N), phosphoprotein (P), and RNA-dependent RNA polymerase (L) encapsulate the viral RNA to form a helical assembly termed the ribonucleoprotein complex (RNP) [8]. This structure protects the RNA and forms the minimal replication machinery [8]. RSV possesses three integral membrane proteins: the receptor attachment glycoprotein (G), the fusion protein (F), and a short hydrophobic (SH) protein [8]. The G protein is involved in viral attachment to the host cell, while the F protein is responsible for fusion [8]. The SH protein forms a pentameric ion channel [8]. Much like other paramyxoviruses, the polymerization of the matrix protein (M) is regarded as the main force that drives RSV assembly and budding [8]. M is a membrane-

associated protein that consists of both positively charged and hydrophobic domains that are important for cytoplasmic membrane binding [8]. The three additional genes contained in the genome are the two nonstructural proteins (NS1 and NS2) and M2. NS1 and NS2 are type I interferon antagonists [8]. The M2 gene encodes two distinct proteins, M2-1 and M2-2, which have been shown to function in genome transcription and replication [8].

RSV primarily infects respiratory epithelial cells lining the nasal passages and respiratory tract [5]. During infection, a host-acquired lipid bilayer consisting of the viral glycoproteins surrounds the RSV virion, and entry of the viral nucleocapsid into the host cell involves virus-specific membrane fusion. Binding and uptake/entry of RSV into host cells is dependent on interactions between the G and F proteins and numerous host cell molecules, both secreted- and surface-bound [9]. While some of these interactions may favor RSV infection or elicit inappropriate immune responses, others may encourage viral clearance [9]. The airway epithelium has a central role in defense against respiratory virus infections by expression of antiviral factors and immune mechanisms that contribute to viral resistance and clearance [10].

Early upon RSV infection, the G protein mediates attachment to the cellular receptor CX3CR1 [11] and the F protein binds to nucleolin [12] and induces fusion of the viral membrane and the plasma membrane. Fusion of the viral envelope with host cell membranes and syncytium formation are essential stages in the RSV life cycle, and both processes require the F protein to be intact (and are enhanced by the G protein) [3]. The F protein, highly conserved among the *Paramyxoviridae* family, is synthesized as a 67 kDa precursor that undergoes proteolytic cleavage to produce two disulfide-linked polypeptides, F1 and F2, from the C- and N-termini respectively [3]. Adjacent to these two

regions are two heptad repeat sequences, denoted HR-C and HR-N, that form a stable trimer of hairpin-like structures that undergo a conformational change to enable the viral and cell membranes to be opposed before viral entry [3]. In addition to the ability of the F protein to bind heparin-containing structures on the cellular surface, the small GTP-binding RhoA, a member of the Ras superfamily, also binds RSV F protein and facilitates virus-induced syncytium formation in Hep-2 cells [3,13]. RhoA is involved in actin mobilization and signal transduction, and infection with RSV upregulates surface expression of RhoA and stimulates RhoA-mediated signaling [3,14]. In addition, the F protein has been shown to interact with, and subsequently signal through, components of the lipopolysaccharide (LPS) receptor system; in particular, the pattern recognition receptors, CD14 and Toll-like receptor 4 (TLR4), have been implicated [3,15]. Following entry into the host cell, virion uncoating release the nucleocapsid along with the L protein (RdRp) into the cytoplasm where viral transcription and replication proceeds [5]. Once in the cytoplasm, encapsidated genomic RNA serves as template for both transcription and replication. The leader (Le) and trailer (Tr) sequences located at the 3' and 5' termini of the genome contain the genomic and antigenomic promoter elements. Transcription of mRNA occurs in a 3' → 5' order from a single promoter near the 3' end resulting in a series of subgenomic mRNAs [5]. Viral mRNAs can be detected by 4 h post infection with peak mRNA synthesis and protein expression occurring 12-20 h postinfection [5]. The level of protein expressed is related to mRNA abundance, thus there are decreased levels of mRNA proportional to the gene distance from promoter sequence [5]. Replication generates a complete positive-sense RNA complement of the genome called the antigenome, which acts as a template for genome synthesis [16].

Upon viral mRNA translation the G protein is produced in two forms, membrane-bound G (G_m) and soluble G (G_s) [5]. The RSV Glycoprotein is one of two major proteins recognized in the antibody response to infection, the other being the F protein [5]. The G protein is a glycosylated type II transmembrane protein, consisting of an N-terminal cytoplasmic domain, a hydrophobic anchor region and an ectodomain made up of two mucin-like regions that are highly variable and rich in serine, threonine and proline, and are heavily glycosylated with N- and O-linked sugars [3]. Thus, the G protein possesses unusual characteristics among viral membrane proteins and lacks homology to any other known Paramyxovirus protein [3]. Previous studies indicate that the cell surface glycosaminoglycans (GAGs), heparin sulfate (HS) and chondroitin sulfate B are important for infection in vitro, by interacting with a putative heparin-binding domain (HBD) in the G protein [3,17]. The mucin-like domains are separated by a 13 amino acid sequence, which contains four cysteine residues that are conserved across RSV strains [3,18]. The conserved nature of the cysteine noose and flanking 13 amino acid segment suggests that this region may be important for attachment, and previous data indicates a possible interaction with the TNF receptor (TNFR) [3]. The G protein and TNFR share homology in the cysteine noose at the C-terminus, which may allow the G protein to interfere with the antiviral and apoptotic effects of TNF, and with TNFR expressed on host cells [3]. In addition, a receptor on endothelial and epithelial cells, annexin II has been shown to bind RSV G protein, heparin and plasminogen [3]. However, there is evidence that binding of the RSV G protein to leukocytes involves different receptors from those on epithelial cells [3]. Malhotra *et al*. have shown that the G protein binds to L-selectin (CD62L), a leukocyte-specific adhesion receptor, in a heparin-dependent manner [3,19].

Previous studies in our laboratory demonstrated that the HBD region of the G protein contains a central-conserved cysteine-rich region that also contains a CX3C chemokine motif at amino acid 182-186, which binds to CX3CR1, the CX3CL1 (fractalkine) receptor [3,5,20]. CX3CL1 mimicry by the G protein has been shown to facilitate RSV infection and alter CX3CL1 chemotaxis of human and mouse leukocytes [20]. Furthermore, this may represent a functional role for the truncated form of the G protein secreted from infected cells, which may be largely responsible for the detrimental inflammatory response [3].

The M protein regulates the assembly of the RSV virions by interacting with the envelope proteins F and G and with the nucleocapsid proteins N, P, and M2-1. Virions assemble at the plasma membrane where nucleocapsids localize with the cell-membrane containing membrane viral glycoproteins [5]. The virions mature in clusters at the apical surface in a filamentous form associated with caveolin-1, and extend from the plasma membrane[5]. The release of progeny virus begins by 10 to 12 hours post infection, reaches peak after 24 hours, and continues until the cells deteriorate [16].

2. RSV-induced Immune Response

RSV infection of respiratory epithelial cells has been shown to alter the tempo and expression patterns of various genes related to protein metabolism, cell growth and proliferation, cytoskeleton organization, regulation of nucleotides and nucleic acid synthesis, and cytokine/chemokine genes linked with inflammation [5]. While a primary function of airway epithelium is to promote gaseous exchange, it also functions as the

interface between the external environment and the host, thus acting as a first-line defense against pathogens [5]. To overcome the repertoire of immune defenses encountered, RSV enlists a variety of immune modulatory and evasion strategies to promote virus infection and replication [5]. RSV delays programmed cell death or apoptosis of epithelial cells to facilitate virus replication [5]. It has been shown that RSV-infected cells have increased expression of the anti-apoptosis gene *IEX-1L* and increased expression of several Bcl-2 family members including myeloid cell leukemia-1 and Bcl-XL [5,21-24]. RSV also modulates the host-cell responses via pattern recognition receptors (PRRs) and toll-like receptors (TLRs) [7]. Viruses that trigger TLRs initiate a complex signaling cascade leading to the expression of a variety of genes and signaling through NF-κB[7]. RSV also interacts with TLRs and PRRs and activates signaling and downstream cellular transcription pathways [7]. TLRs are broadly distributed along the airways by various cell types including: respiratory epithelial cells, alveolar macrophages and dendritic cells (DCs) [7]. RSV infection of respiratory epithelial cells has been shown to result in increased TLR4 expression on the cell surface within 24 hours post-infection (hpi) [5,25,26]. The upregulating of TLR4 leads to increased sensitivity to endotoxin, and upon stimulation with lipopolysaccharide (LPS) enhanced IL-6 and IL-8 production was observed [26]. Like LPS, the RSV F protein can interact with TLR4 and CD14 in human monocytes leading to the activation of NF-κB and the production of proinflammatory cytokines TNF-α, IL-6 and IL-12 [5,15]. A previous study demonstrated that RSV promotes TNF-α, IL-6, MCP-1 and RANTES via interaction with TLR2 and TLR6 [27]. RSV also interferes with the host antiviral cytokine response [5]. Several studies have shown that RSV NS1 and NS2 are important in antagonizing the type I IFN response in infected

epithelial cells as well as suppressing DC maturation [7]. A recent study in MLE-15 lung cells showed that by 24hpi, in the absence of NS1 and NS2 proteins, type I IFN mRNA and IFN-β protein expression were suppressed [5,28]. In this study, a role for RSV G-protein inhibition of IFN-β was revealed and linked to the induction of suppressor of cytokine signaling (SOCS)-1 and SOCS-3 expression. As type I IFNs have an important role in DC maturation, activation of natural killer (NK) cells, differentiation and function of T cells, as well as enhancing primary antibody responses, RSV-mediated inhibition of type I IFN production negatively impacts antiviral immunity and facilitates virus replication [5,29,30].

Although antibody responses are vital for protection against RSV infection, T cell-mediated cellular immune responses have a greater role in virus clearance [5]. RSV-specific CD8+ cytotoxic T-lymphocytes (CTLs) are found in the lungs and peripheral tissues after RSV infection, and they have a major role in viral clearance [5]. In humans, CTLs recognize F, M, M2 and NS2 proteins, but there is little or no recognition of G, P or NS1 [5,31]. In BALB/c mice, CD8+ CTLs primarily recognize M2, F and N proteins, and the role of CTLs in the immune response to RSV is well illustrated by in vivo depletion studies [32-35]. These studies suggest that both CD4+ and CD8+ lymphocytes are important for clearing RSV and that both contribute to the inflammatory response associated with infection [33]. In BALB/c mice, the F protein primes both CD8+ and CD4+ T cells toward a Th1-type biased cytokine response while G protein primes typically CD4+ T cells that are biased towards the Th2-type cytokine response [5,36]. The Th1 and Th2 CD4+ T cells elicited react to a single region comprising amino acids 183-197 of the G protein [5,37]. The importance of CD4+ memory T cells to RSV infection has been investigated; however,

the majority of studies have focused on the response to RSV G protein priming [5]. It has been shown that the memory CD4+ T cell response to the RSV G protein in the lungs of primed BALB/c mice challenged with RSV is dominated by effector T cells expressing a single TCR Vβ chain, such as Vβ14 [38]. CD4+ T cells expressing TCR Vβ14 preferentially proliferate and expand into activated T cells in the lungs rather than the lymph nodes, which drain into the site of infection [39]. Although this study is limited to a specific inbred strain of mice, these findings may be important for understanding the role RSV-specific CD4+ memory T cells have in RSV-induced immunopathology, a feature linked to polarized Th2-type cytokine response and pulmonary eosinophilia [40].

3. RSV Antigens and Vaccine Development

The failures of RSV vaccines, and the fact that natural infection provides limited protection from re-infection and disease, indicate that the task of developing a successful RSV vaccine will be difficult [41]. Nevertheless, these failed vaccines can help identify the critical antigens to include or exclude in the development of RSV vaccines such as sites on surface proteins that are conserved among strains that induce protective antibodies that block disease, that elicit effector and memory responses, and that can be used in vaccine production [41]. RSV infection induces antibody responses against several viral antigens; however, only two major surface glycoproteins (F and G proteins) induce neutralizing antibodies that have a major role in protection [5,42]. In addition, neutralizing antibodies have an important role in protection from RSV infection, although serum and mucosal neutralizing antibodies seem to provide different levels of protection [5]. Serum antibodies

mainly composed of IgG, gain access to the lungs more readily than to the nasal passages via transduction [5]. Mucosal secretory IgA antibodies are short-lived and have less neutralizing activity compared with serum IgG antibodies [5].

3.1. RSV F protein

The RSV F protein is generally conserved among RSV strains and is essential for infectivity and fusion of the viral and cellular membranes [41]. In addition, the F protein can interact with TLR4 and CD14 in human monocytes leading to the activation of NF-κB and the production of proinflammatory cytokines TNF-α, IL-6, and IL-12 [41]. A recent study demonstrated that the N-terminal domain of the F1 segment physically interacts with the TLR4 co-receptor, MD-2 [41].

Recent advances in understanding the structural rearrangements of the F protein during fusion have helped vaccine and antiviral drug discovery for RSV [41]. The F protein is a type I fusion protein that is synthesized in a metastable prefusion form stabilized on the virion [41]. Proteolytic cleavage leads to a conformational change that causes the fusion of adjoining membranes to a highly stable post-fusion structure [41]. Until recently, the known structure of the F protein was the post-fusion form, which contains three known antigenic sites (I, II, and IV) associated with neutralizing activity [41]. However, absorption of human sera with post-fusion F demonstrated that the greater proportion of virus neutralization was not due to antibodies against epitopes in this conformation [41]. Recent studies have identified the structure of pre-fusion F and a novel antigenic site located at the apex of the pre-fusion F trimer, known as site ∅ [41]. Immunization with site ∅-stabilized variants of RSV F in mice and macaques induced levels of RSV-specific

neutralizing activity approximately fourfold higher than that elicited by post-fusion F and approximately 20-fold higher than the protective threshold [41]. In addition, high expression levels of a stabilized pre-fusion F protein has recently been achieved by introducing mutations in the refolding regions (RR1 and RR2) [41]. This highly stable pre-fusion F elicited neutralizing antibodies in cotton rats and induced complete protection from virus replication [41]. However, additional studies may need to be conducted with the prefusion F protein to further elucidate its efficacy and safety, as well as its structural and functional stability [41].

3.2. RSV G protein

The RSV G protein is an important target for the induction of neutralizing antibodies; however, the head of the G protein is antigenically variable, and the sequence homology of G proteins between A and B subtype is only ~53% [41]. Therefore, few G-specific monoclonal antibodies are cross-reactive, while the majority of F-specific monoclonal antibodies are cross-reactive [5]. However, studies have shown that strain-specific antibody responses primarily recognize epitopes within the hypervariable C-terminal region of the RSV G protein [18]. More specifically, the glycosylation pattern of the RSV G protein varies with the infected cell type, indicating that the different glycosylation patterns on the RSV G proteins may be one of the mechanisms used to evade the host immune response via the alteration of the G-protein antigenic profile [18]. This observation highlights the importance of the antibody response specific to the central conserved region (CCR) of the RSV G protein in generating cross-protection

against both strains of RSV [18]. Therefore, antibodies that block G protein binding to host cells and neutralize the virus to prevent disease are the target [41].

Vaccination of mice with a nanoparticle vaccine incorporating the G protein CX3C chemokine motif induced a strong neutralizing antibody response, increased G protein-specific and M2-specific T cell responses, and antibodies to G protein reduce RSV disease [43]. A recent study that evaluated the safety and efficacy of a non-glycosylated G protein vaccine produced in *E. coli* showed that the G protein induced protective immunity and no lung pathology in a mouse model against homologous and heterologous RSV challenge [44]. A recombinant influenza virus carrying the chimeric constructs of hemagglutinin and central conserved-domains of the RSV G protein induced RSV-neutralizing antibodies and protected mice from RSV infection after a single intranasal inoculation [41]. Similarly, another study showed that RSV virus-like particle (VLP) vaccines containing the RSV G alone or plus the F protein induced robust humoral and mucosal RSV-specific antibodies and demonstrated that VLPs carrying the F and G protein induced stronger immune responses than those carrying F alone, protecting mice against virus replication and lung inflammation [41]. Together these results indicate that the RSV G protein is an important antigen to take in consideration when producing a new RSV vaccine [41].

3.3. RSV SH, M2, N, and P proteins

The SH, M2, N, and P proteins of RSV are not typically targeted as vaccine antigens because other than the SH protein, they are internal proteins and typically not targeted by neutralizing antibodies [41]. The SH protein is a transmembrane surface

glycoprotein [41]. During infection, the SH protein accumulates at the lipid-raft structures of the Golgi complex, endoplasmic reticulum, and the cell surface [41]. A minor fraction of SH proteins is modified by glycosylation or expressed as a truncated variant [41]. It is important to note that non-neutralizing antibodies to the SH protein can influence viral replication by ADCC [41]. A recent study produced an RSV vaccine antigen using the SH ectodomain (SHe) peptide conjugated to keyhole limpet hemocyanin, and it showed that immunization of mice and cotton rats induced high levels of SHe-specific IgG, reduced pulmonary RSV replication, and protection against morbidity [41].

Using internal RSV proteins as vaccine antigen have the potential for inducing cross-protective immune response, but since these proteins are not exposed on the virion surface, antibodies directed against them tend to be poorly neutralizing [41]. Vaccination of mice with the RSV N and M2 proteins expressed in *Mycobacterium bovis bacillus Calmette-Guerin* (BCG) induced protective T cell responses against in absence of RSV-neutralizing antibodies [41]. Similarly, calves vaccinated with RSV P, N, and M2-1 proteins have been shown to develop cross-protective cell-mediated immune responses; however, the antibody responses were non-neutralizing [41]. Recently, it was shown that adenovirus-3 and modified Vaccinia Ankara vectors expressing RSV F, N, and M2-1 proteins induce neutralizing antibodies and broad cellular immunity in nonhuman primates [41]. These data suggest that including N, P, or M2 proteins in a vaccine can promote broad RSV-specific T cell responses, but fail to induce neutralizing antibodies, suggesting at least one RSV surface protein should be included in candidate vaccines [41].

4. Determining Correlates of Vaccine-induced Protection and Disease

As indicated above, a variety of host factors affect RSV disease pathogenesis. Although RSV disease phenotypes vary in humans and among animal models, inflammatory mediators have been strongly implicated in RSV pathogenesis [5]. In addition, a large number of studies have demonstrated a link between severe RSV infection during early childhood and increased likelihood to develop either recurrent wheezing or asthma later in life, and that these conditions are associated with enhanced CD4+ T cell responses, inappropriate cytokine expression, inflammation and reduced immune regulation [6,45-55]. Asthma is a chronic inflammatory disease of the lung that is the leading cause of morbidity and mortality in children worldwide [6]. Over the past 20 years, numerous studies have indicated a relationship between early severe RSV infection and an increased risk in developing asthma, yet the exact nature of the relationship remains unclear [6].

A recent study, in a rat model, demonstrated that RSV can spread across the placenta from the respiratory tract of the mother to the fetus, and persist postnatally in the lungs throughout development and into adulthood [56]. Vertical RSV infection was associated with dysregulation of critical neurotrophic pathways during fetal development, leading to aberrant innervation and increased airway reactivity after postnatal reinfection with RSV [56]. In addition, an altered balance between Th1- and Th2-type cytokines is likely responsible for a variety of inflammatory disorders including asthma, yet the role of post-transcriptional mechanisms such as those mediated by microRNAs (miRNAs) in regulating the relative magnitude and balance of the cytokine expression during RSV infection have been largely unexplored [57]. Recent studies have identified miRNA profiles in multiple allergic inflammatory diseases [58-63].

Despite RSV being a major healthcare burden, there is currently no safe and effective vaccine available, and there is a lack of therapeutic interventions [7]. Attempts to develop an effective live, inactivated, or subunit vaccine against RSV have largely been unsuccessful [33,64-66]. Early efforts at vaccinating young children with a formalin-inactivated RSV (FI-RSV) vaccine failed to protect the children from naturally acquired infection and actually enhanced lower respiratory tract disease upon later virus infection [5,33,67-70]. The determination of correlates of protection is an important step in the development of a vaccine [41]. It provides objective criterion for protection associated with vaccination, and in some cases where clinical trials are dangerous, or when testing new combinations of vaccines, it may guide licensure of a vaccine candidate without demonstration of field efficacy [41]. It is important to understand that the correlates of protection induced by vaccination are not necessarily the same correlates that operate to block infection [41]. Cellular immunity is also important for recovery from disease: B cell-deficient humans do recover from measles, whereas T cell deficiency leads to serious and fatal disease [41].

One of the many challenges of developing an RSV vaccine is the lack of an absolute correlate of protection that can be used to predict vaccine efficacy and clinical outcome [41]. For example, the hemagglutination inhibition (HI) titer of 1:40 has been established as an immunologic correlate corresponding to a 50% reduction in the risk of contracting influenza [71,72]. Since various components of the innate and adaptive immune response have shown to be important for controlling RSV infection and disease, it is likely that a combination of immune correlates, and/or biomarkers, will need to be defined to predict vaccine efficacy and safety [41]. Different methods can be used for

biomarker detection and validation; however, some major hurdles are the lack of standardized specimen collection and storage, testing methodologies, and data analysis [41]. Another obstacle includes the validation process, which will require verification that the diagnostic tests will improve the prevention and treatment of RSV disease and reduce healthcare costs [41]. For example, current treatment for infants with bronchiolitis caused by RSV includes supplemental oxygen, nasal suctioning, fluids to prevent dehydration, and other supportive therapies [73]. However, the use of nebulized epinephrine and nebulized ipratropium bromide have been shown to be possibly effective, and the appropriate use of corticosteroids remains controversial [73]. Therefore, determining the appropriate usage criteria for diagnostic tests and treatments for RSV still remains to be elucidated.

4.1. Overall antibody response

Serum neutralizing antibody titers is one of the most common immune correlates measured to assess vaccine efficacy [41]. Estimating the minimum protective antibody concentration to prevent RSV disease is of critical importance in assessing a RSV vaccine candidate [41]. To define a minimal protective antibody titer, one must first choose an antibody assay that best correlates with disease protection [41]. Comparative analysis of enzyme-linked immunosorbent assay (ELISA), microneutralization (MN), and plaque reduction neutralization (PRN) assays have been examined to identify optimal neutralizing and protective IgG levels [41]. In addition, antibodies directed against the RSV G protein CCR have been shown to have antiviral and anti-inflammatory effects that effectively neutralize RSV and protects from disease [41,43]. Anti-F protein antibodies

generated by Palivizumab (Synagis) can prevent severe RSV disease in premature and term infants if administered by passive immune prophylaxis [41]. In addition, a binding competition assay using Palivizumab (Synagis), named the Palivizumab competing antibodies (PCA), has been developed to demonstrate that candidate vaccines induce antibodies binding to the same region of F protein recognized by this efficacious product [74]. Lastly, antibodies in nasal secretions are likely to be a more important correlate of protection than serum antibodies. Low levels of RSV-specific nasal IgA (<1:60) have shown to be a significant risk factor for RSV infection and disease in adults [41]. High level of nasal neutralizing antibodies are associated with reduction or prevention of infection and disease relative to any tier of serum antibodies [41]. Thus, vaccines able to induce durable RSV-specific IgA responses may be more protective than those generating systemic antibody alone [41].

4.2. T cell response

RSV-specific CD4 and CD8 T lymphocyte responses are important in controlling infection and inhibiting virus replication and spread by producing antiviral cytokines, killing virus-infected targets, and regulating innate and adaptive effector functions [41]. Increasing evidence in T cell-deficient hosts suggests that RSV-specific T cell responses reduce severe RSV disease in infants and older adults [41]. It has been shown that CD8+ cytotoxic T lymphocyte (CTL) response peaks within 10 days of infection in infants exposed to RSV for the first time [41]. In addition, a recent study found that vaccine-elicited effector anti-RSV CD8+ T cells protected BALB/c mice against RSV infection and pathogenesis, and waning protection correlated with reduced CD8+ T cell cytokine

expression [75]. A role for T cells in viral clearance is also suggested by a prospective study examining immunocompromised children less than five years of age that showed these individuals suffer more severe disease and shed virus at higher levels for several months, compared with 7-21 days in normal children [76]. Similar findings have also been shown in adult bone marrow transplant recipients [76]. The increased frequency and risk of severe RSV disease seen in elderly adults may similarly be related to the lower numbers and decreased proliferative and functional capacity of IFNγ producing RSV F-protein specific T cells seen in that high-risk population [76]. Despite these data demonstrating the apparent importance of T cells, standardized parameters and additional studies need to be conducted to show the relevance of measuring T cell response in terms of providing an additional correlate of protection in humans for vaccine development. More specifically, the relationship between T cell numbers or function and protection from RSV re-infection is not a simple dynamic, and is complicated by checks and balances in the immune system [76].

4.3 Biomarkers

A biological marker (biomarker) is defined as a characteristic that is objectively measured and evaluated as an indicator of normal biological processes, pathogenic processes, or pharmacologic responses to a therapeutic intervention [77]. Biomarkers have a critical role in improving the drug development, clinical trials, as well as in the larger biomedical research enterprise [78]. More specially, biomarkers can provide a basis for the selection of lead candidates for clinical trials, for contribution to the understanding of the pharmacology and immunology of candidates, and for characterization of the subtypes of

disease for which a therapeutic intervention is most appropriate [77]. In addition, they provide the greatest value in early efficacy and safety evaluations such as *in vitro* studies in tissue samples, *in vivo* studies in animal models, and early-phase clinical trials to establish "proof of concept" [77]. When defining biomarkers, it is of equal importance to distinguish these from clinical endpoints. A clinical endpoint is a characteristic or variable that reflects how a patient or animal model feels, functions, or survives [77]. Although clinical endpoints are the most credible characteristics for the assessment of the benefits and risks of a therapeutic intervention in randomized clinical trials, they are often not accessible during the early developmental stages of drug and vaccine design. Therefore, the development of subset of biomarkers that can function as surrogate endpoints is ideal. A surrogate endpoint is a biomarker that is intended to substitute for a clinical endpoint, in that it is expected to predict clinical benefit based on epidemiologic, therapeutic, pathophysiologic, immunologic, or other scientific evidence [77]. It is also important to point out that the same biomarkers used as surrogate endpoints in preclinical and clinical trials are often extended to clinical practice in which disease responses are similarly measured [77]. Therefore, understanding the relationship between measurable biological processes and clinical outcomes is vital to expanding our arsenal of treatments and vaccines for RSV, and for deepening our understanding of normal, healthy physiology as compared to diseased states. Based on these definitions, it is evident that the establishment of biomarkers that can accurately predict vaccine efficacy and disease outcomes for RSV would serve to expedite vaccine and therapeutic development for target populations, which are urgently needed.

4.3.1. MicroRNAs (miRNAs)

miRNAs are a class of small noncoding, endogenous RNAs (sncRNAs), that can alter gene expression at the post-transcriptional level [62]. miRNA genes constitute one of the most abundant gene families, and they are generally conserved across all eukaryotes and have been substantially expanded during evolution, with only twelve miRNAs having been lost from deuterostomes to mammals [79-81]. The miRNA family is a global regulatory network controlling homeostasis, inflammatory responses, and affecting immunity and disease pathogenesis [82]. miRNA genes are located on the sense/antisense strands in genic/intergenic and introns of genes as independent transcription units called mirtrons [83,84]. Parent genes are typically transcribed by RNA polymerase II [85,86], and in some cases by RNA polymerase III [87] producing long primary transcripts, pri-miRNAs, of varying length in the nucleus [82]. Pri-miRNAs are processed by the microprocessor complex consisting of Drosha and DGCR8 into ~60 nucleotide long hairpin structured pre-miRNAs, which are then exported out of the nucleus by exportin 5 (XPO5) [88]. Exported pre-miRNAs are processed further by a Dicer and Argonaute complex to produce mature miRNA duplexes, 20-25 nucleotides long, that consist of a *guide* strand and a *passenger* strand, which is generally degraded [82]. The guide strand nucleotides 2-8 represent the "seed site" which recognizes a 6-8 nucleotide complementary sequence in the target gene(s) causing either a translational block or transcript decay in a RNA protein complex termed as RNA induced silencing complex (RISC) [82,88]. Some miRNAs can also bind with perfect complementarity with the target transcript [82]. Therefore, the degree of base pairing between the miRNA guide strand and mRNA, and the composition of the RISC

complex determine the downstream pathways [82]. Due to the short sequence complementarity between a miRNA and its target, a single miRNA can regulate the expression of multiple genes [88,89].

More specifically, various miRNAs have been found to have critical roles in regulating key pathogenic mechanisms in asthma and in airway hyper-responsiveness, including polarization of adaptive immune responses, activation of T cells, regulation of eosinophils, and modulation of cytokine-driven responses [57,60,90]. miR-21 has been shown to regulate polarized adaptive immune responses in allergic asthma models, undergoing increased expression during eosinophilia [57,62]. miR-106 regulates IL-10 and Th2 response, and antagonism of miR-106a has been shown to decrease asthma severity[58]. miR-126 regulates the effector function of Th2 cells and the allergic inflammatory response in experimental asthma [59,61]. miR-145 was recently found to be upregulated during eosinophilia and Th2-type response; additionally, antagonism of miR-145 significantly attenuated eosinophil infiltration, mucus production, Th2 cytokine production, and airway hyperreactivity in experimental allergic airway inflammation [59,62,63,91]. miR-146 has been implicated as an inducer of inflammation, and up regulation of this miRNA could potentially suppress Th1 responses and promote Th2 responses [60-63,92,93]. miR-155, which is upregulated during allergic inflammation, regulates polarized T-cell responses to induce a predominantly Th2 response [58,60]. The let-7 family can regulate the production of Th2-bias cytokines, and antagonism of these miRNAs attenuated experimental asthma. The let-7 family is encoded by 12 genes, which includes nine slightly different miRNAs; all Let-7 family members are believed to exert similar

functions because they share a common seed region, which mediates miRNA interaction with target mRNAs [94].

As previously shown in our laboratory, expression patterns of miRNAs vary between normal physiological processes and disease [7,82,95,96]. These differences form the basis as to why miRNA profiles should be exploited as diagnostic tools [82]. Among the various biomolecule classes, miRNAs are very promising biomarkers owing to their stability in a variety of tissues and body fluids, and high stability within a particular sample type [82]. Further, miRNA expression profiling has been used to differentiate cancerous cells. Recently, large-scale sets of cancer specimens revealed that miRNA profiling was able to successfully differentiate the origin tumor cells [97], as well as further tumor sub-classification [98]. In addition, patterns of miRNA expression have successfully predicted clinical disease progression [99,100]. It is important to note that altered miRNA expression patterns and their diagnostic potential are not restricted to cancer diagnosis but have been used to evaluate distinct types of cardiomyopathies [101], musculoskeletal disorders [102], neurodegenerative disorders [103], autoimmune diseases [104-109], and infectious diseases [110-116] which all drive unique miRNA profiles that can be used as potential biomarkers of disease progression and or treatment [82]. Given that novel disease intervention strategies for RSV are urgently needed, an important first step is to increase our understanding of the virus-host interface and secondly develop predictive tools for evaluating disease outcomes and treatment strategies. Therefore, miRNAs implicated in asthma and lung inflammation can be evaluated as biomarkers for assessing the severity of primary RSV and vaccine-enhanced disease.

4.3.2. Cytokines

The pattern of cytokine expression may serve as an immunological biomarker of RSV infection and disease; however, it can be difficult to obtain sufficient specimen volumes for analysis [41]. For example, sputum and nasopharyngeal aspirate samples are both difficult to obtain and limited in their quality and quantity [41], and not all sites express or are exposed to similar cytokine patterns. In contrast, human plasma and serum testing may present a valuable method for evaluating cytokines. Previous studies have evaluated cytokine profiles from these clinical samples as predictors of disease severity during RSV infection [41]. In vivo levels of IFNγ in nasopharyngeal aspirates of infants with RSV lower respiratory tract infection were substantially decreased in mechanically ventilated infants compared to non-ventilated hospitalized infants [41,117]. A recent study assessing serum samples from 52 RSV-infected children with varying degrees of disease severity showed that decreased CD4+ T cell counts and elevated levels of IL-8 and CCL-5 readily discriminated severe from mild RSV infection with 82% sensitivity and 96% specificity [41,118]. In addition, low levels of plasma TNF-α and IL-8 concentrations were associated with enhanced disease severity in infants with severe RSV bronchiolitis [41,119]. Although the results from these two studies differ in terms of levels of IL-8 expression, it should be noted that the level of certain cytokines may not be as important as the patterns of cytokine expression [41]. In addition, the pattern and tempo of cytokine expression differs substantially *in vivo* between areas of localized infection, such as the lungs, BAL, and systemic responses, such as in the blood.

4.3.3. Matrix metalloproteinases

Matrix metalloproteinases (MMPs) are a group of enzymes that participate in extracellular matrix protein degradation. More specifically, MMPs have a vital role in viral infection, inflammation, and remodeling of the airway [41]. Increased mRNA levels of MMP-1, -7, -9, -10, and -19 have been found in human nasal epithelial cells after RSV infection [41,120]. A previous study has shown that RSV infection can induce the expression of MMP-9 in epithelial cells, and MMP inhibitors can reduce syncytia formation and RSV replication [41,121]. A recent study using a $Mmp9^{-/-}$ mouse model demonstrated that MMP-9 exerts antiviral activity against RSV, considerably enhancing neutrophil recruitment and cytokine production and reducing airway hyperresponsiveness [41,122]. These and other findings implicate MMPs as having an important role in RSV pathogenesis and disease progression, and thus, MMPs may serve as biomarkers of RSV disease pathogenesis [41].

4.3.4. Neurotrophins and leukotrienes

Neurotrophins (NTs) are a family of proteins responsible for neuronal survival, growth, and programmed cell death and are continuously present in all vertebrates [41]. Two receptor classes mediate NT responses: the tropomyosin-related tyrosine kinases (Trks) and p75, a member of the tumor necrosis factor receptor superfamily [41]. The lung expresses NTs and their receptors [41]. It has been shown that NTs contribute to lung function and disease pathologies and are critical for the development of airway inflammation and hyperreactivity [41,56,123].

Leukotrienes (LTs) are critically involved in the pathogenesis of asthma and protection against respiratory pathogens [41]. RSV infection in young infants results in the release of LTs and activation of the LT receptor during the acute inflammatory response of the lung airways [41,124]. More specifically, the RSV G protein has been shown to reduce respiratory rates associated with the induction of substance P and G glycoprotein-CX3CR1 interaction, an effect that is inhibited by treatment with anti-G glycoprotein, anti-SP, or anti-CX3CR1 monoclonal antibodies [41,125,126]. It has been shown that substance P is important in the induction of LTs; therefore, interactions between substance P and LTs may represent an important mechanism of airway inflammation in response to RSV infection [41,124]. Previous studies have demonstrated that elevated nasal LT levels mediate neurogenic inflammation in RSV-infected lungs and disease severity [41,124,127,128]. Elevated urinary LTE_4 levels have been found in infants with RSV bronchiolitis and persistent airway obstruction [41,129].

4.3.5. Lung epithelium-specific proteins

The collection of BAL fluid is a common means of sampling the epithelial lining fluid to study the proteins secreted by the lung epithelium and investigate their alterations in lung disorders [130]. However, over the past decade, researchers have shown the presence of these proteins in the bloodstream as well, even though in small amounts, demonstrated using ELISAd significant variations of these proteins' levels in the serum of patients with different interstitial lung diseases [130]. These lung epithelium-specific proteins are mainly, if not exclusively secreted within the respiratory tract; therefore, their presence in the

vascular compartment can be theorized by a number of hypothetical mechanisms [130]. Leakage from the lung into the bloodstream resulting from the increased permeability of lung vessels and barrier destruction between alveolar epithelium and endothelium due to injury to the basement membrane [130].There is increased production by the alveolar type II cells paired with an increase in total type II cells in the lung due to diffuse hyperplasia [130]. Finally, these increased systemic protein levels resulting from diminished clearance rates from the circulation [130].

4.3.5.1. Surfactant-associated Proteins (SPAs)

Pulmonary surfactant is a complex and highly surface active material covering the alveolar space of the lung [130]. A primary function of pulmonary surfactant is to reduce the surface tension at the air-liquid interface of the alveolus, thereby preventing alveolar collapse on expiration [130]. There are four main surfactant-specific proteins, known as surfactant protein- (SP)-A, SP-B, SP-C, and SP-D [130]. Studies have demonstrated that these proteins have an important role in the innate immune system of the lung, and show potential as useful markers for epithelial damage and turnover in the lung [130]. It has been shown that serum SP-D concentration is associated with the severity of RSV bronchiolitis in pediatric patients [131]. Several studies have also indicated that a genetic association exists between SP-D and SP-A gene loci and severe RSV infection. More specifically, SP-D Met11Thr polymorphism as a factor associated with individual disease susceptibility and the severity of RSV bronchiolitis during infancy [132]. In addition, SP-A2 allele $1A^3$ was overrepresented in RSV-infected infants, compared with control patients

[133]. SP-A has also been used as a marker for lung adenocarcinomas to differentiate lung adenocarcinomas from other types, and to detect metastasis of lung adenocarcinomas [134]. The serum SP-A levels also increase in patients with acute respiratory distress syndrome [134].

4.3.5.2. Mucin-associated Antigens

Mucins (MUC) are major components of the mucus layer covering the airway epithelium [130]. They consist of a family of high molecular weight, heavily glycosylated proteins [130]. Mucins are either membrane-bound or secreted at the surface of the respiratory tract [130]. Krebs von den Lungen-(KL)-6/MUC1 is mainly associated with cellular membranes, including alveolar type II and epithelial cells of the respiratory bronchioles [130]. More specifically, KL-6 is a sensitive indicator of damage to alveolar type II cells, which strongly express this mucin at their surface [130]. Several studies have shown that KL-6 is a sensitive marker for interstitial lung diseases such as idiopathic pulmonary fibrosis, collagen vascular disease-associated interstitial pneumonia, radiation pneumonitis, hypersensitivity, pneumonitis and pulmonary sarcoidosis [130]. In terms of respiratory viral infections, it has been shown that the MUC expression by RSV and hMPV differs significantly; more specifically, RSV infection results in stronger expression of MUC8, MUC15, MUC20, MUC21, and MUC22 while the expression of MUC1, MUC2, and MUC5B are induced by hMPV infection [135].

4.3.5.3. Clara Cell Protein (CC16)

The Clara Cell secretory protein-(CC)- 16 is a low molecular weight protein secreted in large amounts into the lumen of the respiratory tract by non-ciliated bronchiolar Clara cells in humans and rodents [130]. CC16 is not an entirely specific and exclusive product of Clara cells or even the lung [130]. Even though the exact *in vivo* function of CC16 remains to be elucidated, evidence is accumulating that CC16 serves as an important immunosuppressive and anti-inflammatory mediator in the lung [130,136]. Serum CC16 increases in acute or chronic lung disorders characterized by increased airway permeability [136]. Additionally, CC16 can inhibit production of IFNγ by peripheral blood mononuclear cells [130]. The sensitivity of serum CC16 to an increased leakiness of the lung allows for the detection of defects of the epithelial barrier at ozone levels below current air-quality guidelines [136].

Conclusions

It has been over 60 years since the identification of RSV, and yet the highlights of RSV research dedicated to prevention and treatment have been relatively few. The reasons for this include the difficulty of working with RSV in the laboratory, the complex host immune responses of the different target populations, confinement of RSV replication in humans and few strong animal models, the early recognition of the complex immune responses to RSV, and the failure of the first vaccine leading to enhanced disease upon subsequent natural infection [2]. Therefore, biomarkers of protection and disease are needed to advance RSV vaccine candidates [41]. Ideally, these biomarkers and immune correlates need to translate among animal models used for predicting RSV vaccine efficacy and safety as well as to humans. This will not only be valuable for

preclinical trials, but also the identification of correlates induced within a few days after vaccination or even at baseline will be of great value in accelerating vaccine testing in clinical trials [137]. In addition, a major challenge to moving toward vaccine licensure is determining which candidate vaccines are likely to succeed [64]. The present approach in animal models has not proven adequate for predicting success in clinical trials and better platforms are needed. Therefore, miRNA biomarkers are a valuable approach for assessing the host immune response, antiviral activity, and disease pathogenesis associate with vaccine candidates as they provide practical application advantages. More specifically, miRNAs are advantageous as they are not only biologically stable, but also miRNA regulatory programs are evolutionarily conserved and their sequence homology among species. In addition, supplementary immune correlates will be useful to provide a systems biology approach to evaluating immunogenicity of potential vaccine candidates.

References

1 Krzyzaniak, M. A., Zumstein, M. T., Gerez, J. A., Picotti, P. & Helenius, A. Host cell entry of respiratory syncytial virus involves macropinocytosis followed by proteolytic activation of the F protein. *PLoS Pathog* **9**, e1003309, doi:10.1371/journal.ppat.1003309 (2013).

2 Wright, P. F. Progress in the prevention and treatment of RSV infection. *N Engl J Med* **371**, 776-777, doi:10.1056/NEJMe1407467 (2014).

3 Harris, J. & Werling, D. Binding and entry of respiratory syncytial virus into host cells and initiation of the innate immune response. *Cell Microbiol* **5**, 671-680 (2003).

4 Castilow, E. M., Meyerholz, D. K. & Varga, S. M. IL-13 is required for eosinophil entry into the lung during respiratory syncytial virus vaccine-enhanced disease. *Journal of immunology* **180**, 2376-2384 (2008).

5 Oshansky, C. M., Zhang, W., Moore, E. & Tripp, R. A. The host response and molecular pathogenesis associated with respiratory syncytial virus infection. *Future microbiology* **4**, 279-297, doi:10.2217/fmb.09.1 (2009).

6 Knudson, C. J. & Varga, S. M. The Relationship Between Respiratory Syncytial Virus and Asthma. *Vet Pathol*, doi:10.1177/0300985814520639 (2014).

7 Bakre, A. *et al.* Respiratory syncytial virus modifies microRNAs regulating host genes that affect virus replication. *J Gen Virol* **93**, 2346-2356, doi:10.1099/vir.0.044255-0 (2012).

8 Kiss, G. *et al.* Structural Analysis of Respiratory Syncytial Virus Reveals the Position of M2-1 between the Matrix Protein and the Ribonucleoprotein Complex. *J Virol* **88**, 7602-7617, doi:10.1128/jvi.00256-14 (2014).

9 Anderson, D. C. & Kodukula, K. Biomarkers in pharmacology and drug discovery. *Biochemical pharmacology* **87**, 172-188, doi:10.1016/j.bcp.2013.08.026 (2014).

10 Tripp, R. A. Respiratory Syncytial Virus (RSV) Modulation at the Virus-Host Interface Affects Immune Outcome and Disease Pathogenesis. *Immune network* **13**, 163-167, doi:10.4110/in.2013.13.5.163 (2013).

11 Johnson, S. M. *et al.* Respiratory Syncytial Virus Uses CX3CR1 as a Receptor on Primary Human Airway Epithelial Cultures. *PLoS Pathog* **11**, e1005318, doi:10.1371/journal.ppat.1005318 (2015).

12 Mastrangelo, P. & Hegele, R. G. RSV fusion: time for a new model. *Viruses* **5**, 873-885, doi:10.3390/v5030873 (2013).

13 Pastey, M. K., Crowe, J. E., Jr. & Graham, B. S. RhoA interacts with the fusion glycoprotein of respiratory syncytial virus and facilitates virus-induced syncytium formation. *J Virol* **73**, 7262-7270 (1999).

14 Gower, T. L., Peeples, M. E., Collins, P. L. & Graham, B. S. RhoA is activated during respiratory syncytial virus infection. *Virology* **283**, 188-196, doi:10.1006/viro.2001.0891 (2001).

15 Kurt-Jones, E. A. *et al.* Pattern recognition receptors TLR4 and CD14 mediate response to respiratory syncytial virus. *Nat Immunol* **1**, 398-401, doi:10.1038/80833 (2000).

16 Collins, P. L. C., J. in *Fields Virology* Vol. 2 (ed D. M.; Howley Knipe, P. M.) Ch. 46, 1601-1646 (Lippincott Williams & Wilkins, 2007).

17 Feldman, S. A., Hendry, R. M. & Beeler, J. A. Identification of a linear heparin binding domain for human respiratory syncytial virus attachment glycoprotein G. *J Virol* **73**, 6610-6617 (1999).

18 Choi, Y. *et al.* Antibodies to the central conserved region of respiratory syncytial virus (RSV) G protein block RSV G protein CX3C-CX3CR1 binding and cross-neutralize RSV A and B strains. *Viral immunology* **25**, 193-203, doi:10.1089/vim.2011.0094 (2012).

19 Malhotra, R. *et al.* Isolation and characterisation of potential respiratory syncytial virus receptor(s) on epithelial cells. *Microbes and infection / Institut Pasteur* **5**, 123-133 (2003).

20 Tripp, R. A. *et al.* CX3C chemokine mimicry by respiratory syncytial virus G glycoprotein. *Nat Immunol* **2**, 732-738, doi:10.1038/90675 (2001).

21 Domachowske, J. B. *et al.* Respiratory syncytial virus infection induces expression of the anti-apoptosis gene IEX-1L in human respiratory epithelial cells. *J Infect Dis* **181**, 824-830, doi:10.1086/315319 (2000).

22 Kotelkin, A., Prikhod'ko, E. A., Cohen, J. I., Collins, P. L. & Bukreyev, A. Respiratory syncytial virus infection sensitizes cells to apoptosis mediated by tumor necrosis factor-related apoptosis-inducing ligand. *J Virol* **77**, 9156-9172 (2003).

23 Lindemans, C. A. *et al.* Respiratory syncytial virus inhibits granulocyte apoptosis through a phosphatidylinositol 3-kinase and NF-kappaB-dependent mechanism. *Journal of immunology* **176**, 5529-5537 (2006).

24 Monick, M. M. *et al.* Activation of the epidermal growth factor receptor by respiratory syncytial virus results in increased inflammation and delayed apoptosis. *J Biol Chem* **280**, 2147-2158, doi:10.1074/jbc.M408745200 (2005).

25 Xie, X. H. *et al.* Lipopolysaccharide induces IL-6 production in respiratory syncytial virus-infected airway epithelial cells through the toll-like receptor 4 signaling pathway. *Pediatric research* **65**, 156-162, doi:10.1203/PDR.0b013e318191f5c6 (2009).

26 Monick, M. M. *et al.* Respiratory syncytial virus up-regulates TLR4 and sensitizes airway epithelial cells to endotoxin. *J Biol Chem* **278**, 53035-53044, doi:10.1074/jbc.M308093200 (2003).

27 Murawski, M. R. *et al.* Respiratory syncytial virus activates innate immunity through Toll-like receptor 2. *J Virol* **83**, 1492-1500, doi:10.1128/JVI.00671-08 (2009).

28 Moore, E. C., Barber, J. & Tripp, R. A. Respiratory syncytial virus (RSV) attachment and nonstructural proteins modify the type I interferon response associated with suppressor of cytokine signaling (SOCS) proteins and IFN-stimulated gene-15 (ISG15). *Virology journal* **5**, 116, doi:10.1186/1743-422x-5-116 (2008).

29 Becker, Y. Respiratory syncytial virus (RSV) evades the human adaptive immune system by skewing the Th1/Th2 cytokine balance toward increased levels of Th2

cytokines and IgE, markers of allergy--a review. *Virus genes* **33**, 235-252, doi:10.1007/s11262-006-0064-x (2006).

30 Bruder, D., Srikiatkhachorn, A. & Enelow, R. I. Cellular immunity and lung injury in respiratory virus infection. *Viral immunology* **19**, 147-155, doi:10.1089/vim.2006.19.147 (2006).

31 Cherrie, A. H., Anderson, K., Wertz, G. W. & Openshaw, P. J. Human cytotoxic T cells stimulated by antigen on dendritic cells recognize the N, SH, F, M, 22K, and 1b proteins of respiratory syncytial virus. *J Virol* **66**, 2102-2110 (1992).

32 Openshaw, P. J. Immunity and immunopathology to respiratory syncytial virus. The mouse model. *Am J Respir Crit Care Med* **152**, S59-62, doi:10.1164/ajrccm/152.4_Pt_2.S59 (1995).

33 Tripp, R. A. & Anderson, L. J. Cytotoxic T-lymphocyte precursor frequencies in BALB/c mice after acute respiratory syncytial virus (RSV) infection or immunization with a formalin-inactivated RSV vaccine. *J Virol* **72**, 8971-8975 (1998).

34 Connors, M. *et al.* Pulmonary histopathology induced by respiratory syncytial virus (RSV) challenge of formalin-inactivated RSV-immunized BALB/c mice is abrogated by depletion of CD4+ T cells. *J Virol* **66**, 7444-7451 (1992).

35 Graham, B. S., Bunton, L. A., Wright, P. F. & Karzon, D. T. Role of T lymphocyte subsets in the pathogenesis of primary infection and rechallenge with respiratory syncytial virus in mice. *J Clin Invest* **88**, 1026-1033, doi:10.1172/JCI115362 (1991).

36 Johnson, T. R. & Graham, B. S. Secreted respiratory syncytial virus G glycoprotein induces interleukin-5 (IL-5), IL-13, and eosinophilia by an IL-4-independent mechanism. *J Virol* **73**, 8485-8495 (1999).

37 Varga, S. M., Wissinger, E. L. & Braciale, T. J. The attachment (G) glycoprotein of respiratory syncytial virus contains a single immunodominant epitope that elicits both Th1 and Th2 CD4+ T cell responses. *Journal of immunology* **165**, 6487-6495 (2000).

38 Varga, S. M., Wang, X., Welsh, R. M. & Braciale, T. J. Immunopathology in RSV infection is mediated by a discrete oligoclonal subset of antigen-specific CD4(+) T cells. *Immunity* **15**, 637-646 (2001).

39 Wissinger, E. L., Stevens, W. W., Varga, S. M. & Braciale, T. J. Proliferative expansion and acquisition of effector activity by memory CD4+ T cells in the lungs following pulmonary virus infection. *Journal of immunology* **180**, 2957-2966 (2008).

40 Tripp, R. A. Pathogenesis of respiratory syncytial virus infection. *Viral immunology* **17**, 165-181, doi:10.1089/0882824041310513 (2004).

41 Jorquera, P. A., Anderson, L. & Tripp, R. A. Understanding respiratory syncytial virus (RSV) vaccine development and aspects of disease pathogenesis. *Expert review of vaccines*, 1-15, doi:10.1586/14760584.2016.1115353 (2015).

42 Groothuis, J. R. The role of RSV neutralizing antibodies in the treatment and prevention of respiratory syncytial virus infection in high-risk children. *Antiviral research* **23**, 1-10 (1994).

43 Jorquera, P. A. *et al.* Nanoparticle vaccines encompassing the respiratory syncytial virus (RSV) G protein CX3C chemokine motif induce robust immunity protecting from challenge and disease. *PLoS One* **8**, e74905, doi:10.1371/journal.pone.0074905 (2013).

44 Schepens, B., Schotsaert, M. & Saelens, X. Small hydrophobic protein of respiratory syncytial virus as a novel vaccine antigen. *Immunotherapy* **7**, 203-206, doi:10.2217/imt.15.11 (2015).

45 Backman, K., Piippo-Savolainen, E., Ollikainen, H., Koskela, H. & Korppi, M. Adults face increased asthma risk after infant RSV bronchiolitis and reduced respiratory health-related quality of life after RSV pneumonia. *Acta paediatrica (Oslo, Norway : 1992)*, doi:10.1111/apa.12662 (2014).

46 Escobar, G. J. *et al.* Recurrent wheezing in the third year of life among children born at 32 weeks' gestation or later: relationship to laboratory-confirmed, medically attended infection with respiratory syncytial virus during the first year of life. *Archives of pediatrics & adolescent medicine* **164**, 915-922, doi:10.1001/archpediatrics.2010.177 (2010).

47 Kusel, M. M. H. *et al.* Early-life respiratory viral infections, atopic sensitization, and risk of subsequent development of persistent asthma. *The Journal of allergy and clinical immunology* **119**, 1105-1110, doi:10.1016/j.jaci.2006.12.669 (2007).

48 Kwon, J. M. *et al.* Prevalence of respiratory viral infection in children hospitalized for acute lower respiratory tract diseases, and association of rhinovirus and influenza virus with asthma exacerbations. *Korean J Pediatr* **57**, 29-34, doi:10.3345/kjp.2014.57.1.29 (2014).

49 Lin, H. C., Hwang, K. C., Yang, Y. H., Lin, Y. T. & Chiang, B. L. Risk factors of wheeze and allergy after lower respiratory tract infections during early childhood. *Journal of microbiology, immunology, and infection = Wei mian yu gan ran za zhi* **34**, 259-264 (2001).

50 Martinez, F. D. *et al.* Asthma and wheezing in the first six years of life. The Group Health Medical Associates. *The New England journal of medicine* **332**, 133-138, doi:10.1056/NEJM199501193320301 (1995).

51 Ruotsalainen, M., Hyvarinen, M. K., Piippo-Savolainen, E. & Korppi, M. Adolescent asthma after rhinovirus and respiratory syncytial virus bronchiolitis. *Pediatr Pulmonol* **48**, 633-639, doi:10.1002/ppul.22692 (2013).

52 Sigurs, N. *et al.* Severe respiratory syncytial virus bronchiolitis in infancy and asthma and allergy at age 13. *American journal of respiratory and critical care medicine* **171**, 137-141, doi:10.1164/rccm.200406-730OC (2005).

53 Sikkel, M. B., Quint, J. K., Mallia, P., Wedzicha, J. A. & Johnston, S. L. Respiratory syncytial virus persistence in chronic obstructive pulmonary disease. *The Pediatric infectious disease journal* **27**, S63-70, doi:10.1097/INF.0b013e3181684d67 (2008).

54 Gern, J. E. Mechanisms of virus-induced asthma. *The Journal of pediatrics* **142**, S9-13; discussion S13-14 (2003).

55 Kallal, L. E. & Lukacs, N. W. The role of chemokines in virus-associated asthma exacerbations. *Current allergy and asthma reports* **8**, 443-450 (2008).

56 Piedimonte, G., Walton, C. & Samsell, L. Vertical transmission of respiratory syncytial virus modulates pre- and postnatal innervation and reactivity of rat airways. *PLoS One* **8**, e61309, doi:10.1371/journal.pone.0061309 (2013).

57 Lu, T. X. *et al.* MicroRNA-21 limits in vivo immune response-mediated activation of the IL-12/IFN-gamma pathway, Th1 polarization, and the severity of delayed-type hypersensitivity. *Journal of immunology (Baltimore, Md. : 1950)* **187**, 3362-3373, doi:10.4049/jimmunol.1101235 (2011).

58 Sharma, A. *et al.* Antagonism of mmu-mir-106a attenuates asthma features in allergic murine model. *Journal of applied physiology (Bethesda, Md. : 1985)* **113**, 459-464, doi:10.1152/japplphysiol.00001.2012 (2012).

59 Collison, A. *et al.* Altered expression of microRNA in the airway wall in chronic asthma: miR-126 as a potential therapeutic target. *BMC pulmonary medicine* **11**, 29, doi:10.1186/1471-2466-11-29 (2011).

60 Lu, T. X. & Rothenberg, M. E. Diagnostic, functional, and therapeutic roles of microRNA in allergic diseases. *The Journal of allergy and clinical immunology* **132**, 3-13; quiz 14, doi:10.1016/j.jaci.2013.04.039 (2013).

61 Mattes, J., Collison, A., Plank, M., Phipps, S. & Foster, P. S. Antagonism of microRNA-126 suppresses the effector function of TH2 cells and the development of allergic airways disease. *Proceedings of the National Academy of Sciences of the United States of America* **106**, 18704-18709, doi:10.1073/pnas.0905063106 (2009).

62 Oglesby, I. K., McElvaney, N. G. & Greene, C. M. MicroRNAs in inflammatory lung disease--master regulators or target practice? *Respiratory research* **11**, 148, doi:10.1186/1465-9921-11-148 (2010).

63 Foster, P. S. *et al.* The emerging role of microRNAs in regulating immune and inflammatory responses in the lung. *Immunol Rev* **253**, 198-215, doi:10.1111/imr.12058 (2013).

64 Anderson, L. J. Respiratory syncytial virus vaccine development. *Seminars in immunology* **25**, 160-171, doi:10.1016/j.smim.2013.04.011 (2013).

65 Polack, F. P. & Karron, R. A. The future of respiratory syncytial virus vaccine development. *The Pediatric infectious disease journal* **23**, S65-73, doi:10.1097/01.inf.0000108194.71892.95 (2004).

66 Jorquera, P. A., Oakley, K. E. & Tripp, R. A. Advances in and the potential of vaccines for respiratory syncytial virus. *Expert review of respiratory medicine* **7**, 411-427, doi:10.1586/17476348.2013.814409 (2013).

67 Bueno, S. M. *et al.* Host immunity during RSV pathogenesis. *International immunopharmacology* **8**, 1320-1329, doi:10.1016/j.intimp.2008.03.012 (2008).

68 Castilow, E. M., Olson, M. R. & Varga, S. M. Understanding respiratory syncytial virus (RSV) vaccine-enhanced disease. *Immunol Res* **39**, 225-239 (2007).

69 Graham, B. S., Johnson, T. R. & Peebles, R. S. Immune-mediated disease pathogenesis in respiratory syncytial virus infection. *Immunopharmacology* **48**, 237-247 (2000).

70 Graham, B. S. Pathogenesis of respiratory syncytial virus vaccine-augmented pathology. *Am J Respir Crit Care Med* **152**, S63-66, doi:10.1164/ajrccm/152.4_Pt_2.S63 (1995).

71 Black, S. *et al.* Hemagglutination inhibition antibody titers as a correlate of protection for inactivated influenza vaccines in children. *The Pediatric infectious disease journal* **30**, 1081-1085, doi:10.1097/INF.0b013e3182367662 (2011).

72 Dunning, A. J. *et al.* Correlates of Protection against Influenza in the Elderly: Results from an Influenza Vaccine Efficacy Trial. *Clin Vaccine Immunol* **23**, 228-235, doi:10.1128/CVI.00604-15 (2016).

73 Steiner, R. W. Treating acute bronchiolitis associated with RSV. *Am Fam Physician* **69**, 325-330 (2004).

74 PD-VAC, W. *Status of Vaccine Research and Development of Vaccines for RSV*, <http://www.who.int/immunization/research/meetings_workshops/WHO_PDVAC_RSV.pdf> (2014).

75 Lee, S. *et al.* Vaccine-elicited CD8+ T cells protect against respiratory syncytial virus strain A2-line19F-induced pathogenesis in BALB/c mice. *J Virol* **86**, 13016-13024, doi:10.1128/JVI.01770-12 (2012).

76 Openshaw, P. J. & Chiu, C. Protective and dysregulated T cell immunity in RSV infection. *Current opinion in virology* **3**, 468-474, doi:10.1016/j.coviro.2013.05.005 (2013).

77 Biomarkers and surrogate endpoints: preferred definitions and conceptual framework. *Clinical pharmacology and therapeutics* **69**, 89-95, doi:10.1067/mcp.2001.113989 (2001).

78 Strimbu, K. & Tavel, J. A. What are biomarkers? *Curr Opin HIV AIDS* **5**, 463-466, doi:10.1097/COH.0b013e32833ed177 (2010).

79 Ha, M. & Kim, V. N. Regulation of microRNA biogenesis. *Nature reviews. Molecular cell biology* **15**, 509-524, doi:10.1038/nrm3838 (2014).

80 Berezikov, E. Evolution of microRNA diversity and regulation in animals. *Nature reviews. Genetics* **12**, 846-860, doi:10.1038/nrg3079 (2011).

81 Grimson, A. *et al.* Early origins and evolution of microRNAs and Piwi-interacting RNAs in animals. *Nature* **455**, 1193-1197, doi:10.1038/nature07415 (2008).

82 Bakre, A., Tripp, R.A. in *Frontiers in RNAi Volume 1* (ed R.A. Tripp, Karpilow, J.) In Press (2014).

83 Sibley, C. R. *et al.* The biogenesis and characterization of mammalian microRNAs of mirtron origin. *Nucleic acids research* **40**, 438-448, doi:10.1093/nar/gkr722 (2012).

84 Berezikov, E., Chung, W. J., Willis, J., Cuppen, E. & Lai, E. C. Mammalian mirtron genes. *Molecular cell* **28**, 328-336, doi:10.1016/j.molcel.2007.09.028 (2007).

85 Cai, X., Hagedorn, C. H. & Cullen, B. R. Human microRNAs are processed from capped, polyadenylated transcripts that can also function as mRNAs. *Rna* **10**, 1957-1966, doi:10.1261/rna.7135204 (2004).

86 Lee, Y. *et al.* MicroRNA genes are transcribed by RNA polymerase II. *The EMBO journal* **23**, 4051-4060, doi:10.1038/sj.emboj.7600385 (2004).

87 Borchert, G. M., Lanier, W. & Davidson, B. L. RNA polymerase III transcribes human microRNAs. *Nature structural & molecular biology* **13**, 1097-1101, doi:10.1038/nsmb1167 (2006).

88 Fabian, M. R., Sonenberg, N. & Filipowicz, W. Regulation of mRNA translation and stability by microRNAs. *Annual review of biochemistry* **79**, 351-379, doi:10.1146/annurev-biochem-060308-103103 (2010).

89 Li, J. H., Liu, S., Zhou, H., Qu, L. H. & Yang, J. H. starBase v2.0: decoding miRNA-ceRNA, miRNA-ncRNA and protein-RNA interaction networks from large-scale CLIP-Seq data. *Nucleic acids research* **42**, D92-97, doi:10.1093/nar/gkt1248 (2014).

90 Lu, T. X. MicroRNA in the Pathogenesis of Allergic Inflammation. (2012).

91 Thornburg, N. J., Hayward, S. L. & Crowe, J. E., Jr. Respiratory syncytial virus regulates human microRNAs by using mechanisms involving beta interferon and NF-kappaB. *MBio* **3**, doi:10.1128/mBio.00220-12 (2012).

92 Jim,Äö√†√∂¬¨©nez-Morales, S. *et al.* MiR-146a polymorphism is associated with asthma but not with systemic lupus erythematosus and juvenile rheumatoid arthritis in Mexican patients. *Tissue antigens* **80**, 317-321, doi:10.1111/j.1399-0039.2012.01929.x (2012).

93 Rusca, N. *et al.* MiR-146a and NF-,âà√≠,Äö√†¬¥B1 regulate mast cell survival and T lymphocyte differentiation. *Molecular and cellular biology* **32**, 4432-4444, doi:10.1128/MCB.00824-12 (2012).

94 Frost, R. J. A. & Olson, E. N. Control of glucose homeostasis and insulin sensitivity by the Let-7 family of microRNAs. *Proceedings of the National*

Academy of Sciences of the United States of America **108**, 21075-21080, doi:10.1073/pnas.1118922109 (2011).

95 Meliopoulos, V. A. *et al.* MicroRNA regulation of human protease genes essential for influenza virus replication. *PLoS One* **7**, e37169, doi:10.1371/journal.pone.0037169 (2012).

96 Bakre, A. *et al.* Identification of Host Kinase Genes Required for Influenza Virus Replication and the Regulatory Role of MicroRNAs. *PLoS One* **8**, e66796, doi:10.1371/journal.pone.0066796 (2013).

97 Lu, J. *et al.* MicroRNA expression profiles classify human cancers. *Nature* **435**, 834-838, doi:10.1038/nature03702 (2005).

98 Volinia, S. *et al.* A microRNA expression signature of human solid tumors defines cancer gene targets. *Proc Natl Acad Sci U S A* **103**, 2257-2261, doi:10.1073/pnas.0510565103 (2006).

99 Takamizawa, J. *et al.* Reduced expression of the let-7 microRNAs in human lung cancers in association with shortened postoperative survival. *Cancer research* **64**, 3753-3756, doi:10.1158/0008-5472.CAN-04-0637 (2004).

100 Calin, G. A. *et al.* A MicroRNA signature associated with prognosis and progression in chronic lymphocytic leukemia. *N Engl J Med* **353**, 1793-1801, doi:10.1056/NEJMoa050995 (2005).

101 van Rooij, E. *et al.* A signature pattern of stress-responsive microRNAs that can evoke cardiac hypertrophy and heart failure. *Proc Natl Acad Sci U S A* **103**, 18255-18260, doi:10.1073/pnas.0608791103 (2006).

102 Eisenberg, I. *et al.* Distinctive patterns of microRNA expression in primary muscular disorders. *Proc Natl Acad Sci U S A* **104**, 17016-17021, doi:10.1073/pnas.0708115104 (2007).

103 Hebert, S. S. & De Strooper, B. Alterations of the microRNA network cause neurodegenerative disease. *Trends in neurosciences* **32**, 199-206, doi:10.1016/j.tins.2008.12.003 (2009).

104 Amarilyo, G. & La Cava, A. miRNA in systemic lupus erythematosus. *Clinical immunology* **144**, 26-31, doi:10.1016/j.clim.2012.04.005 (2012).

105 Bostjancic, E. & Glavac, D. Importance of microRNAs in skin morphogenesis and diseases. *Acta dermatovenerologica Alpina, Pannonica, et Adriatica* **17**, 95-102 (2008).

106 Chan, E. K., Ceribelli, A. & Satoh, M. MicroRNA-146a in autoimmunity and innate immune responses. *Annals of the rheumatic diseases* **72 Suppl 2**, ii90-95, doi:10.1136/annrheumdis-2012-202203 (2013).

107 Moser, J. J. & Fritzler, M. J. Relationship of other cytoplasmic ribonucleoprotein bodies (cRNPB) to GW/P bodies. *Advances in experimental medicine and biology* **768**, 213-242, doi:10.1007/978-1-4614-5107-5_13 (2013).

108 Persengiev, S. P. miRNAs at the crossroad between hematopoietic malignancies and autoimmune pathogenesis. *Discovery medicine* **13**, 211-221 (2012).

109 Wittmann, J. & Jack, H. M. microRNAs in rheumatoid arthritis: midget RNAs with a giant impact. *Annals of the rheumatic diseases* **70 Suppl 1**, i92-96, doi:10.1136/ard.2010.140152 (2011).

110 Al-Quraishy, S., Dkhil, M. A., Delic, D., Abdel-Baki, A. A. & Wunderlich, F. Organ-specific testosterone-insensitive response of miRNA expression of C57BL/6 mice to Plasmodium chabaudi malaria. *Parasitology research* **111**, 1093-1101, doi:10.1007/s00436-012-2937-3 (2012).

111 Delic, D., Dkhil, M., Al-Quraishy, S. & Wunderlich, F. Hepatic miRNA expression reprogrammed by Plasmodium chabaudi malaria. *Parasitology research* **108**, 1111-1121, doi:10.1007/s00436-010-2152-z (2011).

112 Ge, Y. *et al.* Serum microRNA expression profile as a biomarker for the diagnosis of pertussis. *Molecular biology reports* **40**, 1325-1332, doi:10.1007/s11033-012-2176-9 (2013).

113 Ma, L., Shen, C. J., Cohen, E. A., Xiong, S. D. & Wang, J. H. miRNA-1236 inhibits HIV-1 infection of monocytes by repressing translation of cellular factor VprBP. *PLoS One* **9**, e99535, doi:10.1371/journal.pone.0099535 (2014).

114 Podolska, A. *et al.* Profiling microRNAs in lung tissue from pigs infected with Actinobacillus pleuropneumoniae. *BMC genomics* **13**, 459, doi:10.1186/1471-2164-13-459 (2012).

115 Singh, P. K., Singh, A. V. & Chauhan, D. S. Current understanding on micro RNAs and its regulation in response to Mycobacterial infections. *Journal of biomedical science* **20**, 14, doi:10.1186/1423-0127-20-14 (2013).

116 Wang, C. *et al.* Comparative miRNA expression profiles in individuals with latent and active tuberculosis. *PLoS One* **6**, e25832, doi:10.1371/journal.pone.0025832 (2011).

117 Bont, L. *et al.* Local interferon-gamma levels during respiratory syncytial virus lower respiratory tract infection are associated with disease severity. *J Infect Dis* **184**, 355-358, doi:10.1086/322035 (2001).

118 Brand, H. K. *et al.* CD4+ T-cell counts and interleukin-8 and CCL-5 plasma concentrations discriminate disease severity in children with RSV infection. *Pediatric research* **73**, 187-193, doi:10.1038/pr.2012.163 (2013).

119 Mella, C. *et al.* Innate immune dysfunction is associated with enhanced disease severity in infants with severe respiratory syncytial virus bronchiolitis. *J Infect Dis* **207**, 564-573, doi:10.1093/infdis/jis721 (2013).

120 Hirakawa, S. *et al.* Marked induction of matrix metalloproteinase-10 by respiratory syncytial virus infection in human nasal epithelial cells. *J Med Virol* **85**, 2141-2150, doi:10.1002/jmv.23718 (2013).

121 Yeo, S. J. *et al.* Respiratory syncytial virus infection induces matrix metalloproteinase-9 expression in epithelial cells. *Arch Virol* **147**, 229-242 (2002).

122 Dabo, A. J., Cummins, N., Eden, E. & Geraghty, P. Matrix Metalloproteinase 9 Exerts Antiviral Activity against Respiratory Syncytial Virus. *PLoS ONE* **10**, e0135970, doi:10.1371/journal.pone.0135970 (2015).

123 Tortorolo, L. *et al.* Neurotrophin overexpression in lower airways of infants with respiratory syncytial virus infection. *Am J Respir Crit Care Med* **172**, 233-237, doi:10.1164/rccm.200412-1693OC (2005).

124 Wedde-Beer, K., Hu, C., Rodriguez, M. M. & Piedimonte, G. Leukotrienes mediate neurogenic inflammation in lungs of young rats infected with respiratory

syncytial virus. *American journal of physiology. Lung cellular and molecular physiology* **282**, L1143-1150, doi:10.1152/ajplung.00323.2001 (2002).

125 Tripp, R. A., Barskey, A., Goss, L. & Anderson, L. J. Substance P receptor expression on lymphocytes is associated with the immune response to respiratory syncytial virus infection. *J Neuroimmunol* **129**, 141-153 (2002).

126 Tripp, R. A. *et al.* The G glycoprotein of respiratory syncytial virus depresses respiratory rates through the CX3C motif and substance P. *J Virol* **77**, 6580-6584 (2003).

127 Matsuse, H. *et al.* Differential airway inflammatory responses in asthma exacerbations induced by respiratory syncytial virus and influenza virus a. *International archives of allergy and immunology* **161**, 378-382, doi:10.1159/000348381 (2013).

128 Matsuse, H. *et al.* Effects of respiratory syncytial virus infection on dendritic cells and cysteinyl leukotrienes in lung tissues of a murine model of asthma. *Allergology international : official journal of the Japanese Society of Allergology* **56**, 165-169, doi:10.2332/allergolint.O-06-476 (2007).

129 Kott, K. S. *et al.* Effect of secondhand cigarette smoke, RSV bronchiolitis and parental asthma on urinary cysteinyl LTE4. *Pediatr Pulmonol* **43**, 760-766, doi:10.1002/ppul.20853 (2008).

130 Tzouvelekis, A., Kouliatsis, G., Anevlavis, S. & Bouros, D. Serum biomarkers in interstitial lung diseases. *Respir Res* **6**, 78, doi:10.1186/1465-9921-6-78 (2005).

131 Kawasaki, Y. *et al.* Serum SP-D levels as a biomarker of lung injury in respiratory syncytial virus bronchiolitis. *Pediatr Pulmonol* **46**, 18-22, doi:10.1002/ppul.21270 (2011).

132 Lahti, M. *et al.* Surfactant protein D gene polymorphism associated with severe respiratory syncytial virus infection. *Pediatric research* **51**, 696-699, doi:10.1203/00006450-200206000-00006 (2002).

133 Lofgren, J., Ramet, M., Renko, M., Marttila, R. & Hallman, M. Association between surfactant protein A gene locus and severe respiratory syncytial virus infection in infants. *J Infect Dis* **185**, 283-289, doi:10.1086/338473 (2002).

134 Kuroki, Y., Takahashi, H., Chiba, H. & Akino, T. Surfactant proteins A and D: disease markers. *Biochim Biophys Acta* **1408**, 334-345 (1998).

135 Banos-Lara Mdel, R., Piao, B. & Guerrero-Plata, A. Differential mucin expression by respiratory syncytial virus and human metapneumovirus infection in human epithelial cells. *Mediators of inflammation* **2015**, 347292, doi:10.1155/2015/347292 (2015).

136 Broeckaert, F., Clippe, A., Knoops, B., Hermans, C. & Bernard, A. Clara cell secretory protein (CC16): features as a peripheral lung biomarker. *Ann N Y Acad Sci* **923**, 68-77 (2000).

137 Pulendran, B. Systems vaccinology: Probing humanity's diverse immune systems with vaccines. *Proceedings of the National Academy of Sciences* **111**, 12300-12306, doi:10.1073/pnas.1400476111 (2014).

CHAPTER 3

DYSREGULATED LUNG MICRORNA EXPRESSION PROFILES IN BALB/C MICE POST-VACCINATION AND POST-CHALLENGE WITH RESPIRATORY SYNCYTIAL VIRUS [1,2]

[1] A Microparticle Vaccine Carrying the G Protein CX3C Chemokine Motif Induce Protection against the Respiratory Syncytial Virus strains Memphis 37 and B1 in BALB/c mice, Jorquera PA, Anderson LJ, Williams C, Harcourt J, Nagy T, Powell TJ, Tripp RA. To be submitted to *Journal of Immunology*.

[2] MicroRNA Biomarkers for Vaccine Adjuvants: using Respiratory Syncytial Virus as a model. Anderson LJ*, Jorquera PA*, Tripp RA. To be submitted to *AIMS Microbiology*.

Abstract

MicroRNAs (miRNAs) are short single-stranded noncoding RNA molecules involved in post-transcriptional gene regulation. In the airways, miRNAs are implicated in the regulation of antiviral defense, through the modulation of both innate and adaptive immune response in inflammatory and immune effector cells, but also in parenchymal cells of the lung. The primary target of respiratory syncytial virus (RSV), as well as other respiratory viruses, is airway epithelial cells. To address this and provide a better understanding of the virus-host interface, the potential role for miRNAs was examined in BALB/c mice. miRNAs have been shown to have important roles in lung development and in pulmonary diseases, such as regulating pathogenic mechanisms linked to asthma and airway hyperresponsiveness, cystic fibrosis, and chronic obstructive pulmonary disease. The rationale for this study is that understanding the changes in miRNA expression profiles and their contribution to the pathogenesis of the disease could lead to development of new clinical targets as well as diagnostic and prognostic tools for RSV, both of which are urgently needed. Using RT-qPCR to evaluate nine miRNAs in lung samples from BALB/c mice, we provide evidence that miRNA expression patterns are altered between naïve and RSV-infected or vaccinated mice, and that challenge of these mice leads to unique miRNA profiles in mice that recover or develop disease. In addition, the RSV strain utilized for RSV infection and challenge altered the miRNA expression levels. Overall, the miRNA profiles also appear to correlate with lung viral titers and Th1- and Th2- type cytokine expression levels in the lung and bronchoalveolar lavage (BAL), suggesting that these miRNAs may be involved in RSV pathogenesis.

Introduction

Respiratory syncytial virus (RSV), an enveloped non-segmented negative strand RNA virus of the *Paramyxoviridae* family, is the most common cause of lower respiratory tract infections in infants and young children, and frequently recognized as a cause of respiratory illness in the elderly and high-risk adults (1-3). RSV bronchiolitis exhibits similar pathology to bronchiolitis caused by other respiratory viruses such as influenza virus, parainfluenza virus type 3, and adenovirus (4). RSV has a direct cytopathic effect on cells in the lung epithelium; in addition, a peribronchiolar cell infilitrate forms accompanied by submucosal edema and mucus secretion (4). Despite being highly infective, one of the features of RSV that poses a challenge to vaccine development is that natural infection does not provide effective immunological memory therefore re-infections are frequently observed (5, 6). Furthermore, it has been proposed that exposure to RSV early in life can exacerbate and potentially induce the development of recurrent allergic wheezing and asthma (5, 7). There is currently no licensed vaccine or therapeutic treatment for RSV, and so the recommended treatment options are primarily based on supportive care. Passive immunoprophylaxis with monoclonal antibody against a highly conserved RSV F epitope (Synagis) is available, but its efficacy, cost, delivery, and availability limit its usage for susceptible individuals (8). Clearly, new strategies for the prevention and treatment of RSV infections are urgently needed.

Harnessing the immune response by vaccination is the most effective method for control of infectious diseases (8). The identification of novel immune correlates of vaccine efficacy that take into account parameters other than antibody titers has become increasingly more important in the development and the optimization of vaccine

candidates (9). The spectrum of vaccine candidates in development for RSV ranges from live attenuated viruses to vector-based and subunit vaccines in a wide variety of platforms, and it is likely that multiple vaccines will be necessary for the distinct target populations (10, 11). In terms of RSV vaccine development, the current clinical parameters and immune correlates used to assess the efficacy and safety of vaccine candidates are insufficient, often resulting in vaccine failure late in development and costly and time-intensive clinical trials (12). The best-studied model of RSV disease enhancement by the immune system is the formalin-inactivated RSV (FI-RSV) vaccine. In the 1960s, infants and young children immunized with a FI-RSV vaccine developed severe pulmonary disease following natural RSV infection (4, 13, 14). Therefore, the generation of vaccine-enhanced disease remains a major concern for RSV vaccine development, and so the ability to easily monitor the induction of immune correlates by vaccine candidates is becoming of critical concern in clinical development (9). To address these knowledge gaps, a study to address the feasibility of characterizing the immune response and disease severity through lung miRNA profiling was undertaken.

During RSV infection, both viral proteins and mediators released by the host cells have been found to be involved in RSV-induced miRNA expression (1, 15-17). To date however, no previous studies have evaluated host miRNA expression profiles as potential immune correlates for RSV vaccination and subsequent infection. miRNAs are a class of highly conserved non-coding single-stranded RNA molecules approximately 20-22 nucleotide in length that regulate post-transcriptional expression of target genes by mRNA cleavage and destruction or translational repression (18, 19). In addition, miRNAs are evolutionary conserved among different organisms, and all miRNAs share a

common biosynthetic pathway and reaction mechanisms (20). More recently, microRNAs (miRNAs) have emerged as critical gene expression regulators with the potential to have a modulatory role in various pulmonary diseases but also to normal development of the lung and maintenance of its homeostasis (18, 21-23). Extensive research has examined miRNA involvement in the development and fate of immune cells and in both innate and adaptive immune responses (9, 24-26); however, little is known about the role of miRNA expression on signaling pathways and receptors with critical roles in the inflammatory response produced by RSV infection and vaccine-enhanced disease. To evaluate this, a set of miRNAs were selected that have been found to have critical roles in regulating key pathogenic mechanisms in asthma and airway hyperresponsiveness, such as the polarization of the adaptive immune response, the activation of T cells, the regulation of eosinophil development, and the modulation of cytokine-driven responses (27-31).

We hypothesized that miRNAs implicated in chronic inflammatory diseases of the lung would have altered expression patterns between naïve, RSV-infected, or vaccinated mice. Using lung homogenates from retrospective studies in BALB/c mice designed to evaluate vaccine efficacy of a novel microparticle-based vaccine encompassing the RSV G protein CX3C chemokine motif, we evaluated the expression levels of nine miRNAs by RT-qPCR. This set of host miRNAs were evaluated to explore their potential to serve as diagnostic tools, in the context of other immune correlates being evaluated for vaccine efficacy. miRNA profiles were examined after challenge with wild-type RSV strain A and B viruses as well as RSV M37, a clinically derived virus, to determine the significance of RSV strain differences. These studies show that miRNA expression

patterns are altered between naïve and RSV-infected or vaccinated mice, and that RSV challenge of these mice leads to unique miRNA profiles that are linked to recovery or disease. The results appear to correlate with lung viral titers and histopathology, Th1- and Th2- type cytokine expression levels and pro-inflammatory cytokine levels in the lung and BAL, thereby suggesting that these miRNAs may modulate RSV pathogenesis.

Materials and Methods

Animals

Specific-pathogen-free, 6-to-8 weeks old female BALB/c mice (The Jackson Laboratory) were used in all experiments. Mice were housed in microisolator cages and were fed sterilized water and food ad libitum. All experiments were performed in accordance with the guidelines of the University of Georgia Institutional Animal Care and Use Committee (IACUC), with protocols approved by the University of Georgia IACUC.

Virus infection

There are two major antigenic subtypes of RSV, A and B, and additional antigenic variability occurs within the groups (6). RSV M37 is a wild type RSV A strain virus, first isolated from a 4 month old infant and used in human clinical studies (32). Mycoplasma-free virus stocks of wild-type RSV A2, wildtype RSV B1, and RSV Memphis Strain 37 (M37) were propagated in Vero E6 cells (ATCC CRL-1586) as described (33). Briefly, upon detectable cytopathic effect cells were scraped and collected in 50 mL conical tubes, then virus was harvested by sonicating scraped cells three times

for 10 sec intervals at maximum power, followed by centrifugation to pellet the cell debris. Virus supernatant, divided into 1 mL aliquots, was stored at -80°C until needed. Virus titers were determined through plaque assay on Vero E6 cells as described below. All mice were anesthetized by intraperitoneal (i.p.) injection of avertin (2, 2, 2-tribromoethanol) followed by intranasal infection with 10^6 PFU of RSV A2, RSV B1, or RSV M37 in Phosphate Buffered Saline (PBS; GE Healthcare HyClone) in a total volume of 50 µl. The naïve mice received 50 µl of PBS (GE Healthcare HyClone) upon challenge.

Vaccination

LbL microparticles will be suspensed in phosphate buffered saline (PBS; Hyclone, Thermo Scientific) and dispersed by water bath sonication immediately prior to immunization. Doses will be adjusted to deliver either 50 µg DP/100 µL/mouse. Mice will be immunized without adjuvant subcutaneously (s.c.) between the shoulder blades. The control groups receive either 10^6 PFU of live RSV A2, RSV B1, or RSV M37 by intranasal (i.n.) instillation (positive control for protection), 100 µL of PBS per injection (negative control), and either 50 µg DP/100 µL/mouse of the irrelevant microparticle vaccine (irrMP) with the designed peptide containing a malaria amino acid sequence (placebo vaccine). The FI-RSV A2 vaccine group (vaccine-enhanced disease) will receive a 1:25 dilution in PBS of FI-RSV A2 by s.c. injection in a final volume of 50 µL/mouse.

Peptide synthesis

Peptide spanning the G protein CX3C motif of the RSV A2 strain was designed for vaccination. C-terminal amide peptides were synthesized on a CEM, Liberty^{TM} microwave assisted synthesizer using the manufacturer's standard synthesis protocols. Crude reduced peptides were partially purified by C_{18} reversed phase HPLC, correct molecular weight was confirmed by electrospray mass spectrometry (ESMS), and then lyophilized. Oxidative refolding was accomplished by dissolving the peptides at 2-5 mg/mL in redox buffer (2.5 mM reduced glutathione, 2.5 mM oxidized glutathione, 100 mM Tris pH 7.0) for 3h at room temperature then at 4°C overnight. Folding was judged complete by a shift to slightly shorter retention time on analytical HPLC. Following a final HPLC purification step refolding was confirmed by a loss of 4.0 (±0.4) amu in the ESMS spectra relative to that of the reduced peptide, as well as an absence of free thiol as detected by DTNB (Ellman's assay). Correct disulfide bonding is partially confirmed by ESMS of fragments generated from a thermolysin digest of the synthetic peptide. Peptides were aliquoted, lyophilized, and stored at -20°C until use.

Microparticle fabrication and quality control

Microparticles were constructed as previously described (34) on 3μm diameter $CaCO_3$ cores by alternately layering poly-I-glutamic acid (PGA, negative charge) and poly-I-lysine (PLL, positive charge) to build up a seven-layer film where the designed peptide (DP) containing the RSV G protein CX3C motif linked to a cationic sequence was added as the outermost layer. The composition of the film was determined by amino acid analysis (AAA), which showed that a comparable amount of the peptide component was present in each batch. Endotoxin levels were measured using limulus amebocyte

lysate (LAL) assay and were found to be less than 0.1 EU/ug of G peptide. The dispersity of the particle vaccines were monitored by dynamic light scattering (DLS). Stepwise LbL steadily increases the diameter of the particles several fold, from an apparent diameter of about 150nm for uncoated particles to about 400-500 nm for fully coated particles. Some particle aggregation was detected in each batch with a second population of particles in the 1500-2000 nm range.

FI-RSV preparation

This protocol was adapted from the FI-RSV Lot 100 methods described previously (35). Vero E6 cells will be grown to 90% confluency in DMEM with 5% HI-FBS (at least 20 T150cm2 flasks). Cells will be infected with RSV A2, RSV B1, or RSV M37 at a MOI=0.1 in DMEM without serum. When the cells show extensive CPE (~ day 4pi), we will remove all but 2mL of media, scrape the cells and collect all the fluid into a 50mL tube. 5mL will be distributed per tube and placed on ice; the cells will then be sonicated (3 times, 5 sec per time at maximum power) until all cells become debris. We will remove the cell debris by centrifugation at 3,000 rpm for 15 min at 4°C. The supernatant will be transferred to a clean tube and filter sterilized using a 2µm filter. We will determine the protein concentration of the preparation using BCA assay, and the concentration of protein will be adjusted to 1-2 mg/mL, allowing for consistency across batch preparations in the amount of protein used during vaccination. The virus will be inactivated by the addition of 37% formalin (final dilution 1:4,000) incubate at 37°C per 3 days in agitation. Approximately 200µl will be reserved for plaque assay to determine the viral titer and to calculate the ratio between PFU: protein. The virus will be pelleted

by ultracentrifugation for 2 h at 25,000 rpm (Beckman; SW28 rotor). Then re-suspended in serum-free media at 1/25th of the original volume. Adsorbed overnight at room temperature in 4mg/mL aluminum hydroxide. The compound material will be pelleted by centrifugation (1,000 rpm for 15 min at room temperature) and the pellet will be re-suspended in serum-free media (at 1/4th volume of step 7). Optional: use DMEM containing 200 units/ml each of neomycin, streptomycin and polymyxin B, and a 1:40,000 final dilution of benzethonium chloride. This procedure will result in a final vaccine that is concentrated 100-fold and contains 16 mg/ml alum. The vaccine will be aliquoted in 1ml volumes and stored at 4°C.

Lung viral titers

RSV lung virus titers in treatment and control mice were also determined by RSV M gene copy number by RT-qPCR as previously described (36). Briefly, total RNA was extracted and quantified from the homogenized lung samples. Serial dilution of known PFU of RSV RNA was used to obtain a standard reference curve for RT-qPCR as described (37). Expression of RSV A2 M gene was determined by one-step RT-qPCR using the AgPath-ID One-Step RT-qPCR kit (Life Technologies) and the following primers and probe: RSV A2 M gene forward primer: 5'-GGC AAA TAT GGA AAC ATA GCT GAA-3', RSV A2 M gene reverse primer: 5'-TCT TTT TCT AGG ACA TTG TAT TGA ACA G-3', and RSV A2 M gene TaqMan probe: 5'-GTG TGT ATG TGG AGC CTT CGT GAA GCT-3'. RSV B1 M gene forward primer: 5'-GGT GCC TAT GTT CCA GTC ATC-3', RSV B1 M gene reverse primer: 5'-GAC TCG TAG TGA AGG TCC TTT G-3', and RSV B1 M gene TaqMan probe: 5'-TG CAA GCA TCA ACA

TAC TAG TGA AGC AGA-3'. All TaqMan probes were labeled at the 5' end with the reporter molecule 6-carboxyfluorescein (FAM) and labeled with a Blackhole quencher-1 (BHQ1) at the 3' end. Data was analyzed using RT-qPCR analysis software and cycle threshold (Ct) values and corresponding copy numbers were calculated.

Histopathology

Day 5 post-challenge, a subset of mice from each group were sacrificed and lung histopathological evaluation was performed. Briefly, lungs from vaccinated mice were removed post-challenge, perfused with 10% buffered formalin through the heart and trachea and fixed in 10% buffer formalin. The sections were embedded in paraffin, cut in 5μm-thick sections and stained with hematoxylin and eosin. The sections were evaluated by light microscopy. Histopathological evaluation of the pulmonary sections was performed in a blinded fashion using an inflammatory scale of 0 to 4. The definition of the scores is as follows: 0 = no inflammation; 1 = minimal inflammation; 2 = mild inflammation; 3 = moderate inflammation; 4 = maximum inflammation. The following 5 parameters were evaluated histologically: a) peribronchiolitis (presence of peribronchiolar inflammatory infiltrates); b) perivasculitis (presence of perivascular inflammatory infiltrates); c) bronchiolitis (presence of inflammatory cells in the bronchiolar epithelium or presence of necrotic bronchiolar epithelial cells in the bronchiolar lumina); d) alveolitis (presence of inflammatory cells in the alveoli); e) interstitial pneumonitis (presence of inflammatory cells in the alveolar septa) as described by *Prince et al.* (38). The summary value for each of the five parameters was added

together to arrive at a single summary score for each animal as described by *Smith et al.* (39).

BAL collection and quantification of cytokines

Day 5 post-challenge, a subset of mice from each group were sacrificed and tracheotomy was performed. The mouse lungs were flushed three times with 1 ml of PBS and the retained BAL was centrifuged at 400 x g for 5 min at 4°C. The recovered supernatants were collected and stored at -80°C until assessed for cytokine concentration, and the cell pellet were resuspended in 200 μL of FACS staining buffer (PBS containing 1% BSA). Total cell numbers were counted using a hemocytometer. The Luminex® xMAPTM system using a MILLIPLEX MAP mouse cytokine immunoassay (MCYTOMAG-70K, Millipore) was used to quantitate cytokines in BAL supernatants according to the manufacturer protocol. Briefly, beads coupled with anti-IFN-γ, anti-IL-1α, anti-IL-2, anti-IL-4, anti-IL-5, anti-IL-6, anti-IL-9, anti-IL-10, anti-IL-12p40, anti-IL-13, anti-IL-15, anti-IL17A, anti-MCP-1, anti-RANTES, anti-TNF-α, and anti-Eotaxin monoclonal antibodies were sonicated, mixed, and diluted 1:50 in assay buffer. For the assay, 25 μL of beads were mixed with 25 μL of PBS, 25 μL of assay buffer and 25 μL of BAL supernatant and incubated overnight at 4°C. After washing, beads were incubated with biotinylated detection antibodies for 1 h and the reaction mixture was then incubated with streptavidin- phycoerythrin (PE) conjugate for 30 min at room temperature, washed, and resuspended in PBS. The assay was analyzed on a Luminex 200 instrument (Luminex Corporation, Austin, TX) using Luminex xPONENT 3.1 software.

Flow cytometry

Flow cytometry analysis was performed as described by *Jorquera et al.* (40), BAL cell suspensions were incubated in FACS staining buffer and blocked with FcγIII/II receptor antibody (BD), and subsequently stained with antibodies from BD bioscience, i.e. PE-Cy7 or PE-conjugated anti-CD3e (145-2C11), PerCP-Cy5.5 or FITC -conjugated anti-CD8α (53-6.7), PerCP-Cy5.5-conjugated anti-CD4 (RM4-5) and optimized concentration of APC-conjugated MHC class I H-2Kd tetramer complexes bearing the peptide SYIGSINNI (Beckman Coulter) representing the immunodominant epitope of the RSV M2-1 protein. To determine cell types in lungs, cell suspensions were stained for 30 min at 4°C with an optimized concentration of PerCP-Cy5.5-conjugated anti-CD45 (30-F11), FITC-conjugated anti-CD11c (HL3), or PE-conjugated anti-SiglecF (E50-2440). Cells were acquired on a LSRII flow cytometer (BD bioscience) with data analyzed using FlowJo software (v 7.6.5).

RNA isolation

Total RNA was isolated from lung samples using RNAzol®RT (Molecular Research Center, Inc) following manufacture protocol for isolation of total RNA. Briefly, 1 ml of RNAzol®RT (up to 100 mg of tissue per 1 mL of RNAzol®RT) was added to 0.4 ml of each homogenized lung sample. 0.4 mL of water per 1 mL of RNAzol®RT was then added to the homogenate/lysate. The resulting mixture was vigorously shaken for 15 sec and stored at room temperature for 15 minutes. Samples were then centrifuged at 12,000 x g for 15 min at 4°C. Following centrifugation, DNA, protein and most polysaccharides were precipitate at the bottom of the tube. 1ml of the supernatant was

transferred to a new 2 ml microcentrifuge tube. RNA precipitation was accomplished by mixing 1 ml of the supernatant with 1 ml of isopropanol and 1μl of polyacryl carrier (Molecular Research Center, Inc.), samples were stored for 10 minutes at room temperature and then centrifuged at 12,000 x g for 10 min at 4°C. The RNA pellet was washed twice by mixing the RNA pellet with 75% ethanol (v/v) and then centrifuged at 8,000 x g for 3 minutes. Residual alcohol solution was removed using a micropipette, and the RNA pellets was dried using a vacufuge® vacuum concentrator (Eppendorf) at 45 °C for approximately 6 minutes. RNA was solubilized in 20μl of RNase free water. The quantity of total RNA was determined using Epoch™ microplate spectrophotomer controlled with the Gen5 Data Analysis software interface (BioTek).

RT-qPCR for miRNA detection

To elongate the miRNAs, total RNA (1μg of total RNA per sample) was polyadenylated with *E. coli* poly A polymerase (PAP) to generate a poly-A tail at the 3' end of each RNA molecule using the miRNA 1st-Strand cDNA Synthesis Kit (Agilent Technologies Cat. # 600036) following the manufactured protocol. Following polyadenylation, the RNA was used as template to synthesize 1st-strand cDNA using the miRNA 1st-Strand cDNA Synthesis Kit (Agilent Technologies Cat. # 600036) following the manufactured protocol. The cDNA was then diluted in 280 μl of RNase-free water for each 20 μl reaction. Brilliant III Ultra-Fast SYBR Green QPCR Master Mix (Agilent Technologies Cat. # 600886) was used for qPCR to quantify the expression levels of miR-21, miR-106, miR-126, miR-145, miR-146a, miR-146b, miR-155, Let-7d, and Let-7f in each sample. To screen for contamination, a no-PAP control cDNA template was

prepared from the polyadenylated reaction (in which the PAP was omitted) and included in the qPCR reactions. All samples were run in triplicate and n=3 mice per group. All miRNA levels were normalized by mouse-specific 18S rRNA (Applied Biosystems Cat. # 4331182) gene expression. Values were represented as expression/ mock treatment (PBS vaccinated/PBS challenged).

miRNA primers

Mouse-specific miRNA sequences were obtained from miRBase for the miRNAs of interest. Forward primers were designed based on the mature-miRNA sequence with the greatest number of deep-sequencing reads, and synthesized by Integrated DNA Technologies (IDT). The mouse-specific miRNA primers have 100% sequence homology with the human miRNA sequence; with the exception of miR-106a, which has two point mutations (Table 3.1).

Statistical analysis

All statistical analyses were performed using GraphPad Prism 6.0h (La Jolla, CA). The data is presented as the mean±standard error of the mean (SEM). Statistical significance was determined using One-way ANOVA followed by Bonferroni's or Dunnett's post-hoc comparisons tests, a p value ≤ 0.05 was considered significant.

Results

RSV G microparticle vaccination is protective against challenge

To evaluate whether immunization with RSV G protein microparticles induces protective immunity, vaccinated mice were challenged with RSV B1 or RSV M37 at day 55 post-boost immunization and lung virus loads were determined at day 5 post-challenge (Fig.3.1). The naïve group, GA2-MP vaccinated group, and mice vaccinated with live RSV B1 or RSV M37 showed a significant ($p \leq 0.0001$) decrease in lung virus loads compared with irrMP control (Fig.3.2). However, no significant difference in lung virus loads was observed in the FI-RSV vaccinated group compared with irrMP control (Fig.3.2). Therefore, mice vaccinated with the irrMP control or a vaccine known to cause vaccine-enhanced disease (FI-RSV) had enhanced viral replication and lack of clearance in their lungs.

An additional study was performed to determine whether a single immunization with GA2-MP induces protective immunity, vaccinated mice were challenged with RSV A2 at day 28 post-prime immunization and lung virus loads were determined at day 7 post-challenge (Fig.3.5). As expected, the lung viral load was undetectable in the naïve mice and low levels of virus were present in the lungs of mice live RSV A2 vaccinated and subsequently challenged with RSV A2 (Fig.3.6). The irrMP mice showed a significant ($p \leq 0.001$) increase in lung virus loads compared with naïve mice and live RSV A2, FI-RSV, and GA2-MP vaccinated mice (Fig.3.6). GA2-MP vaccinated mice showed a decrease in lung virus loads compared with FI-RSV, but this finding was not statistically significant (Fig.3.6). These findings corroborate those observed with prime-boost immunization and challenge with live RSV B1 or RSV M37, in that mice vaccinated with the irrMP control or FI-RSV show increased lung virus loads. However,

these results also demonstrate that a single immunization with GA2-MP does not provide protective immunity.

Enhanced airway inflammation in FI-RSV vaccinated mice indicative of vaccine-enhanced disease

To determine if vaccination increased disease pathogenesis, lung histopathological examination was performed at 5 days post-challenge with RSV B1 or RSV M37. The FI-RSV vaccinated mice showed a significant increase in airway inflammation compared with all other groups (Fig.3.3). Additionally, the mice vaccinated with live RSV B1 or RSV M37 showed a significant increase in the overall histopathology score (Fig.3.3A) and perivaculitis (Fig.3.3B) compared with the irrMP control and naïve mice. Mice vaccinated with the GA2-MP developed minor airway inflammation (Fig.3.3). Taken together, these results indicate that the FI-RSV vaccinated mice have enhanced airway inflammation, which supports the use of this model as a positive control of vaccine-enhanced disease. In addition, vaccination with the GA2-MP induces decreased disease pathogenesis compared with live RSV and FI-RSV vaccination.

Markers of enhanced eosinophil infiltration and airway inflammation

Vaccination with FI-RSV vaccine or RSV G protein results in enhanced pulmonary disease after live RSV infection (41). Additionally, previous studies have reported that vaccinating BALB/c mice with FI-RSV results in high Th2/Th1 cell ratios, which have been associated with immunopathology (8, 42, 43). Furthermore, T cells

marked with Vβ14 TCR and with specificity for RSV G protein have been deemed responsible for immunopathology including airway hyperresponsiveness, mucus over-production, and pulmonary eosinophilia following some, but not all strategies of vaccination (8, 40, 43-45). Eosinophilia is generally considered to be a component of the Th2-type immune response and airway inflammation (46). Eosinophil recruitment and activation are promoted by numerous factors, including IL-5, IL-4, IL-8, eotaxin, RANTES, mast cell products histamine and tryptase, and leukotriene B4 (46). Therefore, the outcome of vaccination and the induction of a Th2-type biased T cell response following live RSV challenge was investigated. Analysis of cytokines (IL-4, IL-5, and IL-6) and chemokines (RANTES and eotaxin) in BAL supernatant showed a tendency of increased cytokine expression in the FI-RSV vaccinated groups at 5 days post-challenge with live RSV B1 and RSV M37, as a marker for enhanced inflammation in these mice (Fig.3.4). All treatment groups had a higher overall level of cytokine expression with live RSV B1 challenge compared with live RSV M37 (Fig.3.4). This is likely due to the fact that live RSV M37 does not replicate as efficiently as RSV B1 in the mouse model of respiratory syncytial virus. In mice challenged with live RSV B1, the GA2-MP group had equivalent IFN-γ expression compared with irrMP control; in contrast, the naïve, live RSV, and FI-RSV groups had significantly lower levels (Fig.3.4A). The Th2-type cytokines IL-4 (Fig.3.4C), IL-5 (Fig.3.4D), and IL-6 (Fig.3.4E) were substantially lower in all groups except for mice vaccinated with FI-RSV. Elevated eotaxin and RANTES levels were also evaluated as markers of eosinophil infilitration. RANTES expression was increased significantly in the irrMP and live RSV mice after live RSV B1 challenge compared with naïve mice that received PBS (Fig.3.4B). Eotaxin expression was

increased significantly in the irrMP and FI-RSV vaccinated mice after live RSV B1 challenge compared with all other groups, a similar trend was observed in FI-RSV vaccinated mice following RSV M37 challenge (Fig.3.4F). Taken together, these results indicate that elevated eotaxin, RANTES, and Th2-type cytokine levels upon RSV infection can be used as markers of enhanced eosinophil infilitration and airway inflammation.

The effect of vaccination on pulmonary cell recruitment to the lung

To evaluate the role of vaccination in pulmonary cell recruitment to the lung, flow cytometry was used to assess leukocyte recruitment in the BAL of mice at day 7 post-challenge with RSV A2. There was no significant difference in the total $CD45^+$ cells (Fig.3.7A) or total lymphocytes (Fig.3.7B) between vaccination groups, the naïve mice was trending towards reduced total cell numbers compared with all groups but this difference was not significant. Total eosinophil cell numbers were increased significantly ($p \leq 0.5$) in FI-RSV vaccinated mice compared with irrMP mice after RSV A2 challenge (Fig. 7C). There was no significant difference in the total number of eosinophils in naïve, GA2-MP, and live RSV A2 vaccinated mice compared with irrMP mice after RSV A2 challenge (Fig.3.7C). The percentage of $CD45^+$ BAL cells was also evaluated for the proportion of macrophages, lymphocytes, eosinophils, and neutrophils. All groups of mice showed a similar increase in the percentage of lymphocytes and neutrophils compared with the naïve mice (Fig.3.7D). Macrophage cell recruitment was decreased in all groups compared with naïve mice (Fig.3.7D). The most striking difference was observed in the eosinophils, as expected, the FI-RSV vaccinated mice showed increased

eosinophil infiltration (~50%) compare to all groups; however, the GA2-MP vaccinated mice also showed moderately increased eosinophil infiltration (~20%) (Fig.3.7D). Taken together, this data demonstrates that all vaccination groups induce increased lymphocyte recruitment by 7 days post-challenge as compared to the naïve mice. In addition, the FI-RSV and GA2-MP vaccinated mice showed enhanced eosinophil recruitment as compared to the other groups.

Alterations in miRNA expression patterns by vaccination and RSV infection

miRNA biology is a key mechanism for mediating cellular responses under various stress conditions, in particular related to proinflammatory lung diseases (18, 47). In addition, recent studies demonstrate that miRNAs are likely involved in regulating various aspects of innate and acquired immunity, and thereby indirectly involved in a variety of inflammatory lung diseases (18, 48, 49). To evaluate the potential for host miRNAs to serve as diagnostic tools for vaccine efficacy, expression patterns of nine host miRNAs associated with critical roles in asthma and airway hyperresponsiveness were evaluated by RT-qPCR (Table 3.2). miR-21, miR-106, miR-126, miR-145, miR-146a, miR-146b, miR-155, Let-7d, and Let-7f expression levels showed a tendency of increased expression levels in FI-RSV vaccinated mice upon challenge with all RSV strains (A2, B1, and M37) (Fig.3.8). Unique miRNA expression patterns are observed between naïve, RSV-infected, FI-RSV vaccinated, and GA2-MP vaccinated mice (Fig.3.8). The RSV strain (A2, B1, or M37) used for RSV infection and challenge appears to alter the magnitude of miRNA expression levels, but the unique expression profiles are preserved among vaccine candidates and RSV infection (Fig.3.8). Overall,

the miRNA profiles also appear to correlate with lung viral titers and Th1- and Th2- type cytokine expression levels in the lung and bronchoalveolar lavage (BAL), suggesting that these miRNAs may be involved in RSV pathogenesis.

miRNAs as potential biomarkers for characterizing adjuvant-mediated immune response profiles

The goal of vaccination is to generate a strong immune response to the administered antigen that is capable of providing long-term protection against infection (50). To achieve this objective, adjuvants are often used to enhance the immunogenicity of antigens, reduce the amount of antigen or the number of immunizations needed for protective immunity, or to improve the efficacy of vaccines in target populations (50). An additional study was performed to evaluate the potential for adjuvants to enhance the immunogenicity of the GA2-MP vaccine. Briefly, BALB/c mice that received a single immunization with either irrMP, live RSV A2, FI-RSV, GA2-MP, or the GA2-MP with the addition of an adjuvant. Various adjuvants were evaluated based on their abilities to stimulate cellular and humoral immunity: RSV M2 protein epitope (Th1 response), Alum (Th2 response), Poli(I:C) (TLR3 agonist), TBD (Th1/Th17 response), and TiterMax (balance Th1/Th2 response). 28 days after immunization, mice were i.n. challenged with live RSV A2 and immune correlates were measured at 7 days post-challenge (data not shown). Adjuvant safety still remains a major roadblock in new vaccine development; therefore, the identification of miRNA biomarkers that accurately characterize adjuvant-mediated immune responses would be beneficial to adjuvant science and clinical development. In order to evaluate this, retrospective lung homogenates were evaluated

from all mice to determine if the various adjuvants produced unique lung miRNA expression profiles. The expression patterns of the same nine host miRNAs associated with critical roles in asthma and airway hyperresponsiveness were evaluated by RT-qPCR (Fig.S3.1). Among the mice that received the various adjuvants, six miRNAs showed significantly altered expression patterns between groups: miR-21, miR-145, miR-146b, miR-155, let-7d, and let-7f (Table 3.3).

The identification of these six miRNAs in correlation with specific adjuvants provides a novel opportunity to discern the mode of action by which these adjuvants modulate the adaptive immune response to vaccines. Overall, miR-146b, miR-155, Let-7d, and Let-7f showed substantially increased expression levels in GA2 + Titermax, GA2 + Poli(I:C), GA2-MP + TBD vaccinated mice upon RSV challenge (Table 3.3). Interestingly, miR-146a and miR-146b have been found to be upregulated in patients with eosinophilic esophagitis, but the specific role of miR-146b in regulating adaptive immune responses has not been investigated (27). However, a recent study determined that miR-146a selectively suppresses Th1 responses via a STAT-1 dependent mechanism (51), and since miR-146a and miR-146b have an identical seed sequence it is plausible that miR-146b could also regulate STAT-1 expression and suppress Th1 responses (27). miR-155 is expressed by skin T cells, dendritic cells, and mast cells (27), and upregulation has been observed following T cell differentiation into both Th1 and Th2 lineages through the downregulation of CTLA-4 in patients with atopic dermatitis (52). The let-7 family appears to target IL-13 expression, and downregulation likely enhances Th2 responses (27). miR-21 expression was increased significantly in mice that received GA2-MP + TiterMAX compared with irrMP, live RSV, GA2-MP + Poli(I:C), and GA2-

MP + TBD groups (Table 3). While miR-21 induction in cells of the innate immune response represents a key switch in the transition from a pro-inflammatory to anti-inflammatory response, it is also found in both T and B-cells (53). miR-21 has been identified as a major regulator of Th1 versus Th2 response; more specifically, it limits activation of the IL-12/IFN-γ pathway, Th1 polarization, and the severity of delayed-type hypersensitivity (53, 54). Taken together, these results demonstrate that adjuvants alone produce unique miRNA profiles; this is a novel insight that has not previously been studied. Furthermore, the miRNAs identified may work additively or synergistically to initiate and/or maintain an exaggerated Th2 response by targeting different components of the T helper cell polarization pathway (27).

Discussion

The results of this lung miRNA profiling study provide unique insights into the pathogenesis and protection from RSV disease. miRNAs are a rapidly evolving research field, and we are just beginning to understand the contribution of these small non-coding RNA molecules to the function of the immune system and in the regulation of cellular processes that contribute to disease (26). In this study, we found that RSV infection and vaccination compared with naïve mice induced unique miRNA expression profiles. Specifically, miRNAs previously implicated in asthma and airway hyperresponsiveness, as identified by a manual literature search, were differentially expressed in response to vaccine candidates and live RSV vaccination that prime for protection and enhanced disease following RSV challenge. In addition, the differential expression of these miRNA profiles among the vaccine candidates appeared to correlate with other immune correlates

(Th2-type immune response and cytokine production) and markers of disease severity (lung viral load and pulmonary inflammation). To our knowledge, this is the first report of miRNA expression profiles of RSV vaccine candidates. These findings provide proof-of-principle for the utilization of miRNAs as a biomarker for RSV disease pathogenesis and vaccine efficacy.

A limitation of the present study is the sample collection methods used for lung miRNA profiling; the process of collecting lung tissues or bronchial washings is invasive and time-intensive, and ultimately not conducive to clinical development as diagnostic and prognostic tools. Most cells release miRNAs into the extracellular environment, predominantly in association with either vesicles (exosomes, microvesicles, and apoptotic bodies) (55-58) or protein complexes (Argonaute2 and high-density lipoprotein) (55, 59, 60) that protect them from RNAse degradation (9, 61, 62). In recent years, it has been discovered that extracellular miRNAs circulate in the bloodstream, and remain remarkably stable (55, 61, 63). Therefore, the stability of miRNAs in serum and plasma and the ease by which miRNAs can be detected in a quantitative manner by methods such as qPCR and microarrays have generated immense interest in the use of circulating miRNAs as clinical biomarkers (55). To date, miRNAs have been evaluated as circulating biomarkers for diagnosis or prognosis of cardiovascular pathologies (55, 64, 65), cancer (66-70), neurological disorders (71), and most importantly inflammatory disorders (72-75).

Our future studies will focus on identifying blood-circulating miRNAs that are capable of functioning as novel and minimally invasive clinical biomarkers for RSV disease pathogenesis and vaccine outcomes. To enhance these findings, a serum miRNA

screen using microarray analysis can be used to validate these miRNAs as potential biomarkers for RSV vaccine enhanced disease, and also identify additional miRNAs that have a critical role in protection and enhanced disease outcomes. In addition, due to the retrospective nature of these studies the time point for evaluating miRNA expression was limited to post-vaccination/post-challenge. Therefore, future studies need to be conducted to assess additional time points during vaccination and RSV challenge in order to characterize the pattern and tempo of miRNA expression.

The link between dysregulation of miRNAs and the pathogenesis of different pulmonary diseases also offers potentially new targets for enhancing vaccines and the development of therapeutic interventions, which are urgently needed. However, identifying the targets of miRNAs in biological systems and in processes such as inflammation and vaccine efficacy is a great challenge, and one of the most important goals to advancing our understanding of how miRNAs contribute to health and disease (26). In addition, as miRNAs have multiple targets it is likely that the physiological and pharmacological effects observed by modifying function are related to subtle changes in the levels of many target transcripts and potentially other subsidiary miRNAs (26). However, reporter assays and gain- and loss- of function studies to modulate miRNA activity have revealed promising results as validation of a target implicated in a pathological process (28, 76, 77). Recent advances in altering miRNA expression in animal models of related human diseases have also raised the possibility of using these molecules as a new class of therapeutic tools (18). Additionally, mastering an understanding of miRNA utilization, target prediction, and validation is key in harnessing miRNAs to prevent and treat clinical diseases.

Author contributions

Conceived and designed experiments: LA PJ RAT. Performed experiments: LA PJ CW. Analyzed the data: LA PJ RAT. Contributed reagents/materials/analysis: RAT. Wrote the manuscript(s): LA PJ RAT.

References

1. Rossi GA, Silvestri M, Colin AA. Respiratory syncytial virus infection of airway cells: Role of microRNAs. Pediatric Pulmonology. 2015:n/a-n/a.
2. Falsey AR, Hennessey PA, Formica MA, Cox C, Walsh EE. Respiratory syncytial virus infection in elderly and high-risk adults. N Engl J Med. 2005;352(17):1749-59.
3. Hall CB, Weinberg GA, Iwane MK, Blumkin AK, Edwards KM, Staat MA, et al. The burden of respiratory syncytial virus infection in young children. N Engl J Med. 2009;360(6):588-98.
4. Openshaw PJ, Tregoning JS. Immune responses and disease enhancement during respiratory syncytial virus infection. Clin Microbiol Rev. 2005;18(3):541-55.
5. Bueno SM, Gonzalez PA, Pacheco R, Leiva ED, Cautivo KM, Tobar HE, et al. Host immunity during RSV pathogenesis. International immunopharmacology. 2008;8(10):1320-9.
6. Sullender WM. Respiratory syncytial virus genetic and antigenic diversity. Clin Microbiol Rev. 2000;13(1):1-15, table of contents.
7. Matsuse H, Tsuchida T, Fukahori S, Kawano T, Tomari S, Matsuo N, et al. Differential airway inflammatory responses in asthma exacerbations induced by

respiratory syncytial virus and influenza virus a. International archives of allergy and immunology. 2013;161(4):378-82.

8. Hurwitz JL. Respiratory syncytial virus vaccine development. Expert review of vaccines. 2011;10(10):1415-33.

9. de Candia P, Torri A, Pagani M, Abrignani S. Serum microRNAs as Biomarkers of Human Lymphocyte Activation in Health and Disease. Frontiers in immunology. 2014;5:43.

10. Guvenel AK, Chiu C, Openshaw PJ. Current concepts and progress in RSV vaccine development. Expert review of vaccines. 2014;13(3):333-44.

11. Jorquera PA, Anderson L, Tripp RA. Understanding respiratory syncytial virus (RSV) vaccine development and aspects of disease pathogenesis. Expert review of vaccines. 2015:1-15.

12. Jorquera PA, Oakley KE, Tripp RA. Advances in and the potential of vaccines for respiratory syncytial virus. Expert review of respiratory medicine. 2013;7(4):411-27.

13. Polack FP, Teng MN, Collins PL, Prince GA, Exner M, Regele H, et al. A role for immune complexes in enhanced respiratory syncytial virus disease. J Exp Med. 2002;196(6):859-65.

14. Waris ME, Tsou C, Erdman DD, Zaki SR, Anderson LJ. Respiratory synctial virus infection in BALB/c mice previously immunized with formalin-inactivated virus induces enhanced pulmonary inflammatory response with a predominant Th2-like cytokine pattern. J Virol. 1996;70(5):2852-60.

15. Bakre A, Wu W, Hiscox J, Spann K, Teng MN, Tripp RA. Human respiratory syncytial virus non-structural protein NS1 modifies miR-24 expression via transforming growth factor-beta. J Gen Virol. 2015;96(11):3179-91.

16. Meliopoulos VA, Andersen LE, Brooks P, Yan X, Bakre A, Coleman JK, et al. MicroRNA regulation of human protease genes essential for influenza virus replication. PLoS One. 2012;7(5):e37169.

17. Winter J, Jung S, Keller S, Gregory RI, Diederichs S. Many roads to maturity: microRNA biogenesis pathways and their regulation. Nature cell biology. 2009;11(3):228-34.

18. Sessa R, Hata A. Role of microRNAs in lung development and pulmonary diseases. Pulm Circ. 2013;3(2):315-28.

19. Wu Z, Hao R, Li P, Zhang X, Liu N, Qiu S, et al. MicroRNA expression profile of mouse lung infected with 2009 pandemic H1N1 influenza virus. PLoS One. 2013;8(9):e74190.

20. Lee CT, Risom T, Strauss WM. Evolutionary conservation of microRNA regulatory circuits: an examination of microRNA gene complexity and conserved microRNA-target interactions through metazoan phylogeny. DNA Cell Biol. 2007;26(4):209-18.

21. Garofalo M, Romano G, Di Leva G, Nuovo G, Jeon YJ, Ngankeu A, et al. EGFR and MET receptor tyrosine kinase-altered microRNA expression induces tumorigenesis and gefitinib resistance in lung cancers. Nature medicine. 2012;18(1):74-82.

22. Calin GA, Croce CM. MicroRNA signatures in human cancers. Nat Rev Cancer. 2006;6(11):857-66.

23. Zoetis T, Hurtt ME. Species comparison of lung development. Birth Defects Res B Dev Reprod Toxicol. 2003;68(2):121-4.

24. Chen CZ, Schaffert S, Fragoso R, Loh C. Regulation of immune responses and tolerance: the microRNA perspective. Immunol Rev. 2013;253(1):112-28.

25. Globinska A, Pawelczyk M, Kowalski ML. MicroRNAs and the immune response to respiratory virus infections. Expert review of clinical immunology. 2014;10(7):963-71.

26. Foster PS, Plank M, Collison A, Tay HL, Kaiko GE, Li J, et al. The emerging role of microRNAs in regulating immune and inflammatory responses in the lung. Immunol Rev. 2013;253(1):198-215.

27. Lu TX, Rothenberg ME. Diagnostic, functional, and therapeutic roles of microRNA in allergic diseases. The Journal of allergy and clinical immunology. 2013;132:3-13; quiz 4.

28. Mattes J, Collison A, Plank M, Phipps S, Foster PS. Antagonism of microRNA-126 suppresses the effector function of TH2 cells and the development of allergic airways disease. Proceedings of the National Academy of Sciences of the United States of America. 2009;106:18704-9.

29. Collison A, Herbert C, Siegle JS, Mattes J, Foster PS, Kumar RK. Altered expression of microRNA in the airway wall in chronic asthma: miR-126 as a potential therapeutic target. BMC pulmonary medicine. 2011;11:29.

30. Kumar M, Ahmad T, Sharma A, Mabalirajan U, Kulshreshtha A, Agrawal A, et al. Let-7 microRNA-mediated regulation of IL-13 and allergic airway inflammation. J Allergy Clin Immunol. 2011;128(5):1077-85 e1-10.

31. Lu TX. MicroRNA in the Pathogenesis of Allergic Inflammation. 2012.

32. Larios Mora A, Detalle L, Van Geelen A, Davis MS, Stohr T, Gallup JM, et al. Kinetics of Respiratory Syncytial Virus (RSV) Memphis Strain 37 (M37) Infection in the Respiratory Tract of Newborn Lambs as an RSV Infection Model for Human Infants. PLoS One. 2015;10(12):e0143580.

33. Tripp RA, Moore D, Jones L, Sullender W, Winter J, Anderson LJ. Respiratory syncytial virus G and/or SH protein alters Th1 cytokines, natural killer cells, and neutrophils responding to pulmonary infection in BALB/c mice. J Virol. 1999;73(9):7099-107.

34. Powell TJ, Palath N, DeRome ME, Tang J, Jacobs A, Boyd JG. Synthetic nanoparticle vaccines produced by layer-by-layer assembly of artificial biofilms induce potent protective T-cell and antibody responses in vivo. Vaccine. 2011;29(3):558-69.

35. Prince GA, Curtis SJ, Yim KC, Porter DD. Vaccine-enhanced respiratory syncytial virus disease in cotton rats following immunization with Lot 100 or a newly prepared reference vaccine. J Gen Virol. 2001;82(Pt 12):2881-8.

36. Harcourt JL, Caidi H, Haynes LM. RSV growth and quantification by Microtitration and qRT-PCR assays. In: Tripp RA, Jorquera P, editors. Human Respiratory Syncytial Virus: Methods and Protocols. 1 ed: Humana Press; 2016. p. XI, 247.

37. Caidi H, Harcourt JL, Tripp RA, Anderson LJ, Haynes LM. Combination therapy using monoclonal antibodies against respiratory syncytial virus (RSV) G glycoprotein protects from RSV disease in BALB/c mice. PloS one. 2012;7:e51485.

38. Prince GA, Jenson AB, Hemming VG, Murphy BR, Walsh EE, Horswood RL, et al. Enhancement of respiratory syncytial virus pulmonary pathology in cotton rats by prior intramuscular inoculation of formalin-inactiva ted virus. J Virol. 1986;57(3):721-8.

39. Smith G, Raghunandan R, Wu Y, Liu Y, Massare M, Nathan M, et al. Respiratory syncytial virus fusion glycoprotein expressed in insect cells form protein nanoparticles that induce protective immunity in cotton rats. PLoS One. 2012;7(11):e50852.

40. Jorquera PA, Choi Y, Oakley KE, Powell TJ, Boyd JG, Palath N, et al. Nanoparticle vaccines encompassing the respiratory syncytial virus (RSV) G protein CX3C chemokine motif induce robust immunity protecting from challenge and disease. PLoS One. 2013;8(9):e74905.

41. Haynes LM, Jones LP, Barskey A, Anderson LJ, Tripp RA. Enhanced disease and pulmonary eosinophilia associated with formalin-inactivated respiratory syncytial virus vaccination are linked to G glycoprotein CX3C-CX3CR1 interaction and expression of substance P. J Virol. 2003;77(18):9831-44.

42. Graham BS, Bunton LA, Wright PF, Karzon DT. Role of T lymphocyte subsets in the pathogenesis of primary infection and rechallenge with respiratory syncytial virus in mice. J Clin Invest. 1991;88(3):1026-33.

43. Varga SM, Wang X, Welsh RM, Braciale TJ. Immunopathology in RSV infection is mediated by a discrete oligoclonal subset of antigen-specific CD4(+) T cells. Immunity. 2001;15(4):637-46.

44. Varga SM, Wissinger EL, Braciale TJ. The attachment (G) glycoprotein of respiratory syncytial virus contains a single immunodominant epitope that elicits both Th1 and Th2 CD4+ T cell responses. Journal of immunology. 2000;165(11):6487-95.

45. Varga SM, Braciale TJ. RSV-induced immunopathology: dynamic interplay between the virus and host immune response. Virology. 2002;295(2):203-7.

46. Johnson TR, Graham BS. Secreted respiratory syncytial virus G glycoprotein induces interleukin-5 (IL-5), IL-13, and eosinophilia by an IL-4-independent mechanism. J Virol. 1999;73(10):8485-95.

47. Hassan T, McKiernan PJ, McElvaney NG, Cryan SA, Greene CM. Therapeutic modulation of miRNA for the treatment of proinflammatory lung diseases. Expert review of anti-infective therapy. 2012;10(3):359-68.

48. Oglesby IK, McElvaney NG, Greene CM. MicroRNAs in inflammatory lung disease--master regulators or target practice? Respiratory research. 2010;11:148.

49. O'Neill LA, Sheedy FJ, McCoy CE. MicroRNAs: the fine-tuners of Toll-like receptor signalling. Nat Rev Immunol. 2011;11(3):163-75.

50. Petrovsky N, Aguilar JC. Vaccine adjuvants: current state and future trends. Immunol Cell Biol. 2004;82(5):488-96.

51. Lu LF, Boldin MP, Chaudhry A, Lin LL, Taganov KD, Hanada T, et al. Function of miR-146a in controlling Treg cell-mediated regulation of Th1 responses. Cell. 2010;142(6):914-29.

52. Sonkoly E, Janson P, Majuri ML, Savinko T, Fyhrquist N, Eidsmo L, et al. MiR-155 is overexpressed in patients with atopic dermatitis and modulates T-cell proliferative responses by targeting cytotoxic T lymphocyte-associated antigen 4. J Allergy Clin Immunol. 2010;126(3):581-9 e1-20.

53. Sheedy FJ. Turning 21: Induction of miR-21 as a Key Switch in the Inflammatory Response. Frontiers in immunology. 2015;6:19.

54. Lu TX, Hartner J, Lim E-J, Fabry V, Mingler MK, Cole ET, et al. MicroRNA-21 limits in vivo immune response-mediated activation of the IL-12/IFN-gamma pathway, Th1 polarization, and the severity of delayed-type hypersensitivity. Journal of immunology (Baltimore, Md : 1950). 2011;187:3362-73.

55. Creemers EE, Tijsen AJ, Pinto YM. Circulating microRNAs: novel biomarkers and extracellular communicators in cardiovascular disease? Circ Res. 2012;110(3):483-95.

56. Zernecke A, Bidzhekov K, Noels H, Shagdarsuren E, Gan L, Denecke B, et al. Delivery of microRNA-126 by apoptotic bodies induces CXCL12-dependent vascular protection. Sci Signal. 2009;2(100):ra81.

57. Valadi H, Ekstrom K, Bossios A, Sjostrand M, Lee JJ, Lotvall JO. Exosome-mediated transfer of mRNAs and microRNAs is a novel mechanism of genetic exchange between cells. Nature cell biology. 2007;9(6):654-9.

58. Moldovan L, Batte K, Wang Y, Wisler J, Piper M. Analyzing the circulating microRNAs in exosomes/extracellular vesicles from serum or plasma by qRT-PCR. Methods in molecular biology (Clifton, NJ). 2013;1024:129-45.

59. Arroyo JD, Chevillet JR, Kroh EM, Ruf IK, Pritchard CC, Gibson DF, et al. Argonaute2 complexes carry a population of circulating microRNAs independent of vesicles in human plasma. Proc Natl Acad Sci U S A. 2011;108(12):5003-8.

60. Vickers KC, Palmisano BT, Shoucri BM, Shamburek RD, Remaley AT. MicroRNAs are transported in plasma and delivered to recipient cells by high-density lipoproteins. Nature cell biology. 2011;13(4):423-33.

61. Chen X, Ba Y, Ma L, Cai X, Yin Y, Wang K, et al. Characterization of microRNAs in serum: a novel class of biomarkers for diagnosis of cancer and other diseases. Cell Res. 2008;18(10):997-1006.

62. Willeit P, Zampetaki A, Dudek K, Kaudewitz D, King A, Kirkby NS, et al. Circulating microRNAs as novel biomarkers for platelet activation. Circ Res. 2013;112(4):595-600.

63. Mitchell PS, Parkin RK, Kroh EM, Fritz BR, Wyman SK, Pogosova-Agadjanyan EL, et al. Circulating microRNAs as stable blood-based markers for cancer detection. Proc Natl Acad Sci U S A. 2008;105(30):10513-8.

64. Goren Y, Kushnir M, Zafrir B, Tabak S, Lewis BS, Amir O. Serum levels of microRNAs in patients with heart failure. Eur J Heart Fail. 2012;14(2):147-54.

65. van Rooij E, Sutherland LB, Liu N, Williams AH, McAnally J, Gerard RD, et al. A signature pattern of stress-responsive microRNAs that can evoke cardiac hypertrophy and heart failure. Proc Natl Acad Sci U S A. 2006;103(48):18255-60.

66. Liu J, Gao J, Du Y, Li Z, Ren Y, Gu J, et al. Combination of plasma microRNAs with serum CA19-9 for early detection of pancreatic cancer. International journal of cancer Journal international du cancer. 2012;131(3):683-91.

67. Margue C, Reinsbach S, Philippidou D, Beaume N, Walters C, Schneider JG, et al. Comparison of a healthy miRNome with melanoma patient miRNomes: are microRNAs suitable serum biomarkers for cancer? Oncotarget. 2015;6(14):12110-27.

68. Mangolini A, Ferracin M, Zanzi MV, Saccenti E, Ebnaof SO, Poma VV, et al. Diagnostic and prognostic microRNAs in the serum of breast cancer patients measured by droplet digital PCR. Biomark Res. 2015;3:12.

69. Song MY, Pan KF, Su HJ, Zhang L, Ma JL, Li JY, et al. Identification of serum microRNAs as novel non-invasive biomarkers for early detection of gastric cancer. PLoS One. 2012;7(3):e33608.

70. Yang Y, Gu X, Zhou M, Xiang J, Chen Z. Serum microRNAs: A new diagnostic method for colorectal cancer. Biomed Rep. 2013;1(4):495-8.

71. Luo Y, Wang C, Chen X, Zhong T, Cai X, Chen S, et al. Increased serum and urinary microRNAs in children with idiopathic nephrotic syndrome. Clin Chem. 2013;59(4):658-66.

72. Tomofuji T, Yoneda T, Machida T, Ekuni D, Azuma T, Kataoka K, et al. MicroRNAs as serum biomarkers for periodontitis. J Clin Periodontol. 2016;43(5):418-25.

73. Lewis A, Nijhuis A, Mehta S, Kumagai T, Feakins R, Lindsay JO, et al. Intestinal fibrosis in Crohn's disease: role of microRNAs as fibrogenic modulators, serum biomarkers, and therapeutic targets. Inflamm Bowel Dis. 2015;21(5):1141-50.

74. Lv Y, Qi R, Xu J, Di Z, Zheng H, Huo W, et al. Profiling of serum and urinary microRNAs in children with atopic dermatitis. PLoS One. 2014;9(12):e115448.

75. Kamiya Y, Kawada J, Kawano Y, Torii Y, Kawabe S, Iwata N, et al. Serum microRNAs as Potential Biomarkers of Juvenile Idiopathic Arthritis. Clin Rheumatol. 2015;34(10):1705-12.

76. Collison A, Mattes J, Plank M, Foster PS. Inhibition of house dust mite-induced allergic airways disease by antagonism of microRNA-145 is comparable to glucocorticoid treatment. J Allergy Clin Immunol. 2011;128(1):160-7 e4.

77. Quaranta MT, Olivetta E, Sanchez M, Spinello I, Paolillo R, Arenaccio C, et al. miR-146a controls CXCR4 expression in a pathway that involves PLZF and can be used to inhibit HIV-1 infection of CD4(+) T lymphocytes. Virology. 2015;478:27-38.

78. Sharma A, Kumar M, Ahmad T, Mabalirajan U, Aich J, Agrawal A, et al. Antagonism of mmu-mir-106a attenuates asthma features in allergic murine model. Journal of applied physiology (Bethesda, Md : 1985). 2012;113:459-64.

79. Thornburg NJ, Hayward SL, Crowe JE. Respiratory syncytial virus regulates human microRNAs by using mechanisms involving beta interferon and NF-κB. mBio. 2012;3.

80. Comer BS, Camoretti-Mercado B, Kogut PC, Halayko AJ, Solway J, Gerthoffer WT. MicroRNA-146a and microRNA-146b expression and anti-inflammatory

function in human airway smooth muscle. American journal of physiology Lung cellular and molecular physiology. 2014;307(9):L727-34.

81. Rusca N, Dehò L, Montagner S, Zielinski CE, Sica A, Sallusto F, et al. MiR-146a and NF-κB1 regulate mast cell survival and T lymphocyte differentiation. Molecular and cellular biology. 2012;32:4432-44.

82. Vigorito E, Perks KL, Abreu-Goodger C, Bunting S, Xiang Z, Kohlhaas S, et al. microRNA-155 regulates the generation of immunoglobulin class-switched plasma cells. Immunity. 2007;27(6):847-59.

Tables and figures

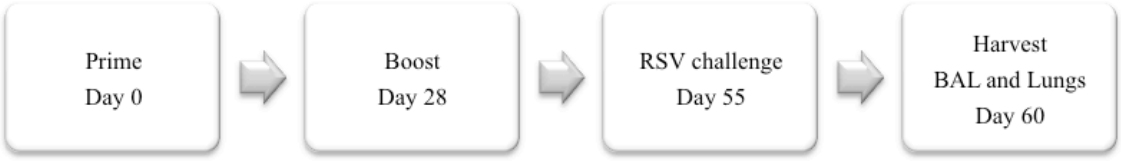

Group	Prime		Boost		Challenge	Route
Naïve	-	-	-	-	PBS	i.n.
Placebo	10µg of irrMP	s.c.	10µg of irrMP	s.c.	$1x10^6$ PFU of RSV M37 or RSV B1	i.n.
Live RSV	$1x10^6$ PFU of RSV M37 or RSV B1	i.n.	$1x10^6$ PFU of RSV M37 or RSV B1	i.n.	$1x10^6$ PFU of RSV M37 or RSV B1	i.n.
FI-RSV	$1x10^6$ PFU equivalent of FI-RSV M37 or FI-RSV B1	i.m.	$1x10^6$ PFU equivalent of FI-RSV M37 or FI-RSV B1	i.m.	$1x10^6$ PFU of RSV M37 or RSV B1	i.n.
GA2-MP	10µg of GA2-MP	s.c.	10µg of GA2-MP	s.c.	$1x10^6$ PFU of RSV M37 or RSV B1	i.n.

Fig. 3.1: Schematic of the experimental design used to determine alterations in miRNA expression profiles in an *in vivo* murine model post-vaccination/post-RSV challenge with RSV M37 or RSV B1 challenge. Female, 6-8 week old BALB/c mice were immunized at days 0 and 28 with placebo vaccine (10 μg of irrelevant microparticle (irrMP)), $1x10^6$ PFU of live RSV M37 or live RSV B1, FI-RSV M37 or FI-RSV B1 equivalent to $1x10^6$ PFU, or 10μg of GA2-MP vaccine (microparticle carrying the amino acidic region 169-196 of the RSV G protein). At day 55, mice were intranasally challenged with $1x10^6$ PFU of either live RSV M37 or live RSV B1. Naïve mice (mock infected) were not prime-boost immunized but challenged with phosphate buffer saline (PBS). At 5 days post-challenge bronchoalveolar lavages (BAL) and lung samples were harvested from all mice.

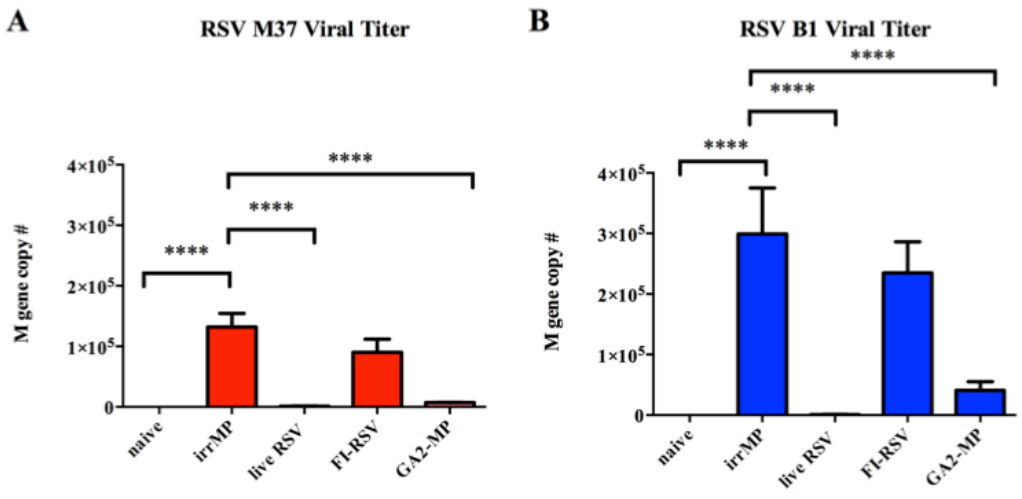

Fig. 3.2: Lung viral titer at 5 days post-challenge of mice post-vaccination/post-RSV challenge with either RSV M37 or RSV B1. Groups of BALB/c mice were vaccinated with either GA2-MP or irrMP (placebo) diluted in PBS to yield 50 µg of designed peptide per dose, 10^6 equivalents of FI-RSV (vaccine enhanced disease), 10^6 PFU of live RSV M37 or RSV B1, or with 100 µL of PBS on days 0 and 28, and challenged i.n. on day 55 with 10^6 PFU of RSV M37 or RSV B1. **(A)** RSV M37 and **(B)** RSV B1 lung viral titers were determined at 5 days post-challenge by RT-qPCR using M gene copy number. Error bars represent the SEM from n=6 mice/group and results were considered significant with a P value ≤ 0.05 (*) as determined by One-way ANOVA and Dunnett's test.

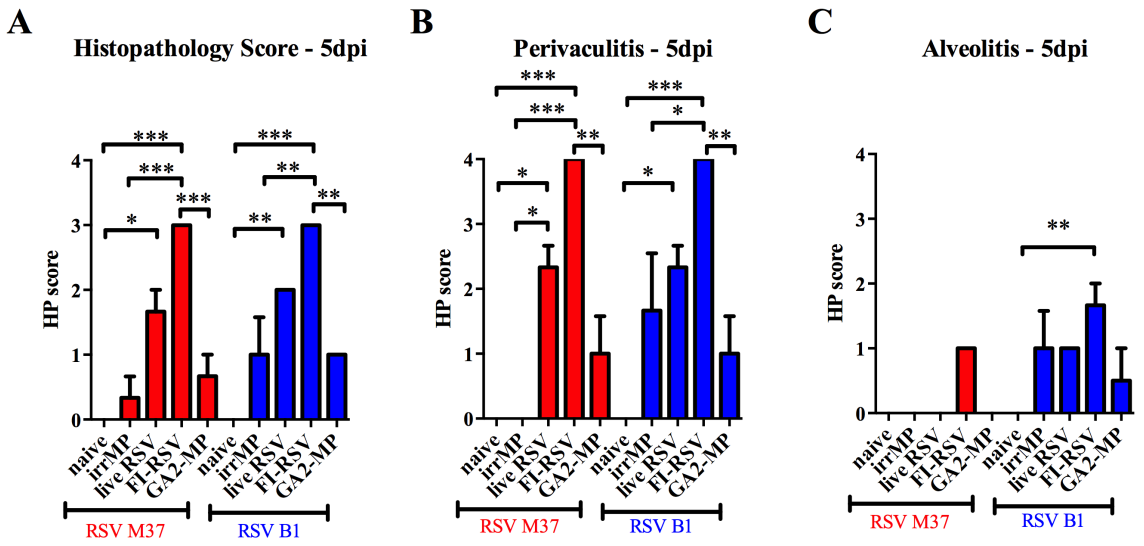

Fig. 3.3: Enhanced airway inflammation in FI-RSV vaccinated mice indicative of vaccine-enhanced disease. Groups of BALB/c mice were vaccinated with either GA2-MP or irrMP (placebo) diluted in PBS to yield 50 µg of designed peptide per dose, 106 equivalents of FI-RSV (vaccine enhanced disease), 106 PFU of live RSV M37 or RSV B1, or with 100 µL of PBS on days 0 and 28, and challenged i.n. on day 55 with 106 PFU of RSV M37 or RSV B1. **(A)** Quantitation of lung inflammation, **(B)** perivaculitis, and **(C)** alveolitis were scored at day 5 post-challenge. Error bars represent the SEM from n=3 mice/group and results were considered significant with a P value ≤ 0.05 (*) as determined by One-way ANOVA and Dunnett's test.

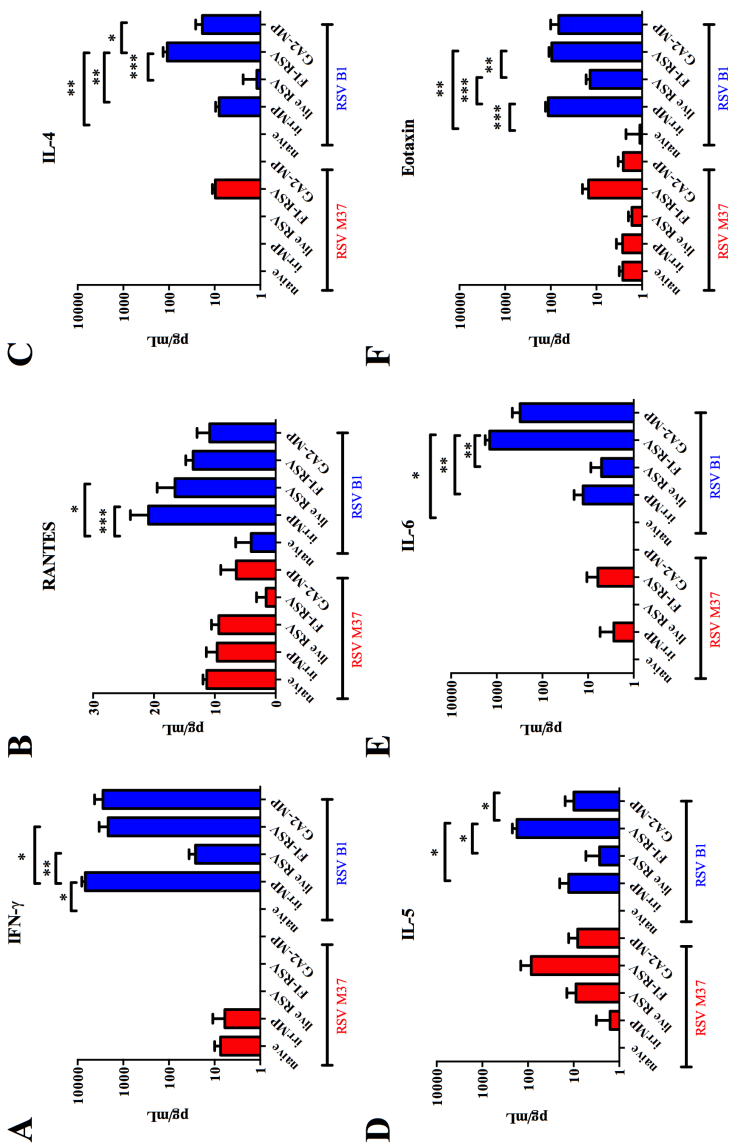
A
IFN-γ
B
RANTES
C
IL-4
D
IL-5
E
IL-6
F
Eotaxin
pg/mL
naïve
IFN-AP
live RSV
FI-RSV
CA2-AP
RSV M37
RSV B1

Fig. 3.4: Elevated eotaxin and RANTES (CCL5) levels and Th2-type cytokine production upon RSV infection as markers of enhanced eosinophil infiltration and airway inflammation. Groups of BALB/c mice were vaccinated with either GA2-MP or irrMP (placebo) diluted in PBS to yield 50 μg of designed peptide per dose, 10^6 equivalents of FI-RSV (vaccine enhanced disease), 10^6 PFU of live RSV M37 or RSV B1, or with 100 μL of PBS on days 0 and 28, and challenged i.n. on day 55 with 10^6 PFU of RSV M37 or RSV B1. The level of **(A)** IFN-γ, **(B)** RANTES, **(C)** IL-4, **(D)** IL-5, **(E)** IL-6, and **(F)** eotaxin were measured in BAL supernatant by Milliplex MAP Mouse Cytokine immunoassay, and the data are presented as picograms of cytokine/ mL of BAL supernatant. Error bars represent the SEM from n=3-5 mice/group and results were considered significant with a P value ≤ 0.05 (*) as determined by One-way ANOVA and Bonferroni's test.

Group	Prime		Challenge	Route
Naïve	PBS	s.c.	PBS	i.n.
Placebo	10µg of irrMP	s.c.	$1x10^6$ PFU of RSV A2	i.n.
Live RSV	$1x10^6$ PFU of RSV A2	i.n.	$1x10^6$ PFU of RSV A2	i.n.
FI-RSV	~$1x10^6$ PFU equivalent of FI-RSV A2	i.m.	$1x10^6$ PFU of RSV A2	i.n.
GA2-MP	10µg of GA2-MP	s.c.	$1x10^6$ PFU of RSV A2	i.n.

Fig. 3.5: Schematic of the experimental design used to determine alterations in miRNA expression profiles in an *in vivo* murine model post-vaccination/post-RSV challenge with RSV A2 challenge. Female, 6-8 week old BALB/c mice were immunized at days 0 with placebo vaccine (10 µg of irrelevant microparticle (irrMP)), $1x10^6$ PFU of live RSV A2, FI-RSV A2 equivalent to $1x10^6$ PFU, or 10µg of GA2-MP vaccine (microparticle carrying the amino acidic region 169-196 of the RSV G protein). At day 28, mice were intranasally challenged with $1x10^6$ PFU of live RSV A2. Naïve mice (mock infected) were not immunized but challenged with phosphate buffer saline (PBS). At 7 days post-challenge bronchoalveolar lavages (BAL) and lung samples were harvested from all mice.

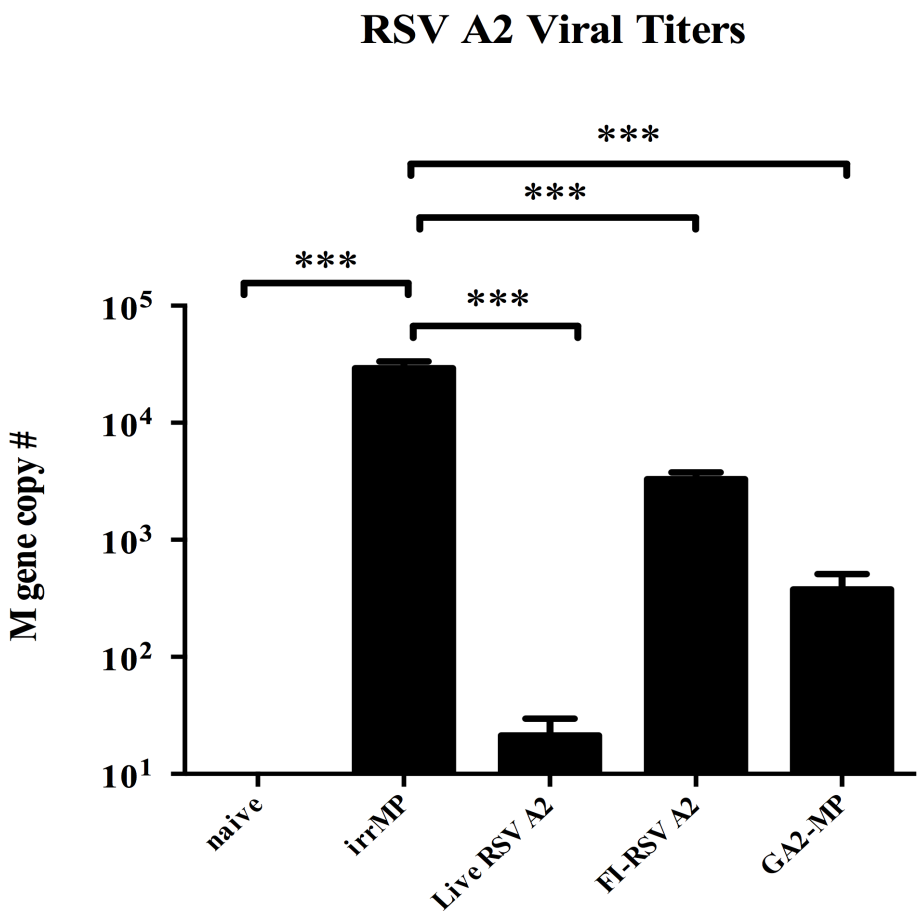

Fig. 3.6: Lung viral titer 7 days post-challenge of mice post-vaccination/post-RSV challenge with RSV A2. Groups of BALB/c mice were vaccinated with either GA2-MP or irrMP (placebo) diluted in PBS to yield 50 μg of designed peptide per dose, 10^6 equivalents of FI-RSV (vaccine enhanced disease), 10^6 PFU of live A2, or with 100 μL of PBS on day 0, and challenged i.n. on day 28 with 10^6 PFU of RSV A2. Lung virus loads were evaluted by RT-qPCR using RSV A2 M gene copy number. Error bars represent the SEM from n=6-8 mice/group and results were considered significant with a P value ≤ 0.05 (*) as determined by One-way ANOVA and Bonferroni's test.

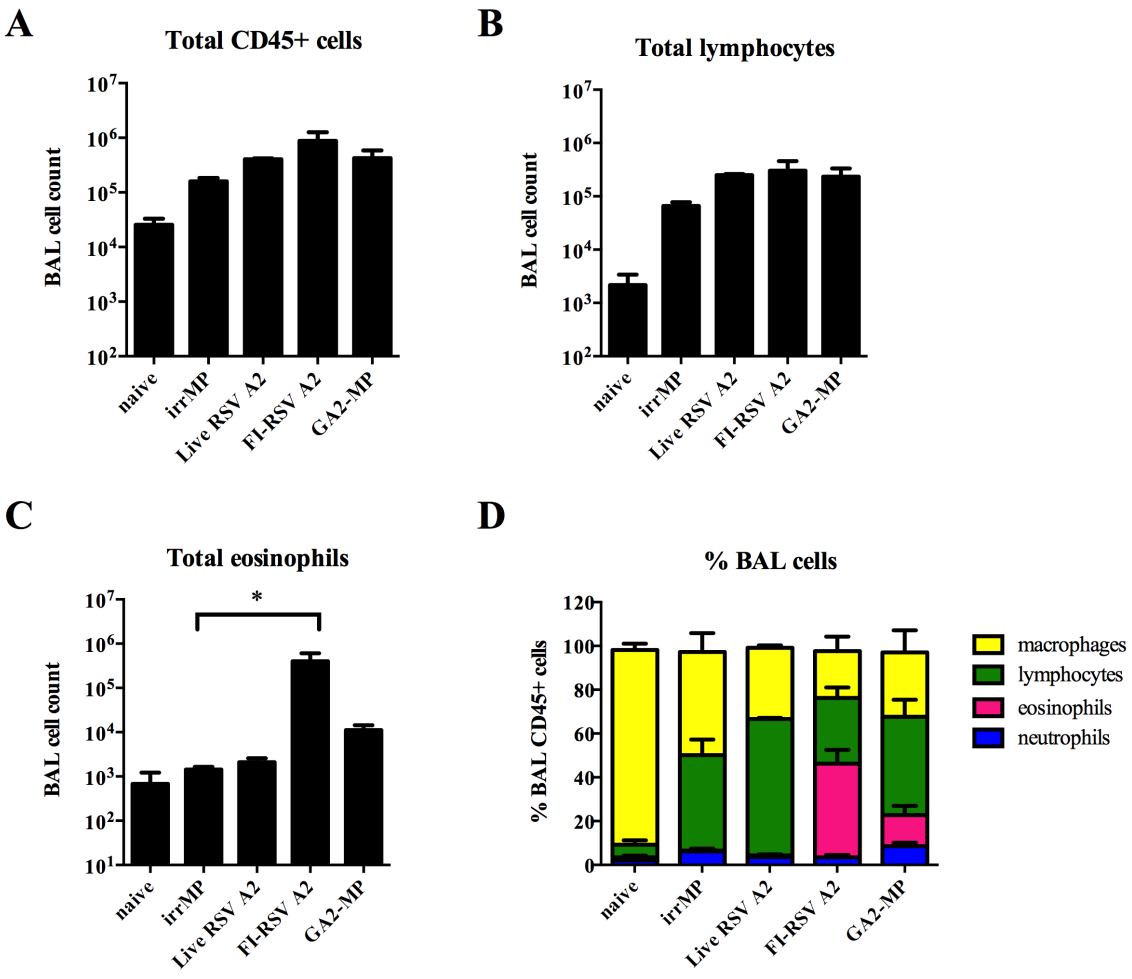
A
Total CD45+ cells
BAL cell count
10^7
10^6
10^5
10^4
10^3
10^2
naive
irrMP
Live RSV A2
FI-RSV A2
GA2-MP
B
Total lymphocytes
BAL cell count
10^7
10^6
10^5
10^4
10^3
10^2
naive
irrMP
Live RSV A2
FI-RSV A2
GA2-MP
C
Total eosinophils
*
BAL cell count
10^7
10^6
10^5
10^4
10^3
10^2
10^1
naive
irrMP
Live RSV A2
FI-RSV A2
GA2-MP
D
% BAL cells
% BAL CD45+ cells
120
100
80
60
40
20
0
naive
irrMP
Live RSV A2
FI-RSV A2
GA2-MP
macrophages
lymphocytes
eosinophils
neutrophils

Fig. 3.7: Pulmonary cell recruitment at 7 days post-challenge with RSV A2. Groups of BALB/c mice were vaccinated with either GA2-MP or irrMP (placebo) diluted in PBS to yield 50 μg of designed peptide per dose, 10^6 equivalents of FI-RSV (vaccine enhanced disease), 10^6 PFU of live A2, or with 100 μL of PBS on day 0, and challenged i.n. on day 28 with 10^6 PFU of RSV A2. Flow cytometry analysis was performed on BAL cells suspensions to evaluated **(A)** Total CD45+ cells, **(B)** Total lymphocytes, **(C)** Total eosinophils, and **(D)** % BAL CD45+ cells by cell type (macrophages, lymphocytes, eosinophils, and neutrophils). Error bars represent the SEM from n=5 mice/group and results were considered significant with a P value ≤ 0.05 (*) as determined by One-way ANOVA and Bonferroni's test.

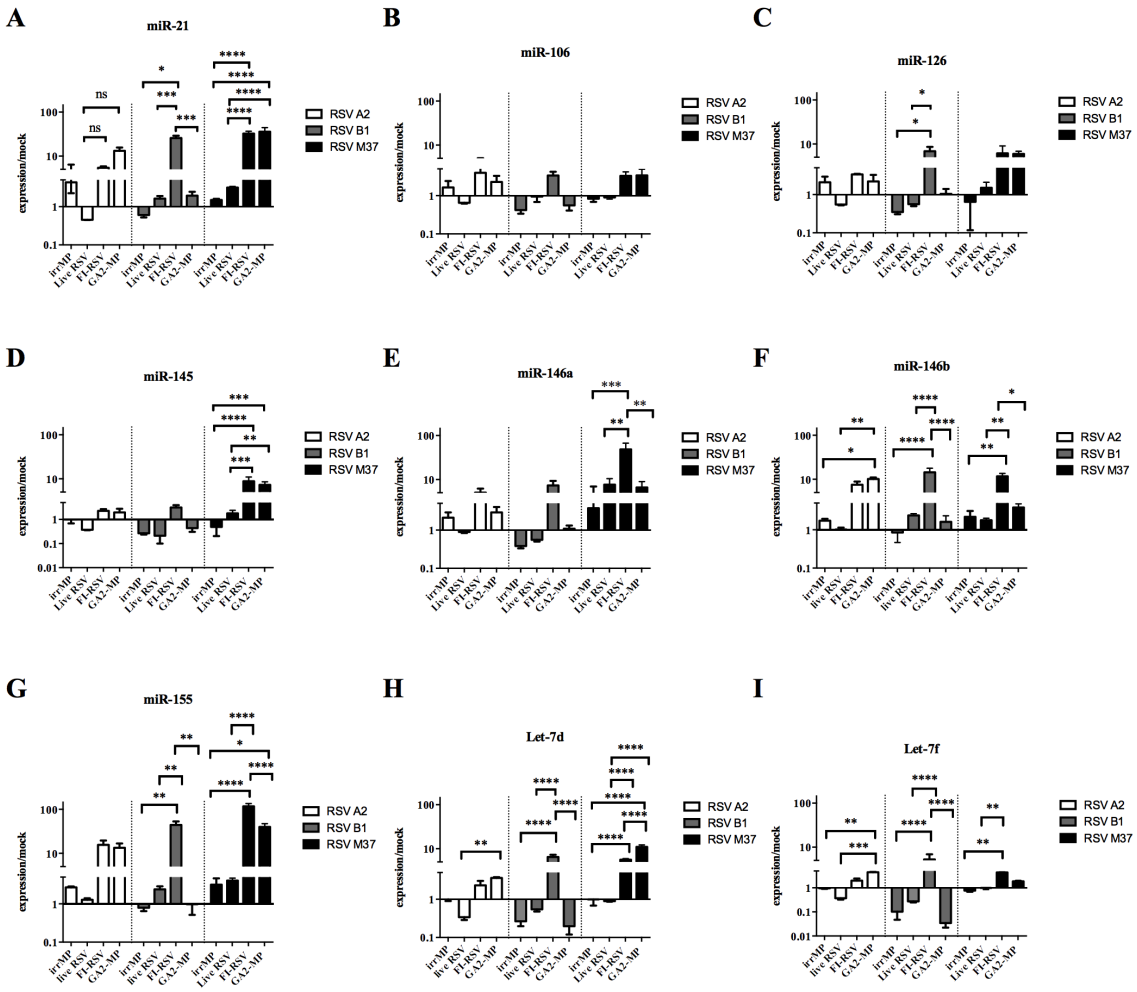
A
miR-21
B
miR-106
C
miR-126
D
miR-145
E
miR-146a
F
miR-146b
G
miR-155
H
Let-7d
I
Let-7f
expression/mock
RSV A2
RSV B1
RSV M37
irrMP
Live RSV
FI-RSV
GA2-MP

Fig. 3.8: Unique miRNA expression patterns between naïve, RSV-infected, and vaccinated mice. Total RNA isolation was performed on lung homogenates from BALB/c mice (n=3 mice/group) and examined for **(A)** miR-21, **(B)** miR-106, **(C)** miR-126, **(D)** miR-145, **(E)** miR-146a, **(F)** miR-146b, **(G)** miR-155, **(H)** Let-7d, **(I)** Let-7f expression levels using RT-qPCR. miRNA expression levels were normalized by 18S rRNA gene expression. Values are represented as expression over mock (naïve/PBS challenge mice). All data is representative of two independent experiments. Error bars represent the SEM and results were considered significant with a P value ≤ 0.05 (*) as determined by One-way ANOVA and Bonferroni's test.

miRNA	Description	Forward Primer Sequence
miR-21	mmu-miR-21a-5p	TAGCTTATCAGACTGATGTTGA
miR-106	mmu-miR-106a-5p	CAAAGTGCTAACAGTGCAGGTAG
miR-126	mmu-miR-126a-3p	TCGTACCGTGAGTAATAATGCG
miR-145	mmu-miR-145a-5p	GTCCAGTTTTCCCAGGAATCCCT
miR-146a	mmu-miR-146a-5p	TGAGAACTGAATTCCATGGGTT
miR-146b	mmu-miR-146b-5p	TGAGAACTGAATTCCATAGGCT
miR-155	mmu-miR-155-5p	TTAATGCTAATTGTGATAGGGGT
Let-7d	mmu-let-7d-5p	AGAGGTAGTAGGTTGCATAGTT
Let-7f	mmu-let-7f-5p	TGAGGTAGTAGATTGTATAGTT

Table 3.1: This table shows the mouse-specific miRNA primer sequences. All of the miRNA primer sequences share 100% sequence homology between mice and humans, with the exception of miR-106. The miR-106 primer sequence contains two point mutations between mice and humans as indicated in red.

miRNA family	Critical roles in asthma and airway hyperresponsiveness
miR-21	↑ During eosinophilia (48, 54), polarization of adaptive immune responses and activation of T cells (27), ↑ in asthma (27), negative regulator of TLR4 signaling (26)
miR-106	Regulates IL-10 expression and Th2-type response (27, 78), ↑ in asthma (27)
miR-126	↑ In Th2-type cells that produce IL-5/IL-13 and allergic inflammatory response (27-29)
miR-145	↑ During eosinophilia, mucus production, and Th2-type response (26, 27, 29, 48, 79)
miR-146	↑ in asthma (80), induces severe inflammation (25), polarization of adaptive immune responses and activation of T cells (27, 81), regulates mast cell survival (81), negative regulator of NF-κB signaling and TNF-α response (26)
miR-155	↑ During allergic inflammation (27), facilitates Th2 cell differentiation (25, 27), ↑ effector and memory CD8+ T cell-mediated antiviral response (25), regulates the generation of immunoglobulin class-switched plasma cells (82), positive regulator of TNF-α response (26)
Let-7	↑ in asthma (25), regulates IL-4, IL-5, and IL-13 expression (27, 30)

Table 3.2: This table lists miRNAs evaluated in this study and their known roles in modulating the host immune response. Seven miRNA families (a total of nine miRNAs) were selected for evaluation based on their critical roles in regulating key pathogenic mechanisms in allergic inflammation, including polarization of adaptive immune responses and activation of T cells, regulation of eosinophil development, and involvement with Th2-type cytokine responses.

miRNA	Vaccine comparison	P value
miR-21	irrMP vs. GA2-MP + TiterMAX	*
	Live RSV vs. GA2-MP + TiterMAX	**
	GA2-MP + Poli(I:C) vs. GA2-MP + TiterMAX	**
	GA2-MP + TBD vs. GA2-MP + TiterMAX	**
miR-145	FI-RSV vs. GA2-MP + Poli(I:C)	*
miR-146b	irrMP vs. FI-RSV	****
	irrMP vs. GA2-MP	****
	irrMP vs. GA2-MP + TiterMAX	***
	live RSV vs. FI-RSV	****
	live RSV vs. GA2-MP	****
	live RSV vs. GA2-MP + TiterMAX	****
	FI-RSV vs. GA2/M2-MP	**
	FI-RSV vs. GA2-MP+alum	**
	FI-RSV vs. GA2-MP + Poli(I:C)	****
	FI-RSV vs. GA2-MP + TBD	***
	GA2-MP vs. GA2/M2-MP	****
	GA2-MP vs. GA2-MP+alum	****
	GA2-MP vs. GA2-MP + Poli(I:C)	****
	GA2-MP vs. GA2-MP + TBD	****
	GA2-MP vs. GA2-MP + TiterMAX	*
	GA2/M2-MP vs. GA2-MP + TiterMAX	**
	GA2-MP+alum vs. GA2-MP + TiterMAX	*
	GA2-MP + Poli(I:C) vs. GA2-MP + TiterMAX	****
	GA2-MP + TBD vs. GA2-MP + TiterMAX	***
miR-155	irrMP vs. FI-RSV	**
	irrMP vs. GA2-MP	*
	live RSV vs. FI-RSV	**
	live RSV vs. GA2-MP	**
	live RSV vs. GA2-MP + TiterMAX	*
	FI-RSV vs. GA2-MP + Poli(I:C)	**
	FI-RSV vs. GA2-MP + TBD	**
	GA2-MP vs. GA2-MP + Poli(I:C)	*
	GA2-MP vs. GA2-MP + TBD	*
	GA2-MP + Poli(I:C) vs. GA2-MP + TiterMAX	*
	GA2-MP + TBD vs. GA2-MP + TiterMAX	*
Let-7d	irrMP vs. GA2-MP	****
	live RSV vs. FI-RSV	**
	live RSV vs. GA2-MP	****
	live RSV vs. GA2-MP+alum	**
	FI-RSV vs. GA2/M2-MP	*
	FI-RSV vs. GA2-MP + Poli(I:C)	**
	GA2-MP vs. GA2/M2-MP	****
	GA2-MP vs. GA2-MP+alum	*
	GA2-MP vs. GA2-MP + Poli(I:C)	****
	GA2-MP vs. GA2-MP + TBD	****
	GA2-MP vs. GA2-MP + TiterMAX	****
	GA2-MP+alum vs. GA2-MP + Poli(I:C)	**
Let-7f	irrMP vs. FI-RSV	*
	irrMP vs. GA2-MP	****
	irrMP vs. GA2-MP+alum	**
	live RSV vs. FI-RSV	****
	live RSV vs. GA2-MP	****
	live RSV vs. GA2-MP+alum	****
	live RSV vs. GA2-MP + TiterMAX	**
	FI-RSV vs. GA2-MP	****
	FI-RSV vs. GA2/M2-MP	*
	FI-RSV vs. GA2-MP + Poli(I:C)	****
	FI-RSV vs. GA2-MP + TBD	*
	GA2-MP vs. GA2/M2-MP	****
	GA2-MP vs. GA2-MP+alum	****
	GA2-MP vs. GA2-MP + Poli(I:C)	****
	GA2-MP vs. GA2-MP + TBD	****
	GA2-MP vs. GA2-MP + TiterMAX	****
	GA2/M2-MP vs. GA2-MP+alum	**
	GA2-MP+alum vs. GA2-MP + Poli(I:C)	****
	GA2-MP+alum vs. GA2-MP + TBD	**
	GA2-MP + Poli(I:C) vs. GA2-MP + TiterMAX	**

Table 3.3: Six miRNAs show significantly altered expression patterns among adjuvants. BALB/c mice were vaccinated with either irrMP (placebo), GA2-MP, GA2/M2-MP (containing RSV-M2 protein epitope) or GA2-MP + adjuvant (alum, Poli(I:C), TBD, TiterMax) diluted in PBS to yield 50 μg of designed peptide per dose, 10^6 equivalents of FI-RSV (vaccine enhanced disease), or 10^6 PFU of live A2 on day 0, and challenged i.n. on day 28 with 10^6 PFU of RSV A2. Total RNA isolation was performed on lung homogenates from BALB/c mice (n=3 mice/group) and miRNA levels were evaluated by RT-qPCR. miR-21, miR-145, miR-146b, miR-155, Let-7d, and Let-7f had significantly altered expression levels among adjuvant and vaccine groups. miRNA expression levels were normalized by 18S rRNA gene expression. Values are represented as expression over mock (naïve/PBS challenge mice). All data is representative of two independent experiments and results were considered significant with a P value ≤ 0.05 (*) as determined by One-way ANOVA and Bonferroni's test.

Supplemental information

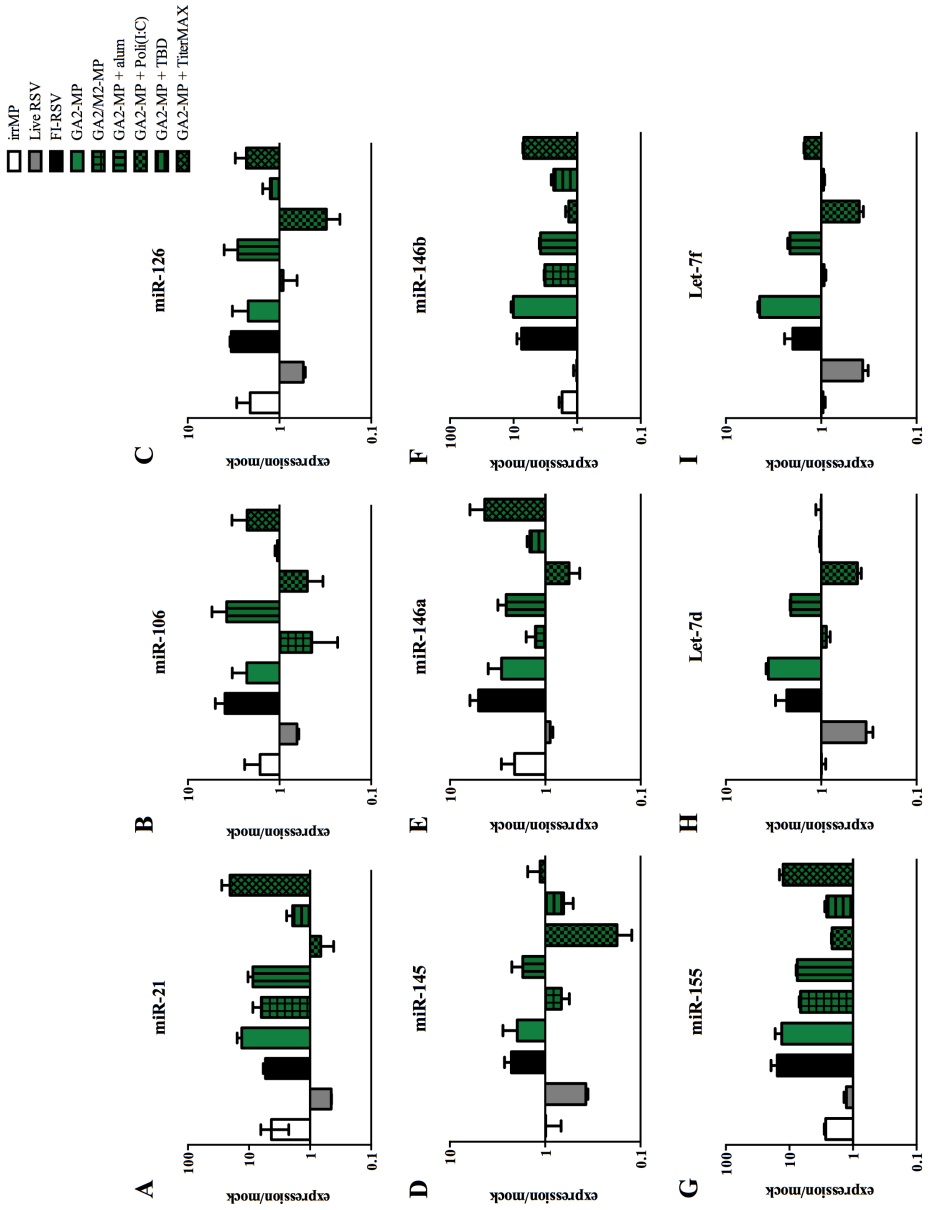

Fig. S3.1: Vaccine adjuvants generate differential miRNA expression patterns. Groups of BALB/c mice were vaccinated with either irrMP (placebo), GA2-MP, GA2/M2-MP (containing RSV-M2 protein epitope) or GA2-MP + adjuvant (alum, Poli(I:C), TBD, TiterMax) diluted in PBS to yield 50 μg of designed peptide per dose, 10^6 equivalents of FI-RSV (vaccine enhanced disease), or 10^6 PFU of live A2 on day 0, and challenged i.n. on day 28 with 10^6 PFU of RSV A2. Total RNA isolation was performed on lung homogenates from BALB/c mice (n=3 mice/group) and examined for **(A)** miR-21, **(B)** miR-106, **(C)** miR-126, **(D)** miR-145, **(E)** miR-146a, **(F)** miR-146b, **(G)** miR-155, **(H)** Let-7d, **(I)** Let-7f expression levels using RT-qPCR. miRNA expression levels were normalized by 18S rRNA gene expression. Values are represented as expression over mock (naïve/PBS challenge mice). All data is representative of two independent experiments and error bars represent the SEM and results were considered not significant with a $P > 0.5$ by One-way ANOVA Bonferroni's test.

CHAPTER 4

MICRORNA BIOMARKERS FOR DETERMINING VACCINE EFFICACY AND PROTECTION FROM RRESPIRATORY SYNCYTIAL VIRUS [1]

[1] Anderson L, Jorquera PA, Williams CM, Tripp RA. To be submitted to *PLOS ONE*.

Abstract

Respiratory syncytial virus (RSV) is the leading cause of severe viral respiratory illness in pediatric populations globally. To date there is no vaccine available for RSV; however, the importance of RSV as a respiratory pathogen makes development of a safe and effective vaccine a high priority. However, due to the spectrum of differences between the four target populations for RSV vaccination, vaccine safety and efficacy concerns as well as vaccine strategies will differ. Therefore, we need to establish precise measures of vaccine protection and disease severity to evaluate a wide range of promising vaccines early in development in order to avoid costly and time-intensive trials. microRNAs (miRNAs) are emerging as promising biomarkers for a variety of diseases. miRNAs are small noncoding RNA molecules that function RNA silencing (RNAi) and post-transcription regulation of gene expression. In this study, we utilized a miRNA PCR array to characterize the serum miRNA expression profiles in BALB/c mice in response to model RSV vaccines and live RSV in order to improve our understanding of how alterations in the host miRNA expression profile may affect the host immune response and disease outcome. In this study, we identified 50 miRNAs post-prime vaccination**,** 75 miRNAs post-boost vaccination, and 50 miRNAs post-challenge with RSV that were differentially expressed among the vaccine candidates from a panel of 84 miRNAs, which corresponded with other known immune correlates and markers of disease severity. To our knowledge, this is the first report to identify miRNA expression profiles as potential biomarkers for RSV vaccine efficacy and disease outcomes, and these findings may provide valuable insights for vaccine development and novel targets

for therapeutic interventions for inflammatory diseases of the lung, which are urgently needed.

Introduction

Respiratory syncytial virus (RSV) is the most common cause of childhood acute lower respiratory infection (ALRI) worldwide and is responsible for over 30 million new ALRI episodes worldwide and up to 199,000 deaths in children under five years old, resulting in more than 3.4 million hospital admission associated with severe RSV disease (1, 2). The elderly are also at risk of severe RSV disease (2). Currently, the only approved RSV prophylactic is passive immunization using palivizumab for high-risk populations, but such treatment has limited applicability due to availability, cost, and treatment logistics (2-4). Unfortunately, efforts to develop a safe and effective RSV vaccine have been largely unsuccessful (5). Attempts in the 1960s to develop a formalin-inactivated RSV (FI-RSV) vaccine candidate were hampered by several factors, including lack of protection against infection in infants and children, and an association with enhanced disease that resulted in two deaths upon subsequent natural RSV infection (2, 5). Concern that any other inactivated RSV vaccine may result in vaccine-enhanced disease upon subsequent natural infection has directed development of live virus vaccines for RSV naïve infants and children. Over the past 35 years, efforts to develop a live-attenuate RSV vaccine candidate using serial cold-passage, chemical mutagenesis, and reverse genetics have been unsuccessful, largely due to the fact that the level of attenuation cannot be predicted precisely often resulting in over- or under- attenuation of the virus (6-12). In addition, natural RSV infection does not provide long-term protective immunity bringing into question the benefit of pursuing live-attenuated RSV vaccine candidates (4). Therefore, additional RSV vaccine platforms have been developed, such as protein subunit (13-16), vectored (17-26), particle-based (27-31), and nucleic acid (32-34)

vaccines. Each of these vaccine strategies has a unique set of advantages and disadvantages in terms of vaccine safety and efficacy, cold-chain logistics, and production costs. Despite these impacts, no vaccine currently exists for RSV, in part due to an incomplete understanding of the host immune response to the virus, which has challenged and delayed RSV vaccine development efforts (2). In addition, the epidemiology of RSV disease implies that there are at least four distinct target populations for RSV vaccines: infants, young children, pregnant women, and the elderly (3). Due to the spectrum of differences between these target populations, vaccine safety and efficacy concerns as well as vaccine strategies will be different (3). Therefore, we need to establish precise measures of vaccine protection and disease severity to evaluate a wide range of promising vaccines early in development in order to avoid costly and time-intensive trials.

A large number of studies have demonstrated a link between severe RSV infection during early childhood and increased likelihood to develop either recurrent wheezing or asthma later in life (35-43). Asthma is a chronic inflammatory disease of the lung that is the leading cause of morbidity and mortality in children worldwide (35). Over the past 20 years, numerous studies have indicated a relationship between early severe RSV infection and an increased risk in developing asthma, yet the exact nature of the relationship is still unclear (35). In addition, an altered balance between Th1- and Th2-type cytokines is responsible for a variety of inflammatory disorders such as asthma, yet the role of post-transcriptional mechanisms such as those mediated by microRNAs (miRNAs) in adjusting the relative magnitude and balance of the cytokine expression have been largely unexplored (44). However, recent studies have identified miRNA

profiles in multiple allergic inflammatory diseases (45-50). Specific miRNAs have been found to have critical roles in regulating key pathogenic mechanisms in asthma and in airway hyperresponsiveness, including polarization of adaptive immune responses, activation of T cells, regulation of eosinophil development, and modulation of cytokine-driven responses (44, 47, 51).

miRNAs are small, endogenous noncoding RNAs, approximately 20-25 nucleotides long that can alter the modulation of gene expression at a post-transcriptional level (49). They govern gene expression by inducing mRNA degradation or translation inhibition, thereby having a critical role in determining the level of protein expression of gene target(s) (49, 52). The multi-target regulation potential of miRNAs themselves presents opportunities to dissect immune signaling networks by decoding the target-recognition information encoded in the miRNA genes (52). In addition, among the various other biomolecule classes, miRNAs are highly stable in a variety of tissues and body fluids, and have high stability within a particular sample type (53). Intensive studies have also shown that their expression patterns vary between normal physiological processes and disease (53-56). These unique advantages have made miRNAs very promising biomarkers for the diagnosis of neurodegenerative disorders (57), autoimmune diseases (58-63), cardiovascular disease (64), and cancers (65, 66). Similarly, these cell-free small RNAs are also involved in the detection of infectious diseases (67-73). Given the emerging role of miRNAs in regulating the immune system and inflammatory responses in the host and their importance in the regulation of the virus-host interface, it is critical to determine if miRNA profiles found in sera can be used as a biomarker for RSV disease pathogenesis and vaccine efficacy.

To date, there are no well-established techniques to quantify the stability or buffering dynamics of immune responses during vaccination and virus infection *in vivo*; however, identification and manipulation of miRNA genes in mice, which generally results in subtle changes to the immune system, presents a unique opportunity to study how miRNA regulation affects the immune signals and memory response induced by vaccination and RSV infection (52). Therefore, the rationale for this study is that characterization of the serum miRNA expression profiles in BALB/c mice in response to vaccination and RSV infection allows for an improved understanding of how alterations in the host miRNA expression profile may affect the host immune response and disease outcome. We hypothesized that vaccination and RSV infection alters the pattern and tempo of host miRNA expression thereby modulating the host immune response and disease outcome, allowing for the identification of miRNA biomarkers for determining vaccine efficacy and protection from RSV. In the present study, we successfully screen miRNAs involved in the activation and differentiation of T cells and B cells in the sera from BALB/c mice at various time points post vaccination/pre-challenge and post vaccination/post-challenge with RSV using a variety of RSV vaccine candidates that demonstrate protection and enhanced disease. The miRNA PCR array was also evaluated for their potential as a biomarker for RSV vaccine development by evaluating miRNA profiles in the context of other known immune correlates for each vaccine candidate. In this study, we identified 50 unique miRNAs post-prime vaccination**,** 75 unique miRNAs post-boost vaccination, and 50 unique miRNAs post-challenge with RSV that were differentially expressed among the model vaccines from a panel of 84 miRNAs. The miRNA profiles identified in the various vaccine candidates correlated with immune

parameters and clinical markers of disease severity. Identification of miRNAs that indirectly or directly modulate the immune response to vaccination and RSV disease can provide valuable novel targets for new approaches to prevent and treat inflammatory diseases of the lung, which are urgently needed.

Materials and Methods

Animals

Specific-pathogen-free, 6-to-8 weeks old female BALB/c mice (The Jackson Laboratory) were used in all experiments. Mice were housed in microisolator cages and were fed sterilized water and food ad libitum. All experiments were performed in accordance with the guidelines of the University of Georgia Institutional Animal Care and Use Committee (IACUC), with protocols approved by the University of Georgia IACUC.

Viruses

RSV A2 is a wild-type strain and RSV CP52 (gifted by Stephen Whitehead and Brian Murphy at LID, National Institute of Allergy and Infectious Diseases, Bethesda, MD) is a cold passage live attenuated virus that lacks the G and SH genes, derived from the RSV B1 strain. RSV CP52 was propogated in vero cells held at 32 °C as described (74). RSV A2 was propagated in Vero E6 cells (ATCC CRL-1586) incubated at 37 °C as described (75). The titer was determined for both viruses by plaque assay on Vero E6 cells, and plaques were enumerated by immunostaining (27, 75).

Peptide synthesis

Peptide spanning the G protein CX3C motif of the RSV A2 strain was designed for vaccination. C-terminal amide peptides were synthesized on a CEM, Liberty^{TM} microwave assisted synthesizer using the manufacturer's standard synthesis protocols. Crude reduced peptides were partially purified by C_{18} reversed phase HPLC, correct molecular weight was confirmed by electrospray mass spectrometry (ESMS), and then lyophilized. Oxidative refolding was accomplished by dissolving the peptides at 2-5 mg/mL in redox buffer (2.5 mM reduced glutathione, 2.5 mM oxidized glutathione, 100 mM Tris pH 7.0) for 3h at room temperature then at 4°C overnight. Folding was judged complete by a shift to slightly shorter retention time on analytical HPLC. Following a final HPLC purification step refolding was confirmed by a loss of 4.0 (±0.4) amu in the ESMS spectra relative to that of the reduced peptide, as well as an absence of free thiol as detected by DTNB (Ellman's assay). Correct disulfide bonding is partially confirmed by ESMS of fragments generated from a thermolysin digest of the synthetic peptide. Peptides were aliquoted, lyophilized, and stored at -20°C until use.

Microparticle fabrication and quality control

Microparticles were constructed as previously described (29) on 3μm diameter $CaCO_3$ cores by alternately layering poly-I-glutamic acid (PGA, negative charge) and poly-I-lysine (PLL, positive charge) to build up a seven-layer film where the designed peptide (DP) containing the RSV G protein CX3C motif linked to a cationic sequence was added as the outermost layer. The composition of the film was determined by amino acid analysis (AAA), which showed that a comparable amount of the peptide component

was present in each batch. Endotoxin levels were measured using limulus amebocyte lysate (LAL) assay and were found to be less than 0.1 EU/ug of G peptide. The dispersity of the particle vaccines were monitored by dynamic light scattering (DLS). Stepwise LbL steadily increases the diameter of the particles several fold, from an apparent diameter of about 150nm for uncoated particles to about 400-500 nm for fully coated particles. Some particle aggregation was detected in each batch with a second population of particles in the 1500-2000 nm range.

FI-RSV A2 preparation

This protocol was adapted from the FI-RSV Lot 100 methods described by Prince *et al*. (76). Briefly, Vero E6 cells infected with RSV A2 at a MOI=0.1 in SF-DMEM (Hyclone). When the cells showed extensive cytopathic effect (~ day 4pi), medium was removed; cells were scraped, collected into a 50mL tube and sonicated. Cell debris was removed by centrifugation at 600 x g for 15 min at 4°C. The supernatant was transferred to a clean tube and filter sterilized using a 2μm filter. Protein concentration was determined by BCA assay, and the final concentration was adjusted to 1-2 mg/mL. The virus was inactivated by the addition of 37% formalin (final dilution 1:4,000) incubated at 37°C per 3 days in agitation. The virus was pelleted by ultracentrifugation for 2 h at 25,000 rpm (Beckman; SW28 rotor) then re-suspended in SF-DMEM (Hyclone) at 1/25th of the original volume, and then adsorbed overnight at room temperature in 4 mg/mL aluminum hydroxide. The compound material was pelleted by centrifugation and the pellet was re-suspended in SF-DMEM and total virus inactivation was confirmed via plaque assay. This procedure resulted in an FI-RSV vaccine that is concentrated 100-fold

and contains 16 mg/ml alum. The vaccine was aliquoted in 1ml volumes and stored at 4°C.

Vaccination

LbL microparticles will be suspended in phosphate buffered saline (PBS; Hyclone, Thermo Scientific) and dispersed by water bath sonication immediately prior to immunization. Doses were adjusted to deliver either 50 μg DP/100 μL/mouse. Mice were immunized with GA2-MP without adjuvant subcutaneously (s.c.) between the shoulder blades. FI-RSV A2 vaccinated mice (positive control for enhanced disease) received a 1:25 dilution of FI-RSV A2 in PBS by intramuscular (i.m.) injection in a final volume of 50 μL/mouse. RSV CP52 vaccinated mice (positive control for protection) received 10^6 PFU of RSV CP52 diluted in PBS **(**GE Healthcare HyClone) by intranasal (i.n.) instillation in a final volume of 50 μL/mouse. PBS vaccinated mice (vehicle control) received 50 μL of PBS (vehicle control) by s.c. injection. Naïve mice did not receive any vaccinations.

Virus challenge

Mice were anesthetized by i.p. administration of Avertin (150-250 mg/kg; Sigma-Aldrich) and challenged i.n. with 10^6 PFU of RSV A2 diluted in PBS **(**GE Healthcare HyClone). Naïve mice were not challenged with RSV A2.

Lung viral titers

RSV lung virus titers in treatment and control mice were determined by plaque assay as previously described (75). Briefly, lungs were aseptically removed from mice at day 5 post-RSV A2 challenge (10^6 PFU /mouse), and individual lung specimens were homogenized at 4°C in 1 mL of SF-DMEM (Hyclone) by use of gentleMACS^{TM} Dissociator (Miltenyi Biotec). Samples were centrifuged for 10 min at 200 x g, the supernatants were transferred to a new tube and used immediately or stored at -80°C until they were assayed. For the plaque assay, 10-fold serial dilutions of the lung homogenates were added to 90% confluent Vero E6 cell monolayers. Following adsorption for 2h at 37°C, cell monolayers were overlaid with 1% methylcellulose medium and incubated at 37°C for 7 days. The plaques were enumerated by immunostaining with monoclonal antibodies against RSV F protein (clone 131-2A) as previously described (27).

Indirect ELISA

At days 14 post boost and 5 post challenge, RSV A2-specific and RSV B1-specific IgG antibodies were detected by ELISA using 96-well high binding plates (Corning, NY) coated with 10^6 PFU/mL RSV A2 or RSV B1 in 0.05 M carbonate-bicarbonate buffer, pH 9.6. Sera were added to plates in serial dilutions. RSV-specific antibodies were detected with horseradish peroxidase (HRP) conjugated antibodies specific for mouse IgG (Southern Biotech) followed by addition of SureBlue TMB 1-Component Microwell Peroxidase Substrate (KPL, Inc.) for 15 min. Antibody titers were determined as the last sample dilution that generated an OD_{450} reading of greater than 0.2 (mean OD value of background plus 2 standard deviation of the mean).

Microneutralization assay

Six two-fold serial dilutons (1:50-1:1600) of serum were made with SF-DMEM (Hyclone). The diluted serum was incubated with $1x10^5$ PFU/well of RSV A2 for one hour at 37 °C, 5% CO_2 (77). Synagis (palivizumab) was used as a positive control for neutralizing activity. Positive control wells of virus without sera and negative control wells without virus or sera were included in triplicate on each plate. The serum and virus mixture was transferred to ~80-90% confluent monolayers of Vero cells in 96-well plates and incubated for 2 h at 37 °C, 5% CO_2. The virus overlay was then aspirated, and 150 μl/well of DMEM-10% FBS was added and plates were recovered for 3-4 days at 37 °C, 5% CO_2. Then plates were fixed with 80% acetone in PBS (GE Healthcare HyClone) for 10 minutes at 4 °C, fixative was then aspirated, and plates were rinsed twice with PBS (GE Healthcare HyClone). The plates were then rinsed three times with 150 μl/well of wash buffer (PBS + 0.1% Tween-20). A monoclonal antibody to the RSV F protein (clone 131-2A) was diluted in PBS with 0.5% gelatin + 0.15% Tween 20 and incubated for 1 h at 37 °C, 5% CO_2. Wells were rinsed with wash buffer and HRP conjugated goat anti-mouse IgG (Southern Biotech) was added, followed by another 1 h incubation. After washing, TMB substrate (Thermo Fisher Scientific) was added and absorbance was measured at 450/650 nm dual wavelength using the Epoch™ microplate spectrophotometer controlled with the Gen5 Data Analysis software interface (BioTek. The percentage of neutralization was calculated, and all samples were normalized to the average value from the no serum control wells to account for background absorbance.

ELISPOT analysis

24hr prior to the assay, 96-well Multiscreen plates (Millipore) were coated with the anti-mouse IL-4 or anti-mouse IFN-γ capture antibody (R&D Systems) and incubated overnight at 4°C. The plates were then blocked by the addition of 200 μL of RPMI-10 medium (RPMI 1640 supplemented with 10% FBS, 100 U/mL penicillin, 100 μg/mL streptomycin, 50 μM 2-mercaptoethanol and 2 mM L-glutamine) and incubated for 2 h at 37°C. In parallel, spleens were harvested from treatment and naïve mice at 5 days and 7 days post challenge with RSV A2 and prepared to a single cell suspension using a syringe plunger and a 70 μm mesh nylon strainer. The cell suspensions were collected by centrifugation for 10 min at 200 x g and suspended in RPMI-10 at a concentration of 10^7 cells/mL. Spleen cell suspensions were added to each well, and cells were stimulated with either 10 μg/mL RSV M2 (82-90) peptide, 10 μg/mL RSV F (51-66) peptide, 10 μg/mL RSV G (183-198) peptide or 10 μg/mL GFP (irrelevant peptide control) for 24h at 37°C and 5% CO_2. Plates were washed 4 times with wash buffer (0.05% Tween-20 in PBS), anti-mouse IL-4 or anti-mouse IFN-γ detection antibody (R&D Systems) was added and plates were incubated overnight at 4°C. Detection antibody was removed, plates were washed and cytokine spots were developed using NBT/BCIP substrate (Thermo Fisher Scientific). Spots were counted using an ELISPOT reader (CTL-ImmunoSpot®).

BAL and serum collection and quantification of cytokines

3 days and 5 days post-challenge, a subset of mice from each group was sacrificed and tracheotomy was performed and sera were collected. The mouse lungs were flushed three times with 1 ml of PBS and the retained BAL was centrifuged at 400 x g for 5 min

at 4°C. The recovered supernatants were collected and stored at -80°C until assessed for cytokine concentration, and the cell pellet were resuspended in 200 μL of FACS staining buffer (PBS containing 1% BSA). Total cell numbers were counted using a hemocytometer. The Luminex® xMAPTM system using a MILLIPLEX MAP mouse cytokine immunoassay (MCYTOMAG-70K, Millipore) was used to quantitate cytokines in BAL supernatants and sera according to the manufacturer protocol. Briefly, beads coupled with anti-IFN-γ, anti-IL-1α, anti-IL-2, anti-IL-4, anti-IL-5, anti-IL-6, anti-IL-9, anti-IL-10, anti-IL-12p40, anti-IL-13, anti-IL-15, anti-IL17A, anti-MCP-1, anti-RANTES, anti-TNF-α, and anti-Eotaxin monoclonal antibodies were sonicated, mixed, and diluted 1:50 in assay buffer. For the assay, 25 μL of beads were mixed with 25 μL of PBS (for BAL samples) or serum matrix (for serum samples), 25 μL of assay buffer and 25 μL of BAL supernatant or serum and incubated overnight at 4°C. After washing, beads were incubated with biotinylated detection antibodies for 1 h and the reaction mixture was then incubated with streptavidin- phycoerythrin (PE) conjugate for 30 min at room temperature, washed, and resuspended in PBS. The assay was analyzed on a Luminex 200 instrument (Luminex Corporation, Austin, TX) using Luminex xPONENT 3.1 software.

RNA isolation

Whole blood was collected from mice in 1.5 ml microcentrifuge tubes (Fisher Scientific) and allowed to clot at room temperature for 30 to 60 minutes. The tubes were then centrifuged for 10 minutes at 3000 rpm and 4 °C. The upper serum phase was transferred to a new 1.5 ml microcentrifuge tube. The serum samples were then

centrifuged for 10 minutes at 16,000 x g and 4 °C and the cleared supernatant was carefully transferred to a new microcentrifuge tube without disturbing the pellet. Samples were then processed for RNA isolation, or stored at -80 °C until further processing. Total RNA was isolated from sera samples collected from mice using the miRNeasy Serum/Plasma Kit (Qiagen) following manufacture protocol for isolation of total RNA. A total volume of 100 μl of serum was used per mouse for total RNA isolation, and RNA was eluted in 20 μl of RNase-free water. The miRNeasy Serum/Plasma Spike-In Control (Qiagen) was spiked in to each sample prior to RNA purification as an internal control for miRNA expression profiling in serum to allow for monitoring of RNA recovery and reverse transcription efficiency. RNA concentration was determined using Epoch™ microplate spectrophotometer controlled with the Gen5 Data Analysis software interface (BioTek).

miRNA PCR arrays and data analysis

cDNA synthesis was performed on 200 ng per sera RNA sample using the miScript II RT kit with miScript HiSpec Buffer (Qiagen) following manufacture protocol. Reactions were incubated for 60 min at 37 °C followed by 5 min at 95 °C. The undiluted cDNA was then stored at -20 °C. Prior to real-time PCR, cDNA was diluted 1:10 (200 μl of RNase-free water was added to each 20 μl reaction). Real-time PCR for mature miRNA expression profiling was performed using the miScript miRNA PCR Array Mouse T-Cell & B-Cell Activation (Qiagen) following manufacture protocol. Briefly, each PCR array contains a miScript Primer Assay for 84 T-Cell and B-Cell related mature miRNAs. For controls, the PCR arrays contain duplicate wells of the *C. elegans*

miR-39 miScript Primer Assays that can be used as an alternative normalizer for array data (Ce), six snoRNA/snRNA controls SNORD61, SNORD95, SNORD96A, SNORD68, SNORD72, RNU6B (RNU6-2) (SN1/2/3/4/5/6), duplicate wells of reverse transcription controls (miRTC), and duplicate wells of positive PCR controls (PPC). The miScript Primer Assay for *C. elegans* miR-39 (Qiagen) is included on each PCR Array to detect the miRNeasy Serum/Plasma Spike-In Control (Qiagen). The miScript Primer Assays for miR-16, miR-21, and miR-191 are included in the miScript miAll PCR arrays were run on Stratagene models Mx3005P and Mx3000P and the specificity of the SYBR Green PCR signal was confirmed by melting curve analysis. The results were analyzed using miScript miRNA PCR Array data analysis tool (Qiagen) using the $\Delta\Delta C_T$ method of relative quantification and interpretation of the control assays. Briefly, ΔCT value for each mature miRNA profiled in the plate is calculated using the formula $\Delta C_T = C_T$miRNA – AVG C_T $^{SN1/2/3/4/5/6}$. $\Delta\Delta C_T$ for each miRNA across 2 miScript miRNA PCR Arrays or 2 samples is calculated using the formula: $\Delta\Delta C_T = \Delta C_T$ (sample 2) – ΔC_T (sample 1) where sample 1 is the control sample (vehicle or naïve mice) and sample 2 is the experimental sample. Fold-change for each gene from sample 1 to sample 2 is calculated as $2^{(-\Delta\Delta CT).}$ If the fold-change was > 2, the result was reported as a fold upregulation. If the fold-change was < 0.5, the result was reported as a fold downregulation.

RT-qPCR for miRNA validation

The relative expression levels of candidate miRNAs selected from the PCR array analysis were validated by RT-qPCR. Briefly, cDNA was prepared using the miScript II

RT kit with miScript HiSpec Buffer (Qiagen) and diluted 1:10 (200 μl of RNase-free water was added to each 20 μl reaction) and real-time PCR was performed using the miScript SYBR Green PCR Kit (Qiagen) following manufacture protocol. Mouse-specific miRNA sequences were obtained from miRBase for the miRNAs of interest. Forward primers were designed based on the mature-miRNA sequence with the greatest number of deep-sequencing reads, and synthesized by Integrated DNA Technologies (IDT). All qPCR reactions were run on Stratagene models Mx3005P and Mx3000P and the specificity of the SYBR Green PCR signal was confirmed by melting curve analysis. miRNA levels were normalized by RU6B (RNU6-2) (Qiagen) gene expression and all samples were run in duplicate. The 2^-ΔΔCt method was utilized to calculate expression fold change over mock (naïve or vehicle mice).

Statistical analysis

All statistical analyses were performed using GraphPad software (San Diego, CA). Statistical significance was determined using a student's t-test, One-way ANOVA or Two-way ANOVA followed by Bonferroni's post-hoc comparisons tests, a p value ≤ 0.05 was considered significant.

Results

The model vaccines induce predicted protection against RSV replication and RSV-specific antibody responses

To demonstrate that the model vaccines induce protective immunity, vaccinated mice were challenged with RSV A2 (10^6 PFU/mouse) at 6 weeks post-boost immunization, and the lung virus loads and antibody responses were determined (Fig.S4.1). At 5 days post-challenge, mice vaccinated with RSV CP52 and GA2-MP showed a significant ($p \leq 0.05$) decrease in lung virus loads compared to PBS vaccinated mice, while FI-RSV vaccinated mice showed no significant difference in lung virus clearance (Fig.4.1A). Sera antibody titers were determined at 14 days after the second immunization (boost) by ELISA using plates coated with either RSV A2 or RSV B1 virus. Immunization with RSV CP52 and FI-RSV elicited higher titers of anti-RSV A2 IgG and higher titers of cross-reactive anti-RSV B1 IgG compared to PBS vaccinated mice, however the difference was not statistically significant (Fig.4.1B and 4.1C). Immunization with GA2-MP elicited low levels of anti-RSV A2 IgG, but no difference was observed in the levels of cross-reactive anti-RSV B1 IgG compared to PBS vaccinated mice at 14 days post-boost (Fig.4.1B and 4.1C). Sera antibody levels were re-evaluated at 5 days post-challenge with RSV A2. Immunization with RSV CP52 elicited significantly ($p \leq 0.0001$) higher titers of anti-RSV A2 IgG and the anti-RSV B1 IgG levels were significantly ($p \leq 0.001$) higher compared to PBS vaccinated mice (Fig.4.1D and 4.1E). Immunization with FI-RSV and GA2-MP also elicited higher anti-RSV A2 IgG titers compared to PBS vaccinated mice, however this difference was not statistically significant (Fig.4.1D and 4.1E). Immunization with FI-RSV elicited higher titers of cross-reactive anti-RSV B1 IgG compared to PBS vaccinated mice, but immunization with GA2-MP did not increase anti-RSV B1 IgG levels (Fig.4.1E). The inability of the GA2-MP vaccine to elicit cross-reactive antibodies against RSV B1 is likely due to the

fact that the microparticle-based vaccine carries the CX3C motif of the RSV A2 G protein (78). Taken together, these results demonstrate that immunization with both RSV CP52 (positive control for protection) and GA2-MP (microparticle-based vaccine candidate) induced protective immunity and RSV-specific antibodies, whereas immunization with FI-RSV (positive control for enhanced disease) did not protect from RSV infection despite eliciting an equivalent antibody response. These findings are consistent with previous studies showing that RSV CP52 is able to induce RSV serum-neutralizing antibody responses in cotton rats, African green monkeys, and chimpanzees (79, 80).

Vaccination with RSV CP52 induces neutralizing antibodies

Neutralizing antibodies are a critical component of an efficacious vaccine. To evaluate whether immunization with the model vaccines induced neutralizing antibodies, an *in vitro* microneutralization assay was performed using sera from mice vaccinated and subsequently challenged with RSV A2 (10^6 PFU/mouse), and Synagis® (palivizumab) was used as a positive control for neutralization. At day 3 and day 5 post-challenge, RSV CP52 vaccinated mice showed a significant ($p \leq 0.0001$) increase in neutralizing antibody titer compared to PBS vaccinated mice, while neither FI-RSV nor GA2-MP vaccinated mice showed substantial increases in neutralization titer compared to PBS vaccinated mice (Fig.4.2A and 4.2B).

The model vaccines induce a predicted Th1 and Th2 memory response

To evaluate the memory T cell response induced by the model vaccines, the Th1- (IFN-γ) and Th2-type (IL-4) cell frequencies were measured by ELISPOT assay at 14 days post-boost vaccination. Mice immunized with PBS, FI-RSV, or GA2-MP had significantly lower frequencies of M2- ($p \leq 0.0001$) and F-specific ($p \leq 0.001$) IFN-γ secreting cells than RSV CP52 vaccinated mice (Fig.4.3A). Th1-type cytokines (IFN-γ, IL-1α, TNF-α, IL-2) and chemokines (MCP-1 and RANTES) were also evaluated in sera and BAL supernatant among the model vaccines by luminex assay. RSV CP52 vaccinated mice induced moderate IFN-γ expression levels compared to all groups, however this difference was not statistically significant (Fig.4.4A). IL-1α expression levels were higher in the sera compared to the BAL, however there was no significant difference in expression levels between vaccination groups (Fig.4.4B). TNF-α and IL-2 expression levels were low in both sera and BAL, and there were no substantial differences among the vaccination groups (Fig.4.4C and 4.4D). MCP-1 expression levels were higher in the BAL of FI-RSV vaccinated mice, however this difference was not statistically significant compared to all groups (Fig.4.4E). RANTES expression levels were significantly ($p \leq 0.5$) lower in the sera of GA2-MP vaccinated mice compared to PBS vaccinated mice, but there was no difference among the other vaccinated groups (Fig.4.4F). In contrast, FI-RSV vaccinated mice had significantly ($p \leq 0.05$) higher frequencies of M2-, F-, G-, and GFP-specific IL-4 secreting cells compared to mice immunized with PBS, CP52, and GA2-MP (Fig.4.3B). In addition, GA2-MP vaccinated mice had significantly ($p \leq 0.0001$) higher G-specific IL-4 secreting cells compared to mice vaccinated with PBS and RSV CP52 (Fig.4.3B). Analysis of Th2-type cytokines (IL-4, IL-5, IL-6, IL-10, IL-13) in sera and BAL supernatant showed that FI-RSV

vaccinated mice had higher expression levels overall compared to all groups, however this difference was not statistically significant (Fig.4.5A-E). Eotaxin expression levels were substantially higher in the sera compared to the BAL, however there was no significant difference in expression levels among the vaccination groups (Fig.4.5F). Taken together, these results indicate that RSV CP52 vaccination induces a strong Th1-type T cell response where as FI-RSV vaccination induces a strong Th2-type T cell response, and GA2-MP vaccination induces a balanced Th1/Th2 T cell response.

The model vaccines induced unique temporal patterns of differential miRNA expression

To understand the potential for host miRNAs as biomarkers of vaccine efficacy and RSV disease severity, we evaluate the miRNA expression profiles in mouse sera post-vaccination/pre-RSV challenge and post-vaccination/post-RSV challenge. Using a miRNA PCR array, 84 miRNAs were evaluated to identify unique miRNA profiles for the model vaccines in the context of other known immune correlates and markers of disease severity. PCR array analysis showed that the model vaccines induced unique temporal-specific miRNA expression patterns. Among the 84 miRNAs on the miRNA PCR array, 65 (~77%) were detected in the sera of GA2-MP vaccinated mice, 70 (~83%) were detected in the sera of FI-RSV vaccinated mice, and 58 (69%) were detected in the sera of RSV CP52 vaccinated mice (Fig.4.6). Characteristically, more differentially expressed miRNAs were aroused post-boost vaccination compared to post-prime and post-challenge among all vaccine candidates (Fig.4.6). We identified miRNAs that were differentially expressed in each model vaccine for the duration of vaccination (post-

prime, post-boost, and post-challenge) and RSV challenge; more specifically, 11 miRNAs were found for GA2-MP vaccinated mice, 18 miRNAs were found for FI-RSV vaccinated mice, and 8 miRNAs were obtained from RSV CP52 vaccinated mice (Table 4.1-4.3). Therefore, the miRNA expression patterns induced by the GA2-MP, FI-RSV, and RSV CP52 vaccines were temporal-specific. The ability to detect a group of common and unique miRNAs for the RSV vaccine platforms at various time points during vaccination and subsequent RSV-challenge demonstrates their potential as biomarkers of vaccine efficacy, and their importance in forwarding RSV vaccine development.

Differentially expressed miRNAs in response to the model vaccines

In order to understand the potential for these miRNAs to distinguish between protective and enhanced disease outcomes, we evaluated the differentially expressed miRNAs in a vaccine-specific manner across a range of time points during vaccination and after RSV-challenge. At 7 days post-prime a total of 42 miRNAs were differentially expressed among the model vaccines, of which 34 miRNAs showed upregulated expression levels and 8 miRNAs showed downregulated expression levels compared to PBS control (Fig.4.7A). The GA2-MP vaccinated mice had a total of 9 miRNAs, FI-RSV vaccinated mice had 38 miRNAs, and RSV CP52 had 15 miRNAs that showed a group of unique and common miRNAs at 7 days post-prime (Fig.4.7A). At 14 days post-prime, 23 miRNAs showed altered expression levels among the vaccine groups, and of those 14 miRNAs were upregulated and 9 miRNAs were downregulated (Fig.4.7B and Fig.4.8). In terms of altered miRNA expression patterns by vaccine groups at 14 days post-prime, FI-RSV vaccinated mice induced 7 miRNAs, GA2-MP vaccinated mice induced 13

miRNAs, and RSV CP52 vaccinated mice induced 8 miRNAs (Fig.4.7B). The greatest numbers of differentially expressed miRNAs among the vaccinated mice were induced at 7 days post-boost vaccination, with 73 miRNAs (~87%) from the miRNA PCR array showing altered expression levels (Fig.4.7C). Of those 73 miRNAs, the number of upregulated miRNAs dramatically increased to 72 (~99%) of the total differentially expressed miRNAs; however 1 miRNA (miR-182-5p) showed downregulation in GA2-MP vaccinated and RSV CP52 vaccinated mice but FI-RSV vaccinated mice induced upregulated expression levels (Fig.4.8). Of the altered miRNA expression levels induced by the model vaccines, FI-RSV vaccinated mice induced 66 miRNAs, GA2-MP vaccinated mice induced 56 miRNAs, and RSV CP52 vaccinated mice induced 35 miRNAs (Fig.4.7C). By 14 days post-boost the amount of miRNAs that showed altered expression levels had decreased substantially to a total of 29 miRNAs (~35%) from the miRNA PCR array; among them, 22 (~76%) were upregulated and 6 (~21%) were downregulated, and 1 (miR-184-3p) was upregulated in FI-RSV vaccinated mice but downregulated in GA2-MP vaccinated mice (Fig.4.7D and Fig.4.8). Of the 29 miRNAs differentially expressed at 14 days post-boost, 3 were induced in FI-RSV vaccinated mice, 7 were induced in the GA2-MP vaccinated mice, and 21 were induced by RSV CP52 vaccinated mice (Fig.4.7D). A total of 50 miRNAs were differentially expressed post-challenge, 3 days and 5 days post-RSV challenge combined (Fig.4.7E-F). At 3 days post-challenge, 27 miRNAs showed altered expression levels; among these, 24 were upregulated and 3 were downregulated (Fig.4.7E and Fig.4.8). Mice vaccinated with FI-RSV induced differential expression of 1 miRNA (miR-483-5p), and GA2-MP and RSV CP52 vaccinated mice induced 6 and 22 miRNAs, respectively (Fig.4.7E). By 5 days

post-challenge, 44 miRNAs were differentially expressed; of these, 35 were upregulated and 9 were downregulated (Fig.4.7F and Fig. 4.8). Furthermore, FI-RSV vaccinated mice had 25 differentially expressed miRNAs, GA2-MP had 35 differentially expressed miRNAs, and RSV CP52 had 12 differentially expressed miRNAs (Fig.4.7F).

Common and distinct differentially expressed miRNAs induced by the model vaccines

Post-prime vaccination all vaccines induced distinct differentially expressed miRNA profiles; however, groups of common miRNAs were also identified among the model vaccines (Fig.4.9A-B). Let-7a-5p, miR-467f, miR-142a-5p, and miR-20b-5p were downregulated in all vaccine groups at 7 days post-prime; however, by 14 days post-prime only miR-467f was downregulated in all groups (Fig.4.9A-B). Let-7f-5p expression was also in GA2-MP vaccinated mice at both 7 days (~4.52 fold) and 14 days post-prime (~2.52 fold), and FI-RSV vaccinated mice (~2.84 fold) had upregulated expression levels at 7 days post-prime (Fig.4.9A-B). miR-483-5p expression levels were downregulated in FI-RSV vaccinated mice at 7 days (~0.36 fold) and 14 days post-prime (~0.36 fold), and RSV CP52 (~0.46 fold) vaccinated mice at 7 days post-prime (Fig.4.9A-B). miR-26b-5p expression levels were increased in GA2-MP vaccinated mice at 7 days (~2.23 fold) and 14 days post-prime (~2.45 fold) (Fig.4.9A-B). miR-15a-5p was upregulated in GA2-MP vaccinated mice (~2.11 fold) and FI-RSV vaccinated mice (~6.62 fold) at 7 days post-prime (Fig.4.9A). Expression levels of miR-17-5p, miR-195a-5p, miR-19b-3p, and miR-20a-5p were increased in FI-RSV vaccinated mice and RSV CP52 vaccinated mice at 7d post-prime (Fig.4.9A); however, miR-182-5p was

downregulated in mice vaccinated with FI-RSV (~0.13 fold) and RSV CP52 (~0.08 fold) at 7 days post prime (Fig.4.9A). Let-7e-5p, miR-181a-5p, and miR-15a-5p expression levels were upregulated in GA2-MP vaccinated mice and RSV CP52 vaccinated mice at 14 days post-prime (Fig.4.9B).

The overall post-boost miRNA profile identified a total of 75 differentially expressed miRNAs at both time points combined (Fig.4.10). At 7 days post-boost, miR-98-5p, miR-26a-5p, miR-155-5p, miR-223-3p, miR-669e-5p expression levels were upregulated in GA2-MP vaccinated mice and RSV CP52 vaccinated mice, where as miR-182-5p expression levels were downregulated in these vaccine groups (Fig.4.10A). miR-1196-5p and miR-483-5p expression levels were increased in FI-RSV vaccinated mice and RSV CP52 vaccinated mice at 7 days post-boost (Fig.4.10A). miR-714 expression levels were increased in GA2-MP and RSV CP52 vaccinated mice at 14 days post-boost (Fig.4.10B). miR-483-5p, miR-467f, miR-669f-3p, miR-466g, and miR-98-5p expression levels were downregulated in GA2-MP vaccinated mice at 14 days post-boost (Fig.4.10B). miR-146b was upregulated in FI-RSV vaccinated mice at both 7d post-boost (~2.10 fold) and 14d post-boost (~2.25 fold) (Fig.4.10A-B). miR-669f was upregulated in GA2-MP vaccinated mice at 7d post-boost (~2.48 fold) and downregulated by 14d post-boost (~0.45 fold) (Fig.4.10A-B).

Among the 84 miRNAs on the miRNA PCR array, 50 miRNAs were differentially expressed among all of the model vaccines at post-challenge time points. miR-145a and miR-346 were differentially expressed in GA2-MP vaccinated mice at 3d and 5d post challenge as well as in RSV CP52 vaccinated mice at 5d post-challenge (Fig.4.11A-B). miR-98 expression was upregulated in RSV CP52 vaccinated mice at 3d

post-challenge (~2.12 fold) and 5d post-challenge (~3.05 fold), however FI-RSV vaccinated mice also showed increased expression levels at 5d post-challenge (~3.4 fold) (Fig.4.11A-B). miR-467f expression was highly upregulated in GA2-MP vaccinated mice (~12.31 fold) and RSV CP52 vaccinated mice (~8.54 fold) at 3 days post-challenge (Fig.4.11A). At 5 days post-challenge, a total of 44 unique miRNAs were differentially expressed (Fig.4.11B). The following miRNA profile was upregulated in FI-RSV vaccinated mice and GA2-MP vaccinated mice at 5 days post-challenge: miR-93-5p, miR-195a-5p, miR-30e-5p, miR-15a-5p, miR-17-5p, miR-142a-3p, miR-106a-5p, miR-106b-5p, miR-20a-5p, miR-20b-5p, miR-31-5p, and let-7g-5p (Fig.4.11B). miR-346-5p expression levels were increased in GA2-MP vaccinated mice and RSV CP52 vaccinated mice, however miR-365-3p and miR-145a-5p expression levels were downregulated in these vaccinated mice at 5 days post-challenge (Fig.4.11B). miR-346-5p expression levels were upregulated in GA2-MP vaccinated mice and RSV CP52 vaccinated mice at 5 days post-challenge (Fig.4.11B). Taken together, this data demonstrates that a group of common and unique miRNA profiles can be identified for each vaccine (GA2-MP, FI-RSV, and RSV CP52), and temporal changes are observed in their expression patterns.

Discussion:

Blood-circulating miRNAs have the potential to become highly valuable biomarkers in the near future. In particular, the identification of serum miRNA profiles capable of directly reporting the differential activation state of clinically relevant lymphocytic subsets may become an innovative tool to provide vital information with regards to the immune responses occurring during vaccination and disease (81). In this

study, we identified vaccine- and temporal-specific differentially miRNA expression patterns in mouse sera at various time points during vaccination and post-RSV challenge. Specifically, groups of common and distinct miRNAs were differentially expressed in response to the model vaccines that prime for protection (RSV CP52 vaccine) and disease (FI-RSV vaccine), as well as a microparticle-based RSV vaccine platform (GA2-MP). To our knowledge this is the first report of miRNA expression profiles as biomarkers for vaccine efficacy and disease outcomes in the mouse model. The identification of differentially expressed host miRNAs is just an initial step toward understanding miRNA regulation of host-virus interactions during vaccination. However, the biological basis of the difference in protection and disease outcomes for RSV vaccine candidates remains largely unknown, and the identification of novel biomarkers such as these may provide a reliable and accessible option for assessing vaccines during development.

In addition, the assessment of known immune correlates for the model vaccines provided an accurate framework for the assessment of the miRNA profiles induced during vaccination. These results indicated that vaccination was successful for all vaccines as indicated by the induction of RSV-specific antibodies. However, a reduction in lung viral load was only observed for the RSV CP52 and GA2-MP vaccinated mice, but not for the FI-RSV vaccinated mice or the PBS control. In addition, RSV CP52 vaccination induced a strong Th1-type T cell response where as FI-RSV vaccination induced a strong Th2-type T cell response, and GA2-MP vaccination induces a balanced Th1/Th2 T cell response. Taken together, these results demonstrate that the model vaccines induced appropriate immune responses; more specifically, the RSV CP52 vaccine induced protection from RSV disease and the FI-RSV vaccine induced vaccine

enhanced disease. Therefore, we were able to successfully profile a novel RSV vaccine candidate, GA2-MP, using this miRNA profiling platform.

Although this study generated a unique list of candidate miRNAs that potentially regulate RSV vaccine efficacy and immune responsiveness, additional studies are warranted to clarify the mechanisms behind how these candidate miRNAs mediate host-virus interactions during RSV vaccination and subsequent infection. In addition, a potential limitation of this study is that it is limited to the mouse model. Although miRNAs are evolutionarily conserved, there are mainly physiological and immunological differences between animal species. Thus, it is plausible to assume that differences in host genetic factors and immune system components may have an important role in the regulation of miRNA expression during vaccination and RSV infection. Therefore, additional animal models need to be evaluated to validate these miRNA profiles.

Acknowledgments

The authors' would like to thank Jeff Powell (Artificial Cell Technologies, New Haven, CT) for providing the GA2-MP vaccine.

Funding sources

This project was supported by the ARCS Foundation and the Georgia Research Alliance.

Author Contributions

Conceived and designed the experiments: LJA PAJ RAT. Performed the experiments: LJA PAJ CMW. Analyzed the data: LJA PAJ CMW RAT. Contributed reagents/materials/analysis tools: RAT. Wrote the manuscript: LJA PAJ RAT.

References

1. Nair H, Nokes DJ, Gessner BD, Dherani M, Madhi SA, Singleton RJ, et al. Global burden of acute lower respiratory infections due to respiratory syncytial virus in young children: a systematic review and meta-analysis. Lancet. 2010;375(9725):1545-55.

2. PATH Vaccine Resource Library. Respiratory syncytial virus (RSV) 2016 [Available from: http://www.path.org/vaccineresources/rsv.php.

3. Jorquera PA, Anderson L, Tripp RA. Understanding respiratory syncytial virus (RSV) vaccine development and aspects of disease pathogenesis. Expert review of vaccines. 2015:1-15.

4. Jorquera PA, Oakley KE, Tripp RA. Advances in and the potential of vaccines for respiratory syncytial virus. Expert review of respiratory medicine. 2013;7(4):411-27.

5. Rey GU, Miao C, Caidi H, Trivedi SU, Harcourt JL, Tripp RA, et al. Decrease in formalin-inactivated respiratory syncytial virus (FI-RSV) enhanced disease with RSV G glycoprotein peptide immunization in BALB/c mice. PLoS One. 2013;8(12):e83075.

6. Wright PF, Karron RA, Belshe RB, Thompson J, Crowe JE, Jr., Boyce TG, et al. Evaluation of a live, cold-passaged, temperature-sensitive, respiratory syncytial virus vaccine candidate in infancy. J Infect Dis. 2000;182(5):1331-42.

7. Friedewald WT, Forsyth BR, Smith CB, Gharpure MA, Chanock RM. Low-temperature-grown RS virus in adult volunteers. Jama. 1968;204(8):690-4.

8. Gharpure MA, Wright PF, Chanock RM. Temperature-sensitive mutants of respiratory syncytial virus. J Virol. 1969;3(4):414-21.

9. McKay E, Higgins P, Tyrrell D, Pringle C. Immunogenicity and pathogenicity of temperature-sensitive modified respiratory syncytial virus in adult volunteers. J Med Virol. 1988;25(4):411-21.

10. Pringle CR, Filipiuk AH, Robinson BS, Watt PJ, Higgins P, Tyrrell DA. Immunogenicity and pathogenicity of a triple temperature-sensitive modified respiratory syncytial virus in adult volunteers. Vaccine. 1993;11(4):473-8.

11. Karron RA, Wright PF, Belshe RB, Thumar B, Casey R, Newman F, et al. Identification of a recombinant live attenuated respiratory syncytial virus vaccine candidate that is highly attenuated in infants. J Infect Dis. 2005;191(7):1093-104.

12. Whitehead SS, Bukreyev A, Teng MN, Firestone CY, St Claire M, Elkins WR, et al. Recombinant respiratory syncytial virus bearing a deletion of either the NS2 or SH gene is attenuated in chimpanzees. J Virol. 1999;73(4):3438-42.

13. Cherukuri A, Stokes KL, Patton K, Kuo H, Sakamoto K, Lambert S, et al. An adjuvanted respiratory syncytial virus fusion protein induces protection in aged BALB/c mice. Immun Ageing. 2012;9(1):21.

14. Nguyen TN, Power UF, Robert A, Haeuw JF, Helffer K, Perez A, et al. The respiratory syncytial virus G protein conserved domain induces a persistent and protective antibody response in rodents. PLoS One. 2012;7(3):e34331.

15. Prince GA, Capiau C, Deschamps M, Fabry L, Garcon N, Gheysen D, et al. Efficacy and safety studies of a recombinant chimeric respiratory syncytial virus FG glycoprotein vaccine in cotton rats. J Virol. 2000;74(22):10287-92.

16. Remot A, Roux X, Dubuquoy C, Fix J, Bouet S, Moudjou M, et al. Nucleoprotein nanostructures combined with adjuvants adapted to the neonatal immune context: a candidate mucosal RSV vaccine. PLoS One. 2012;7(5):e37722.

17. Fu Y, He J, Zheng X, Wu Q, Zhang M, Wang X, et al. Intranasal immunization with a replication-deficient adenoviral vector expressing the fusion glycoprotein of respiratory syncytial virus elicits protective immunity in BALB/c mice. Biochemical and biophysical research communications. 2009;381(4):528-32.

18. Fu YH, He JS, Zheng XX, Wang XB, Xie C, Shi CX, et al. Intranasal vaccination with a helper-dependent adenoviral vector enhances transgene-specific immune responses in BALB/c mice. Biochemical and biophysical research communications. 2010;391(1):857-61.

19. Krause A, Xu Y, Ross S, Wu W, Joh J, Worgall S. Absence of vaccine-enhanced RSV disease and changes in pulmonary dendritic cells with adenovirus-based RSV vaccine. Virology journal. 2011;8:375.

20. Elliott MB, Chen T, Terio NB, Chong SY, Abdullah R, Luckay A, et al. Alphavirus replicon particles encoding the fusion or attachment glycoproteins of respiratory syncytial virus elicit protective immune responses in BALB/c mice and functional serum antibodies in rhesus macaques. Vaccine. 2007;25(41):7132-44.

21. Chen M, Hu KF, Rozell B, Orvell C, Morein B, Liljestrom P. Vaccination with recombinant alphavirus or immune-stimulating complex antigen against respiratory syncytial virus. Journal of immunology. 2002;169(6):3208-16.

22. Fleeton MN, Chen M, Berglund P, Rhodes G, Parker SE, Murphy M, et al. Self-replicative RNA vaccines elicit protection against influenza A virus, respiratory syncytial virus, and a tickborne encephalitis virus. J Infect Dis. 2001;183(9):1395-8.

23. Mok H, Lee S, Utley TJ, Shepherd BE, Polosukhin VV, Collier ML, et al. Venezuelan equine encephalitis virus replicon particles encoding respiratory syncytial virus surface glycoproteins induce protective mucosal responses in mice and cotton rats. J Virol. 2007;81(24):13710-22.

24. Kim S, Chang J. Baculovirus-based Vaccine Displaying Respiratory Syncytial Virus Glycoprotein Induces Protective Immunity against RSV Infection without Vaccine-Enhanced Disease. Immune network. 2012;12(1):8-17.

25. McGinnes LW, Gravel KA, Finberg RW, Kurt-Jones EA, Massare MJ, Smith G, et al. Assembly and immunological properties of Newcastle disease virus-like particles containing the respiratory syncytial virus F and G proteins. J Virol. 2011;85(1):366-77.

26. Schmidt MR, McGinnes LW, Kenward SA, Willems KN, Woodland RT, Morrison TG. Long-term and memory immune responses in mice against Newcastle disease virus-like particles containing respiratory syncytial virus glycoprotein ectodomains. J Virol. 2012;86(21):11654-62.

27. Jorquera PA, Choi Y, Oakley KE, Powell TJ, Boyd JG, Palath N, et al. Nanoparticle vaccines encompassing the respiratory syncytial virus (RSV) G protein CX3C chemokine motif induce robust immunity protecting from challenge and disease. PLoS One. 2013;8(9):e74905.

28. Garlapati S, Garg R, Brownlie R, Latimer L, Simko E, Hancock RE, et al. Enhanced immune responses and protection by vaccination with respiratory syncytial virus fusion protein formulated with CpG oligodeoxynucleotide and innate defense regulator peptide in polyphosphazene microparticles. Vaccine. 2012;30(35):5206-14.

29. Powell TJ, Palath N, DeRome ME, Tang J, Jacobs A, Boyd JG. Synthetic nanoparticle vaccines produced by layer-by-layer assembly of artificial biofilms induce potent protective T-cell and antibody responses in vivo. Vaccine. 2011;29(3):558-69.

30. Quan FS, Kim Y, Lee S, Yi H, Kang SM, Bozja J, et al. Viruslike particle vaccine induces protection against respiratory syncytial virus infection in mice. J Infect Dis. 2011;204(7):987-95.

31. Kamphuis T, Meijerhof T, Stegmann T, Lederhofer J, Wilschut J, de Haan A. Immunogenicity and protective capacity of a virosomal respiratory syncytial virus vaccine adjuvanted with monophosphoryl lipid A in mice. PLoS One. 2012;7(5):e36812.

32. Li X, Sambhara S, Li CX, Ewasyshyn M, Parrington M, Caterini J, et al. Protection against respiratory syncytial virus infection by DNA immunization. J Exp Med. 1998;188(4):681-8.

33. Bartholdy C, Olszewska W, Stryhn A, Thomsen AR, Openshaw PJ. Gene-gun DNA vaccination aggravates respiratory syncytial virus-induced pneumonitis. J Gen Virol. 2004;85(Pt 10):3017-26.

34. Geall AJ, Verma A, Otten GR, Shaw CA, Hekele A, Banerjee K, et al. Nonviral delivery of self-amplifying RNA vaccines. Proc Natl Acad Sci U S A. 2012;109(36):14604-9.

35. Knudson CJ, Varga SM. The Relationship Between Respiratory Syncytial Virus and Asthma. Veterinary pathology. 2014:0300985814520639-.

36. Backman K, Piippo-Savolainen E, Ollikainen H, Koskela H, Korppi M. Adults face increased asthma risk after infant RSV bronchiolitis and reduced respiratory health-related quality of life after RSV pneumonia. Acta paediatrica (Oslo, Norway : 1992). 2014.

37. Escobar GJ, Ragins A, Li SX, Prager L, Masaquel AS, Kipnis P. Recurrent wheezing in the third year of life among children born at 32 weeks' gestation or later: relationship to laboratory-confirmed, medically attended infection with respiratory syncytial virus during the first year of life. Archives of pediatrics & adolescent medicine. 2010;164:915-22.

38. Kusel MMH, de Klerk NH, Kebadze T, Vohma V, Holt PG, Johnston SL, et al. Early-life respiratory viral infections, atopic sensitization, and risk of subsequent development of persistent asthma. The Journal of allergy and clinical immunology. 2007;119:1105-10.

39. Kwon J-M, Shim JW, Kim DS, Jung HL, Park MS, Shim JY. Prevalence of respiratory viral infection in children hospitalized for acute lower respiratory tract diseases, and association of rhinovirus and influenza virus with asthma exacerbations. Korean journal of pediatrics. 2014;57:29-34.

40. Lin HC, Hwang KC, Yang YH, Lin YT, Chiang BL. Risk factors of wheeze and allergy after lower respiratory tract infections during early childhood. Journal of

microbiology, immunology, and infection = Wei mian yu gan ran za zhi. 2001;34:259-64.

41. Martinez FD, Wright AL, Taussig LM, Holberg CJ, Halonen M, Morgan WJ. Asthma and wheezing in the first six years of life. The Group Health Medical Associates. The New England journal of medicine. 1995;332:133-8.

42. Ruotsalainen M, Hyvarinen MK, Piippo-Savolainen E, Korppi M. Adolescent asthma after rhinovirus and respiratory syncytial virus bronchiolitis. Pediatr Pulmonol. 2013;48(7):633-9.

43. Sigurs N, Gustafsson PM, Bjarnason R, Lundberg F, Schmidt S, Sigurbergsson F, et al. Severe respiratory syncytial virus bronchiolitis in infancy and asthma and allergy at age 13. Am J Respir Crit Care Med. 2005;171(2):137-41.

44. Lu TX, Hartner J, Lim E-J, Fabry V, Mingler MK, Cole ET, et al. MicroRNA-21 limits in vivo immune response-mediated activation of the IL-12/IFN-gamma pathway, Th1 polarization, and the severity of delayed-type hypersensitivity. Journal of immunology (Baltimore, Md : 1950). 2011;187:3362-73.

45. Sharma A, Kumar M, Ahmad T, Mabalirajan U, Aich J, Agrawal A, et al. Antagonism of mmu-mir-106a attenuates asthma features in allergic murine model. Journal of applied physiology (Bethesda, Md : 1985). 2012;113:459-64.

46. Collison A, Herbert C, Siegle JS, Mattes J, Foster PS, Kumar RK. Altered expression of microRNA in the airway wall in chronic asthma: miR-126 as a potential therapeutic target. BMC pulmonary medicine. 2011;11:29.

47. Lu TX, Rothenberg ME. Diagnostic, functional, and therapeutic roles of microRNA in allergic diseases. The Journal of allergy and clinical immunology. 2013;132:3-13; quiz 4.

48. Mattes J, Collison A, Plank M, Phipps S, Foster PS. Antagonism of microRNA-126 suppresses the effector function of TH2 cells and the development of allergic airways disease. Proceedings of the National Academy of Sciences of the United States of America. 2009;106:18704-9.

49. Oglesby IK, McElvaney NG, Greene CM. MicroRNAs in inflammatory lung disease--master regulators or target practice? Respiratory research. 2010;11:148.

50. Foster PS, Plank M, Collison A, Tay HL, Kaiko GE, Li J, et al. The emerging role of microRNAs in regulating immune and inflammatory responses in the lung. Immunol Rev. 2013;253(1):198-215.

51. Lu TX. MicroRNA in the Pathogenesis of Allergic Inflammation. 2012.

52. Chen CZ, Schaffert S, Fragoso R, Loh C. Regulation of immune responses and tolerance: the microRNA perspective. Immunol Rev. 2013;253(1):112-28.

53. Bakre A, Tripp, R.A. Host-Encoded miRNAs Involved in Host-Pathogen Interactions. 2014. In: Frontiers in RNAi Volume 1 [Internet]. [In Press].

54. Bakre A, Mitchell P, Coleman JK, Jones LP, Saavedra G, Teng M, et al. Respiratory syncytial virus modifies microRNAs regulating host genes that affect virus replication. J Gen Virol. 2012;93(Pt 11):2346-56.

55. Meliopoulos VA, Andersen LE, Brooks P, Yan X, Bakre A, Coleman JK, et al. MicroRNA regulation of human protease genes essential for influenza virus replication. PLoS One. 2012;7(5):e37169.

56. Bakre A, Andersen LE, Meliopoulos V, Coleman K, Yan X, Brooks P, et al. Identification of Host Kinase Genes Required for Influenza Virus Replication and the Regulatory Role of MicroRNAs. PLoS One. 2013;8(6):e66796.

57. Hebert SS, De Strooper B. Alterations of the microRNA network cause neurodegenerative disease. Trends in neurosciences. 2009;32(4):199-206.

58. Amarilyo G, La Cava A. miRNA in systemic lupus erythematosus. Clinical immunology. 2012;144(1):26-31.

59. Bostjancic E, Glavac D. Importance of microRNAs in skin morphogenesis and diseases. Acta dermatovenerologica Alpina, Pannonica, et Adriatica. 2008;17(3):95-102.

60. Chan EK, Ceribelli A, Satoh M. MicroRNA-146a in autoimmunity and innate immune responses. Annals of the rheumatic diseases. 2013;72 Suppl 2:ii90-5.

61. Moser JJ, Fritzler MJ. Relationship of other cytoplasmic ribonucleoprotein bodies (cRNPB) to GW/P bodies. Advances in experimental medicine and biology. 2013;768:213-42.

62. Persengiev SP. miRNAs at the crossroad between hematopoietic malignancies and autoimmune pathogenesis. Discovery medicine. 2012;13(70):211-21.

63. Wittmann J, Jack HM. microRNAs in rheumatoid arthritis: midget RNAs with a giant impact. Annals of the rheumatic diseases. 2011;70 Suppl 1:i92-6.

64. van Rooij E, Sutherland LB, Liu N, Williams AH, McAnally J, Gerard RD, et al. A signature pattern of stress-responsive microRNAs that can evoke cardiac hypertrophy and heart failure. Proc Natl Acad Sci U S A. 2006;103(48):18255-60.

65. Lu J, Getz G, Miska EA, Alvarez-Saavedra E, Lamb J, Peck D, et al. MicroRNA expression profiles classify human cancers. Nature. 2005;435(7043):834-8.

66. Volinia S, Calin GA, Liu CG, Ambs S, Cimmino A, Petrocca F, et al. A microRNA expression signature of human solid tumors defines cancer gene targets. Proc Natl Acad Sci U S A. 2006;103(7):2257-61.

67. Al-Quraishy S, Dkhil MA, Delic D, Abdel-Baki AA, Wunderlich F. Organ-specific testosterone-insensitive response of miRNA expression of C57BL/6 mice to Plasmodium chabaudi malaria. Parasitology research. 2012;111(3):1093-101.

68. Delic D, Dkhil M, Al-Quraishy S, Wunderlich F. Hepatic miRNA expression reprogrammed by Plasmodium chabaudi malaria. Parasitology research. 2011;108(5):1111-21.

69. Ge Y, Zhao K, Qi Y, Min X, Shi Z, Qi X, et al. Serum microRNA expression profile as a biomarker for the diagnosis of pertussis. Molecular biology reports. 2013;40(2):1325-32.

70. Ma L, Shen CJ, Cohen EA, Xiong SD, Wang JH. miRNA-1236 inhibits HIV-1 infection of monocytes by repressing translation of cellular factor VprBP. PLoS One. 2014;9(6):e99535.

71. Podolska A, Anthon C, Bak M, Tommerup N, Skovgaard K, Heegaard PM, et al. Profiling microRNAs in lung tissue from pigs infected with Actinobacillus pleuropneumoniae. BMC genomics. 2012;13:459.

72. Singh PK, Singh AV, Chauhan DS. Current understanding on micro RNAs and its regulation in response to Mycobacterial infections. Journal of biomedical science. 2013;20:14.

73. Wang C, Yang S, Sun G, Tang X, Lu S, Neyrolles O, et al. Comparative miRNA expression profiles in individuals with latent and active tuberculosis. PLoS One. 2011;6(10):e25832.

74. Feldman SA, Audet S, Beeler JA. The fusion glycoprotein of human respiratory syncytial virus facilitates virus attachment and infectivity via an interaction with cellular heparan sulfate. J Virol. 2000;74(14):6442-7.

75. Tripp RA, Moore D, Jones L, Sullender W, Winter J, Anderson LJ. Respiratory syncytial virus G and/or SH protein alters Th1 cytokines, natural killer cells, and neutrophils responding to pulmonary infection in BALB/c mice. J Virol. 1999;73(9):7099-107.

76. Prince GA, Curtis SJ, Yim KC, Porter DD. Vaccine-enhanced respiratory syncytial virus disease in cotton rats following immunization with Lot 100 or a newly prepared reference vaccine. J Gen Virol. 2001;82(Pt 12):2881-8.

77. Falsey AR, Formica MA, Walsh EE. Microneutralization assay for the measurement of neutralizing antibodies to human metapneumovirus. J Clin Virol. 2009;46(4):314-7.

78. Jorquera PA, Oakley KE, Powell TJ, Palath N, Boyd JG, Tripp RA. Layer-By-Layer Nanoparticle Vaccines Carrying the G Protein CX3C Motif Protect against RSV Infection and Disease. Vaccines (Basel). 2015;3(4):829-49.

79. Karron RA, Buonagurio DA, Georgiu AF, Whitehead SS, Adamus JE, Clements-Mann ML, et al. Respiratory syncytial virus (RSV) SH and G proteins are not essential for viral replication in vitro: clinical evaluation and molecular characterization of a cold-passaged, attenuated RSV subgroup B mutant. Proc Natl Acad Sci U S A. 1997;94(25):13961-6.

80. Crowe JE, Jr., Bui PT, Firestone CY, Connors M, Elkins WR, Chanock RM, et al. Live subgroup B respiratory syncytial virus vaccines that are attenuated, genetically stable, and immunogenic in rodents and nonhuman primates. J Infect Dis. 1996;173(4):829-39.

81. de Candia P, Torri A, Pagani M, Abrignani S. Serum microRNAs as Biomarkers of Human Lymphocyte Activation in Health and Disease. Frontiers in immunology. 2014;5:43.

Tables and figures

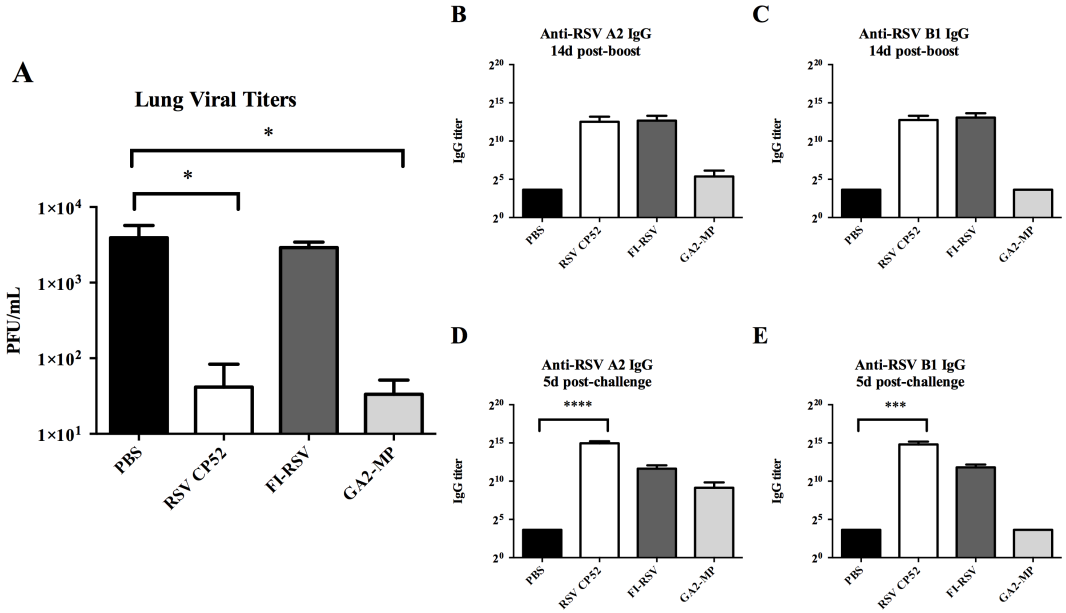

Fig. 4.1: Lung viral titers and RSV-specific antibody response. Groups of BALB/c mice were vaccinated twice with vehicle (PBS), the live-attenuated vaccine (RSV CP52), the inactivated vaccine (FI-RSV), or the microparticle-based vaccine (GA2-MP) using a prime-boost regimen. Control mice (naïve) received no vaccinations. Three weeks after the boost vaccination mice were challenged with $1x10^6$ PFU of RSV A2 via i.n. delivery. **(A)** Lung virus titers were determined 5 days post-challenge by plaque assay (n=4 mice/group). Sera were obtained from blood taken 14 days post-boost and **(B)** RSV A2-specific IgG levels and **(C)** RSV B1-specific IgG levels were determined by indirect ELISA (n=4 mice/group). Sera were obtained from blood taken at 5 days post challenge and **(D)** RSV A2-specific IgG levels and E) RSV B1-specific IgG levels were determined by indirect ELISA (n=4 mice/group). Error bars represent the SEM and results were considered significant with a P value ≤0.05 (*), ≤0.01 (**), ≤0.001 (***), and ≤0.0001 (****) as determined by one-way ANOVA and Bonferroni's test.

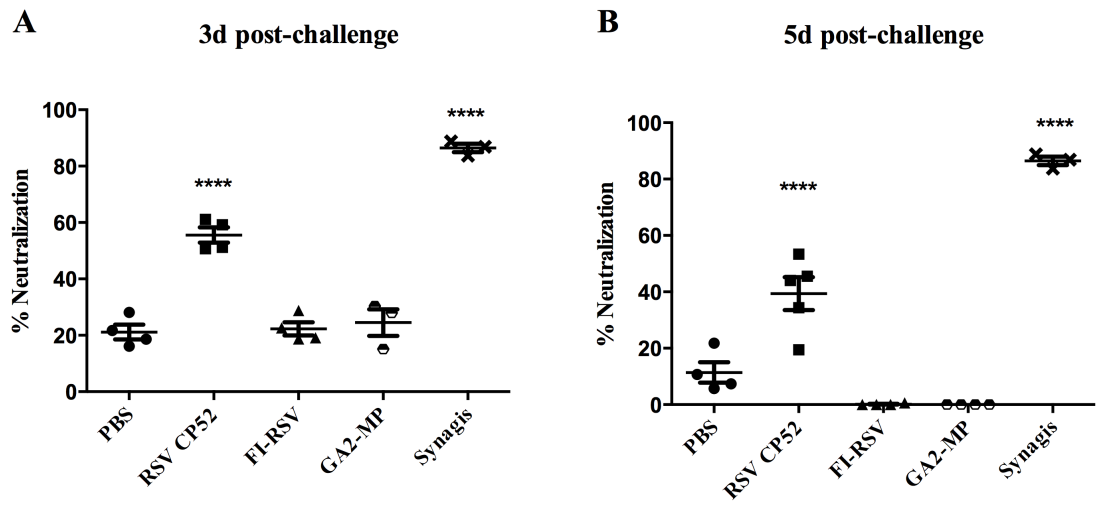

Fig. 4.2: Immunization with RSV CP52 generates RSV-neutralizing antibodies. Groups of BALB/c mice were vaccinated twice with vehicle (PBS), the live-attenuated vaccine (RSV CP52), the inactivated vaccine (FI-RSV), or the microparticle-based vaccine (GA2-MP) using a prime-boost regimen. Three weeks after the boost vaccination mice were challenged with $1x10^6$ PFU of RSV A2 via i.n. delivery. At **(A)** 3 days post-challenge and **(B)** 5 days post-challenge, sera were collected and tested for RSV-neutralizing activity using a microneutralization assay. All samples were assayed in duplicate and n=4 mice/group. Horizontal lines represent the mean antibody titer of each group and results were considered significant with a a P value ≤0.05 (*), ≤0.01 (**), ≤0.001 (***), and ≤0.0001 (****) as determined by one-way ANOVA and Bonferroni's test.

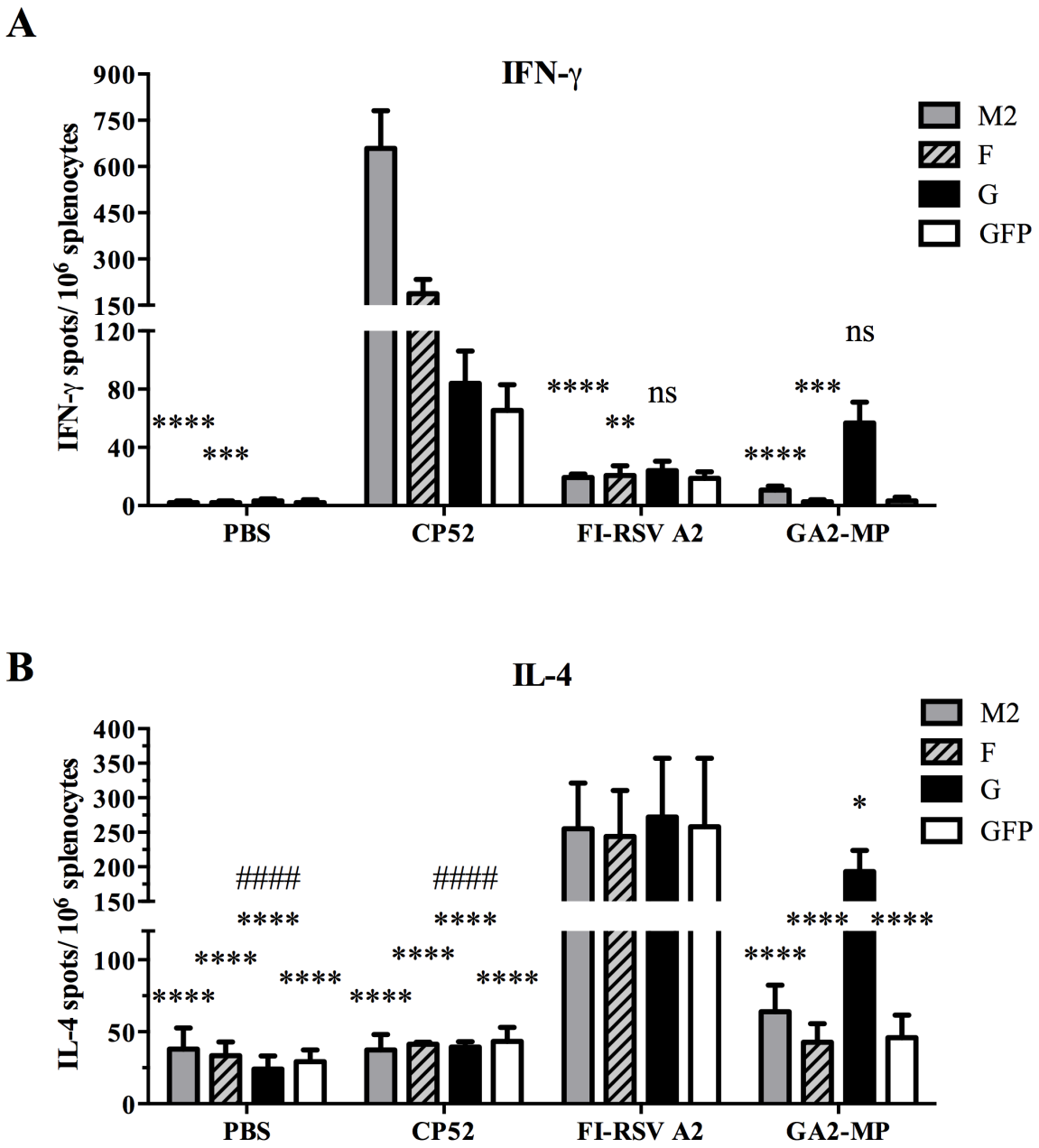
A
IFN-γ
IFN-γ spots/ 10^6 splenocytes
900
750
600
450
300
150
120
80
40
0
M2
F
G
GFP
****
***
****
**
ns
***
****
ns
PBS
CP52
FI-RSV A2
GA2-MP
B
IL-4
IL-4 spots/ 10^6 splenocytes
400
350
300
250
200
150
100
50
0
M2
F
G
GFP
####
####
****
*
PBS
CP52
FI-RSV A2
GA2-MP

Fig. 4.3: Frequency of RSV-specific IFNγ and IL-4 secreting cells after virus challenge. Groups of BALB/c mice were vaccinated using a prime-boost regimen at days 0 and 21 with vehicle (PBS), the live-attenuated vaccine (RSV CP52), the inactivated vaccine (FI-RSV), or the microparticle-based vaccine (GA2-MP). The number of $M2_{82-90}$-specific, F_{51-66}-specific, $G_{183-198}$-specific, and GFP-specific (irrelevant peptide control) IL-4 and IFNγ producing splenocytes were determined by ELISPOT in cells harvested at 14 days post-boost vaccination. **(A)** IFNγ producing splenocytes and **(B)** IL-4 producing splenocytes. The data are presented as cytokine spots/10^6 splenocytes. For IFNγ, the asterisks (*) represent a p-value significant compared to RSV CP52. For IL-4, the astericks (*) represent a p-value significant compared to FI-RSV A2 and hashtags (#) represent a p-value significant compared to GA2-MP. Error bars represent the SEM from n=4 mice/group and results were considered significant with a P value ≤0.05 (*/#), ≤0.01 (**/##), ≤0.001 (***/###) and ≤0.0001 (****/####) as determined by two-way ANOVA and Bonferroni's test.

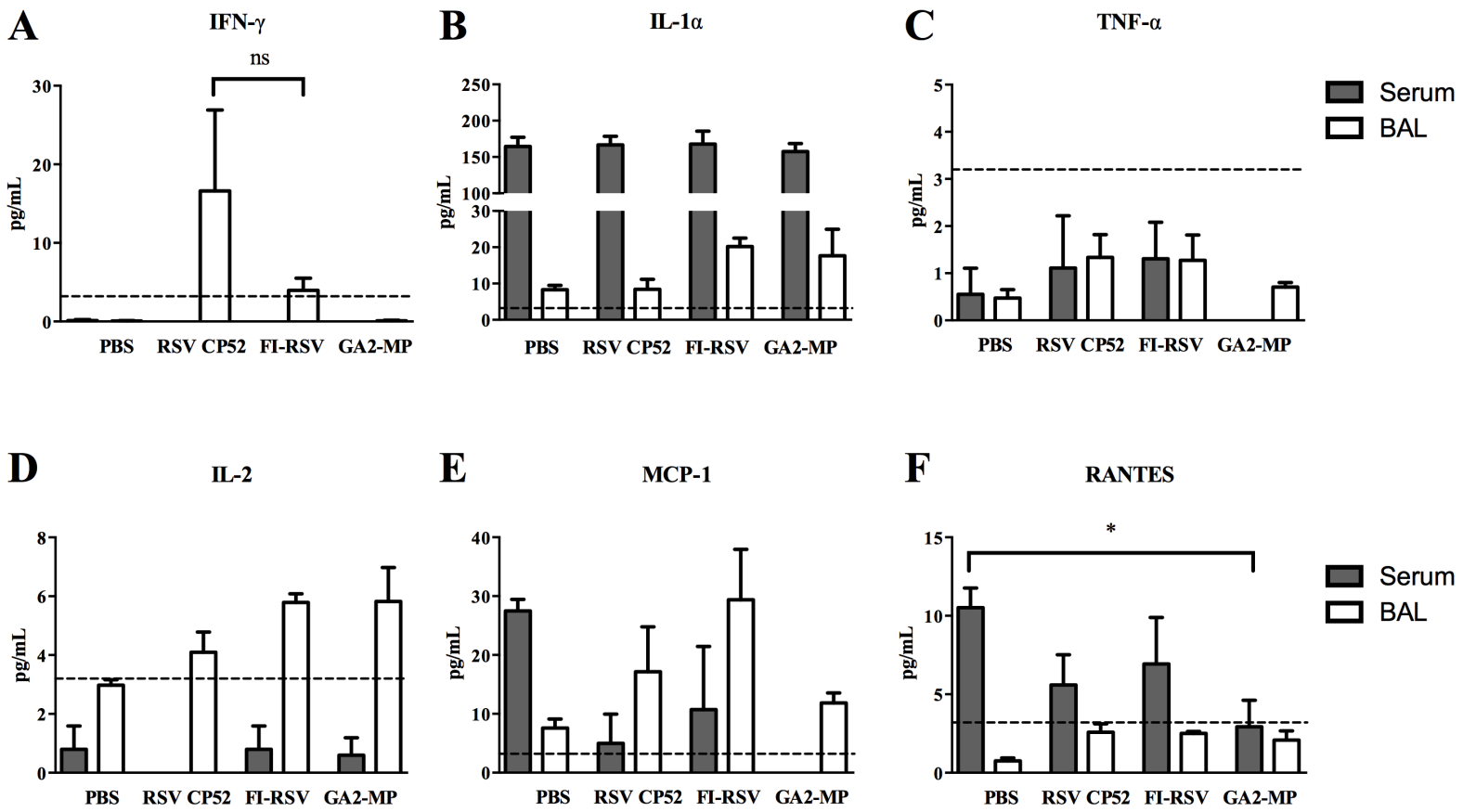
A
IFN-γ
ns
pg/mL
30
20
10
0
PBS
RSV CP52
FI-RSV
GA2-MP
B
IL-1α
pg/mL
250
200
150
100
30
20
10
0
PBS
RSV CP52
FI-RSV
GA2-MP
C
TNF-α
pg/mL
5
4
3
2
1
0
PBS
RSV CP52
FI-RSV
GA2-MP
Serum
BAL
D
IL-2
pg/mL
8
6
4
2
0
PBS
RSV CP52
FI-RSV
GA2-MP
E
MCP-1
pg/mL
40
30
20
10
0
PBS
RSV CP52
FI-RSV
GA2-MP
F
RANTES
*
pg/mL
15
10
5
0
PBS
RSV CP52
FI-RSV
GA2-MP
Serum
BAL

Fig. 4.4: Differential Th1-type cytokine and chemokine expression among vaccine groups. Groups of BALB/c mice were vaccinated twice with vehicle (PBS), the live-attenuated vaccine (RSV CP52), the inactivated vaccine (FI-RSV), or the microparticle-based vaccine (GA2-MP) using a prime-boost regimen. Three weeks after the boost vaccination mice were challenged with $1x10^6$ PFU of RSV A2 via i.n. delivery. The level of **(A)** IFN-γ, **(B)** IL-1α, **(C)** TNFα, **(D)** IL-2, **(E)** MCP-1, and **(F)** RANTES were measured in sera and BAL supernatant by Luminex assay, and the data are presented as picograms (pg) of cytokine/ ml of BAL supernatant at 3 days post challenge (n=4-6 mice/group). The dashed line indicates the limit of detection (LOD) = 3.2 pg/ ml. Error bars represent the SEM and results were considered significant with a P value ≤ 0.05 (*) as determined by one-way ANOVA and Bonferroni's test.

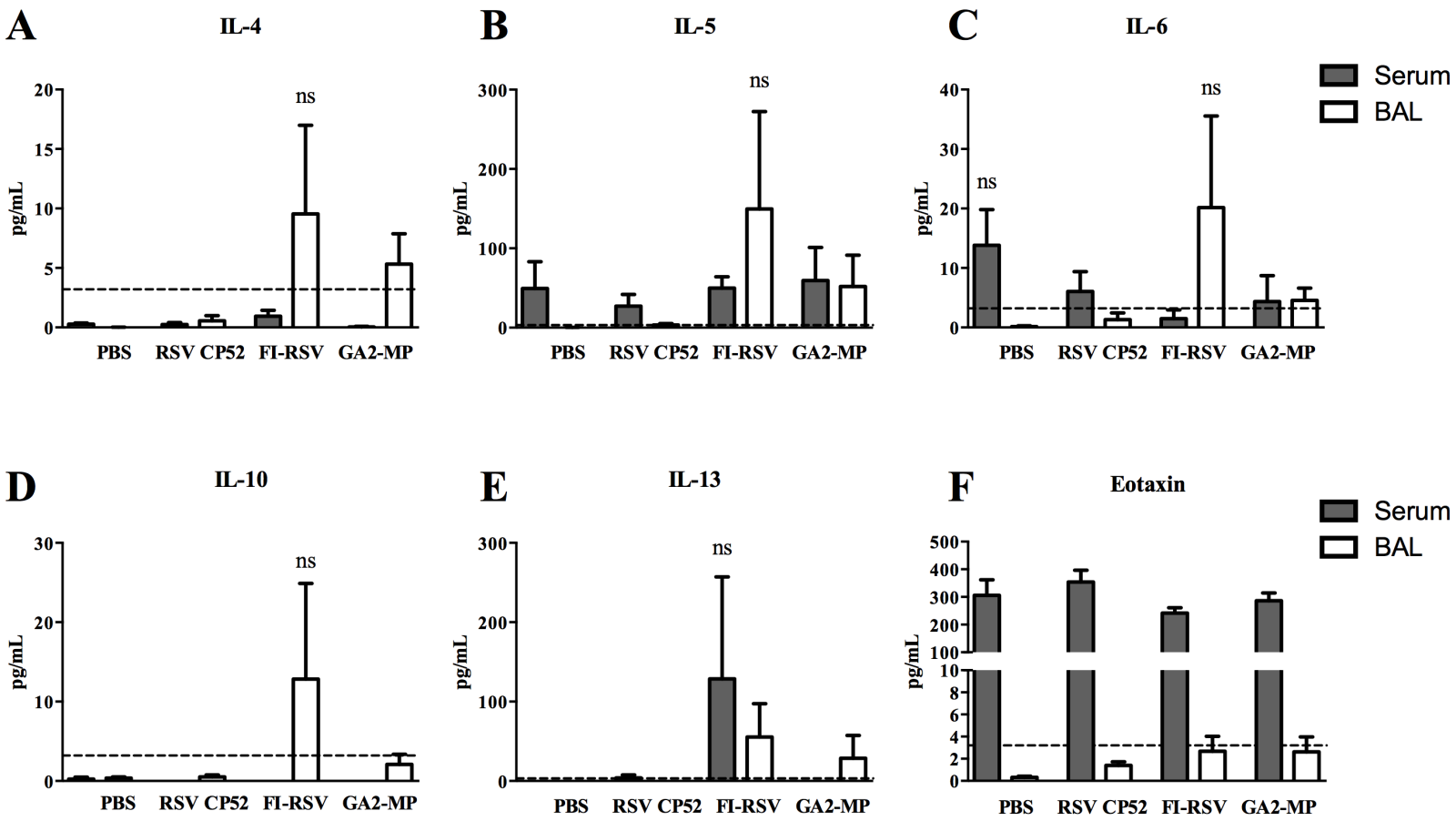
A
IL-4
B
IL-5
C
IL-6
D
IL-10
E
IL-13
F
Eotaxin
pg/mL
ns
PBS
RSV CP52
FI-RSV
GA2-MP
Serum
BAL

Fig. 4.5: Differential Th2-type cytokine and chemokine expression among vaccine groups. Groups of BALB/c mice were vaccinated twice with vehicle (PBS), the live-attenuated vaccine (RSV CP52), the inactivated vaccine (FI-RSV), or the microparticle-based vaccine (GA2-MP) using a prime-boost regimen. Three weeks after the boost vaccination mice were challenged with $1x10^6$ PFU of RSV A2 via i.n. delivery. The level of **(A)** IL-4, **(B)** IL-5, **(C)** IL-6, **(D)** IL-10, **(E)** IL-13, and **(F)** eotaxin were measured in sera and BAL supernatant by Luminex assay, and the data are presented as picograms (pg) of cytokine/ ml of BAL supernatant at 3 days post challenge (n=4-6 mice/group). The dashed line indicates the limit of detection (LOD) = 3.2 pg/ ml. Error bars represent the SEM and results were considered significant with a P value ≤0.05 (*) as determined by one-way ANOVA and Bonferroni's test.

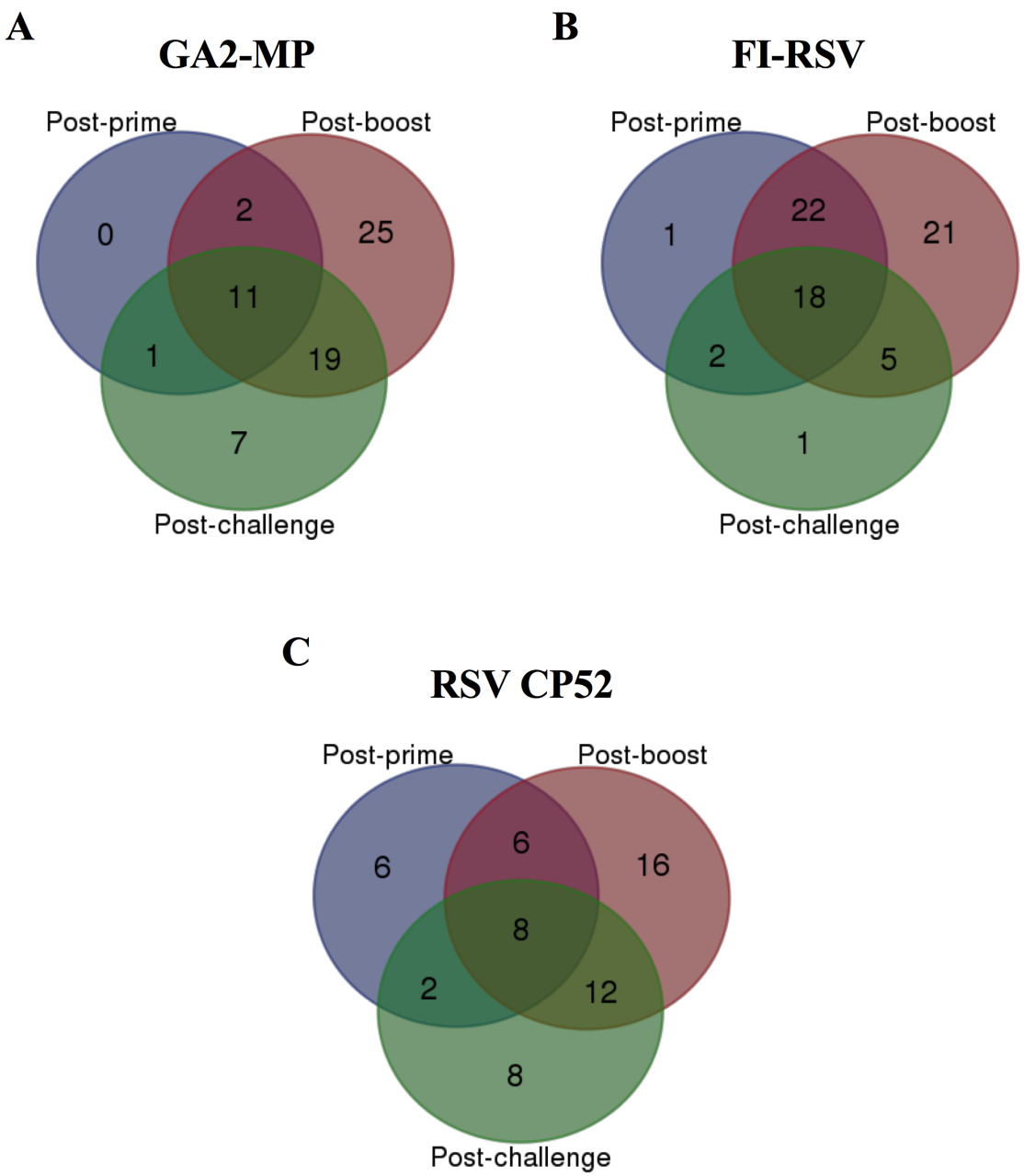
A
GA2-MP
Post-prime
Post-boost
Post-challenge
0
2
25
11
1
19
7
B
FI-RSV
Post-prime
Post-boost
Post-challenge
1
22
21
18
2
5
1
C
RSV CP52
Post-prime
Post-boost
Post-challenge
6
6
16
8
2
12
8

Fig. 4.6: Temporal pattern of differential miRNA expression in the model vaccines. BALB/c mice (n=4/group) were vaccinated twice with vehicle (PBS), the live-attenuated vaccine (RSV CP52), the inactivated vaccine (FI-RSV), or the microparticle-based vaccine (GA2-MP) using a prime-boost regimen. Three weeks after the boost vaccination mice were challenged with $1x10^6$ PFU of RSV A2 via i.n. delivery. Using a miRNA PCR array, 84 miRNAs were evaluated to identify unique sera miRNA profiles in mice for the model vaccines. The tempo of common and unique differentially expressed miRNAs for **(A)** GA2-MP, **(B)** FI-RSV, and **(C)** RSV CP52 vaccinated mice at post-prime (7 and 14 days), post-boost (7 and 14 days), and post-RSV challenge (3 and 5 days). miRNA expression levels are normalized by SN1/2/3/4/5/6 expression. Values are represented as expression/mock treatment (PBS vaccinated/RSV A2 challenge) and fold change was calculated using $2^{(-\Delta\Delta CT)}$ method. Differential expression was determined using the following criteria, if the fold change was > 2, the result was reported as a fold upregulation. If the fold change was < 0.5, the result was reported as a fold downregulation.

A 7 days post-prime

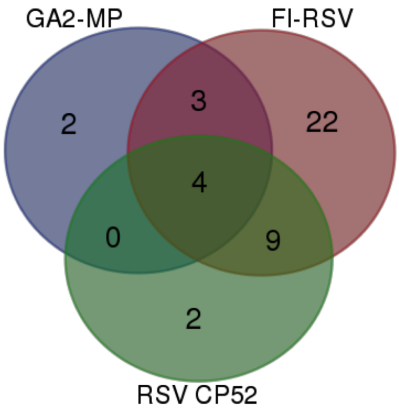

B 14 days post-prime

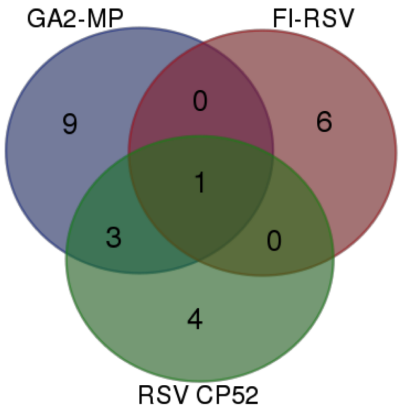

C 7 days post-boost

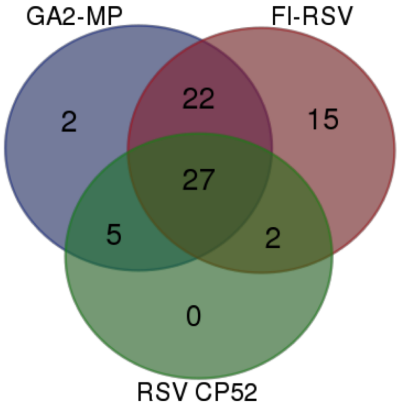

D 14 days post-boost

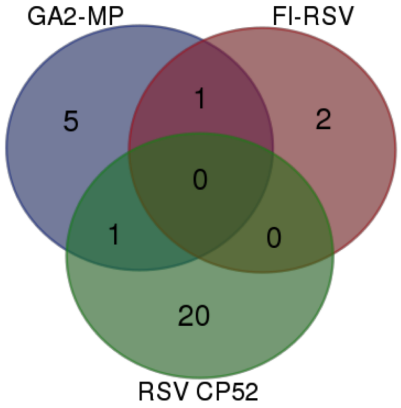

E 3 days post-challenge

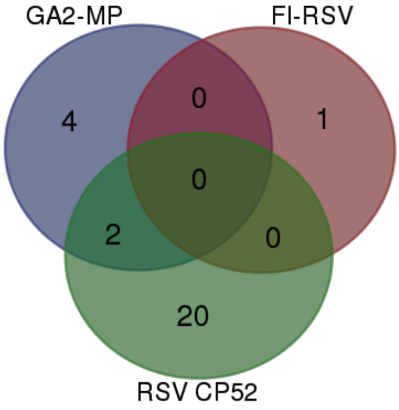

F 5 days post-challenge

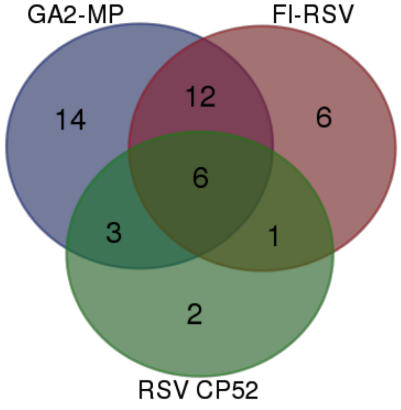

Fig. 4.7: Common and unique differential miRNA profiles in the model vaccines. Groups of BALB/c mice were vaccinated twice with vehicle (PBS), the live-attenuated vaccine (RSV CP52), the inactivated vaccine (FI-RSV), or the microparticle-based vaccine (GA2-MP) using a prime-boost regimen. Three weeks after the boost vaccination mice were challenged with $1x10^6$ PFU of RSV A2 via i.n. delivery. Sera miRNA profiles of vaccinated mice (n=4/group) were evaluated at **(A)** 7 days post-prime, **(B)** 14 days post-prime, **(C)** 7 days post-boost, **(D)** 14 days post-boost, **(E)** 3 days post-challenge, and **(F)** 5 days post-challenge using a miRNA PCR array. The venn diagrams depict the miRNA profiles for all vaccine candidates by time points. miRNA expression levels are normalized by SN1/2/3/4/5/6 expression. Values are represented as expression/mock treatment (PBS vaccinated/RSV A2 challenge) and fold change was calculated using $2^{(-\Delta\Delta CT)}$ method. Differential expression was determined using the following criteria, if the fold change was > 2, the result was reported as a fold upregulation. If the fold change was < 0.5, the result was reported as a fold downregulation.

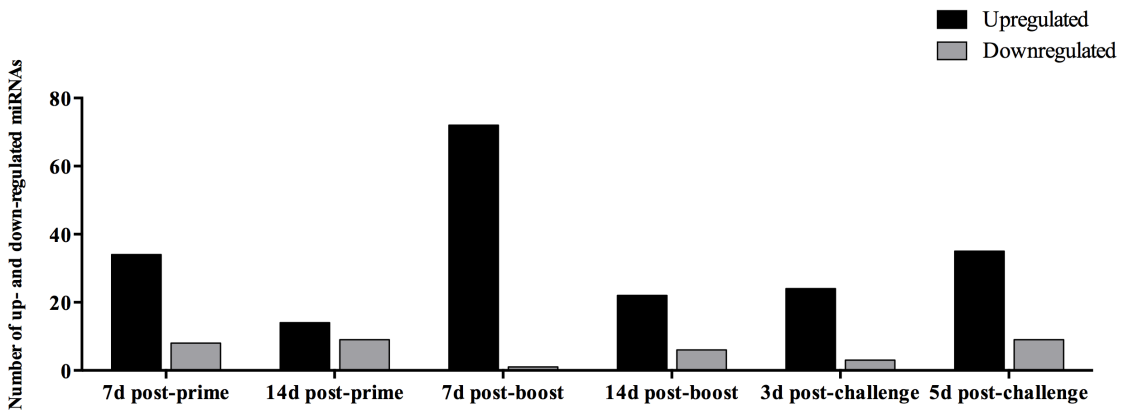

Fig. 4.8: The number of differentially expressed miRNAs during vaccination and post-RSV challenge. Sera miRNA profiles of vaccinated mice (n=4/group) were evaluated at 7 days post-prime, 14 days post-prime, 7 days post-boost, 14 days post-boost, 3 days post-challenge, and 5 days post-challenge using a miRNA PCR array. The y-axis indicates the number of differentially expressed miRNAs. Significance was determined using a fold change threshold of > 2, the result was reported as a fold upregulation. If the fold change was < 0.5, the result was reported as a fold downregulation.

A

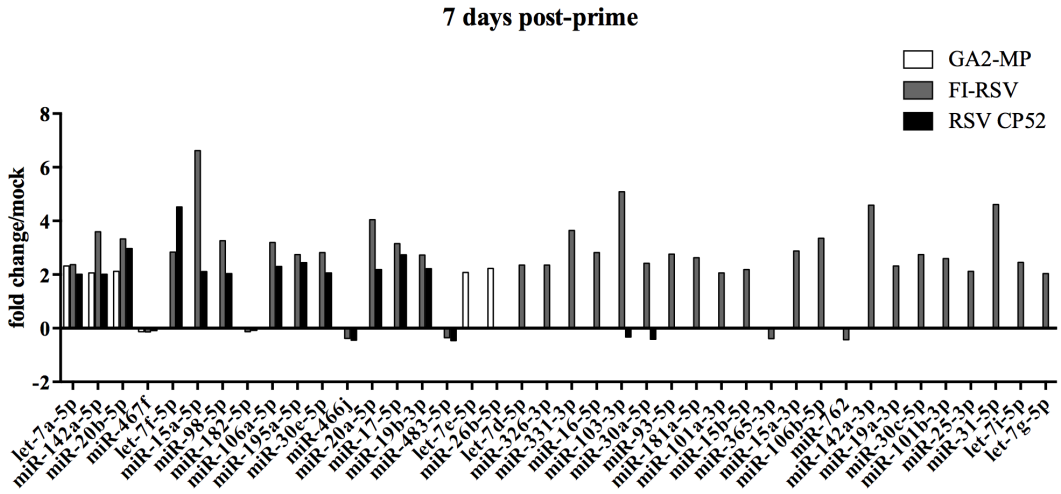
7 days post-prime
GA2-MP
FI-RSV
RSV CP52
fold change/mock
8
6
4
2
0
-2
let-7a-5p
miR-142a-5p
miR-20b-5p
miR-467f
let-7f-5p
miR-15a-5p
miR-98-5p
miR-182-5p
miR-106a-5p
miR-195a-5p
miR-30e-5p
miR-466j
miR-20a-5p
miR-17-5p
miR-19b-3p
miR-483-5p
let-7e-5p
miR-26b-5p
let-7d-5p
miR-326-3p
miR-331-3p
miR-16-5p
miR-103-3p
miR-30a-5p
miR-93-5p
miR-181a-5p
miR-101a-3p
miR-15b-5p
miR-365-3p
miR-15a-3p
miR-106b-5p
miR-762
miR-142a-3p
miR-19a-3p
miR-30c-5p
miR-101b-3p
miR-25-3p
miR-31-5p
let-7i-5p
let-7g-5p

B

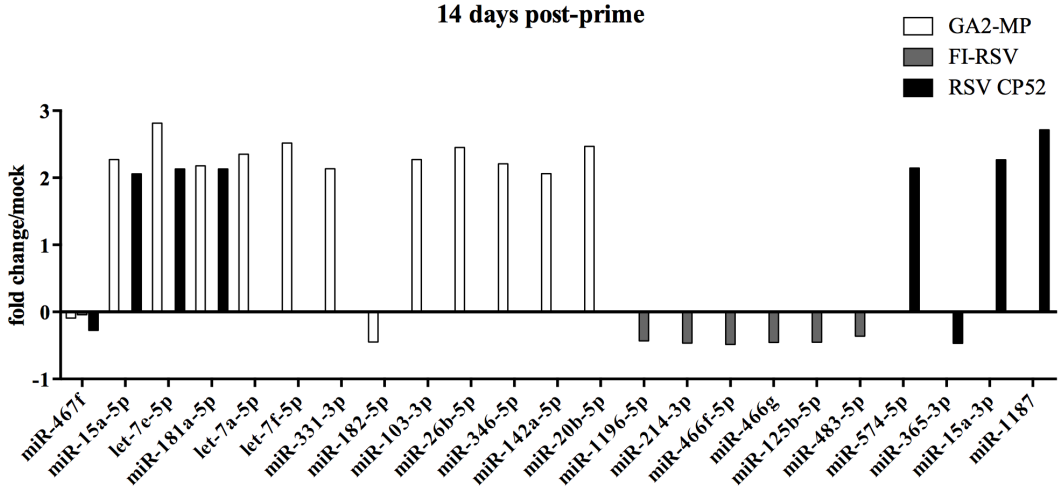
14 days post-prime
GA2-MP
FI-RSV
RSV CP52
fold change/mock
3
2
1
0
-1
miR-467f
miR-15a-5p
let-7e-5p
miR-181a-5p
let-7a-5p
let-7f-5p
miR-331-3p
miR-182-5p
miR-103-3p
miR-26b-5p
miR-346-5p
miR-142a-5p
miR-20b-5p
miR-1196-5p
miR-214-3p
miR-466f-5p
miR-466g
miR-125b-5p
miR-483-5p
miR-574-5p
miR-365-3p
miR-15a-3p
miR-1187

Fig. 4.9: Common and distinct differentially expressed miRNAs induced by the model vaccines at post-prime vaccination. Sera miRNA profiles of vaccinated mice (n=4/group) were evaluated at **(A)** 7 days and **(B)** 14 days post-prime using a miRNA PCR array. The relative expression levels of candidate miRNAs selected from the PCR array analysis were validated by RT-qPCR. Values are represented as fold change/mock (PBS vaccinated/RSV A2 challenge). miRNA levels were normalized by RU6B gene expression and all samples were run in duplicate. Fold change was calculated using $2^{(-\Delta\Delta CT)}$ method. Differential expression was determined using the following criteria, if the fold change was > 2, the result was reported as a fold upregulation. If the fold change was < 0.5, the result was reported as a fold downregulation.

A

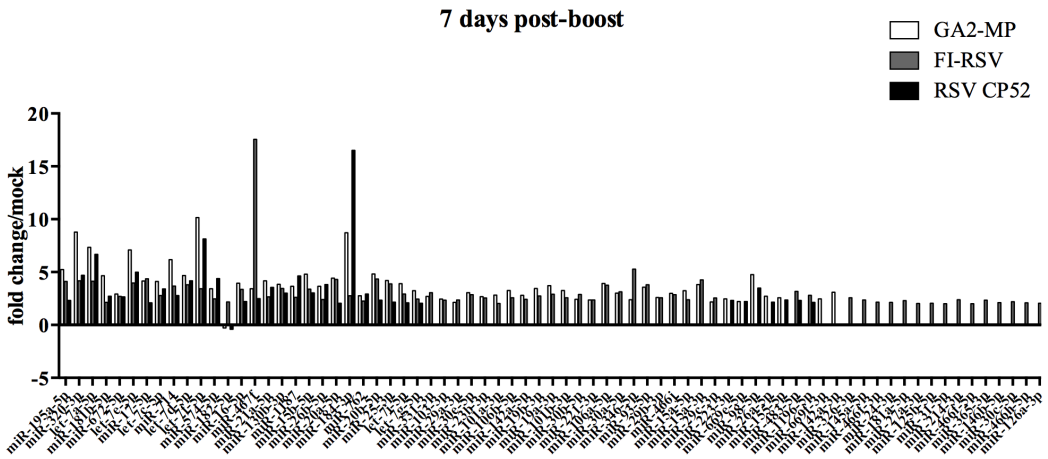
7 days post-boost
GA2-MP
FI-RSV
RSV CP52
fold change/mock
20
15
10
5
0
-5

B

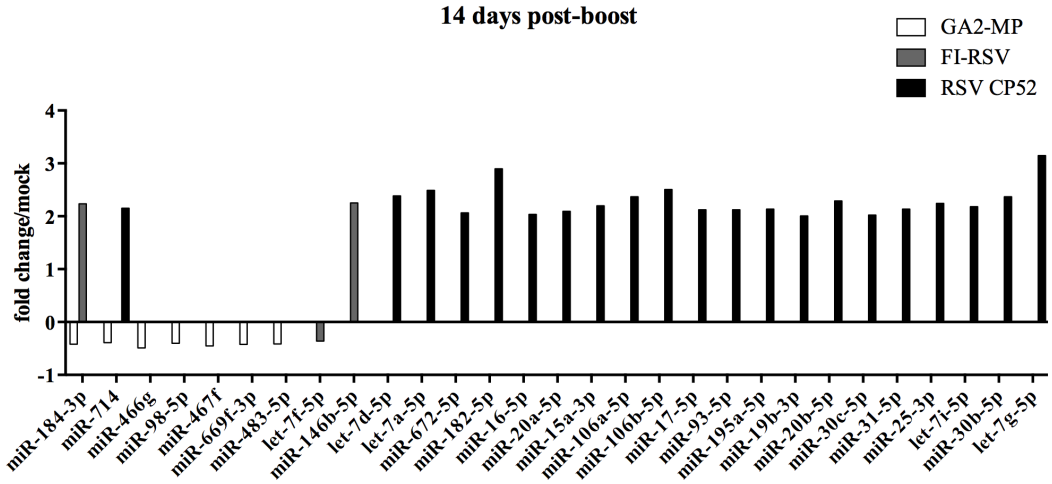
14 days post-boost
GA2-MP
FI-RSV
RSV CP52
fold change/mock
4
3
2
1
0
-1
miR-184-3p
miR-714
miR-466g
miR-98-5p
miR-467f
miR-669f-3p
miR-483-5p
let-7f-5p
miR-146b-5p
let-7d-5p
let-7a-5p
miR-672-5p
miR-182-5p
miR-16-5p
miR-20a-5p
miR-15a-3p
miR-106a-5p
miR-106b-5p
miR-17-5p
miR-93-5p
miR-195a-5p
miR-19b-3p
miR-20b-5p
miR-30c-5p
miR-31-5p
miR-25-3p
let-7i-5p
miR-30b-5p
let-7g-5p

Fig. 4.10: Common and distinct differentially expressed miRNAs induced by the model vaccines at post-boost vaccination. Sera miRNA profiles of vaccinated mice (n=4/group) were evaluated at **(A)** 7 days and **(B)** 14 days post-boost using a miRNA PCR array. The relative expression levels of candidate miRNAs selected from the PCR array analysis were validated by RT-qPCR. Values are represented as fold change/mock (PBS vaccinated/RSV A2 challenge). miRNA levels were normalized by RU6B gene expression and all samples were run in duplicate. Fold change was calculated using $2^{(-\Delta\Delta CT)}$ method. Differential expression was determined using the following criteria, if the fold change was > 2, the result was reported as a fold upregulation. If the fold change was < 0.5, the result was reported as a fold downregulation.

A

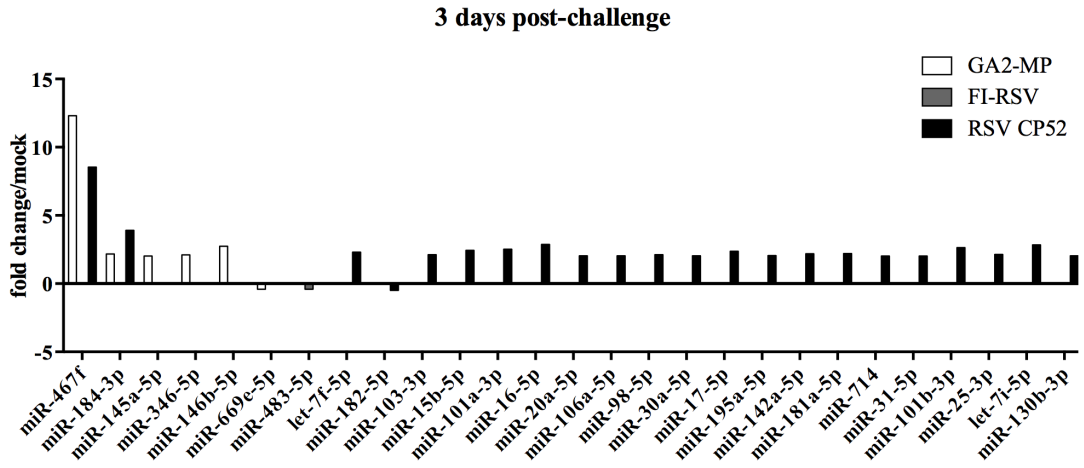
3 days post-challenge
GA2-MP
FI-RSV
RSV CP52
fold change/mock
15
10
5
0
-5
miR-467f
miR-184-3p
miR-145a-5p
miR-346-5p
miR-146b-5p
miR-669e-5p
miR-483-5p
let-7f-5p
miR-182-5p
miR-103-3p
miR-15b-5p
miR-101a-3p
miR-16-5p
miR-20a-5p
miR-106a-5p
miR-98-5p
miR-30a-5p
miR-17-5p
miR-195a-5p
miR-142a-5p
miR-181a-5p
miR-714
miR-31-5p
miR-101b-3p
miR-25-3p
let-7i-5p
miR-130b-3p

B

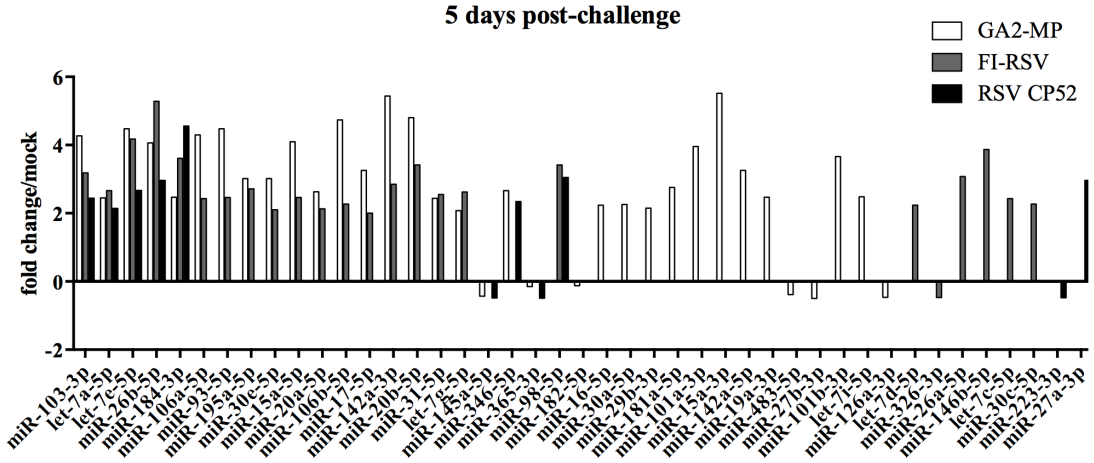
5 days post-challenge
GA2-MP
FI-RSV
RSV CP52
fold change/mock
6
4
2
0
-2
miR-103-3p
let-7a-5p
let-7e-5p
miR-26b-5p
miR-184-3p
miR-106a-5p
miR-93-5p
miR-195a-5p
miR-30c-5p
miR-15a-5p
miR-20a-5p
miR-106b-5p
miR-17-5p
miR-142a-3p
miR-20b-5p
miR-31-5p
let-7g-5p
miR-145a-5p
miR-346-5p
miR-365-3p
miR-98-5p
miR-182-5p
miR-16-5p
miR-30a-5p
miR-29b-3p
miR-181a-5p
miR-101a-3p
miR-15a-3p
miR-142a-5p
miR-19a-3p
miR-483-5p
miR-27b-3p
miR-101b-3p
let-7i-5p
miR-126a-3p
let-7d-5p
miR-326-3p
miR-26a-5p
miR-146b-5p
let-7c-5p
miR-30c-5p
miR-223-3p
miR-27a-3p

Fig. 4.11: Common and distinct differentially expressed miRNAs induced by the model vaccines at post-challenge with RSV A2. Sera miRNA profiles of vaccinated mice (n=4/group) were evaluated at **(A)** 3 days and **(B)** 5 days post-challenge with 10^6 PFU of RSV A2 using a miRNA PCR array. The relative expression levels of candidate miRNAs selected from the PCR array analysis were validated by RT-qPCR. Values are represented as fold change/mock (PBS vaccinated/RSV A2 challenge). miRNA levels were normalized by RU6B gene expression and all samples were run in duplicate. Fold change was calculated using $2^{(-\Delta\Delta CT)}$ method. Differential expression was determined using the following criteria, if the fold change was > 2, the result was reported as a fold upregulation. If the fold change was < 0.5, the result was reported as a fold downregulation.

Time point of differential miRNA expression	Number of miRNAs	miRNAs
Post-prime, post-boost, and post-challenge	11	miR-103-3p, let-7a-5p, let-7e-5p, miR-142a-5p, let-7f-5p, miR-182-5p, miR-467f, miR-346-5p, miR-15a-5p, miR-26b-5p, miR-20b-5p
Post-prime and post-boost	2	miR-331-3p, miR-98-5p
Post-prime and post-challenge	1	miR-181a-5p
Post-boost and post-challenge	19	miR-195a-5p, miR-30e-5p, miR-669e-5p, miR-101a-3p, miR-106b-5p, miR-15-5p, miR-142a-3p, miR-483-5p, miR-19a-3p, miR-16-5p, miR-106a-5p, miR-30a-5p, miR-93-5p, miR-29b-3p, miR-20a-5p, miR-15a-3p, miR-184-3p, let-7i-5p, let-7g-5p
Post-boost	25	miR-466g, miR-669f-3p, miR-29a-3p, miR-320-3p, miR-223-3p, miR-23b-3p, miR-181b-5p, miR-672-5p, miR-19b-3p, let-7c-5p, miR-714, miR-30b-5p, miR-221-3p, let-7d-5p, miR-574-5p, miR-26a-5p, miR-466j, miR-21a-5p, miR-1187, miR-130b-3p, miR-15b-5p, miR-762, miR-155-5p, miR-29c-3p, miR-25-3p
Post-challenge	7	miR-145a-5p, miR-27b-3p, miR-31-5p, miR-101b-3p, miR-365-3p, miR-146b-5p, miR-126a-3p

Table 4.1: Temporal miRNA expression of GA2-MP vaccinated mice. BALB/c mice (n=4/group) were vaccinated twice with vehicle (PBS), the live-attenuated vaccine (RSV CP52), the inactivated vaccine (FI-RSV), or the microparticle-based vaccine (GA2-MP) using a prime-boost regimen. Three weeks after the boost vaccination mice were challenged with $1x10^6$ PFU of RSV A2 via i.n. delivery. Using a miRNA PCR array, 84 miRNAs were evaluated to identify unique sera miRNA profiles in mice for the model vaccines. This table shows the tempo of common and unique differentially expressed miRNAs for GA2-MP vaccinated mice at post-prime (7 and 14 days), post-boost (7 and 14 days), and post-RSV challenge (3 and 5 days). miRNA expression levels are normalized by SN1/2/3/4/5/6 expression. Values are represented as expression/mock treatment (PBS vaccinated/RSV A2 challenge) and fold change was calculated using $2^{(-\Delta\Delta CT)}$ method. Differential expression was determined using the following criteria, if the fold change was > 2, the result was reported as a fold upregulation. If the fold change was < 0.5, the result was reported as a fold downregulation.

Time point of differential miRNA expression	Number of miRNAs	miRNAs
Post-prime, post-boost, and post-challenge	18	miR-326-3p, miR-103-3p, miR-195a-5p, miR-30e-5p, let-7a-5p, miR-106b-5p, miR-17-5p, miR-483-5p, miR-31-5p, let-7d-5p, let-7f-5p, miR-106a-5p, miR-93-5p, miR-15a-5p, miR-20a-5p, miR-20b-5p, miR-30c-5p, let-7g-5p
Post-prime and post-boost	22	miR-331-3p, miR-181a-5p, miR-101a-3p, miR-125b-5p, miR-142a-5p, miR-19b-3p, miR-19a-3p, miR-101b-3p, miR-214-3p, miR-182-5p, miR-16-5p, miR-467f, miR-30a-5p, miR-466j, miR-1196-5p, miR-466f-5p, miR-15b-5p, miR-15a-3p, miR-365-3p, miR-762, miR-25-3p, let-7i-5p
Post-prime and post-challenge	2	miR-98-5p, miR-142a-3p
Post-boost and post-challenge	5	Let-7e-5p, let-7c-5p, miR-26b-5p, miR-184-3p, miR-146b-5p
Post-prime	1	miR-466g
Post-boost	21	miR-145a-5p, miR-466f-3p, miR-24-3p, miR-29a-3p, miR-320-3p, miR-23b-3p, miR-181b-5p, miR-672-5p, miR-27a-3p, miR-714, miR-30b-5p, miR-221-3p, miR-574-5p, miR-346-5p, miR-29b-3p, miR-21a-5p, miR-1187, miR-130b-3p, miR-29c-3p, miR-466h-5p, miR-126a-3p
Post-challenge	1	miR-26a-5p

Table 4.2: Temporal miRNA expression of FI-RSV vaccinated mice. BALB/c mice (n=4/group) were vaccinated twice with vehicle (PBS), the live-attenuated vaccine (RSV CP52), the inactivated vaccine (FI-RSV), or the microparticle-based vaccine (GA2-MP) using a prime-boost regimen. Three weeks after the boost vaccination mice were challenged with $1x10^6$ PFU of RSV A2 via i.n. delivery. Using a miRNA PCR array, 84 miRNAs were evaluated to identify unique sera miRNA profiles in mice for the model vaccines. This table shows the tempo of common and unique differentially expressed miRNAs for FI-RSV vaccinated mice at post-prime (7 and 14 days), post-boost (7 and 14 days), and post-RSV challenge (3 and 5 days). miRNA expression levels are normalized by SN1/2/3/4/5/6 expression. Values are represented as expression/mock treatment (PBS vaccinated/RSV A2 challenge) and fold change was calculated using $2^{(-\Delta\Delta CT)}$ method. Differential expression was determined using the following criteria, if the fold change was > 2, the result was reported as a fold upregulation. If the fold change was < 0.5, the result was reported as a fold downregulation.

Time point of differential miRNA expression	Number of miRNAs	miRNAs
Post-prime, post-boost, and post-challenge	8	miR-182-5p, miR-106a-5p, miR-467f-miR-195a-5p, let-7a-5p, let-7e-5p, miR-20a-5p, miR-17-5p
Post-prime and post-boost	6	miR-574-5p, miR-1187, miR-15a-3p, miR-19b-3p, miR-483-5p, miR-20b-5p
Post-prime and post-challenge	2	miR-181a-5p, miR-365-3p
Post-boost and post-challenge	12	Let-7f-5p, miR-16-5p, miR-223-3p, miR-130b-3p, miR-15b-5p, miR-26b-5p, miR-98-5p, miR-184-3p, miR-714, miR-31-5p, miR-25-3p, let-7i-5p
Post-prime	6	miR-466f-3p, miR-30e-5p, miR-466j, miR-15a-5p, miR-142a-5p, miR-467b-3p, let-7d-5p
Post-boost	16	Let-7d-5p, miR-26a-5p, miR-93-5p, miR-320-3p, miR-21a-5p, miR-669e-5p, miR-181b-5p, miR-1196-5p, miR-672-5p, miR-106b-5p, miR-762, miR-155-5p, miR-30c-5p, let-7c-5p, miR-30b-5p, let-7g-5p
Post-challenge	8	miR-103-3p, miR-145a-5p, miR-30a-5p, miR-346-5p, miR-101a-3p, miR-27a-3p, miR-142a-3p, miR-101b-3p

Table 4.3: Temporal miRNA expression of RSV CP52 vaccinated mice. BALB/c mice (n=4/group) were vaccinated twice with vehicle (PBS), the live-attenuated vaccine (RSV CP52), the inactivated vaccine (FI-RSV), or the microparticle-based vaccine (GA2-MP) using a prime-boost regimen. Three weeks after the boost vaccination mice were challenged with $1x10^6$ PFU of RSV A2 via i.n. delivery. Using a miRNA PCR array, 84 miRNAs were evaluated to identify unique sera miRNA profiles in mice for the model vaccines. This table shows the tempo of common and unique differentially expressed miRNAs for RSV CP52 vaccinated mice at post-prime (7 and 14 days), post-boost (7 and 14 days), and post-RSV challenge (3 and 5 days). miRNA expression levels are normalized by SN1/2/3/4/5/6 expression. Values are represented as expression/mock treatment (PBS vaccinated/RSV A2 challenge) and fold change was calculated using $2^{(-\Delta\Delta CT)}$ method. Differential expression was determined using the following criteria, if the fold change was > 2, the result was reported as a fold upregulation. If the fold change was < 0.5, the result was reported as a fold downregulation.

Supplemental information

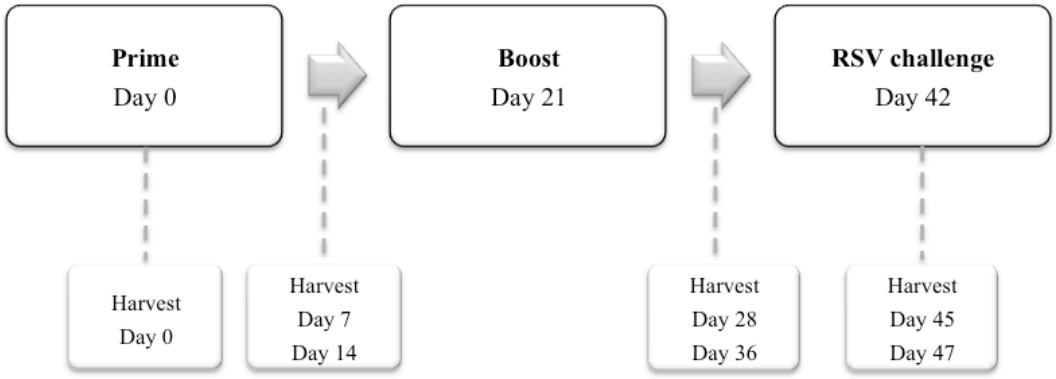

Group	Vaccine	Route	Challenge
Naïve	-	-	-
Vehicle	PBS	s.c.	$1x10^6$ PFU of RSV A2
Live-attenuated vaccine	RSV CP52	i.n.	$1x10^6$ PFU of RSV A2
Inactivated vaccine	FI-RSV A2	i.m.	$1x10^6$ PFU of RSV A2
Microparticle-based vaccine	GA2-MP	s.c.	$1x10^6$ PFU of RSV A2

Fig. S4.1: Vaccination schedule for *in vivo* BALB/c mouse studies. 4 mice per group were vaccinated twice with vehicle (PBS), the live-attenuated vaccine (RSV CP52), the inactivated vaccine (FI-RSV A2), or the microparticle-based vaccine (GA2-MP) using a prime-boost regimen. Control mice (naïve) received no vaccinations. At day 42 (three weeks after boost vaccination) mice were challenged with $1x10^6$ PFU of RSV A2 via i.n. delivery. Naïve mice did not receive virus. Mice were sacrificed at various time points post-prime, post-boost, and post-challenge to harvest sera and tissues to assess miRNA expression levels and other immune correlates.

CHAPTER 5

CHARACTERIZATION OF MICRORNAS IN LUNG EPITHELIAL CELLS IN RESPSONSE TO RSV ANTIGENS AND VACCINES[1]

[1] Anderson L, Jorquera PA, Williams CM, Tripp RA. To be submitted to *Journal of Virology*.

Abstract

Respiratory syncytial virus (RSV) is the leading cause of viral bronchiolitis and pneumonia worldwide, and therefore a major health and economic burden (1). Despite over half a century of dedicated research, there remains no licensed vaccine and no effective licensed therapeutics. A large number of studies suggest that early inflammatory and immune events characteristic of the innate host response may be crucial in determining the outcome of acute RSV infection as well as its potential long-term consequences, such as asthma and airway hyperresponsiveness (2-5). Various microRNAs (miRNAs) have been identified to have critical roles in modulating multiple allergic airway inflammatory diseases (6-11). To date however, few studies have been performed to elucidate the role of miRNA-dependent mechanisms in virus-induced immune response in the airways. Airway epithelial cells are the main targets for RSV infection, as well as the preliminary site for the activation of the innate immune response (1, 2). The rationale for this study is that by utilizing an *in vitro* model of lung epithelial cells, we are able to determine alterations in the expression of miRNAs implicated in the innate immune response to RSV. In addition, the expression of miRNAs was also evaluated intracellularly using a novel P19 protein-based immunostaining method, and demonstrate that both RSV-infected and uninfected cells produce miRNAs during RSV infection. Our studies indicate that miRNAs appear to have an important role in the host response to RSV infection, and multiple miRNAs are induced by infection in lung epithelial cells.

Introduction

The innate immune response is the first line of host defense against invading pathogens. The respiratory epithelium provides a protective physical barrier against injurious inhaled stimuli, and therefore is the main target of RSV (2). Following infection of the local respiratory epithelium, respiratory syncytial virus (RSV) spreads along the respiratory tract via cell-to-cell transfer of the virus along the intracytoplasmic bridges (2). After attachment to epithelial cells, RSV induces NF-κB-mediated gene transcription promoting an antiviral state (1). Epithelial cells also express a variety of pathogen pattern recognition receptors (PRRs), such as Toll-like receptors (TLRs) and nucleotide binding and oligomerization domain-like receptors (NLRs), which recognize pathogens or pathogen-associated molecular patterns (PAMPs) (12). Recognition of RSV by TLRs on respiratory epithelial cells promotes the secretion of inflammatory cytokines and chemokines. Accordingly, within hours after RSV infection, an enhanced expression of genes related to local inflammatory responses, antigen processing and chemoattraction are observed in the lung epithelium (1). These processes promote the production of chemokines and the recruitment of eosinophils, NK cells, and CD4+ T cells to the airways (1). However, the immune response must maintain a balance between pro-inflammatory and anti-inflammatory mediators, as excessive inflammation can exacerbate tissue damage and cause chronic inflammatory diseases (12).

miRNAs, a class of small noncoding RNA molecules, may participate in the modulation of epithelial immune responses at various steps of the innate immune system, including production and release of cytokines and chemokines, expression of adhesion and costimulatory molecules, shuttling of miRNAs through release of extracellular

vesicles, and feedback regulation of immune homeostasis (12). Furthermore, the immune response to respiratory viruses such as rhinovirus, influenza virus, and respiratory syncytial virus is associated with an altered expression of distinct miRNAs, and alterations in the miRNA expression profile in epithelial cells may contribute to the pathogensis of both acute and chronic airway disease (13). By affecting post-transcriptional gene expression, acting on mRNAs by either translational inhibition or mRNA decay, miRNAs are involved in the regulation of immunological and nonimmunological cellular functions (13). In addition, miRNAs can be shuttled through epithelial cell-derived exosomes. Exosomes are small 30-90 nm extracellular vesicles derived from the multivesicular body sorting pathway and are produced by a variety of cells including epithelial cells (12). More specifically, a variety of cellular gene products, such as proteins, mRNAs, and miRNAs, are packaged in exosomes, and exosome secretion allows the contents to be transferred to recipient cells (12, 14). Previous studies have shown that there exists a class of miRNAs that are preferentially sorted into exosomes, such as miR-320 (15-20)29,41,52,55,56 and miR-150 (15, 18, 19, 21-23).

Previous studies in our laboratory have demonstrated that specific miRNAs show altered expression patterns between naïve, RSV-infected, and vaccinated mice, which correlate with other immune correlates and clinical endpoints suggesting that these miRNAs may modulate RSV pathogenesis (unpublished work). We hypothesized that miRNAs implicated in chronic inflammatory diseases of the lung will show altered expression profiles in lung epithelial cells during RSV infection, allowing for the potential identification and development of miRNA biomarkers. Using mouse lung epithelial (MLE-15) cells and human airway epithelial (CALU3) cells, an *in vitro* model

was developed to evaluate both cellular and exosome-derived miRNA expression patterns in RSV-infected cells by RT-qPCR. Expression of miRNAs was also evaluated *in vitro* using a novel P19 protein-based staining technique. P19 is a 19 kDa protein that binds 21-25 mer double-stranded RNAs (dsRNAs) with high affinity in a size dependent and sequence independent fashion, making it a pan-miRNA marker of cellular processes.

Materials and Methods

Cell culture and viruses

MLE-15 cells (ATCC CRL-2110) were cultured in HITES media [RPMI 1640 media (Cellgro, Manassas, VA) with 10 nM hydrocortisone (Sigma-Aldrich, St. Louis, MO), 10 nM β-estradiol (Sigma-Aldrich), 2 mM L-glutamine (Gibco, Carlsbad, CA), and 1% ITS (insulin-transferring-selenium; Gibco)] with 4% exosome-free FBS (Systems Bioscience, Inc., Palo Alto, CA). CALU3 cells (ATCC HTB-55) were cultured in Dulbecco's modified Eagle's medium (DMEM; Cellgro) with 1% Non-essential amino acids (NEAA-100x; Gibco), 2 mM L-glutamine (Gibco), 0.1% HEPES buffer (Gibco), and 20% exosome-free FBS (Systems Bioscience, Inc.). Mycoplasma-free virus stock of wild type RSV A2 was propagated in Vero E6 cells (ATCC CRL-1586) as described (24). Briefly, upon detectable cytopathic effect cells were scraped and collected in 50 mL conical tubes, then virus was harvested by sonicating scraped cells three times for 10 sec intervals at maximum power, followed by centrifugation to pellet the cell debris. Virus supernatant, divided into 1 mL aliquots, was stored at -80°C until needed. Virus titers were determined through immunostaining plaque assay on Vero E6 cells as described previously (25). The RSV A2 was ultraviolet (UV)-inactivated (> 170 J/m^2) by exposure

to UV light on ice, and inactivated viruses were assayed by immunostaining plaque assay to confirm inactivation (25).

Infection assays

24h prior to RSV infection, MLE-15 and CALU3 cells were seeded on 24-well plates (Corning Life Sciences, Corning, NY). MLE-15 and CALU3 cells were then infected for 2h incubation at 37°C with live RSV A2 at multiplicity of infection (MOI) = 1 or 0.1, UV-inactivated RSV A2 (uvRSV) equivalent to MOI=1 , or mock (Vero E6 cell lysate). After 2h incubation at 37°C, cells were rinsed with PBS and replenished with culture media without virus. Supernatants were harvested at 8h, 24h, and 48h after infection and exosome isolation was performed, and subsequently RNA isolation from the exosome pellet. RNAzol®RT (Molecular Research Center, Inc. Cincinnati, OH) was then added to each well to harvest cell lysate and total RNA isolation was performed.

Exosome isolation

500 µl of supernatant per well was used for exosome isolation using ExoQuick-TC™ for Tissue Culture Media and Urine (System Biosciences (SBI), Palo Alto, CA) as directed by manufacturer's protocol. Briefly, the supernatant was centrifuged at 3,000 x g for 15 minutes to remove cells and cell debris. The supernatant was transferred to a sterile 1.5 ml microcentrifuge tube and incubated with 100 µl of ExoQuick-TC overnight at 4°C. The ExoQuick-TC/supernatant mixture was centrifuged at 1,500 x g for 30 min at 4°C. The supernatant was aspirated, and the residual ExoQuick-TC was spun down by centrifugation at 1,500 x g for 5 min at 4°C. All traces of fluid were removed by

aspiration, taking great care not to disturb the precipitated exosomes in pellet. Exosome RNA isolation was then performed using RNAzol®RT (Molecular Research Center, Inc.).

RNA isolation

Total RNA was isolated from cell lysate or exosome pellet using RNAzol®RT (Molecular Research Center, Inc) following manufacture protocol for isolation of total RNA. Briefly, 1 ml of RNAzol®RT (up to 100 mg of tissue per 1 mL of RNAzol®RT) was added to cell lysate or exosome pellet. 0.4 mL of water per 1 mL of RNAzol®RT was then added to the homogenate/lysate. The resulting mixture was vigorously shaken for 15 sec and stored at room temperature for 15 minutes. Samples were then centrifuged at 12, 000 x g for 15 min at 4°C. Following centrifugation, DNA, protein and most polysaccharides were precipitate at the bottom of the tube. 1ml of the supernatant was transferred to a new 2 ml microcentrifuge tube. RNA precipitation was accomplished by mixing 1 ml of the supernatant with 1 ml of isopropanol and 1µl of polyacryl carrier (Molecular Research Center, Inc.), samples were stored for 10 minutes at room temperature and then centrifuged at 12,000 x g for 10 min at 4°C. The RNA pellet was washed twice by mixing the RNA pellet with 75% ethanol (v/v) and then centrifuged at 8, 000 x g for 3 minutes. Residual alcohol solution was removed using a micropipette, and the RNA pellet was dried using a vacufuge® vacuum concentrator (Eppendorf) at 45 °C for approximately 6 minutes. RNA was solubilized in 20µl of RNase free water. The quantity of total RNA was determined using Epoch™ microplate spectrophotomer controlled with the Gen5 Data Analysis software interface (BioTek).

RT-qPCR for miRNA detection

To elongate the miRNAs, total RNA (100 ng of total RNA per sample) was polyadenylated with *E. coli* poly A polymerase (PAP) to generate a poly-A tail at the 3' end of each RNA molecule using the miRNA 1st-Strand cDNA Synthesis Kit (Agilent Technologies Cat. # 600036) following the manufactured protocol. Following polyadenylation, the RNA was used as template to synthesize 1st-strand cDNA using the miRNA 1st-Strand cDNA Synthesis Kit (Agilent Technologies Cat. # 600036) following the manufactured protocol. The cDNA was then diluted in 280 μl of RNase-free water for each 20 μl reaction. Brilliant III Ultra-Fast SYBR Green QPCR Master Mix (Agilent Technologies Cat. # 600886) was used for qPCR to quantify the expression levels of miR-21, miR-106, miR-126, miR-145, miR-146a, miR-146b, miR-155, Let-7d, and Let-7f in each sample. To screen for contamination, a no-PAP control cDNA template was prepared from the polyadenylated reaction (in which the PAP was omitted) and included in the qPCR reactions. All samples were run in triplicate and n=4 wells per group. All miRNA levels were normalized by mouse-specific 18S rRNA (Applied Biosystems Cat. # 4331182) gene expression. The 2^-ΔΔCt method was utilized to calculate expression fold change infected/mock.

P19 protein-based staining

At 8h, 24h, and 48h post-infection, media was removed from the 24-well transwell plates (Corning Life Sciences) and MLE-15 cells were washed three times with Phosphate Buffered Saline (PBS; GE Healthcare HyClone). The MLE-15 cells were then fixed at room temperature overnight by adding 10% Buffered Formalin (Fisher

Scientific) to the basal and apical chambers of the transwell plates. The following day, formalin was removed and discarded in appropriate waste container and cells were washed three times with PBS (GE Healthcare HyClone) to remove residual formalin. The fixed cells were then permeabilized by adding 0.5% Triton X-100 diluted in PBS (GE Healthcare HyClone) to basal and apical chambers and incubating at room temperature for 15 minutes. The 0.5% Triton X-100 was then removed and cells were washed three times with PBS (GE Healthcare HyClone). The transwell plates were then blocked (both basal and apical chambers) with 3% BSA + 0.01% Tween-20 in PBS for one hour at room temperature on rocker. The transwell plates were then washed three times with 0.01% Tween-20 in PBS for 15 minutes at room temperature on the rocker. Monoclonal antibodies against RSV F protein (clone 131-2A) were then added (1:500 dilution in 3% BSA + 0.01% Tween-20 in PBS) and incubated for one hour at room temperature on the rocker. Transwell plates were then washed three times with 0.01% Tween-20 in PBS at room temperature on the rocker. Secondary antibody goat anti-mouse IgG conjugated to Alexa Fluor 546 (ThermoFisher Scientific Cat. # A-11030) was added (1:1000 dilution in 3% BSA + 0.01% Tween-20 in PBS) and incubated for one hour at room temperature on the rocker. Transwell plates were then washed three times with 0.01% Tween-20 in PBS at room temperature on the rocker. P19 binding protein (New England BioLabs Inc. Cat. # M0310L) was added (1:50 dilution in 3% BSA + 0.01% Tween-20 in PBS) and incubated for one hour at room temperature on the rocker. Transwell plates were then washed three times with 0.01% Tween-20 in PBS at room temperature on the rocker. Anti-CBD monoclonal antibody (New England BioLabs Inc. Cat. # E8034S) was added (1:50 dilution in 3% BSA + 0.01% Tween-20 in PBS) and incubated for one hour at room

temperature on the rocker. Transwell plates were then washed three times with 0.01% Tween-20 in PBS at room temperature on the rocker. Secondary antibody goat anti-rabbit IgG conjugated to Alexa Fluor 488 (ThermoFisher Scientific Cat. # A-11008) was added (1:1000 dilution in 3% BSA + 0.01% Tween-20 in PBS) and incubated for one hour at room temperature on the rocker. 4',6-diamidino-2-phenylindole (DAPI) (at 1:5000 dilution in 3% BSA + 0.01% Tween-20 in PBS) was then added for 5 minutes at room temperature on the rocker. Transwell plates were then washed three times with 0.01% Tween-20 in PBS at room temperature on the rocker. The transwell membrane from each well was removed using a scalpel blade and mounted on microscope slides, then 1 drop of ProLong Diamond Antifade Mountant (ThermoFisher Scientific Cat. # P36961) was added to each transwell membrane and a coverslip was placed on top. The slides sat overnight in a Biological Safety Cabinet (BSC) with the fan on and protected from light. The following day, the edges where the slide and coverslip meet were sealed with clear nail varnish. The slides were then imaged on the EVOS FL Cell Imaging System (ThermoFisher Scientific).

miRNA primers

Mouse-specific miRNA sequences were obtained from miRBase for the miRNAs of interest. Forward primers were designed based on the mature-miRNA sequence with the greatest number of deep-sequencing reads, and synthesized by Integrated DNA Technologies (IDT). The mouse-specific miRNA primers have 100% sequence homology with the human miRNA sequence; with the exception of miR-106a, which has two point mutations (Table 5.1).

Statistical analysis

All statistical analyses were performed using GraphPad Prism 6.0h (La Jolla, CA). The data is presented as the mean±standard error of the mean (SEM). Statistical significance was determined using One-way ANOVA followed by Bonferroni's or Dunnett's post-hoc comparisons tests, a P value ≤ 0.05 was considered significant.

Results

Alterations in miRNA expression patterns in lung epithelial cells during infection with live RSV and uvRSV.

The constant battle between the host and the virus for survival necessitates the continued evolution of novel and improved mechanisms of gene regulation (26). A newly emerging approach of gene regulation is that of miRNAs that can regulate gene expression at the level of mRNA stability and translational efficiency (26). In order to fully comprehend the intricate interaction of the host and the virus during infection, the impact of miRNAs on changes in gene regulation and cellular communication is an important consideration. To determine the differential miRNA expression profile of MLE-15 and CALU3 cells to RSV infection, cells were infected for 2h incubation at 37°C with live RSV A2 at MOI = 1 or 0.1, UV-inactivated RSV A2 (uvRSV) equivalent to MOI = 1, or mock (Vero E6 cell lysate) and RNA was harvested from the cell lysate and exosomes at 8h, 24, and 48h post infection (Fig.S5.1). The pattern and tempo of expression for nine host miRNAs associated with critical roles in asthma and airway hyperresponsiveness were evaluated by RT-qPCR to define those that were RSV- and

uvRSV- specific. In addition, cellular and exosomal miRNA expression levels were evaluated to determine if lung epithelial cells undergo a preferential sorting mechanism that guides specific intracellular miRNAs to exosomes during RSV infection. Overall, 24 hpi appears to be the optimal time point for assessing miRNA expression levels (Table 2).

A unique pattern and tempo of miR-21 expression was observed between the epithelial cell types, and within that the alterations in miRNA expression appear to be time point and MOI dependent (Fig. 5.1). The fold change in miR-21 expression levels ranged from 0.4-6.8 in the cell lysate and 0.5-12.0 in the exosomes in MLE-15 cells (Fig.5.1A); where as in CALU3 cells, the fold change in miR-21 expression levels ranged from 0.1 to 22.0 and 0.07 to 6.9 in cell lysate and exosomes, respectively (Fig.5.1B). miR-106 expression levels were increased, in general, among all infection conditions across all time points in MLE-15 cells (Fig.5.2A), however miR-106 expression levels were only upregulated at 24 hpi in CALU3 cells (Fig.5.2B). MLE-15 and CALU3 cells showed differential miR-126 expression levels at all time points (8, 24, and 48 hpi) (Fig.5.3), with a notable increase in exosome-derived miR-126 expression levels in MLE-15 cells among all infection conditions at 24 hpi and 48 hpi (Fig.5.3A). Overall miR-145, miR-146a, and miR-146b expression levels were lower in CALU3 cells compared to MLE-15 cells, however there was a unique pattern and tempo of expression among the time points in both cell lines (Fig.5.4-5.6). In addition, miR-146b expression levels were upregulated among all infection conditions by 8 hpi in both MLE-15 and CALU3 cells (Fig.5.6). MLE-15 cells showed enhanced exosome-derived miR-155 expression at 24 hpi and 48 hpi among all infection conditions, with the fold changes ranging from 1.7 to

53.9 folds (Fig.5.7A). At 24 hpi, exosome-derived miR-155 expression was highly upregulated in CALU3 cells infected with live RSV A2 at MOI=1 (~116.1 fold change), live RSV A2 at MOI=0.1 (~73.9 fold change), and UvRSV (~37.6 fold change) over mock treated cells, however this tempo of expression was reduced by 48 hpi (Fig.5.7B). Let-7d and let-7f expression levels were substantially increased in MLE-15 cells compared to CALU3 cells (Fig.5.8-5.9). Interestingly, MLE-15 cells showed upregulated exosome-derived let-7d expression levels among all infection conditions at 24 hpi (Fig.5.8A), where as CALU3 cells did not show a similar trend until 48 hpi (Fig.5.8B). Taken together, this data demonstrates that miRNAs have a unique pattern and tempo of expression in RSV-infected lung epithelial cells, and that certain miRNAs are potentially preferentially loaded into exosomes. In addition, MLE-15 and CALU3 cells infected with uvRSV were still capable of producing detectable miRNA expression levels, demonstrating that viral replication is not necessary for miRNA induction.

Both RSV-infected and uninfected epithelial cells induce intracellular miRNA expression

Expression of miRNAs was also evaluated intracellularly using a novel P19 protein-based immunostaining technique. P19 RNA binding protein from the Carnation Italian ringspot virus (CIRV), a plant tombusvirus, is an RNA-silencing suppressor that binds small interfering RNA (siRNA) with high affinity (27). The dimeric P19 protein binds 21-25 mer dsRNA in a size-dependent sequence-independent manner (27). To visualize miRNA expression in RSV-infected lung epithelial cells, MLE-15 cells were infected with live RSV A2 (MOI=1 and 0.1), uvRSV (equivalent to MOI=1), or mock

(Vero E6 cell lysate). RSV F protein expression, miRNA expression, and DAPI staining was evaluated by immunofluorescence at 8, 24, and 48 hpi. At all time points miRNA expression was visible in live RSV A2, uvRSV, and mock infected cells (Fig.5-10-5.12). In addition, miRNA expression was visible in both RSV-infected cells and uninfected cells at all time points (Fig.5.10-5.12), but appeared reduced in uvRSV-infected cells by 24 and 48 hpi (Fig.5.11-5.12). miRNA expression was also visible outside the nucleus of the cells, as shown by the overlay + DAPI images (Fig.5.10-5.12). Taken together, these studies provide proof-of-concept for a novel immunostaining technique for the visualization of intracellular miRNA expression. In addition, both RSV-infected and uninfected lung epithelial cells induced miRNA expression. However additional epithelial cell surface markers and confocal microscopy is required to determine the precise location of the miRNAs (Fig.5.10-5.12).

Discussion

These studies identified key differences in cellular and exosome miR-associated expression patterns in RSV-infected cells, and also evaluated the pattern and tempo of intracellular and exosome-derived miRNA expression levels using live RSV and uvRSV. In addition, our studies indicate that exosomes preferentially incorporate specific miRNAs as their cargo during RSV infection, as noted by the upregulated exosome-derived miR-associated expression patterns of miR-126, miR-155, let-7d, and let-7f.

Interestingly, miR-155 has been found as enriched in exosomes derived from tumor cell lines or peripheral blood from cancer patients (15, 21, 23), providing evidentiary support for preferential sorting of this miRNA into exosomes. In addition,

recent literature indicates that mammals may response with miRNAs as a part of the host inflammatory response mounted against pathogens, including cytokines such as interferons (IFNs) (28). IFN-β treatment has been shown to induce miR-155 expression in macrophage cells in a Jun N-terminal protein kinase (JNK)-dependent manner, possibly dependent upon TNF-α (28, 29).

Members of the let-7 family also target IL-6 expression, and has an extensive list of other experimentally validated targets, including SOCS4, caspase-3, p27, TLR4, IL-13, and IL10 (28). Let-7 regulation could be a mechanism of IL-6 secretion during RSV infection (28). As RSV infection induces secretion of numerous proinflammatory cytokines, including type I and type II IFNs, TNF-α, IL-12, and IL-6 (28, 30-32). In addition, two RSV nonstructural proteins, NS1 and NS2, inhibit the induction of host miRNAs, revealing how complex and multilayered the interaction is between paramyxoviruses and the innate response in epithelial cells (28, 33).

In summary, miRNAs appear to have an important role in the host response to RSV infection, and multiple miRNAs are induced by infection, in a cell-type-specific fashion. The miRNA profiles evaluated here are linked to expression in epithelial cells, however other cell types are likely contributing to the miRNA environment during RSV infection. Furthermore, using a novel P19 protein-based staining technique, we are able to demonstrate that both RSV-infected and uninfected cells produce miRNAs, and that these miRNA profiles are detectable by 8 hpi, and sustained till at least 48 hpi. In addition, our results have identified common miRNAs whose expression change in regard to inflammatory responses, therefore commonalities in the changing expression of specific miRNAs during the host inflammatory responses suggest that these miRNAs

may have a critical role in the innate response mounted against pathogens and other lung injuries.

References

1. Bueno SM, Gonzalez PA, Pacheco R, Leiva ED, Cautivo KM, Tobar HE, et al. Host immunity during RSV pathogenesis. International immunopharmacology. 2008;8(10):1320-9.
2. Garofalo RP, Haeberle H. Epithelial regulation of innate immunity to respiratory syncytial virus. American journal of respiratory cell and molecular biology. 2000;23(5):581-5.
3. Everard ML. The relationship between respiratory syncytial virus infections and the development of wheezing and asthma in children. Current opinion in allergy and clinical immunology. 2006;6(1):56-61.
4. Wang SZ, Forsyth KD. Asthma and respiratory syncytial virus infection in infancy: is there a link? Clinical and experimental allergy : journal of the British Society for Allergy and Clinical Immunology. 1998;28(8):927-35.
5. Openshaw PJ, Dean GS, Culley FJ. Links between respiratory syncytial virus bronchiolitis and childhood asthma: clinical and research approaches. The Pediatric infectious disease journal. 2003;22(2 Suppl):S58-64; discussion S-5.
6. Sharma A, Kumar M, Ahmad T, Mabalirajan U, Aich J, Agrawal A, et al. Antagonism of mmu-mir-106a attenuates asthma features in allergic murine model. Journal of applied physiology (Bethesda, Md : 1985). 2012;113:459-64.

7. Collison A, Herbert C, Siegle JS, Mattes J, Foster PS, Kumar RK. Altered expression of microRNA in the airway wall in chronic asthma: miR-126 as a potential therapeutic target. BMC pulmonary medicine. 2011;11:29.

8. Lu TX, Rothenberg ME. Diagnostic, functional, and therapeutic roles of microRNA in allergic diseases. The Journal of allergy and clinical immunology. 2013;132:3-13; quiz 4.

9. Mattes J, Collison A, Plank M, Phipps S, Foster PS. Antagonism of microRNA-126 suppresses the effector function of TH2 cells and the development of allergic airways disease. Proceedings of the National Academy of Sciences of the United States of America. 2009;106:18704-9.

10. Oglesby IK, McElvaney NG, Greene CM. MicroRNAs in inflammatory lung disease--master regulators or target practice? Respiratory research. 2010;11:148.

11. Foster PS, Plank M, Collison A, Tay HL, Kaiko GE, Li J, et al. The emerging role of microRNAs in regulating immune and inflammatory responses in the lung. Immunol Rev. 2013;253(1):198-215.

12. Zhou R, O'Hara SP, Chen XM. MicroRNA regulation of innate immune responses in epithelial cells. Cell Mol Immunol. 2011;8(5):371-9.

13. Globinska A, Pawelczyk M, Kowalski ML. MicroRNAs and the immune response to respiratory virus infections. Expert review of clinical immunology. 2014;10(7):963-71.

14. Valadi H, Ekstrom K, Bossios A, Sjostrand M, Lee JJ, Lotvall JO. Exosome-mediated transfer of mRNAs and microRNAs is a novel mechanism of genetic exchange between cells. Nature cell biology. 2007;9(6):654-9.

15. Zhang J, Li S, Li L, Li M, Guo C, Yao J, et al. Exosome and exosomal microRNA: trafficking, sorting, and function. Genomics, proteomics & bioinformatics. 2015;13(1):17-24.

16. Skog J, Wurdinger T, van Rijn S, Meijer DH, Gainche L, Sena-Esteves M, et al. Glioblastoma microvesicles transport RNA and proteins that promote tumour growth and provide diagnostic biomarkers. Nature cell biology. 2008;10(12):1470-6.

17. Liao J, Liu R, Yin L, Pu Y. Expression profiling of exosomal miRNAs derived from human esophageal cancer cells by Solexa high-throughput sequencing. Int J Mol Sci. 2014;15(9):15530-51.

18. Guduric-Fuchs J, O'Connor A, Camp B, O'Neill CL, Medina RJ, Simpson DA. Selective extracellular vesicle-mediated export of an overlapping set of microRNAs from multiple cell types. BMC genomics. 2012;13:357.

19. Squadrito ML, Baer C, Burdet F, Maderna C, Gilfillan GD, Lyle R, et al. Endogenous RNAs modulate microRNA sorting to exosomes and transfer to acceptor cells. Cell Rep. 2014;8(5):1432-46.

20. Huang X, Yuan T, Tschannen M, Sun Z, Jacob H, Du M, et al. Characterization of human plasma-derived exosomal RNAs by deep sequencing. BMC genomics. 2013;14:319.

21. Rana S, Malinowska K, Zoller M. Exosomal tumor microRNA modulates premetastatic organ cells. Neoplasia. 2013;15(3):281-95.

22. Ogata-Kawata H, Izumiya M, Kurioka D, Honma Y, Yamada Y, Furuta K, et al. Circulating exosomal microRNAs as biomarkers of colon cancer. PLoS One. 2014;9(4):e92921.

23. Taylor DD, Gercel-Taylor C. MicroRNA signatures of tumor-derived exosomes as diagnostic biomarkers of ovarian cancer. Gynecol Oncol. 2008;110(1):13-21.

24. Tripp RA, Moore D, Jones L, Sullender W, Winter J, Anderson LJ. Respiratory syncytial virus G and/or SH protein alters Th1 cytokines, natural killer cells, and neutrophils responding to pulmonary infection in BALB/c mice. J Virol. 1999;73(9):7099-107.

25. Murphy BR, Sotnikov AV, Lawrence LA, Banks SM, Prince GA. Enhanced pulmonary histopathology is observed in cotton rats immunized with formalin-inactivated respiratory syncytial virus (RSV) or purified F glycoprotein and challenged with RSV 3-6 months after immunization. Vaccine. 1990;8(5):497-502.

26. Bruce SR, Alcorn JL. RSV Induced Changes in miRNA Expression in Lung. 2011. In: Human Respiratory Syncytial Virus Infection [Internet]. InTech. Available from: http://www.intechopen.com/books/human-respiratory-syncytial-virus-infection/rsv-induced-changes-in-mirna-expression-in-lung.

27. Jin J, Cid M, Poole CB, McReynolds LA. Protein mediated miRNA detection and siRNA enrichment using p19. Biotechniques. 2010;48(6):xvii-xxiii.

28. Thornburg NJ, Hayward SL, Crowe JE. Respiratory syncytial virus regulates human microRNAs by using mechanisms involving beta interferon and NF-κB. mBio. 2012;3.

29. O'Connell RM, Taganov KD, Boldin MP, Cheng G, Baltimore D. MicroRNA-155 is induced during the macrophage inflammatory response. Proc Natl Acad Sci U S A. 2007;104(5):1604-9.

30. Garofalo R, Mei F, Espejo R, Ye G, Haeberle H, Baron S, et al. Respiratory syncytial virus infection of human respiratory epithelial cells up-regulates class I MHC expression through the induction of IFN-beta and IL-1 alpha. Journal of immunology. 1996;157(6):2506-13.

31. Konig B, Streckert HJ, Krusat T, Konig W. Respiratory syncytial virus G-protein modulates cytokine release from human peripheral blood mononuclear cells. J Leukoc Biol. 1996;59(3):403-6.

32. Krishnan S, Craven M, Welliver RC, Ahmad N, Halonen M. Differences in participation of innate and adaptive immunity to respiratory syncytial virus in adults and neonates. J Infect Dis. 2003;188(3):433-9.

33. Bakre A, Wu W, Hiscox J, Spann K, Teng MN, Tripp RA. Human respiratory syncytial virus non-structural protein NS1 modifies miR-24 expression via transforming growth factor-beta. J Gen Virol. 2015;96(11):3179-91.

Tables and figures

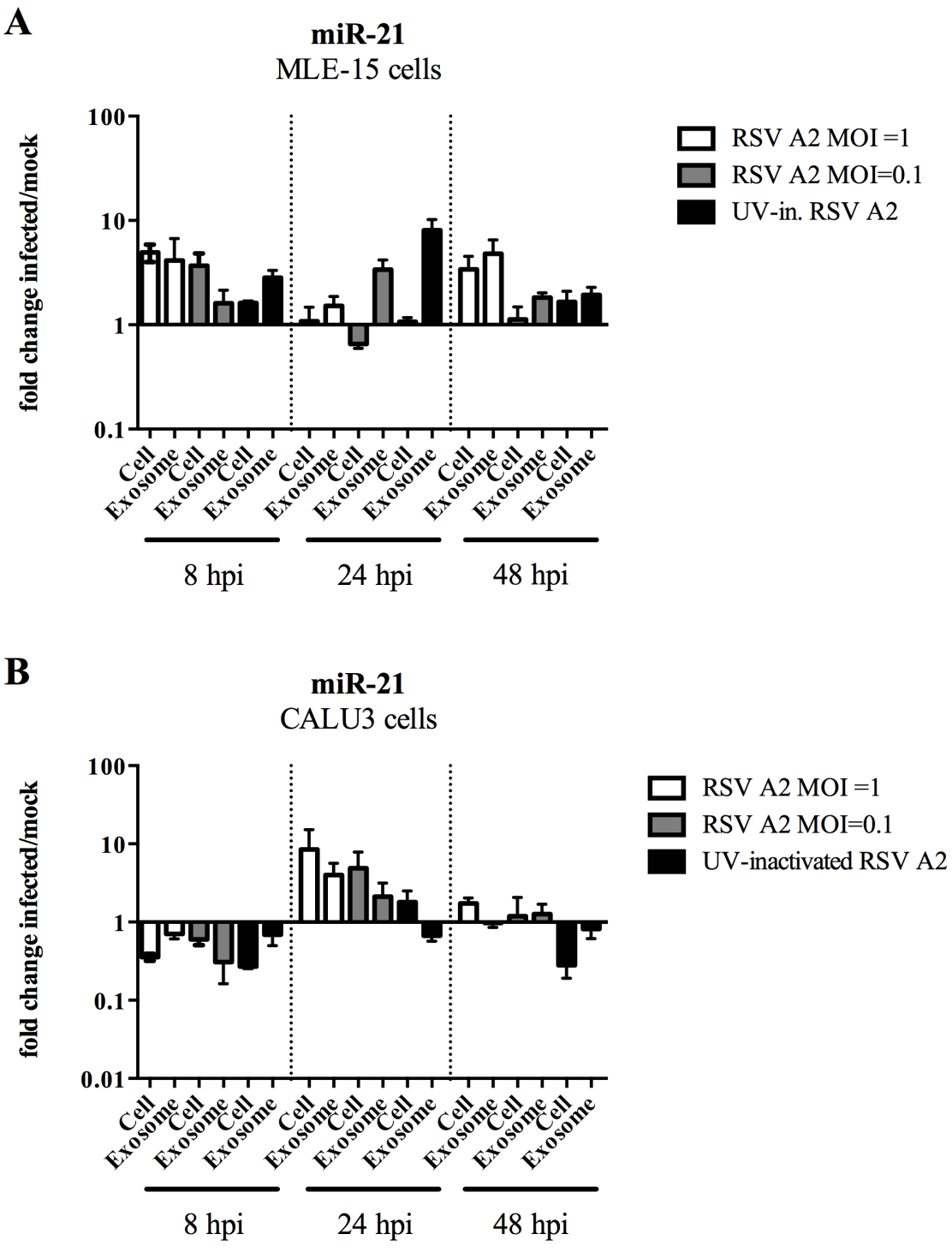

Fig. 5.1: Pattern and tempo of miR-21 expression levels in lung epithelial cells with live and UV-inactivated RSV A2 infection. 24h prior to RSV infection, MLE-15 and CALU3 cells were seeded on 24-well plates. Then the cells were infected for 2h incubation at 37°C with live RSV A2 at multiplicity of infection (MOI) = 1 or 0.1, UV-inactivated RSV A2 equivalent to MOI = 1, or mock (Vero E6 cell lysate). At 8, 24, and 48 hpi, cell lysate and supernatant were collected from **(A)** MLE-15 cells and **(B)** CALU3 cells, and miRNA expression levels were determined by RT-qPCR. miR-21 expression levels are normalized by 18s rRNA gene expression and values are represented as expression over mock (vero E6 cell lysate). All data is representative of three independent experiments with n=3 wells/condition. Error bars represent the SEM and results were considered significant with a P value ≤ 0.05 (*) by a One-way ANOVA and Bonferroni's test.

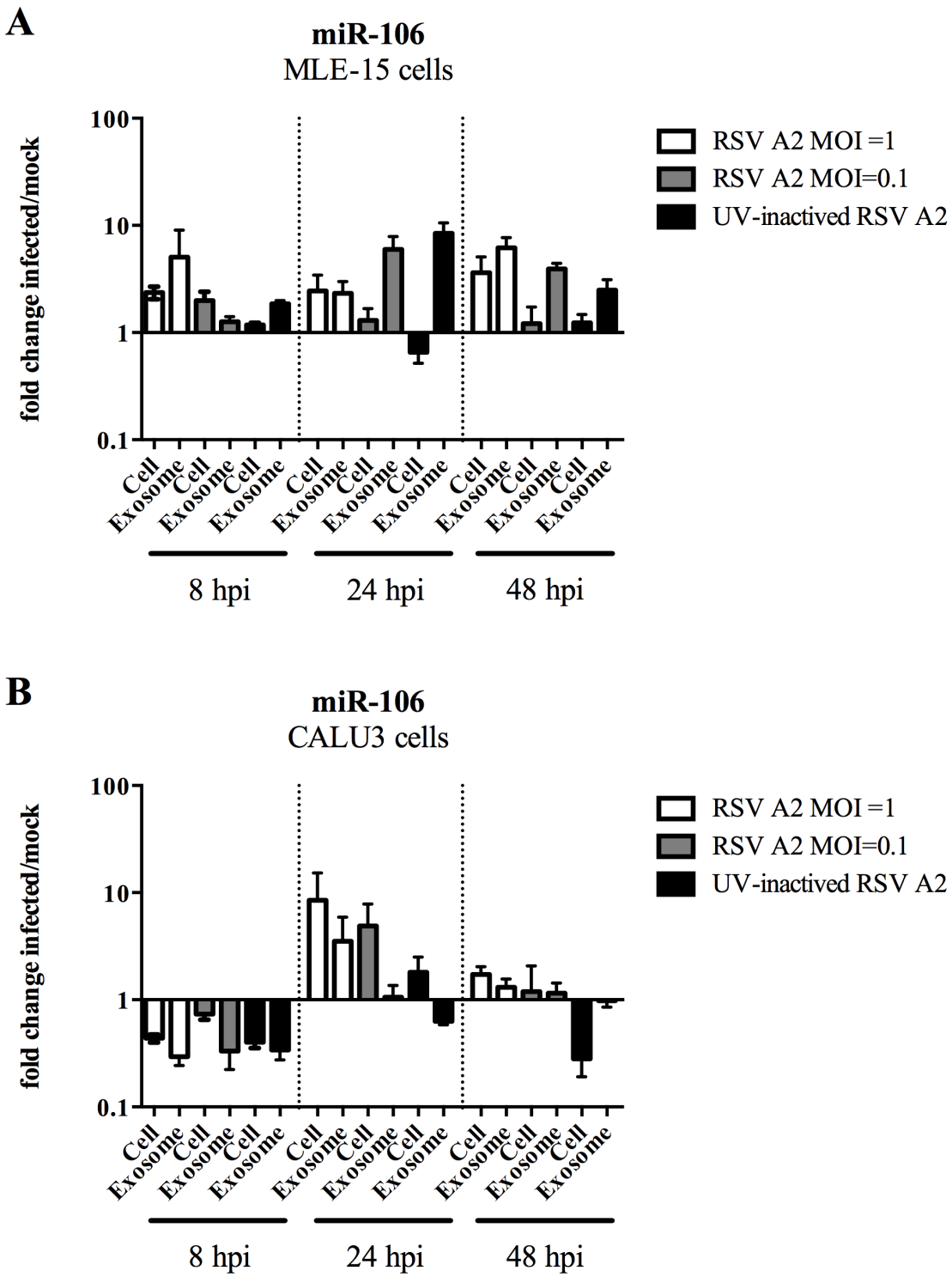
A
miR-106
MLE-15 cells
fold change infected/mock
100
10
1
0.1
RSV A2 MOI =1
RSV A2 MOI=0.1
UV-inactived RSV A2
Cell
Exosome
8 hpi
24 hpi
48 hpi
B
miR-106
CALU3 cells
fold change infected/mock
100
10
1
0.1
RSV A2 MOI =1
RSV A2 MOI=0.1
UV-inactived RSV A2
Cell
Exosome
8 hpi
24 hpi
48 hpi

Fig. 5.2: Pattern and tempo of miR-106 expression levels in lung epithelial cells with live and UV-inactivated RSV A2 infection. 24h prior to RSV infection, MLE-15 and CALU3 cells were seeded on 24-well plates. Then the cells were infected for 2h incubation at 37°C with live RSV A2 at multiplicity of infection (MOI) = 1 or 0.1, UV-inactivated RSV A2 equivalent to MOI = 1, or mock (Vero E6 cell lysate). At 8, 24, and 48 hpi, cell lysate and supernatant were collected from **(A)** MLE-15 cells and **(B)** CALU3 cells, and miRNA expression levels were determined by RT-qPCR. miR-106 expression levels are normalized by 18s rRNA gene expression and values are represented as expression over mock (vero E6 cell lysate). All data is representative of three independent experiments with n=3 wells/condition. Error bars represent the SEM and results were considered significant with a P value ≤ 0.05 (*) by a One-way ANOVA and Bonferroni's test.

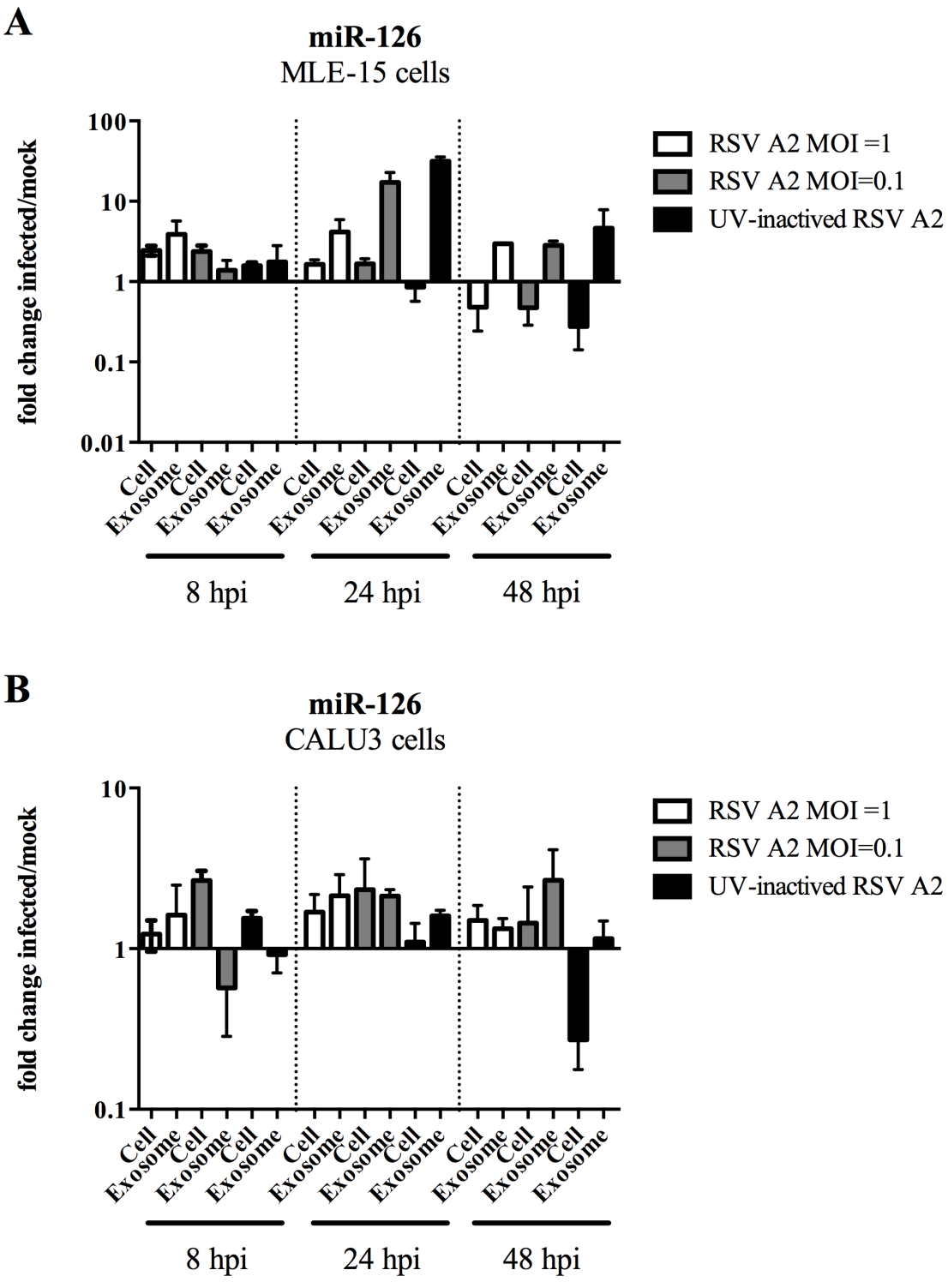
A
miR-126
MLE-15 cells
fold change infected/mock
100
10
1
0.1
0.01
Cell
Exosome
8 hpi
24 hpi
48 hpi
RSV A2 MOI =1
RSV A2 MOI=0.1
UV-inactived RSV A2
B
miR-126
CALU3 cells
fold change infected/mock
10
1
0.1
Cell
Exosome
8 hpi
24 hpi
48 hpi
RSV A2 MOI =1
RSV A2 MOI=0.1
UV-inactived RSV A2

Fig. 5.3: Pattern and tempo of miR-126 expression levels in lung epithelial cells with live and UV-inactivated RSV A2 infection. 24h prior to RSV infection, MLE-15 and CALU3 cells were seeded on 24-well plates. Then the cells were infected for 2h incubation at 37°C with live RSV A2 at multiplicity of infection (MOI) = 1 or 0.1, UV-inactivated RSV A2 equivalent to MOI = 1, or mock (Vero E6 cell lysate). At 8, 24, and 48 hpi, cell lysate and supernatant were collected from **(A)** MLE-15 cells and **(B)** CALU3 cells, and miRNA expression levels were determined by RT-qPCR. miR-126 expression levels are normalized by 18s rRNA gene expression and values are represented as expression over mock (vero E6 cell lysate). All data is representative of three independent experiments with n=3 wells/condition. Error bars represent the SEM and results were considered significant with a P value ≤ 0.05 (*) by a One-way ANOVA and Bonferroni's test.

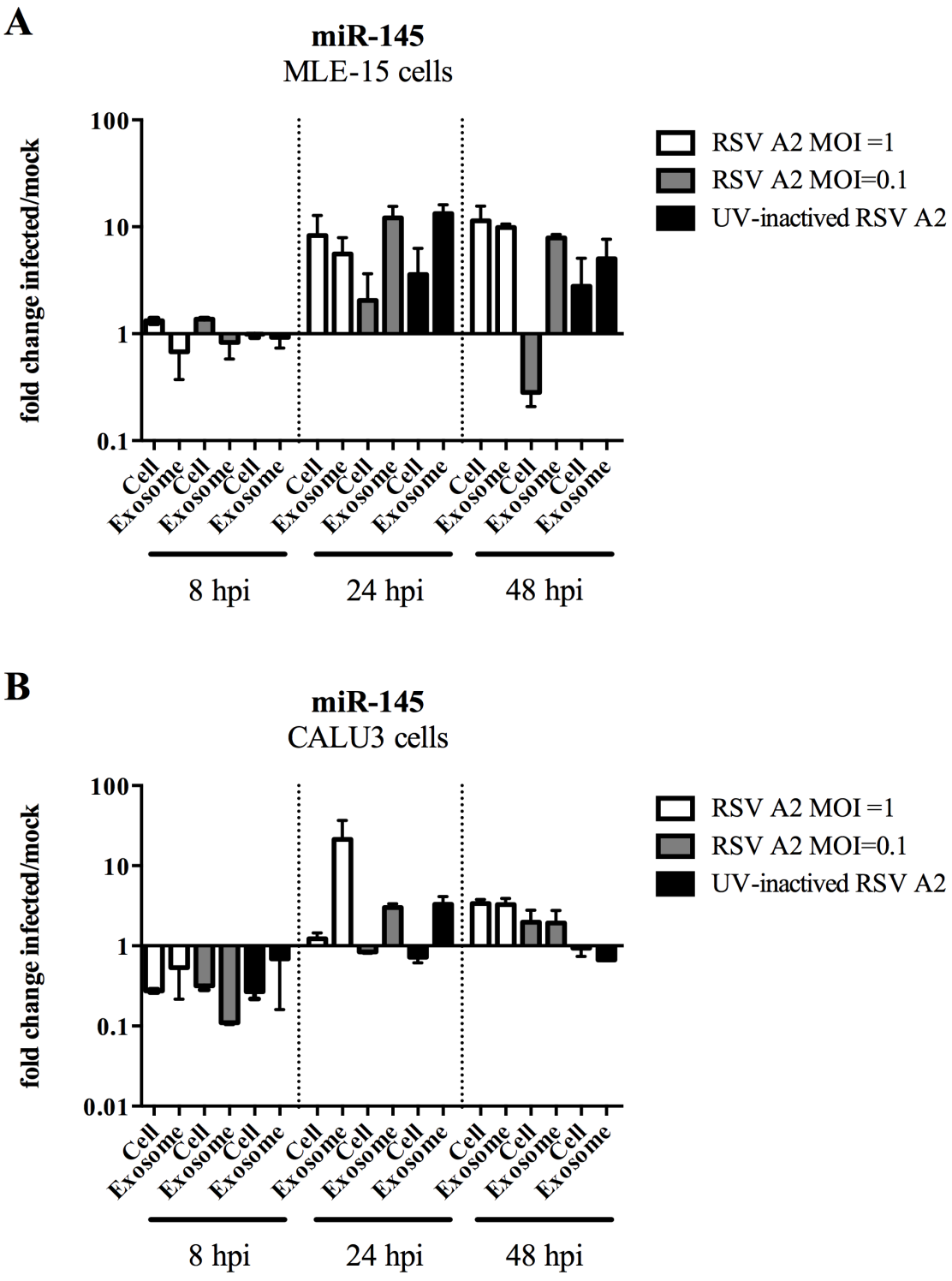
A
miR-145
MLE-15 cells
fold change infected/mock
100
10
1
0.1
Cell
Exosome
8 hpi
24 hpi
48 hpi
RSV A2 MOI =1
RSV A2 MOI=0.1
UV-inactived RSV A2
B
miR-145
CALU3 cells
fold change infected/mock
100
10
1
0.1
0.01
Cell
Exosome
8 hpi
24 hpi
48 hpi
RSV A2 MOI =1
RSV A2 MOI=0.1
UV-inactived RSV A2

Fig. 5.4: Pattern and tempo of miR-145 expression levels in lung epithelial cells with live and UV-inactivated RSV A2 infection. 24h prior to RSV infection, MLE-15 and CALU3 cells were seeded on 24-well plates. Then the cells were infected for 2h incubation at 37°C with live RSV A2 at multiplicity of infection (MOI) = 1 or 0.1, UV-inactivated RSV A2 equivalent to MOI = 1, or mock (Vero E6 cell lysate). At 8, 24, and 48 hpi, cell lysate and supernatant were collected from **(A)** MLE-15 cells and **(B)** CALU3 cells, and miRNA expression levels were determined by RT-qPCR. miR-145 expression levels are normalized by 18s rRNA gene expression and values are represented as expression over mock (vero E6 cell lysate). All data is representative of three independent experiments with n=3 wells/condition. Error bars represent the SEM and results were considered significant with a P value ≤0.05 (*) by a One-way ANOVA and Bonferroni's test.

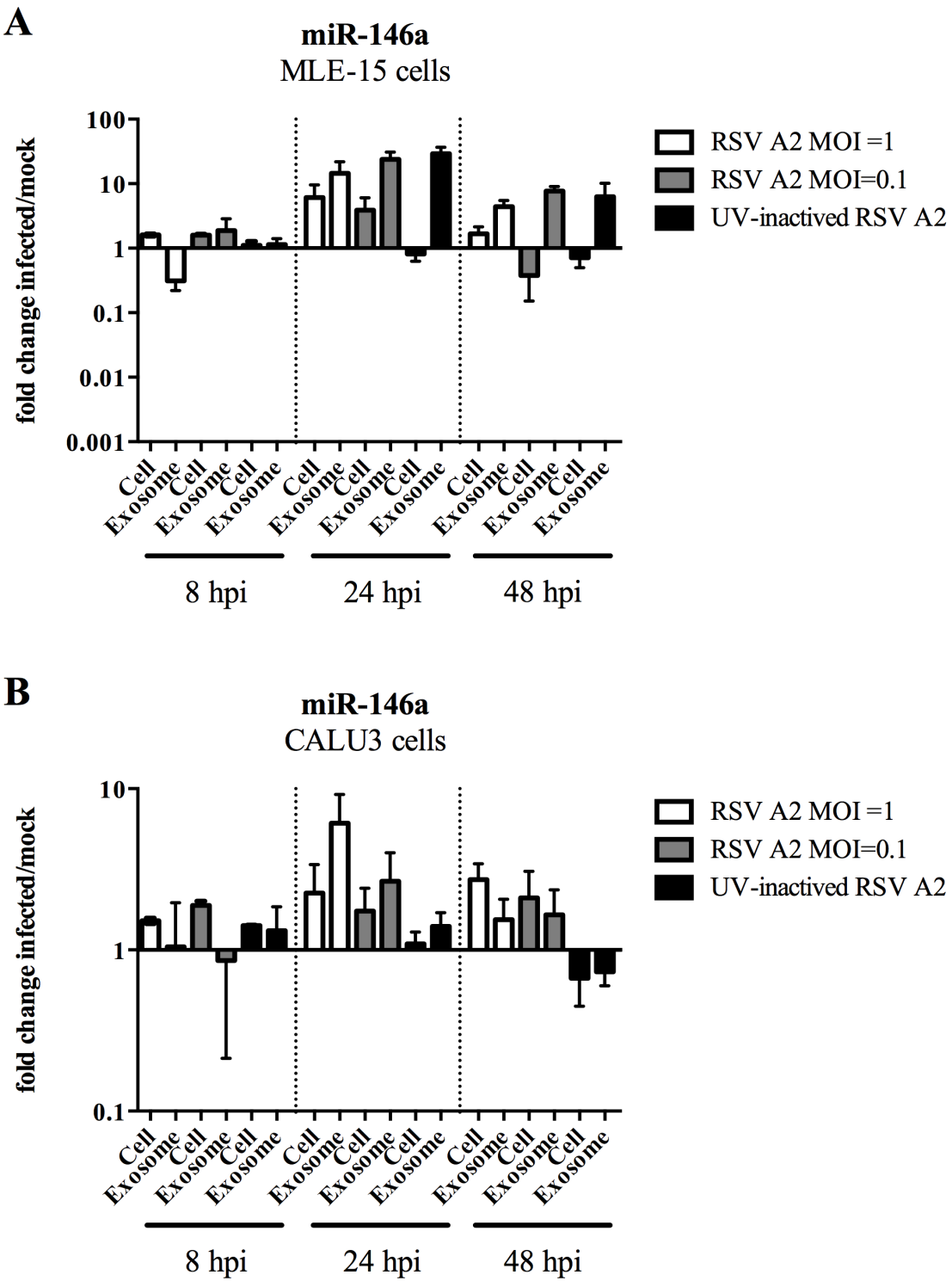
A
miR-146a
MLE-15 cells
fold change infected/mock
100
10
1
0.1
0.01
0.001
Cell
Exosome
8 hpi
24 hpi
48 hpi
RSV A2 MOI =1
RSV A2 MOI=0.1
UV-inactived RSV A2
B
miR-146a
CALU3 cells
fold change infected/mock
10
1
0.1
Cell
Exosome
8 hpi
24 hpi
48 hpi
RSV A2 MOI =1
RSV A2 MOI=0.1
UV-inactived RSV A2

Fig. 5.5: Pattern and tempo of miR-146a expression levels in lung epithelial cells with live and UV-inactivated RSV A2 infection. 24h prior to RSV infection, MLE-15 and CALU3 cells were seeded on 24-well plates. Then the cells were infected for 2h incubation at 37°C with live RSV A2 at multiplicity of infection (MOI) = 1 or 0.1, UV-inactivated RSV A2 equivalent to MOI = 1, or mock (Vero E6 cell lysate). At 8, 24, and 48 hpi, cell lysate and supernatant were collected from **(A)** MLE-15 cells and **(B)** CALU3 cells, and miRNA expression levels were determined by RT-qPCR. miR-146a expression levels are normalized by 18s rRNA gene expression and values are represented as expression over mock (vero E6 cell lysate). All data is representative of three independent experiments with n=3 wells/condition. Error bars represent the SEM and results were considered significant with a P value ≤ 0.05 (*) by a One-way ANOVA and Bonferroni's test.

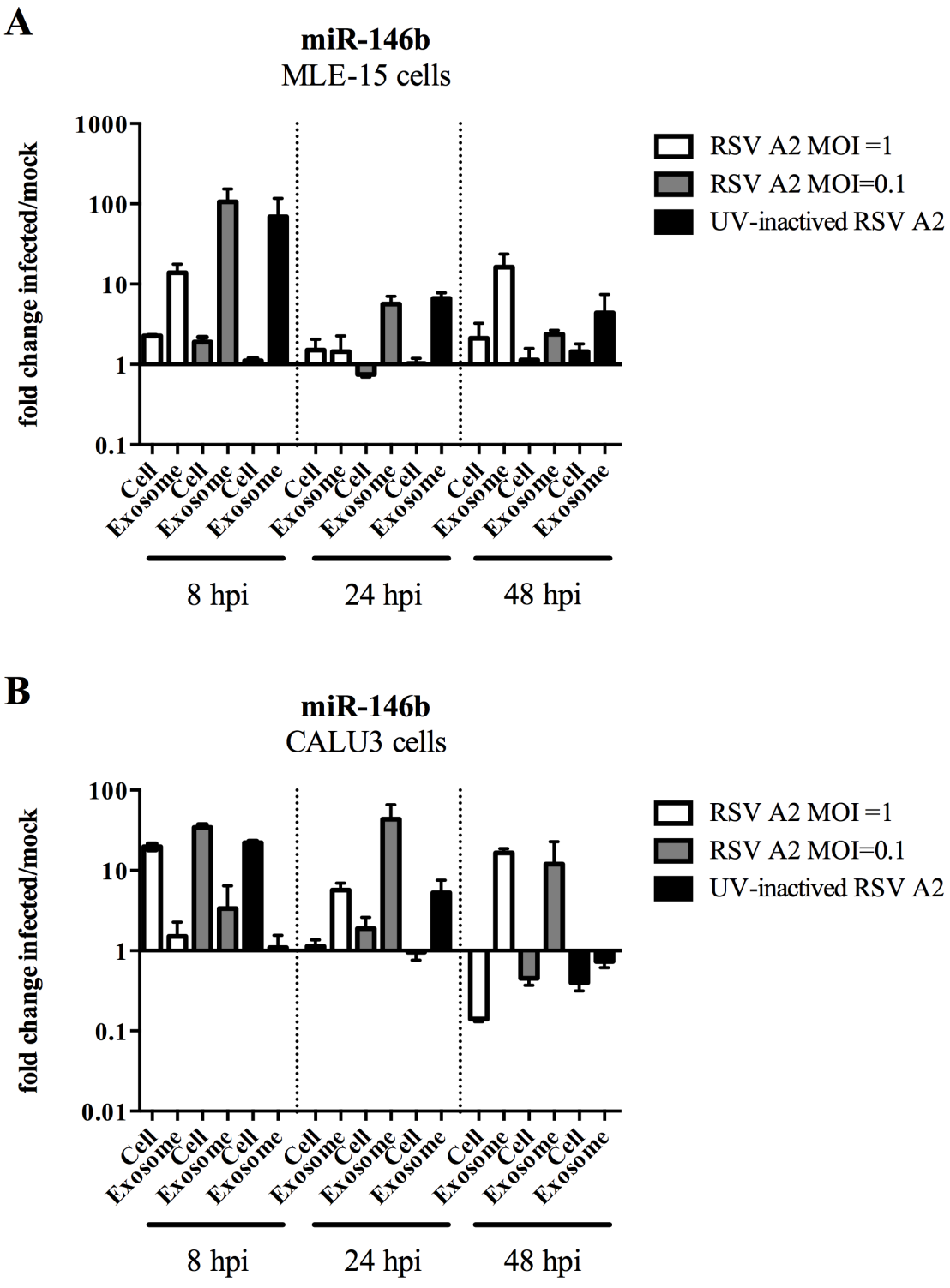
A
miR-146b
MLE-15 cells
fold change infected/mock
1000
100
10
1
0.1
Cell
Exosome
8 hpi
24 hpi
48 hpi
RSV A2 MOI =1
RSV A2 MOI=0.1
UV-inactived RSV A2
B
miR-146b
CALU3 cells
fold change infected/mock
100
10
1
0.1
0.01
Cell
Exosome
8 hpi
24 hpi
48 hpi
RSV A2 MOI =1
RSV A2 MOI=0.1
UV-inactived RSV A2

Fig. 5.6: Pattern and tempo of miR-146b expression levels in lung epithelial cells with live and UV-inactivated RSV A2 infection. 24h prior to RSV infection, MLE-15 and CALU3 cells were seeded on 24-well plates. Then the cells were infected for 2h incubation at 37°C with live RSV A2 at multiplicity of infection (MOI) = 1 or 0.1, UV-inactivated RSV A2 equivalent to MOI = 1, or mock (Vero E6 cell lysate). At 8, 24, and 48 hpi, cell lysate and supernatant were collected from **(A)** MLE-15 cells and **(B)** CALU3 cells, and miRNA expression levels were determined by RT-qPCR. miR-146b expression levels are normalized by 18s rRNA gene expression and values are represented as expression over mock (vero E6 cell lysate). All data is representative of three independent experiments with n=3 wells/condition. Error bars represent the SEM and results were considered significant with a P value ≤ 0.05 (*) by a One-way ANOVA and Bonferroni's test.

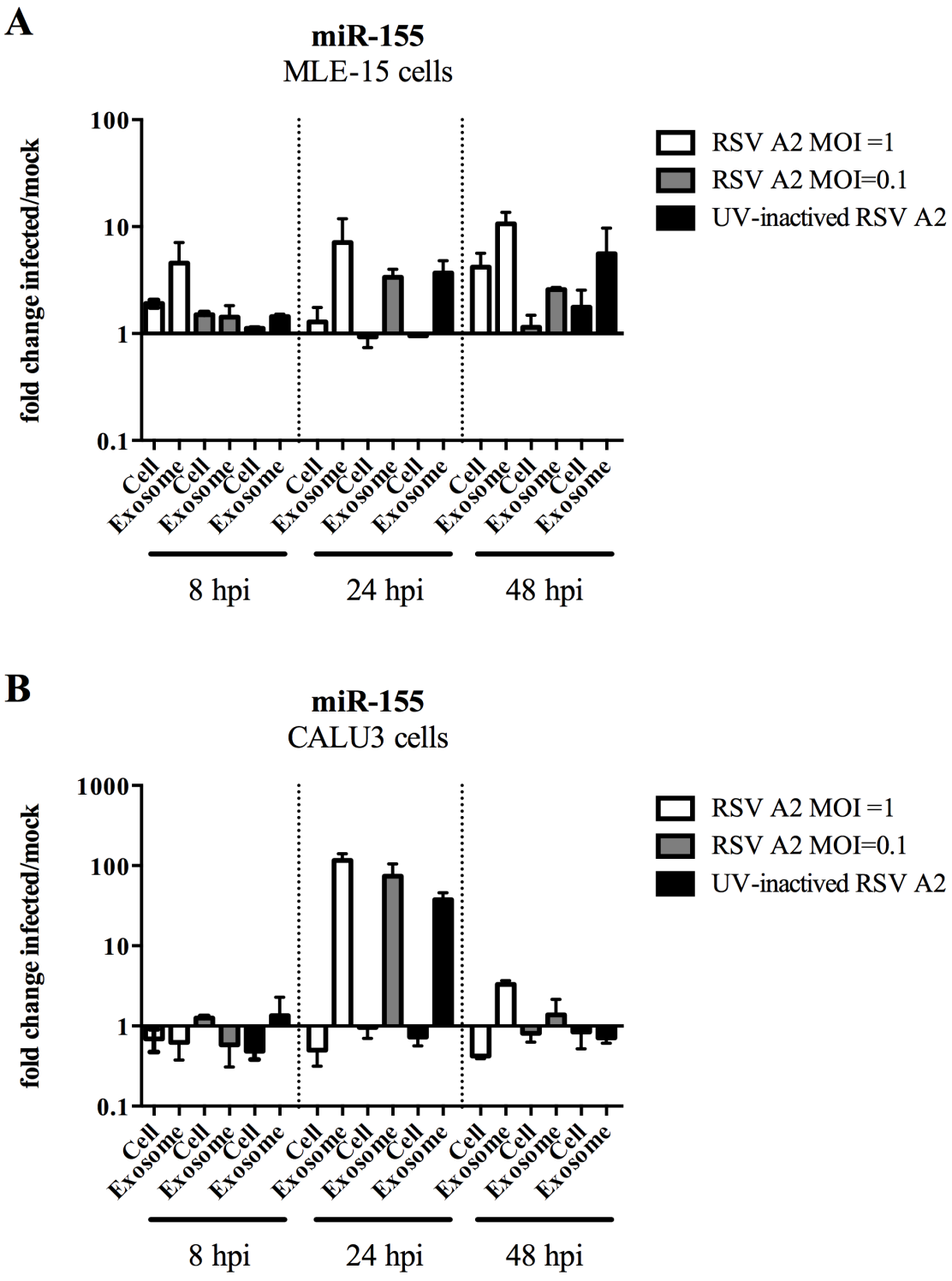
A
miR-155
MLE-15 cells
fold change infected/mock
100
10
1
0.1
Cell
Exosome
8 hpi
24 hpi
48 hpi
RSV A2 MOI =1
RSV A2 MOI=0.1
UV-inactived RSV A2
B
miR-155
CALU3 cells
fold change infected/mock
1000
100
10
1
0.1
Cell
Exosome
8 hpi
24 hpi
48 hpi
RSV A2 MOI =1
RSV A2 MOI=0.1
UV-inactived RSV A2

Fig. 5.7: Pattern and tempo of miR-155 expression levels in lung epithelial cells with live and UV-inactivated RSV A2 infection. 24h prior to RSV infection, MLE-15 and CALU3 cells were seeded on 24-well plates. Then the cells were infected for 2h incubation at 37°C with live RSV A2 at multiplicity of infection (MOI) = 1 or 0.1, UV-inactivated RSV A2 equivalent to MOI = 1, or mock (Vero E6 cell lysate). At 8, 24, and 48 hpi, cell lysate and supernatant were collected from **(A)** MLE-15 cells and **(B)** CALU3 cells, and miRNA expression levels were determined by RT-qPCR. miR-155 expression levels are normalized by 18s rRNA gene expression and values are represented as expression over mock (vero E6 cell lysate). All data is representative of three independent experiments with n=3 wells/condition. Error bars represent the SEM and results were considered significant with a P value ≤0.05 (*) by a One-way ANOVA and Bonferroni's test.

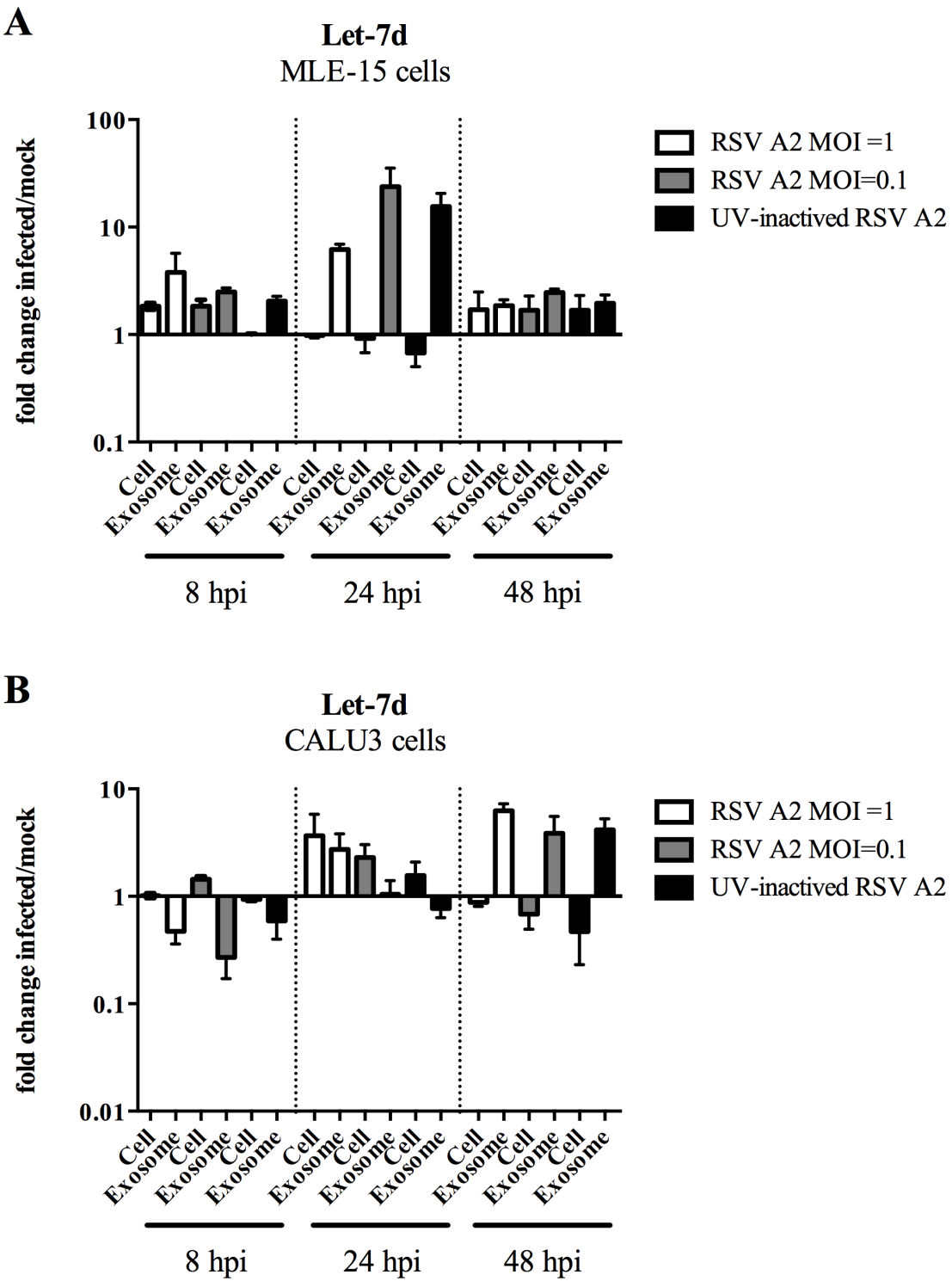
A
Let-7d
MLE-15 cells
fold change infected/mock
100
10
1
0.1
Cell
Exosome
8 hpi
24 hpi
48 hpi
RSV A2 MOI =1
RSV A2 MOI=0.1
UV-inactived RSV A2
B
Let-7d
CALU3 cells
fold change infected/mock
10
1
0.1
0.01
Cell
Exosome
8 hpi
24 hpi
48 hpi
RSV A2 MOI =1
RSV A2 MOI=0.1
UV-inactived RSV A2

Fig. 5.8: Pattern and tempo of let-7d expression levels in lung epithelial cells with live and UV-inactivated RSV A2 infection. 24h prior to RSV infection, MLE-15 and CALU3 cells were seeded on 24-well plates. Then the cells were infected for 2h incubation at 37°C with live RSV A2 at multiplicity of infection (MOI) = 1 or 0.1, UV-inactivated RSV A2 equivalent to MOI = 1, or mock (Vero E6 cell lysate). At 8, 24, and 48 hpi, cell lysate and supernatant were collected from **(A)** MLE-15 cells and **(B)** CALU3 cells, and miRNA expression levels were determined by RT-qPCR. Let-7d expression levels are normalized by 18s rRNA gene expression and values are represented as expression over mock (vero E6 cell lysate). All data is representative of three independent experiments with n=3 wells/condition. Error bars represent the SEM and results were considered significant with a P value ≤0.05 (*) by a One-way ANOVA and Bonferroni's test.

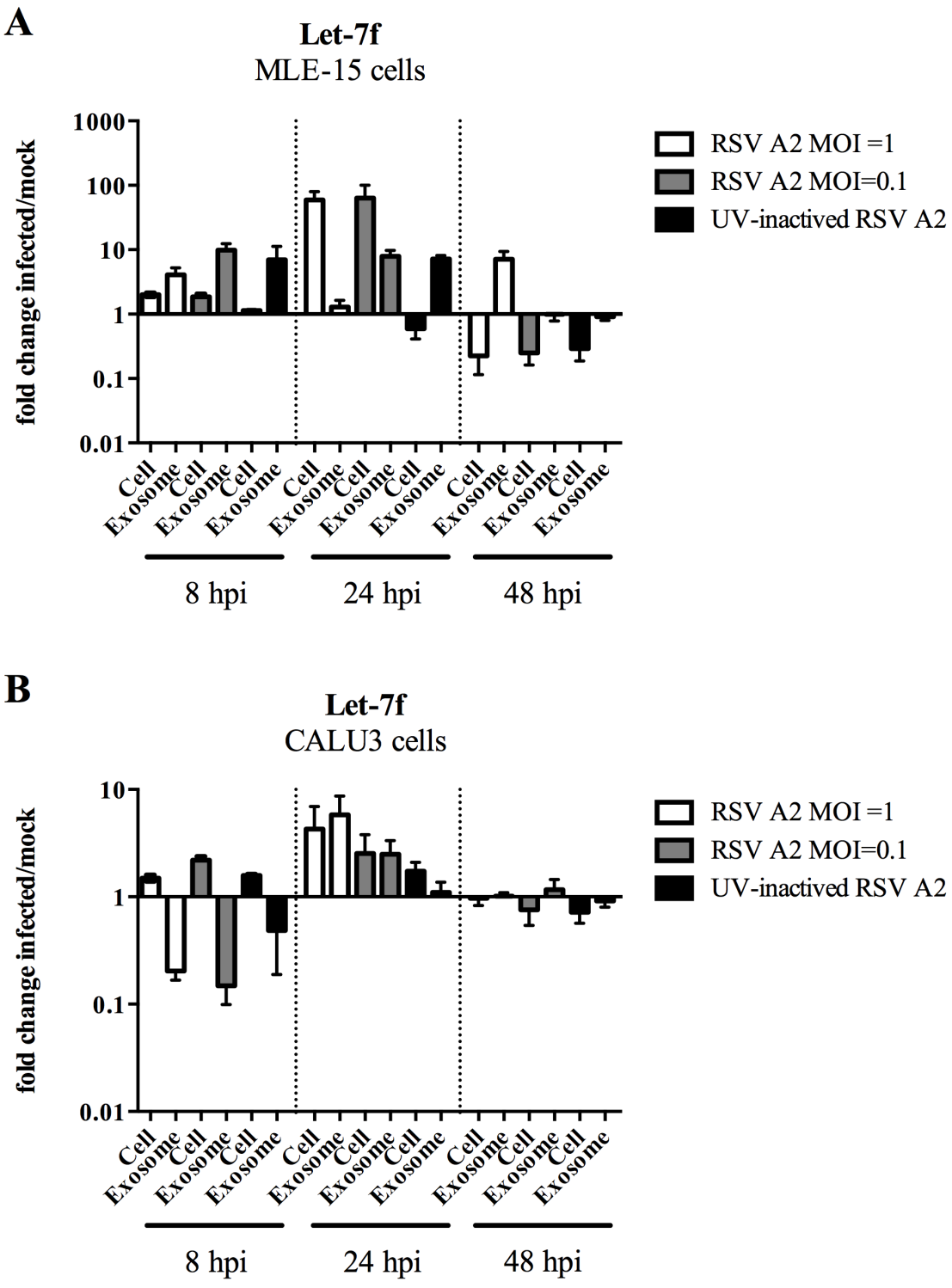
A
Let-7f
MLE-15 cells
fold change infected/mock
1000
100
10
1
0.1
0.01
Cell
Exosome
8 hpi
24 hpi
48 hpi
RSV A2 MOI =1
RSV A2 MOI=0.1
UV-inactived RSV A2
B
Let-7f
CALU3 cells
fold change infected/mock
10
1
0.1
0.01
Cell
Exosome
8 hpi
24 hpi
48 hpi
RSV A2 MOI =1
RSV A2 MOI=0.1
UV-inactived RSV A2

Fig. 5.9: Pattern and tempo of let-7f expression levels in lung epithelial cells with live and UV-inactivated RSV A2 infection. 24h prior to RSV infection, MLE-15 and CALU3 cells were seeded on 24-well plates. Then the cells were infected for 2h incubation at 37°C with live RSV A2 at multiplicity of infection (MOI) = 1 or 0.1, UV-inactivated RSV A2 equivalent to MOI = 1, or mock (Vero E6 cell lysate). At 8, 24, and 48 hpi, cell lysate and supernatant were collected from **(A)** MLE-15 cells and **(B)** CALU3 cells, and miRNA expression levels were determined by RT-qPCR. Let-7f expression levels are normalized by 18s rRNA gene expression and values are represented as expression over mock (vero E6 cell lysate). All data is representative of three independent experiments with n=3 wells/condition. Error bars represent the SEM and results were considered significant with a P value ≤0.05 (*) by a One-way ANOVA and Bonferroni's test.

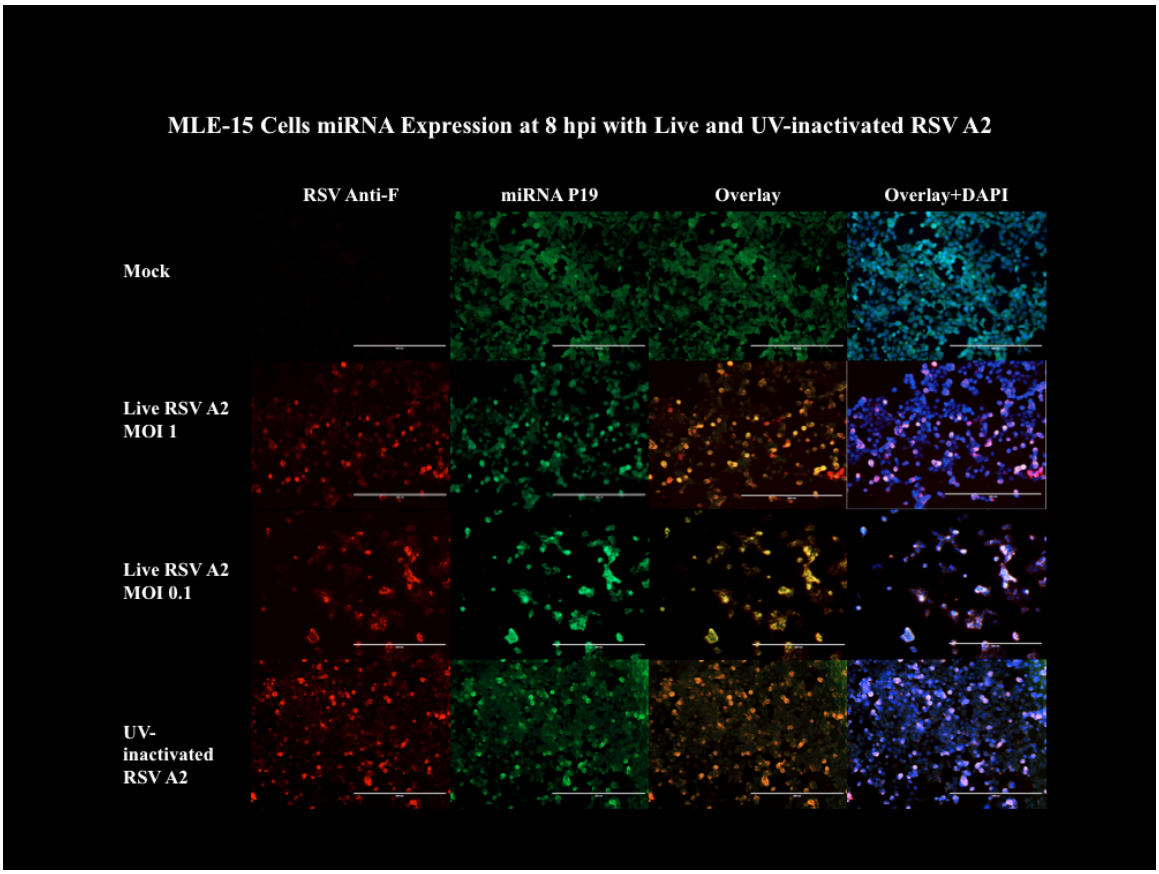

Fig. 5.10: miRNA expression in MLE-15 cells at 8 hpi with live and UV-inactivated RSV. MLE-15 cells were infected with live RSV A2 at MOI = 1 and 0.1, UV-inactivated RSV A2 (equivalent to MOI = 1), or mock (Vero E6 cell lysate). At 8 hours post-infection (8 hpi), RSV (anti-F) and miRNA expression (P19 binding protein) was evaluated by immunofluorescence, and DAPI staining was used to label the nuclear DNA of cells. All data is representative of three independent experiments with n=3 wells/condition.

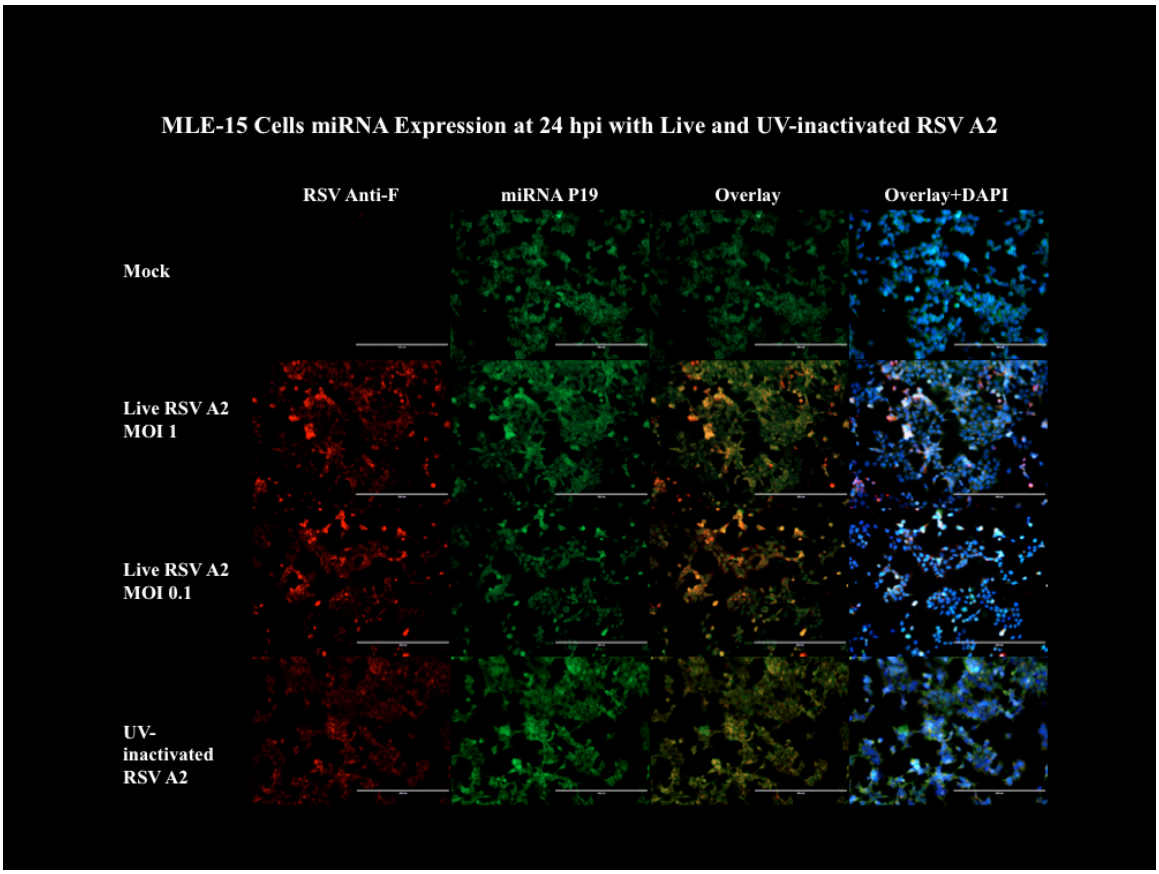

Fig. 5.11: miRNA expression in MLE-15 cells at 24 hpi with live and UV-inactivated RSV. MLE-15 cells were infected with live RSV A2 at MOI = 1 and 0.1, UV-inactivated RSV A2 (equivalent to MOI = 1), or mock (Vero E6 cell lysate). At 24 hpi, RSV (anti-F) and miRNA expression (P19 binding protein) was evaluated by immunofluorescence, and DAPI staining was used to label the nuclear DNA of cells. All data is representative of three independent experiments with n=3 wells/condition.

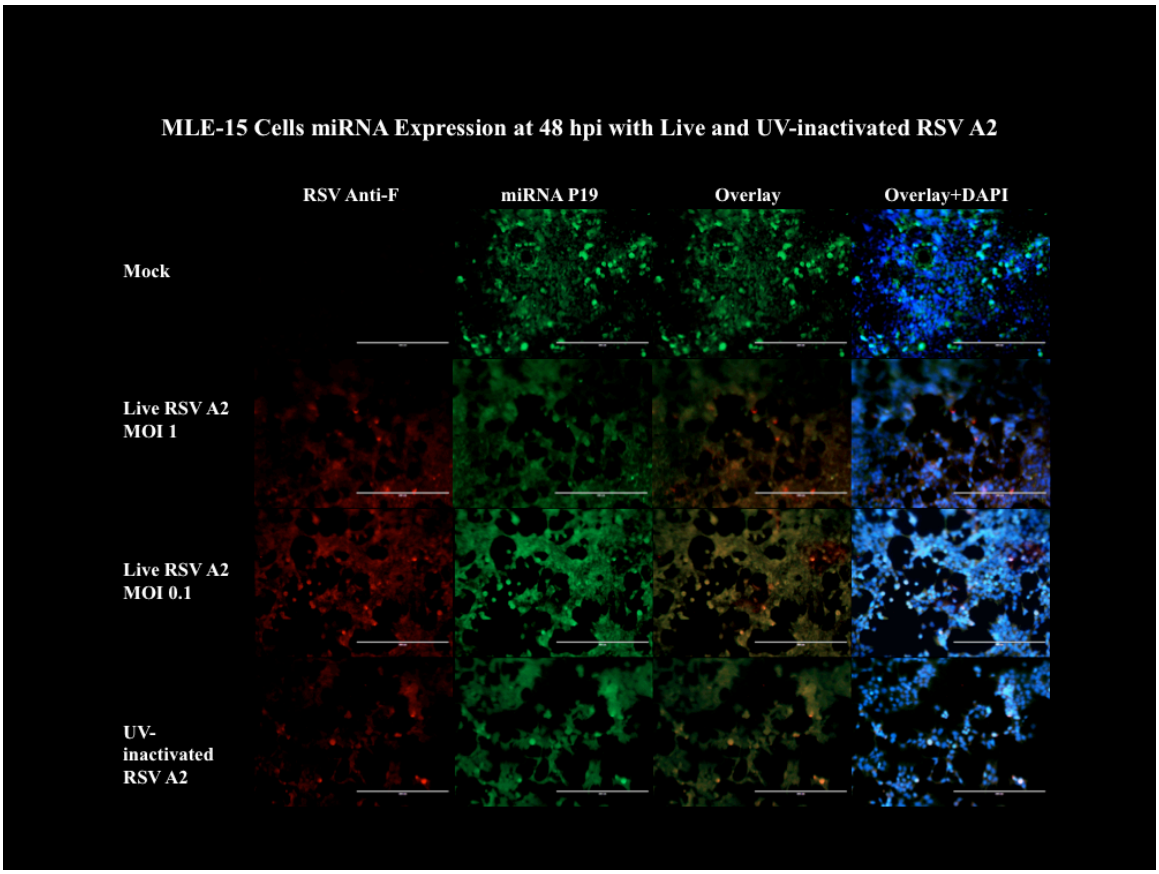

Fig. 5.12: miRNA expression in MLE-15 cells at 48 hpi with live and UV-inactivated RSV. MLE-15 cells were infected with live RSV A2 at MOI = 1 and 0.1, UV-inactivated RSV A2 (equivalent to MOI = 1), or mock (Vero E6 cell lysate). At 48 hpi, RSV (anti-F) and miRNA expression (P19 binding protein) was evaluated by immunofluorescence, and DAPI staining was used to label the nuclear DNA of cells. All data is representative of three independent experiments with n=3 wells/condition.

miRNA	Description	Forward Primer Sequence
miR-21	mmu-miR-21a-5p	TAGCTTATCAGACTGATGTTGA
miR-106	mmu-miR-106a-5p	CAAAGTGCTAACAGTGCAGGTAG
miR-126	mmu-miR-126a-3p	TCGTACCGTGAGTAATAATGCG
miR-145	mmu-miR-145a-5p	GTCCAGTTTTCCCAGGAATCCCT
miR-146a	mmu-miR-146a-5p	TGAGAACTGAATTCCATGGGTT
miR-146b	mmu-miR-146b-5p	TGAGAACTGAATTCCATAGGCT
miR-155	mmu-miR-155-5p	TTAATGCTAATTGTGATAGGGGT
Let-7d	mmu-let-7d-5p	AGAGGTAGTAGGTTGCATAGTT
Let-7f	mmu-let-7f-5p	TGAGGTAGTAGATTGTATAGTT

Table 5.1: miRNA forward primer sequences. All of the miRNA primer sequences share 100% sequence homology between mice and humans, with the exception of miR-106. The miR-106 primer sequence contains two point mutations between mice and humans as indicated in red.

miRNA	MLE-15 exosome miRNA	MLE-15 cellular miRNA	CALU3 exosome miRNA	CALU3 cellular miRNA
miR-21	↑	✖	↑	↑
miR-106	↑	↑	↑	↑
miR-126	↑↑	↑	↑	↑
miR-145	↑↑	↑	↑	✖
miR-146a	↑↑	↑	↑	↑
miR-146b	↑↑ @ 8 hpi	✖	↑	✖
miR-155	↑	✖	↑↑	↓
Let-7d	↑↑	↓	✖	↑
Let-7f	↑	↑↑	↑	↑

> 1.2 = ↑ 0.8-1.2 = ✖ < 0.8 = ↓

Table 5.2: Summary of miRNA expression levels in lung epithelial cells infected with live RSV A2 normalized to mock at 24 hpi. Table provides summary of cell lysate and exosome-derived expression levels of nine miRNAs evaluated in MLE-15 and CALU3 cells by RT-qPCR. If the fold-change was > 1.2, the result was reported as a fold upregulation. If the fold-change was < 0.8, the result was reported as a fold downregulation, and if the fold-change was between 0.8-1.2 the result was reported as no change. All data is representative of three independent experiments with n=3 wells/condition.

Supplemental information

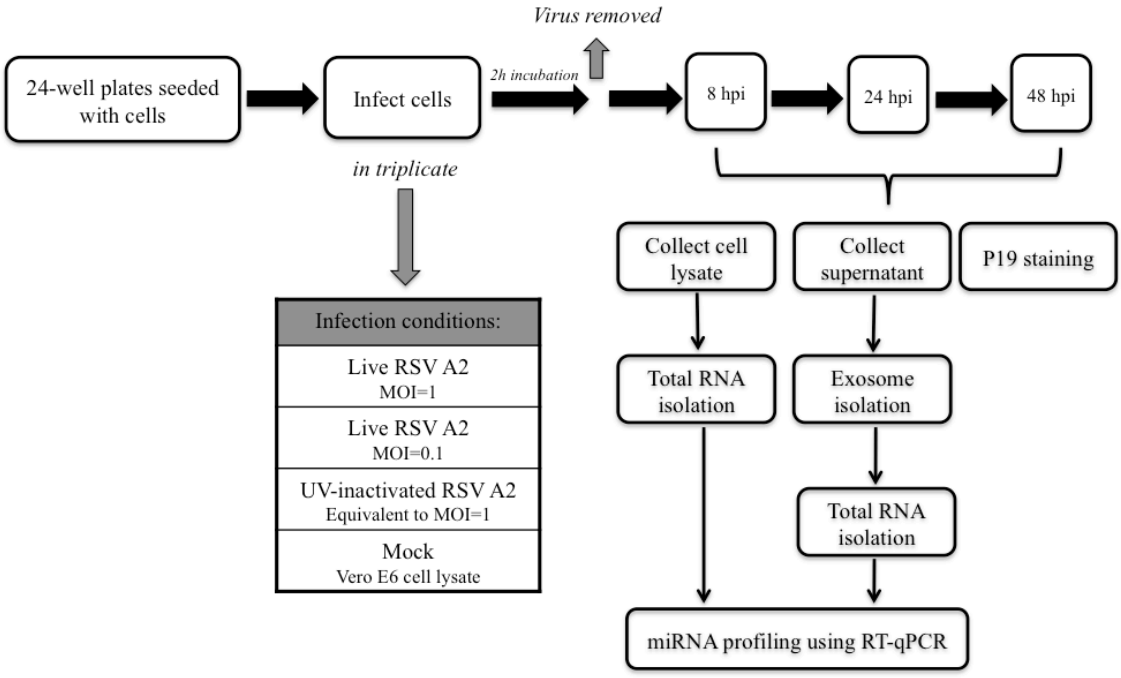

Fig S5.1: Schematic of the experimental design for *in vitro* infection of MLE-15 and CALU3 cells with RSV A2. 24h prior to RSV infection, MLE-15 and CALU3 cells were seeded on 24-well plates, and then infected for 2h incubation at 37°C with live RSV A2 at multiplicity of infection (MOI) = 1 or 0.1, UV-inactivated RSV A2 equivalent to MOI = 1, or mock (Vero E6 cell lysate). At 8, 24, and 48 hpi, cell lysate and supernatant were collected from all wells and miRNA expression levels were determined by RT-qPCR, a subset of wells were used for P19 protein-based staining. All data is representative of three independent experiments with n=3 wells/condition.

CHAPTER 6

INHIBITION OF MIR-467F EXACERBATES ENHANCED DISEASE ASSOCIATED WITH FORMALIN-INACTIVATED RESPIRATORY SYNCYTIAL VIRUS VACCINATION [1]

[1] Anderson LJ, Jorquera PA, Williams CW, Howerth EW, Tripp RA. To be submitted to *Journal of Virology*.

Abstract

Respiratory syncytial virus (RSV) is a high priority target for vaccine development. Previous efforts to develop live or inactivated vaccines have been unsuccessful. In studies conducted in the 1960s, children immunized with a formalin-inactivated respiratory syncytial virus (FI-RSV) vaccine developed severe pulmonary disease following natural RSV infection. The development of vaccine enhanced disease, in immunized subjects and animal models, remains a major concern in the development of a safe and efficacious RSV vaccine, as the mechanism and immunological basis for enhanced disease is not completely understood. To address this and provide a better understanding of the virus-host interface the potential role for microRNAs (miRNAs) was examined. miRNAs have been shown to have important roles in regulating key pathogenic mechanisms linked to asthma and in airway hyperresponsiveness. In this study, we hypothesize that upon RSV infection of vaccinated mice memory cells produce miR-467f that promotes T cell activation and a safe inflammatory response that prevents vaccine-enhanced disease; however, inhibition of miR-467f will result in exacerbation of vaccine enhanced disease. We demonstrate the use of RNAi technology for *in vivo* delivery of exogenous miRNA to both rescue and further exacerbate the FI-RSV induced enhanced disease phenotype induced upon subsequent RSV challenge. By inducing gain- and loss- of-function, these studies indicate a biologically relevant role for miR-467f in linking the innate and adaptive immune response that responds to FI-RSV induced enhanced disease, and its potential as a novel therapeutic target for RSV patients.

Importance

Respiratory syncytial virus (RSV) is the most common cause of serious lower respiratory tract infections in infants and young children and the elderly, and a high priority target for vaccine development. Despite many decades of research, there still remains no licensed vaccine or therapeutic treatment against RSV. The failure of the formalin-inactivated RSV (FI-RSV) vaccine has been a major obstacle in developing novel RSV vaccines. A better understanding of the host factors governing vaccine-enhanced disease is necessary to overcome these hurdles. It has been shown that RSV can modulate the immune response to infection by regulating host gene expression through induction of microRNAs (miRNAs) related to the antiviral response. To date, no information is currently available regarding the role of miR-467f in respiratory virus infections. Using gain- and loss- of function studies, the role of miR-467f is revealed regarding cellular and humoral immune responses to vaccination and subsequent RSV infection.

Introduction

Respiratory syncytial virus (RSV) is the most common cause of lower respiratory tract infections in infants and young children, and increasingly recognized as a cause of respiratory illness in adults (1, 2). RSV can also cause serious lower respiratory tract disease in high-risk populations such as the elderly and immunocompromised (3, 4). RSV is a 15 kb negative-sense single-strand RNA virus in the Paramyxoviridae family (5, 6). RSV generally induces a localized lung infection resulting in a host inflammatory response that recruits immune cells required for viral clearance (7). Although the host inflammatory response is necessary for viral clearance, accumulating evidence strongly suggests that this response is linked with pulmonary pathogenesis and inflammation (7). Despite many decades of research, there still remains no licensed vaccine or therapeutic treatment options against RSV (4). There is passive immune prophylaxis (palivizumab), a humanized anti-RSV F protein monoclonal antibody preparation (8), which can be used in specific high-risk populations, however its usage is limited due to high cost and restrictive qualification criteria. Therefore, supportive care, such as supplemental oxygen, mechanical ventilation, and fluid replacement, is the mainstay therapy for RSV infection (4, 9).

The first candidate vaccine, formalin-inactivated RSV (FI-RSV) resulted in tremendous failure, as it did not prevent RSV infection in recipient infants, resulted in enhanced disease following natural infection (3, 10-12). The failure of the FI-RSV vaccine in the 1960s has been a major obstacle in developing novel RSV vaccines. Therefore, a better understanding of both the virus-host interface and vaccine-enhanced disease is necessary to overcome these hurdles. Although the host inflammatory response

is necessary for viral clearance, accumulating evidence strongly suggests that an exacerbated inflammatory response is linked to the pathogenesis of the pulmonary changes observed following RSV infection (13). It has been shown that RSV can modulate the immune response to infection by regulating host gene expression through induction of microRNAs (miRNAs) related to the anti-viral response(14). miRNAs are small, 20-25 nucleotide long noncoding RNAs, which modulate gene expression at a post-transcriptional level by inhibiting translation or inducing degradation of mRNA via their specific interactions with those target genes (15-17). Due to the short sequence complementarity between a miRNA and its target, a single miRNA can regulate the expression of multiple genes (18, 19). The miRNA family is a global regulatory network controlling homeostasis, inflammatory responses, and affecting immunity and disease pathogenesis (20). Therefore, by regulating cellular gene expression trough miRNAs, RSV can modulate host innate immune response, and by extension, the potency of the memory immune response to RSV.

The discovery of RNA interference (RNAi) has expanded our understanding of the mechanisms regulating host gene expression, and considerable interest has been placed on the role of miRNA species (21). In the last decade, it has been reported that different cell types can produce and secrete exosomes containing miRNAs to the extra-cellular space in response to different stimuli. Several studies have shown that upon antigen exposure and lymphocyte activation, B and T cells secrete a set of miRNAs that can further modulate cell activation and differentiation; for example, when CD4 T cells are activated, they downregulate intracellular miR-150 while accumulating in extracellular vesicles (22). When the intracellular miR-150 is reduced, several genes are

de-repressed, among them c-Myb (23, 24) a transcription factor that promotes lymphocyte survival and Notch3 (25) a receptor protein that is crucial for T cell differentiation. In addition to detection in extracellular vesicles, circulating miRNAs have been detected in cell-free bodily fluids such as serum, plasma and other bodily fluids (26-28); therefore, they can be easily profiled through microarray, RT-qPCR and sequencing. Different groups have explored this via measurement of serum miRNAs and nowadays blood-circulating miRNAs are considered one of the most promising clinical biomarkers for the diagnosis, prognosis, and therapeutic options.

Previous studies in our laboratory utilizing a miRNA PCR array identified upregulated expression of miR-467f in serum of mice vaccinated with protective RSV vaccines, but not in FI-RSV vaccinated mice upon subsequent RSV infection (manuscript in preparation). miR-467f has not been previously reported in any miRNA screens for respiratory viruses; however, a microarray-based approach to examine the miRNA expression in mice with HIV-associated nephropathy (HIVAN) showed that treatment with rapamycin (an mTOR inhibitor) to slow down HIVAN progression induces up-regulation of miR-467f expression (16). Interestingly rapamycin inhibits RSV-induced mTOR activation, and increases the frequency of RSV-$M2_{82-90}$ -specific CD8 T cells and RSV-specific memory T cell precursors in mice (29). Although the gene target(s) for miR-467f is unknown, its role is predicted in a variety of major signal transduction pathways, such as the apoptosis, cytokines, transforming grow factor beta (TGF-β), fibroblast growth factor (FGF) and PI3 kinase (PI3K) signaling pathways (16, 30).

It has been shown that RSV vaccine candidates that promote a safe immune response induce protective antibodies and RSV-specific CD8 T cells that protect mice

from vaccine-enhanced disease upon RSV infection. We hypothesize that upon RSV infection of vaccinated mice host memory cells produce miR-467f that promotes T cell activation and a safe inflammatory response that prevents vaccine-enhanced disease; however, inhibition of miR-467f will result in exacerbation of vaccine enhanced disease. In this study, we evaluate the potential immunomodulatory role of intranasal delivery of exogenous miR-467f mimic and miR-467f inhibitor in mice using a model of FI-RSV induced enhanced disease. In addition, we examine features of the antiviral effect, host immune response, histopathology, and *in vivo* tracking of miR-467f treatment.

Materials and Methods

Animals

Specific-pathogen-free, 6-to-8 weeks old female BALB/c mice (The Jackson Laboratory) were used in all experiments. Mice were housed in microisolator cages and were fed sterilized water and food ad libitum. All experiments were performed in accordance with the guidelines of the University of Georgia Institutional Animal Care and Use Committee (IACUC), with protocols approved by the University of Georgia IACUC.

Virus infection and vaccination

RSV A2 was propagated in Vero E6 cells (ATCC CRL-1586) as described (31). Mice were anesthetized by intraperitoneal administration of Avertin (150-250 mg/kg; Sigma-Aldrich) and intranasally challenged with 10^6 PFU of RSV A2 in Phosphate Buffered Saline (PBS; GE Healthcare HyClone). The FI-RSV A2 vaccinated mice

received a 1:50 dilution in PBS of FI-RSV A2 (prepared as described below) by intramuscular (i.m.) injection in a final volume of 50 µL/mouse. Control mice (naïve and naïve+RSV) did not receive any vaccination.

FI-RSV A2 preparation:

This protocol was adapted from the FI-RSV Lot 100 methods described by Prince *et al*. (32). Briefly, Vero E6 cells infected with RSV A2 at a MOI=0.1 in DMEM without serum (SF-DMEM). When the cells showed extensive cytopathic effect (~ day 4pi), medium was removed; cells were scraped, collected into a 50mL tube and sonicated. Cell debris was removed by centrifugation at 600 x g for 15 min at 4°C. The supernatant was transferred to a clean tube and filter sterilized using a 2µm filter. Protein concentration was determined by BCA assay, and the final concentration was adjusted to 1-2 mg/mL. The virus was inactivated by the addition of 37% formalin (final dilution 1:4,000) incubated at 37°C per 3 days in agitation. The virus was pelleted by ultracentrifugation for 2 h at 25,000 rpm (Beckman; SW28 rotor) then re-suspended in SF-DMEM at 1/25th of the original volume, and then adsorbed overnight at room temperature in 4 mg/mL aluminum hydroxide. The compound material was pelleted by centrifugation and the pellet was re-suspended in SF-DMEM and total virus inactivation was confirmed via plaque assay. This procedure resulted in an FI-RSV vaccine that is concentrated 100-fold and contains 16 mg/ml alum. The vaccine was aliquoted in 1ml volumes and stored at 4°C.

In vivo miRNA treatment

The miR-467f mimic, miR-467f inhibitor, and miRNA scramble were resuspended in 500µl of Opti-MEM® (ThermoFisher), then 5µl of DharmaFECT1 (GE Dharmacon, Lafayette, CO) was added, mixed gently by pipetting and incubated for 20 minutes at room temperature. At 24 h prior to RSV A2 mice received 5 nmol of miR-467f mimic, miR-467f inhibitor, or miRNA scramble in 50µl of transfection mixture via I.N. delivery. Mice in the vehicle control group received 50µl of the transfection mixture as a treatment control. Control mice (naïve and naïve+RSV) did not receive any treatment.

RNA isolation

Total RNA was isolated from sera samples collected from mice using the miRNeasy Serum/Plasma Kit (Qiagen) following manufacture protocol for isolation of total RNA. A total volume of 100 µl of serum was used per mouse for total RNA isolation, and RNA was eluted in 20 µl of RNase-free water. Lung RNA was isolated from lung samples using RNAzol®RT (Molecular Research Center, Inc) following manufacture protocol for isolation of total RNA. Lugs samples were homogenized with RNAzol®RT (up to 100 mg of tissue per 1 mL of RNAzol®RT) and total RNA was solubilized in 20µl of RNase free water. RNA concentration was determined using Epoch™ microplate spectrophotometer controlled with the Gen5 Data Analysis software interface (BioTek).

RT-qPCR for miRNA detection

For the total RNA isolated from the sera, the miScript II RT Kit (Qiagen Cat. # 218161) was used to generate cDNA for sensitive and specific miRNA detection. cDNA detection by miScript SYBR® Green PCR Kit (Qiagen Cat. # 218073) was used to quantify the expression levels of miR-467f in each sample. All miRNA levels were normalized by RNU6 (Qiagen Cat. # MS00033740) and all samples were run in duplicate. For the total RNA isolated from the lungs, the miRNA 1st-Strand cDNA Synthesis Kit (Agilent Technologies Cat. # 600036) was used for the polyadenylation of the miRNAs at the 3' end from the total RNA and reverse transcription to convert the polyadenylated miRNA to cDNA. cDNA detection by Brilliant III Ultra-Fast SYBR Green QPCR Master Mix (Agilent Technologies Cat. # 600886) was used to quantify the expression levels of miR-467f in each sample. All miRNA levels were normalized by mouse-specific 18S rRNA (Applied Biosystems Cat. # 4331182) gene expression and all samples were run in duplicate. The 2^-ΔΔCt method was utilized to calculate expression fold change over mock (naïve mice).

miRNA primer

The mouse-specific miR-467f sequence was obtained from miRBase, and the forward primer was designed based on the mature miRNA sequence with the greatest number of deep-sequencing reads, and synthesized by Integrated DNA Technologies (IDT). The final primer sequence was 21 nt in length with the following sequence: 5'-ATA TAC ACA CAC ACA CCT ACA-3'.

Lung viral titer by plaque assay

RSV lung virus titers in treatment and control mice were determined by plaque assay as previously described (31). Briefly, lungs were aseptically removed from mice at day 5 post-RSV A2 challenge (10^6 PFU /mouse), and individual lung specimens were homogenized at 4°C in 1 mL of SF-DMEM (Hyclone) by use of gentleMACS^{TM} Dissociator (Miltenyi Biotec). Samples were centrifuged for 10 min at 200 x g, the supernatants were transferred to a new tube and used immediately or stored at -80°C until they were assayed. For the plaque assay, 10-fold serial dilutions of the lung homogenates were added to 90% confluent Vero E6 cell monolayers. Following adsorption for 2h at 37°C, cell monolayers were overlaid with 1% methylcellulose medium and incubated at 37°C for 7 days. The plaques were enumerated by immunostaining with monoclonal antibodies against RSV F protein (clone 131-2A) as previously described (33).

Lung viral titer by RT-qPCR

RSV lung virus titers in treatment and control mice were also determined by RSV A2 M gene copy number by RT-qPCR as previously described (34). Briefly, total RNA was extracted and quantified from the homogenized lung samples. Serial dilution of known PFU of RSV A2 RNA was used to obtain a standard reference curve for RT-qPCR (35). Expression of RSV A2 M gene was determined by one-step RT-qPCR using the AgPath-ID One-Step RT-qPCR kit (Life Technologies) and the following primers and probe: RSV A2 M gene forward primer: 5'-GGC AAA TAT GGA AAC ATA GCT GAA-3', RSV A2 M gene reverse primer: 5'-TCT TTT TCT AGG ACA TTG TAT TGA ACA G-3', and TaqMan probe: 5'-GTG TGT ATG TGG AGC CTT CGT GAA GCT-3', labeled at the 5' end with the reporter molecule 6-carboxyfluorescein (FAM) and labeled

with a Blackhole quencher-1 (BHQ1) at the 3' end. Data was analyzed using RT-qPCR analysis software and cycle threshold (Ct) values and corresponding copy numbers were calculated.

ELISPOT analysis

24h prior to the assay, 96-well Multiscreen plates (Millipore) were coated with the anti-mouse IL-4, anti-mouse IFN-γ, or anti-mouse IL-5 capture antibody (R&D Systems) and incubated overnight at 4°C. The plates were then blocked by the addition of 200 μL of RPMI-10 medium (RPMI 1640 supplemented with 10% FBS, 100 U/mL penicillin, 100 μg/mL streptomycin, 50 μM 2-mercaptoethanol and 2 mM L-glutamine) and incubated for 2 h at 37°C. In parallel, spleens were harvested from treatment and naïve mice at 5 days and 7 days post-challenge with RSV A2 and prepared to a single cell suspension using a syringe plunger and a 70 μm mesh nylon strainer. The cell suspensions were collected by centrifugation for 10 min at 200 × g and suspended in RPMI-10 at a concentration of 10^7 cells/mL. Spleen cell suspensions were added to each well, and cells were stimulated with either 10 μg/mL RSV M2 (82-90) peptide, 10 μg/mL RSV F (51-66) peptide, 10 μg/mL RSV G (183-198) peptide or 10 μg/mL GFP (irrelevant peptide control) for 24h at 37°C and 5% CO_2. Plates were washed 4 times with wash buffer (0.05% Tween-20 in PBS), anti-mouse IL-4, anti-mouse IFN-γ, or anti-mouse IL-5 detection antibody (R&D Systems) was added and plates were incubated overnight at 4°C. Detection antibody was removed, plates were washed and cytokine spots were developed using NBT/BCIP substrate (Thermo Fisher Scientific). Spots were counted using an ELISPOT reader (CTL-ImmunoSpot®).

BAL collection and quantification of cytokines

Day 5 and 7 post-challenge, a subset of mice from each group was sacrificed and tracheotomy was performed. The mouse lungs were flushed three times with 1 ml of PBS and the retained BAL was centrifuged at 400 x g for 5 min at 4°C. The recovered supernatants were collected and stored at -80°C until assessed for cytokine concentration, and the cell pellet were resuspended in 200 μL of FACS staining buffer (PBS containing 1% BSA). Total cell numbers were counted using a hemocytometer. The Luminex® xMAPTM system using a MILLIPLEX MAP mouse cytokine immunoassay (MCYTOMAG-70K, Millipore) was used to quantitate cytokines in BAL supernatants according to the manufacturer protocol. Briefly, beads coupled with anti-IFN-γ, anti-IL-1α, anti-IL-2, anti-IL-4, anti-IL-5, anti-IL-6, anti-IL-9, anti-IL-10, anti-IL-12p40, anti-IL-13, anti-IL-15, anti-IL17A, anti-MCP-1, anti-RANTES, anti-TNF-α, and anti-Eotaxin monoclonal antibodies were sonicated, mixed, and diluted 1:50 in assay buffer. For the assay, 25 μL of beads were mixed with 25 μL of PBS, 25 μL of assay buffer and 25 μL of BAL supernatant and incubated overnight at 4°C. After washing, beads were incubated with biotinylated detection antibodies for 1 h and the reaction mixture was then incubated with streptavidin- phycoerythrin (PE) conjugate for 30 min at room temperature, washed, and resuspended in PBS. The assay was analyzed on a Luminex 200 instrument (Luminex Corporation, Austin, TX) using Luminex xPONENT 3.1 software.

Flow cytometry

For flow cytometry analysis, cell suspensions were incubated in FACS staining buffer and blocked with FcγIII/II receptor antibody (BD Bioscience), and subsequently

stained with optimized concentrations of anti-mouse antibodies obtained from BD bioscience, i.e. PE-conjugated anti-CD3e (145-2C11), Alexa fluor 488-conjugated anti-CD8α (53-6.7), PerCP-Cy5.5-conjugated anti-CD4 (RM4-5), PE-Cy7 conjugated anti-CD69 (H1.2F3) and APC-conjugated MHC class I H-2K^{d} tetramer complexes bearing the peptide SYIGSINNI (Beckman Coulter) representing the immunodominant epitope of the RSV M2-1 protein [55]. To determine cell types in lungs, BAL cell suspensions were stained for 60 min at 4°C with an optimized concentration of PerCP-Cy5.5-conjugated anti-CD45 (30-F11), APC-conjugated anti-CD11c (HL3), PE-conjugated anti-SiglecF (E50-2440), Alexa fluor 488-conjugated anti-CD125 (T21) and PE-Cy7 conjugated anti-CD69 (H1.2F3). Cells were acquired on a LSRII flow cytometer (BD Bioscience) with data analyzed using FlowJo software (v 7.6.5). Based on cell surface markers expression three different cell types were identified: SCC^{high} CD45^{+} SiglecF^{+} CD11c^{low} as eosinophils, SSChigh CD45^{+} SiglecF^{+} CD11c^{high} as alveolar macrophages [56] and SCC^{med} CD45^{+} SiglecF^{-} CD11c^{low} as other granulocytes (basophils or neutrophils). These three cell types were subsequently classified according to the level of expression of CD125 (IL-5 receptor α subunit) as IL-5R negative, medium or high.

Indirect ELISA

RSV A2-specific IgG antibodies were detected by ELISA using 96-well high binding plates (Corning, NY) coated with 10^{6} PFU/mL RSV A2 in 0.05 M carbonate-bicarbonate buffer, pH 9.6. Sera or BAL supernatant were added to plates in serial dilutions. RSV-specific antibodies were detected with horseradish peroxidase (HRP) conjugated antibodies specific for mouse IgG (Southern Biotech) followed by addition of

SureBlue TMB 1-Component Microwell Peroxidase Substrate (KPL, Inc.) for 15 min. Antibody titers were determined as the last sample dilution that generated an OD_{450} reading of greater than 0.2 (mean OD value of background plus 2 standard deviations of the mean).

Bioinformatics Analysis

Predicted gene targets for miR-467f were identified by DIANA TarBase v7.0 based on the criteria of experimentally validated genes and successful binding of miR-467f to the 3'UTR of these chosen gene targets. Important pathways associated with these gene targets were identified through GeneCards®: Human Genome Database. Ingenuity IPA (Qiagen) was also used to identify 56 potential gene targets of miR-467f.

Statistics

All statistical analyses were performed using GraphPad software (San Diego, CA). Statistical significance was determined using a Student's t-test, One-way ANOVA or Two-way ANOVA followed by Bonferroni's post-hoc comparisons tests, a p value $\leq$ 0.05 was considered significant.

Results

miR-467f mimic enhances mucosal and systemic antibody response

A RSV vaccine-enhanced disease model was established in mice using the FI-RSV vaccine prepared as previously described (32). A miR-467f mimic and a miR-467f inhibitor were used to either enhance or attenuate the effects of endogenous miR-467f,

respectively. BALB/c mice were primed and boosted by i.m. vaccination on day -42 and -21, respectively, with 50 μL of FI-RSV (10^6 PFU equivalents of RSV A2), treated with 5 nmol of miRNA (i.n.) or 50 μL of vehicle on day -1, and challenged with 10^6 PFU of RSV A2 on day 0 (Fig. S6.1). Age- and sex-matched naïve control groups received no FI-RSV immunization. 24 hours post miRNA treatment all mice were challenged with live RSV A2, except the naïve group that received no virus (Fig. S6.1). To determine whether miR-467f inhibitor treatment exacerbates vaccine-enhanced disease, body weight loss was recorded daily from the day RSV challenge (day 0) until all mice were sacrificed on day 7 post-infection (pi). As shown in Fig.6.1A, miR-467f mimic or inhibitor treatment had no detectable affect on body weight loss, as there was no significant difference in body weight loss among treatment groups at any time point post infection (Fig.6.1A). Next, the effect of miR-467f mimic and inhibitor on the systemic and mucosal antibody response was assessed at day 7 pi. RSV A2-specific antibody levels were measured in the serum and the bronchoalveolar lavage (BAL) (Fig.6.1B-D). All groups vaccinated with FI-RSV elicited high levels of RSV-specific IgG in the serum (Fig.6.1B), where the FI-RSV vaccinated mice had a ~60-fold increase in IgG titers compared to naïve mice infected with RSV (day 7 pi). Only mice treated with miR-467f mimic elicited significantly ($p \leq 0.01$) higher serum RSV A2-specific IgG titers (Fig.6.1B). Interestingly, a similar trend was observed in the mucosal antibody response, where miR-467f mimic treated mice elicited significantly ($p \leq 0.05$) higher RSV-specific IgG levels in the BAL as compared to the vehicle group, and the miR-467f inhibitor group, but not the miRNA scramble control (Fig.6.1C). RSV-specific IgA levels in BAL showed a similar trend to the IgG levels, but were not statistically significant (Fig.6.1D). It is not surprising that

there was no substantial difference in antibody titers between naïve and naïve+RSV mice (day 7 pi). This likely due to the time it takes (approximately 15 days) for IgG, and longer for IgA, to reach detectable levels in the serum and mucosal tissues (36, 37). Overall, these findings demonstrate that the FI-RSV vaccination elicited an RSV-specific B cell memory response, which upon RSV challenge resulted in high RSV-specific IgG and IgA levels in the serum and the BAL. Quite interestingly, it appears that local enhancement of miR-467f using a miR-467f mimic potentiated the mucosal and systemic RSV-specific antibody response, but the local inhibition of miR-467f with a miR-467f inhibitor had no detectable impact on the antibody response.

MiR-467f expression levels in the sera and lungs of mice following RSV challenge

To evaluate the *in vivo* effect of the miR-467f mimic and inhibitor treatment on the endogenous levels of miR-467f, miR-467f expression was measured in the sera and the lungs of mice at day 7 post-challenge with RSV (Fig.6.2 and Fig.S6.1). The scramble miRNA control group was used to control for off-target effects; the vehicle group was used to control for the transfection mixture used for i.n. delivery; the naïve+RSV group was used to demonstrate the endogenous levels of miR-467f during live RSV infection and the naïve uninfected control was used to calculate the base line expression of miR-467f (Fig.6.2). As seen in Fig.2A at day 7 pi, the miR-467f level in the sera was significantly ($p \leq 0.05$) higher in the miR-467f mimic group than in naïve+RSV group or the other groups, indicating that i.n. administration of miR-467f mimic on day -1 enhanced the systemic levels of this miRNA. Conversely, miR-467f expression levels in the sera of the mice treated with a miR-467f inhibitor were equivalent to that of the

naïve+RSV, vehicle, and scramble groups (Fig.6.2A). In the lung tissue, expression of miR-467f was reduced in all treatment groups compared to naïve+RSV mice, and as expected mice treated with miR-467f inhibitor showed the most significant ($p \leq 0.05$) difference compared to the vehicle control (Fig.6.2B). Surprisingly, the group of mice treated with miR-467f mimic showed no significant increase in the pulmonary levels of miR-467f at day 7 pi compared to the vehicle control (Fig.6.2B). These results show that FI-RSV vaccination prior to RSV infection induces immunological changes that result in reduced miR-467 expression in the lungs. Further, these results show that i.n. delivery of miR-467f mimic results in an increase of serum miR-467f by day 7 pi (day 8 post treatment), with no change in pulmonary levels. This data suggests that miR-467f may access the blood stream or could stimulate immune cells to produce miR-467f resulting in elevated levels of this miRNA. It is possible that at an earlier time point post miRNA administration may generate detectable miR-467f expression levels in the lungs.

Enhancement or attenuation of miR-467f does not affect lung viral titers

Previous studies that characterized the FI-RSV vaccine-enhanced disease phenotype showed that mice exhibited reduced viral titers in the lung following RSV challenge (12, 38, 39). In addition, there is convincing evidence that the degree of RSV virus load correlates with disease severity (40-43). In the earliest phases of the infection, activation of host defense mechanisms and regulation of viral replication is governed by a variety of mechanisms that involve gene expression that are subsequently governed by other factors (37, 40, 44, 45). miRNAs have recently emerged as gene expression regulators that have a modulatory role in virus infection by altering the host response in

inflammatory and immune cells as well as airway epithelial cells (21, 40, 46-48). To evaluate the role of miR-467f in RSV replication, *in vitro* studies were performed using mouse lung epithelial (MLE-15) cells transfected for 48 hours with miRNA scramble, miR-467f mimic, miR-467f inhibitor, or vehicle (transfection reagent control) and subsequently infected with live RSV A2 at MOI=0.5. The MLE-15 cells transfected with miR-467f mimic had a significantly ($p \leq 0.01$) higher viral titers as compared to the vehicle and the miRNA scramble control (Fig.S6.2A). Conversely, the miR-467f inhibitor treated cells had reduced viral titers compared to the vehicle control and similar to miRNA scramble control (Fig.S6.2A). To substantiate that the observed changes in viral titers relate to alterations in the miRNA expression levels, RT-qPCR was performed to assess miR-467f expression levels among groups. Compared to the miRNA scramble control, all groups showed equivalent miR-467f expression levels with the exception of the miR-467f mimic where significantly ($p \leq 0.001$) higher levels were observed (Fig.S6.2B). Taken together, these *in vitro* results show that the miR-467f inhibitor has an antiviral effect whereas the miR-467f mimic has a proviral effect on RSV replication.

To assess the relationship between viral load and miR-467f expression *in vivo*, lung virus titers were determined at days 5 and 7 post-challenge. At day 5 post-challenge (peak of RSV replication) all groups vaccinated with FI-RSV had considerably lower lung viral titers as compared to the naïve+RSV group due to the partial protection induced by the FI-RSV vaccine (Fig.6.3A). Mice treated with vehicle control and miR-467f mimic had lower lung viral titers than miRNA scramble or miR-467f inhibitor, but this difference was not significant indicating that miRNA treatment has no effect on RSV replication (Fig.6.3A). Moreover, no substantial reduction in RSV genome copy number

was observed at daya 5 and 7 pi, indicating that although livr RSV clearance occurs, RSV genome remains in the lungs for longer periods of time (Fig.6.3B). Thus, these results indicate that though miR-467f has a proviral effect *in vitro* at 24 hpi and does not detectably affect RSV replication or viral clearance *in vivo* at days 5 and 7 pi, however it does have an impact in the RSV-specific antibody response (Fig.6.1). Therefore, these results are suggestive that miR-467f may be linked to the host immune response to RSV infection.

MiR-467f inhibition alters the Th1/Th2 phenotype

It is well known that the FI-RSV vaccine is not a safe and efficacious vaccine as it resulted in vaccine-enhanced disease in recipients upon exposure to live RSV (49-53). The vaccine enhanced disease is a complex phenomenon that can be in part described as the presence of pulmonary eosinophilia and a Th2 biased response in FI-RSV vaccinated animals challenged with RSV (39, 51, 54-57), with a predominant increase in IL-4 expression and other Th2-type cytokines (54). To investigate whether treatment with the miR-467f mimic and miR-467f inhibitor altered the Th1/Th2 memory response, the frequencies of IFNγ (Th1) and IL-4 (Th2) secreting cells were measured in the spleens of treated mice by ELISPOT assay at day 5 and day 7 post-challenge. Splenocytes were stimulated with peptides representing the RSV-derived CD4 epitopes F_{51-66} and $G_{183-198}$ and the immunodominant RSV-specific CD8 epitope $M2_{82-90}$ (58). As expected, at day 5 pi naïve mice infected with RSV developed RSV-specific Th1-type cell response directed against the M2 and F proteins (Fig.6.4A), and at day 7 pi most of the cells producing IFNγ were $M2_{82-90}$-specific T cells, most likely CD8 T cells (Fig.6.4B). Overall, FI-RSV

vaccinated mice challenged with RSV showed increased levels of cells producing IL-4 expressing cells compared to naïve+RSV mice (Fig.6.4C and 6.4D), with a clear Th2-type bias response; compared to the mice in the vehicle group of mice there was no significant difference in IFNγ-secreting cells among all of the groups at 5 dpi (Fig.6.4A) and 7 dpi (Fig.6.4B). However, FI-RSV vaccinated mice treated with the miR-467f inhibitor had significantly ($p \leq 0.05$) higher frequencies of IL-4 secreting cells as compared to the vehicle group at day 5 post-challenge (Fig.6.4C). Similarly at day 7 post-challenge, the miR-467f inhibitor group also had higher frequencies of IL-4 secreting cells than the vehicle group, however this difference was not significant (Fig.6.4D). Overall, mice vaccinated with FI-RSV had an exacerbated response to peptide stimulation (including the irrelevant peptide GFP) independently of the miRNA treatment (Fig.6.4).

Analysis of cytokines (IFNγ, IL-1α, TNF-α, and IL-2) and chemokines (MCP-1 and RANTES) in BAL supernatant showed a trend towards of increased cytokine expression in the FI-RSV vaccinated groups at days 5 and 7 pi independently of miRNA treatment, as a marker for enhanced inflammation in these mice (Fig.6.5). All treatment groups had similar IL-1α (Fig.6.5B) and IL-2 (Fig.6.5D) expression at day 5 and day 7 post-challenge as compared to the respective vehicle groups, but the expression decreased by day 7 post-challenge. There was no substantial difference in TNF-α levels among treatment groups at days 5 and 7 pi as compared to the vehicle control groups (Fig.6.5C). Only the miR-467f mimic group showed significant ($p \leq 0.01$) upregulation of RANTES expression as compared to the vehicle control groups (Fig.6.5F). IFNγ, IL-5 and Eotaxin were significantly increased in the mice treated with miR-467f inhibitor as compared to

the vehicle group (Fig.6.5A, 6.6B and 6.6F). At day 5 post-challenge, the levels of MCP-1 were also higher in the miR-467f inhibitor group compared to the vehicle group, however this difference was not statistically significant and expression among all groups had diminished by day 7 post-challenge (Fig.6.5E). To investigate this further, the frequency of IL-5 producing splenocytes was determined by ELISPOT assay at day 7 post-challenge. Although there was no significant difference in IL-5 secreting cells as compared to the vehicle group, all FI-RSV vaccinated mice had higher frequency of IL-5 producing cells than naïve+RSV mice (Fig.6.6C). These findings are particularly important, as various studies have shown that of the inflammatory mediators postulated to contribute to the regulation of eosinophil trafficking and degranulation, only IL-5 (59-64) and eotaxin (65-68) have been identified to selectively regulate eosinophil function (69). Taken together, these results indicate that enhancement of endogenous miR-467f levels using the miR-467f mimic does not promote a Th1-type cytokine phenotype; however, attenuation of endogenous miR-467f levels using the miR-467f inhibitor promotes a Th2-type biased phenotype as compared to the vehicle control. Therefore, lack of miR-467f expression appears to further exacerbate the Th2-type response previously reported in FI-RSV induced enhanced disease. Importantly, the elevated levels of IL-5 and eotaxin in the BAL supernatant of mice treated with the miR-467f inhibitor are indicative of eosinophilic inflammation of the airways, which has a critical role in the pathogenesis of asthma (69).

Treatment with miR-467f mimic is associated with enhancement of the pulmonary CD4+ T cell response and reduced RSV M2-specfic CD8+ T cell response

It was important to evaluate the role of miR-467f in pulmonary infiltration and T cell activation, as these are characteristics linked to FI-RSV vaccine enhanced disease (12, 54, 70). Flow cytometry was used to determine T cell types and CD69 expression was used as a marker for T cell activation (71-73). miR-467f mimic treatment was associated with a significant ($p \leq 0.01$) increase in pulmonary recruitment of $CD3^+$ T cells compared to mice treated with the miR-467f inhibitor (Fig.6.7A), and this increase was consistent with recruitment of $CD4^+$ T cells (Fig.6.7B) over $CD8^+$ T cells (Fig.6.7C). The overall increase in $CD4^+$ T cells observed was also reflected in an increase in the total amount of activated $CD69^+$ $CD4^+$ T cells recruited to the lungs (Fig.6.7D). Treatment with miR-467f mimic or inhibitor had no impact in the overall proportions of activated $CD69^+$ CD4 or $CD69^+$ CD8 T cells compared to the total number of $CD3^+$ T cells (Fig.6.8A). Mice vaccinated with FI-RSV had a lower percentage of RSV-specific CD8 T cells following RSV infection compared to naïve+RSV mice (~20% vs ~60%), likely due to the Th2-type biased response induced by the vaccine (Fig.6.8B). Within FI-RSV vaccinated mice, treatment with miR-467f mimic and miR-467f inhibitor had no detectable influence on the recruitment of RSV M2-specific $CD8^+$ T cells (Fig.6.8B). However, the miR-467f mimic had a significantly ($p \leq 0.05$) lower percentage of RSV M2-specific $CD8^+$ $CD69^+$ T cells compared to the miR-467f inhibitor (Fig.6.8C), while this difference was not observed for the $CD8^+$ $CD69^-$ T cells (Fig.6.8D). In summary, these results demonstrate that treatment with the miR-467f mimic is linked to enhanced pulmonary $CD4^+$ T cell infiltration, resulting in an increase in the number of activated $CD4^+$ T cells, reducing the percentage of RSV M2-specific activated $CD8^+$ T cells. This

data suggests that miR-467f has an important role in $CD4^+$ and RSV-specific $CD8^+$ T cell activation in the airways during vaccine enhanced disease.

miR-467f regulates pulmonary infiltration of granulocyte cells

IL-5 functions synergistically with the Th2-type cytokines IL-4 and IL-13 (74), and with the eosinophil chemoattractant eotaxin to promote eosinophil activation and recruitment into tissues in acute inflammatory responses (74). More specifically, IL-5 expression has a critical role in eosinophil and basophil differentiation, exerting its effects through the IL-5 receptor (IL-5R) (75). Given the considerably elevated levels of IL-5 and eotaxin expression induced by the miR-467f inhibitor, it was important to determine the correlation with pulmonary granulocyte trafficking and activation. A unique finding showed that by flow cytometry macrophage, eosinophil, and other granulocyte cells had differential IL-5R α subunit (CD125) expression levels (Fig.6.9). Overall, alveolar macrophages (SSC^{high} $CD45^+$ $SiglecF^+$ $CD11c^{high}$) showed moderate levels of IL-5R expression (IL-5R ^{medium}), whereas contrary to what we expected, most of the eosinophils (SCC^{high} $CD45^+$ $SiglecF^+$ $CD11c^{low}$) showed low or no detectable expression of IL-5R ($IL\text{-}5R^{neg}$), and a third population of granulocytes (SCC^{med} $CD45^+$ $SiglecF^-$ $CD11c^{low}$) showed the highest levels of IL-5R expression (Fig.6.9 and Fig.S6.3B). The naïve+RSV group had significantly ($p \leq 0.05$) higher numbers of $IL\text{-}5R^{med}$ macrophages as compared to the miR-467f inhibitor treated mice, but there was no important differences between the miR-467f mimic and miR-467f inhibitor treated mice in the number of $IL\text{-}5R^{neg}$, $IL\text{-}5R^{med}$ or $IL\text{-}5R^{hi}$ macrophages (Fig.6.9A). The miR-467f inhibitor treated mice had substantially higher numbers of $IL\text{-}5R^{neg}$ eosinophils as compared to the naïve,

naïve+RSV, and vehicle groups (Fig.6.9B). There was no significant difference between the miR-467f mimic and miR-467f inhibitor treated mice in the number of IL-5R^{neg}, IL-5R^{med} or IL-5R^{hi} eosinophils (Fig.6.9B). We had anticipated finding increased levels of IL-5R expression in the eosinophil population of the miR-467f inhibitor group since this group had upregulation of IL-5 and eotaxin levels in the BAL; however, this may be explained by prior *in vivo* studies that have shown that IL-5-activated eosinophils may lose membrane IL-5Rα (mIL-5Rα) and release soluble IL-5Rα (sIL-5Rα) (76, 77). The miR-467f inhibitor group had significantly ($p \leq 0.05$) higher numbers of IL-5R^{med} granulocytes compared to the naïve and naïve+RSV groups (Fig.6.9C). Interestingly, the miR-467f inhibitor treated mice had considerably higher numbers of IL-5R^{hi} granulocytes compared to the naïve ($p \leq 0.0001$), naïve+RSV ($p \leq 0.0001$), vehicle ($p \leq 0.0001$), scramble ($p \leq 0.01$), and miR-467f mimic ($p \leq 0.0001$) groups (Fig.6.9C). It is highly likely that this other granulocyte population is basophils, due to their high IL-5R expression levels and granularity; however, additional basophil activation and functional markers are needed to confirm this.

From these different cell populations, leukocyte activation was evaluated using CD69 expression in the context of negative-, medium-, and high- IL-5R expression. Similar to what we previously observed, the naïve+RSV mice had a significantly ($p \leq 0.01$) higher number of CD69^{+} IL-5R^{med} macrophages as compared to the miR-467f inhibitor, but there was no substantial difference between the miR-467f mimic and miR-467f inhibitor treated mice (Fig.6.9D). The miR-467f inhibitor group had a significantly ($p \leq 0.05$) higher number of CD69^{+} IL-5R^{med} eosinophils compared to the naïve and naïve+RSV mice, but there was no difference in CD69^{+} IL-5R expression between the

miR-467f inhibitor and the miR-467f mimic treated mice (Fig.6.9E). The miR-467f inhibitor treated mice had a significant ($p \leq 0.05$) increase in the number of IL-5R^{med} and IL-5R^{hi} CD69^{+} granulocytes compared to all other groups (Fig.6.9F). CD69 expression on basophils has been shown as a useful *in vitro* as well as *in vivo* marker of activation of these cells by IL-3 (78). Taken together, these results indicate that attenuation of miR-467f expression levels substantially increases pulmonary granulocyte infiltration, and likely basophil recruitment. However, enhancement or attenuation of miR-467f expression had no substantial effect on pulmonary infiltration of macrophage and eosinophil cells. Mast cells, basophils and eosinophils express many of the same receptors and cytokines; yet have different effector functions (79). Recent data from mouse models show a direct role for basophils in antigen presentation for induction of Th2-type responses, with expression of MHC class II molecules and IL-4 production (79). Given the data shown, basophils may be a crucial component of the allergic inflammation observed in vaccine-enhanced disease.

Identifying functionally relevant gene targets of miR-467f

In order to understand the biological role of miR-467f, we identified the predicted host gene targets and the associated major signal transduction pathways. 56 gene targets were identified for miR-467f (Fig.6.S4). Of these predicted gene targets for miR-467f, the top 10 functionally relevant gene targets were identified by DIANA TarBase v7.0 based on the criteria of experimentally validated genes and successful binding of miR-467f to the 3'UTR of these chosen gene targets (Table 6.1). These are associated with 11 major signal transduction pathways (Table 6.1). Of these major signal transduction pathways

both PI3K-Akt signaling (80, 81) and TGFβ signaling (82-84) have been previously described as having a role in various aspects of RSV infection. Therefore, we examined Pten and Klf6 gene expression levels in the lungs of all mice at day 5 post-RSV challenge. There were no substantial differences in Pten or Klf6 expression between the groups of mice examined at 5 dpi (Fig.S6.5). Overall FI-RSV vaccinated mice had somewhat higher Klf6 expression levels as compared to the naïve+RSV group mice, however this difference was not statistically significant (Fig.S6.5). Taken together, these results suggest that miR-467f regulates the expression of genes other than Pten and Klf6. miR-467f is predicted to modulate at least 56 different genes (Fig.S6.4) belonging to various pathways, several of which have already been implicated in RSV replication, immune response and cell cycle. However, further studies need to be conducted to better elucidate the mechanism of action by which miR-467f influences the adaptive immune response to FI-RSV induced enhanced disease. Overall, these results demonstrate that miR-467f promotes antibody responses and $CD4^+$ T cell recruitment to the lungs of RSV-challenged mice, without affecting RSV replication *in vivo*; where as, inhibition of miR-467f enhances expression of proinflammatory cytokines (i.e. IL-5 and eotaxin) that results in recruitment of IL-$5R^{med}$ and IL-$5R^{hi}$ granulocytes and enhanced lung pathogenesis.

Discussion

The present study provides novel insights into the potential immunomodulatory effects of miR-467f expression on the host-virus interface and vaccine enhanced disease. Host genetic studies are beginning to outline factors associated with severity of RSV

disease; for example, certain polymorphisms in RANTES, IL-8, IL-4, and IL-13 genes have been associated with RSV disease (85). However, very little is known about how the host miRNA response induced during vaccination and in response to RSV infection modulates enhanced disease. These studies demonstrate that attenuation of endogenous miR-467f levels *in vivo* using the miR-467f inhibitor elicits a higher Th2 RSV-specific T cell response as compared to the vehicle control. Therefore, the miR-467f inhibitor appears to further exacerbate the Th2-type response previously reported in FI-RSV induced enhanced disease. The significantly elevated levels of IL-5 and eotaxin in the BAL supernatant of mice treated with the miR-467f inhibitor also support the notion of eosinophilic inflammation of the airways. Furthermore, numerous studies have shown a strong correlation between the presence of eosinophils and their products in the airways, disease severity, and airway hyperreactivity (AHR) (69, 86-90). Therefore, these studies demonstrate a specific role for miR-467f in the regulation of critical features of vaccine enhanced disease and allergic disease.

As well as augmenting the cellular immune response resulting in exacerbation of FI-RSV induced enhanced disease; this data suggests a role for miR-467f in mechanisms related to antibody-mediated protection from RSV. IgA is particularly well suited for the control of respiratory virus infections as this isotype is localized to the mucosal lining of the respiratory tract (49). IgG can also cross epithelial cells into the respiratory tract and, in the absence of IgA, can protect against RSV disease (49) . This study demonstrates that mice treated with miR-467f mimic show higher RSV A2-specific IgG and IgA levels in the BAL as compared to the other groups.

In vitro studies showed that enhancement of endogenous miR-467f expression using a miR-467f mimic had a considerable proviral effect as compared to the miRNA scramble control. However, no changes in RSV replication were seen in mice treated with miR-467f mimic. It is possible that by day 5 post-challenge (6 days post miRNA treatment) any initial proviral effect is no longer evident because at this stage RSV has completed more than one round of replication. Importantly, mice treated with miR-467f mimic showed an increase in local RSV-specific antibody and CD4 T cell response, with a substantial increase in $CD69^+$ CD4 T cells, which indirectly suggest that miR-467f may increase RSV replication in epithelial cells at early time points, enhancing the amounts of viral antigen and triggering stronger local immune response. Another possibility affecting the correlation between the *in vitro* and *in vivo* results could be related to the chosen route of delivery, low transfection efficiency of miR-467f mimic into airway epithelial cells *in vivo*, as well as lower local concentration of miRNA compared to an *in vitro* setting; but more importantly it highlights the importance of *in vivo* studies when assessing the role of miRNAs on viral replication and pathogenesis. Intranasal delivery of the miRNA mimic and inhibitor was chosen to target airway epithelial cells and immune cells infiltrating the lung, as this route has been shown previously to be effective (91-94). In addition, several studies have used a transfection reagent for *in vivo* miRNA and siRNA delivery in order to protect the naked RNA from rapid degradation. This study utilized *in vivo* tracking using a Dy547-labeled miRNA to demonstrate that the exogenous miRNA is in fact penetrating the upper and lower respiratory tract and remaining viable during the course of live RSV infection. More specifically, these results demonstrate that the miRNA was present in lymphocyte ($CD45^+$) cells obtained from the

BAL, lungs, and trachea of mice at 24 hours pre- and 3 days post-infection with RSV (Fig.S6.6).

By inducing gain- and loss- of-function, we describe a physiological role for miR-467f in linking the innate and adaptive immune response that responds to FI-RSV induced enhanced disease. However, further investigation is needed into the subsequent impact of miR-467f on key downstream mechanisms that modulate the innate and memory contributing to inflammation. Activation of the PI3K-Akt pathway has been demonstrated to occur during the early phase of infection by numerous cytopathic viruses, such as human immunodeficiency virus, RSV, rubella virus, Coxsackie B virus, herpes simplex virus, flaviviruses, influenza virus, adenovirus, hepatitis B virus, and severe acute respiratory syndrome-associated coronavirus, and to prolong survival of infected cells and thereby promote virus replication (95-97). Based on this information from previous studies and as Pten was identified as the top gene target, we evaluated Pten mRNA expression in the lungs of all mice. However, we did not observe any change in Pten mRNA expression levels among the naïve+RSV, vehicle, scramble, miR-467f mimic, and miR-467f inhibitor treated mice at 5 days post-challenge (Fig.S5). This observation has caveats, as it is likely that Pten mRNA expression may have been altered at earlier time points post-miR-467f mimic treatment, and perhaps day 5 pi was too late to see any differences or perhaps genes further downstream in the pathway may have shown differential expression at this time point. It remains possible that we may need to assess PTEN protein expression to corroborate these findings. There are also other miRNAs that target the PI3k/Akt signaling pathway, and thereby perhaps modulating the functionality of that pathway by directly or indirectly interacting with miR-467f.

In conclusion, our data shows that miR-467f modifies the host immune response to vaccination and subsequent RSV challenge. Thus, the present study provides the proof-of-concept that miRNAs are intimately involved in the cellular and adaptive immune response and intracellular mechanisms controlling RSV replication and disease pathogenesis, and can be measured as parameters of disease severity and manipulated for therapeutic purposes. Further functional investigation of miR-467f in models of vaccine enhanced disease and airway inflammation will not only enhance our understanding of the mechanisms employed by miR-467f, but also perhaps lead to the development of novel therapeutic strategies for RSV patients.

Funding sources

This project was supported by the ARCS Foundation and the Georgia Research Alliance.

References

1. Falsey AR, Hennessey PA, Formica MA, Cox C, Walsh EE. Respiratory syncytial virus infection in elderly and high-risk adults. N Engl J Med. 2005;352(17):1749-59.
2. Hall CB, Weinberg GA, Iwane MK, Blumkin AK, Edwards KM, Staat MA, et al. The burden of respiratory syncytial virus infection in young children. N Engl J Med. 2009;360(6):588-98.
3. Haynes LM, Jones LP, Barskey A, Anderson LJ, Tripp RA. Enhanced disease and pulmonary eosinophilia associated with formalin-inactivated respiratory syncytial

virus vaccination are linked to G glycoprotein CX3C-CX3CR1 interaction and expression of substance P. J Virol. 2003;77(18):9831-44.

4. Jorquera PA, Anderson L, Tripp RA. Understanding respiratory syncytial virus (RSV) vaccine development and aspects of disease pathogenesis. Expert review of vaccines. 2015:1-15.

5. Knudson CJ, Varga SM. The Relationship Between Respiratory Syncytial Virus and Asthma. Veterinary pathology. 2014:0300985814520639-.

6. Bakre A, Mitchell P, Coleman JK, Jones LP, Saavedra G, Teng M, et al. Respiratory syncytial virus modifies microRNAs regulating host genes that affect virus replication. J Gen Virol. 2012;93(Pt 11):2346-56.

7. Christiaansen AF, Knudson CJ, Weiss KA, Varga SM. The CD4 T cell response to respiratory syncytial virus infection. Immunologic research. 2014.

8. Fenton C, Scott LJ, Plosker GL. Palivizumab: a review of its use as prophylaxis for serious respiratory syncytial virus infection. Paediatr Drugs. 2004;6(3):177-97.

9. Krilov LR. Respiratory Syncytial Virus: Update on Infection, Treatment, and Prevention. Curr Infect Dis Rep. 2001;3(3):242-6.

10. Sawada A, Nakayama T. Experimental animal model for analyzing immunobiological responses following vaccination with formalin-inactivated respiratory syncytial virus. Microbiology and immunology. 2016;60(4):234-42.

11. Derscheid RJ, Gallup JM, Knudson CJ, Varga SM, Grosz DD, van Geelen A, et al. Effects of formalin-inactivated respiratory syncytial virus (FI-RSV) in the perinatal lamb model of RSV. PLoS One. 2013;8(12):e81472.

12. Connors M, Kulkarni AB, Firestone CY, Holmes KL, Morse HC, 3rd, Sotnikov AV, et al. Pulmonary histopathology induced by respiratory syncytial virus (RSV) challenge of formalin-inactivated RSV-immunized BALB/c mice is abrogated by depletion of CD4+ T cells. J Virol. 1992;66(12):7444-51.

13. Christiaansen AF, Knudson CJ, Weiss KA, Varga SM. The CD4 T cell response to respiratory syncytial virus infection. Immunologic research. 2014.

14. Thornburg NJ, Hayward SL, Crowe JE, Jr. Respiratory syncytial virus regulates human microRNAs by using mechanisms involving beta interferon and NF-kappaB. MBio. 2012;3(6).

15. Oglesby IK, McElvaney NG, Greene CM. MicroRNAs in inflammatory lung disease--master regulators or target practice? Respiratory research. 2010;11:148.

16. Cheng K, Rai P, Plagov A, Lan X, Mathieson PW, Saleem MA, et al. Rapamycin-induced modulation of miRNA expression is associated with amelioration of HIV-associated nephropathy (HIVAN). Exp Cell Res. 2013;319(13):2073-80.

17. Xiong Y, Chen S, Liu L, Zhao Y, Lin W, Ni J. Increased serum microRNA-155 level associated with nonresponsiveness to hepatitis B vaccine. Clin Vaccine Immunol. 2013;20(7):1089-91.

18. Fabian MR, Sonenberg N, Filipowicz W. Regulation of mRNA translation and stability by microRNAs. Annual review of biochemistry. 2010;79:351-79.

19. Li JH, Liu S, Zhou H, Qu LH, Yang JH. starBase v2.0: decoding miRNA-ceRNA, miRNA-ncRNA and protein-RNA interaction networks from large-scale CLIP-Seq data. Nucleic acids research. 2014;42(Database issue):D92-7.

20. Bakre A, Tripp, R.A. Host-Encoded miRNAs Involved in Host-Pathogen Interactions. 2014. In: Frontiers in RNAi Volume 1 [Internet]. [In Press].

21. Othumpangat S, Walton C, Piedimonte G. MicroRNA-221 modulates RSV replication in human bronchial epithelium by targeting NGF expression. PLoS One. 2012;7(1):e30030.

22. de Candia P, Torri A, Gorletta T, Fedeli M, Bulgheroni E, Cheroni C, et al. Intracellular modulation, extracellular disposal and serum increase of MiR-150 mark lymphocyte activation. PLoS One. 2013;8(9):e75348.

23. Xiao C, Calado DP, Galler G, Thai TH, Patterson HC, Wang J, et al. MiR-150 controls B cell differentiation by targeting the transcription factor c-Myb. Cell. 2007;131(1):146-59.

24. Salomoni P, Perrotti D, Martinez R, Franceschi C, Calabretta B. Resistance to apoptosis in CTLL-2 cells constitutively expressing c-Myb is associated with induction of BCL-2 expression and Myb-dependent regulation of bcl-2 promoter activity. Proc Natl Acad Sci U S A. 1997;94(7):3296-301.

25. Ghisi M, Corradin A, Basso K, Frasson C, Serafin V, Mukherjee S, et al. Modulation of microRNA expression in human T-cell development: targeting of NOTCH3 by miR-150. Blood. 2011;117(26):7053-62.

26. Chen X, Ba Y, Ma L, Cai X, Yin Y, Wang K, et al. Characterization of microRNAs in serum: a novel class of biomarkers for diagnosis of cancer and other diseases. Cell Res. 2008;18(10):997-1006.

27. Zen K, Zhang CY. Circulating microRNAs: a novel class of biomarkers to diagnose and monitor human cancers. Med Res Rev. 2012;32(2):326-48.

28. Lu TX, Rothenberg ME. Diagnostic, functional, and therapeutic roles of microRNA in allergic diseases. The Journal of allergy and clinical immunology. 2013;132:3-13; quiz 4.

29. de Souza AP, de Freitas DN, Antuntes Fernandes KE, D'Avila da Cunha M, Antunes Fernandes JL, Benetti Gassen R, et al. Respiratory syncytial virus induces phosphorylation of mTOR at ser2448 in CD8 T cells from nasal washes of infected infants. Clin Exp Immunol. 2016;183(2):248-57.

30. Krukovets I, Legerski M, Sul P, Stenina-Adognravi O. Inhibition of hyperglycemia-induced angiogenesis and breast cancer tumor growth by systemic injection of microRNA-467 antagonist. FASEB journal : official publication of the Federation of American Societies for Experimental Biology. 2015;29(9):3726-36.

31. Tripp RA, Moore D, Jones L, Sullender W, Winter J, Anderson LJ. Respiratory syncytial virus G and/or SH protein alters Th1 cytokines, natural killer cells, and neutrophils responding to pulmonary infection in BALB/c mice. J Virol. 1999;73(9):7099-107.

32. Prince GA, Curtis SJ, Yim KC, Porter DD. Vaccine-enhanced respiratory syncytial virus disease in cotton rats following immunization with Lot 100 or a newly prepared reference vaccine. J Gen Virol. 2001;82(Pt 12):2881-8.

33. Jorquera PA, Choi Y, Oakley KE, Powell TJ, Boyd JG, Palath N, et al. Nanoparticle vaccines encompassing the respiratory syncytial virus (RSV) G protein CX3C chemokine motif induce robust immunity protecting from challenge and disease. PLoS One. 2013;8(9):e74905.

34. Harcourt JL, Caidi H, Haynes LM. RSV growth and quantification by Microtitration and qRT-PCR assays. In: Tripp RA, Jorquera P, editors. Human Respiratory Syncytial Virus: Methods and Protocols. 1 ed: Humana Press; 2016. p. XI, 247.

35. Caidi H, Harcourt JL, Tripp RA, Anderson LJ, Haynes LM. Combination therapy using monoclonal antibodies against respiratory syncytial virus (RSV) G glycoprotein protects from RSV disease in BALB/c mice. PloS one. 2012;7:e51485.

36. Dorner T, Radbruch A. Antibodies and B cell memory in viral immunity. Immunity. 2007;27(3):384-92.

37. Openshaw PJ, Tregoning JS. Immune responses and disease enhancement during respiratory syncytial virus infection. Clin Microbiol Rev. 2005;18(3):541-55.

38. Castilow EM, Varga SM. Overcoming T cell-mediated immunopathology to achieve safe RSV vaccination. Future Virol. 2008;3(5):445-54.

39. Graham BS, Henderson GS, Tang YW, Lu X, Neuzil KM, Colley DG. Priming immunization determines T helper cytokine mRNA expression patterns in lungs of mice challenged with respiratory syncytial virus. Journal of immunology. 1993;151(4):2032-40.

40. Rossi GA, Silvestri M, Colin AA. Respiratory syncytial virus infection of airway cells: Role of microRNAs. Pediatric Pulmonology. 2015:n/a-n/a.

41. DeVincenzo JP, El Saleeby CM, Bush AJ. Respiratory syncytial virus load predicts disease severity in previously healthy infants. J Infect Dis. 2005;191(11):1861-8.

42. El Saleeby CM, Bush AJ, Harrison LM, Aitken JA, Devincenzo JP. Respiratory syncytial virus load, viral dynamics, and disease severity in previously healthy naturally infected children. J Infect Dis. 2011;204(7):996-1002.

43. Scagnolari C, Midulla F, Selvaggi C, Monteleone K, Bonci E, Papoff P, et al. Evaluation of viral load in infants hospitalized with bronchiolitis caused by respiratory syncytial virus. Med Microbiol Immunol. 2012;201(3):311-7.

44. Oshansky CM, Zhang W, Moore E, Tripp RA. The host response and molecular pathogenesis associated with respiratory syncytial virus infection. Future microbiology. 2009;4(3):279-97.

45. Rossi GA, Colin AA. Infantile respiratory syncytial virus and human rhinovirus infections: respective role in inception and persistence of wheezing. The European respiratory journal. 2015;45(3):774-89.

46. Globinska A, Pawelczyk M, Kowalski ML. MicroRNAs and the immune response to respiratory virus infections. Expert review of clinical immunology. 2014;10(7):963-71.

47. Foster PS, Plank M, Collison A, Tay HL, Kaiko GE, Li J, et al. The emerging role of microRNAs in regulating immune and inflammatory responses in the lung. Immunol Rev. 2013;253(1):198-215.

48. Inchley CS, Sonerud T, Fjaerli HO, Nakstad B. Nasal mucosal microRNA expression in children with respiratory syncytial virus infection. BMC Infect Dis. 2015;15:150.

49. Hurwitz JL. Respiratory syncytial virus vaccine development. Expert review of vaccines. 2011;10(10):1415-33.

50. Castilow EM, Olson MR, Varga SM. Understanding respiratory syncytial virus (RSV) vaccine-enhanced disease. Immunol Res. 2007;39(1-3):225-39.

51. Anderson LJ. Respiratory syncytial virus vaccine development. Seminars in immunology. 2013;25(2):160-71.

52. Anderson LJ, Dormitzer PR, Nokes DJ, Rappuoli R, Roca A, Graham BS. Strategic priorities for respiratory syncytial virus (RSV) vaccine development. Vaccine. 2013;31 Suppl 2:B209-15.

53. Blanco JC, Boukhvalova MS, Shirey KA, Prince GA, Vogel SN. New insights for development of a safe and protective RSV vaccine. Human vaccines. 2010;6(6):482-92.

54. Connors M, Giese NA, Kulkarni AB, Firestone CY, Morse HC, 3rd, Murphy BR. Enhanced pulmonary histopathology induced by respiratory syncytial virus (RSV) challenge of formalin-inactivated RSV-immunized BALB/c mice is abrogated by depletion of interleukin-4 (IL-4) and IL-10. J Virol. 1994;68(8):5321-5.

55. Polack FP, Teng MN, Collins PL, Prince GA, Exner M, Regele H, et al. A role for immune complexes in enhanced respiratory syncytial virus disease. J Exp Med. 2002;196(6):859-65.

56. Waris ME, Tsou C, Erdman DD, Zaki SR, Anderson LJ. Respiratory synctial virus infection in BALB/c mice previously immunized with formalin-inactivated virus induces enhanced pulmonary inflammatory response with a predominant Th2-like cytokine pattern. J Virol. 1996;70(5):2852-60.

57. De Swart RL, Kuiken T, Timmerman HH, van Amerongen G, Van Den Hoogen BG, Vos HW, et al. Immunization of macaques with formalin-inactivated

respiratory syncytial virus (RSV) induces interleukin-13-associated hypersensitivity to subsequent RSV infection. J Virol. 2002;76(22):11561-9.

58. McDermott DS, Knudson CJ, Varga SM. Determining the breadth of the respiratory syncytial virus-specific T cell response. J Virol. 2014;88(6):3135-43.

59. Clutterbuck EJ, Hirst EM, Sanderson CJ. Human interleukin-5 (IL-5) regulates the production of eosinophils in human bone marrow cultures: comparison and interaction with IL-1, IL-3, IL-6, and GMCSF. Blood. 1989;73(6):1504-12.

60. Hamid Q, Azzawi M, Ying S, Moqbel R, Wardlaw AJ, Corrigan CJ, et al. Expression of mRNA for interleukin-5 in mucosal bronchial biopsies from asthma. J Clin Invest. 1991;87(5):1541-6.

61. Alexander AG, Barkans J, Moqbel R, Barnes NC, Kay AB, Corrigan CJ. Serum interleukin 5 concentrations in atopic and non-atopic patients with glucocorticoid-dependent chronic severe asthma. Thorax. 1994;49(12):1231-3.

62. Lopez AF, Sanderson CJ, Gamble JR, Campbell HD, Young IG, Vadas MA. Recombinant human interleukin 5 is a selective activator of human eosinophil function. J Exp Med. 1988;167(1):219-24.

63. Robinson DS, Hamid Q, Ying S, Tsicopoulos A, Barkans J, Bentley AM, et al. Predominant TH2-like bronchoalveolar T-lymphocyte population in atopic asthma. N Engl J Med. 1992;326(5):298-304.

64. Yamaguchi Y, Hayashi Y, Sugama Y, Miura Y, Kasahara T, Kitamura S, et al. Highly purified murine interleukin 5 (IL-5) stimulates eosinophil function and prolongs in vitro survival. IL-5 as an eosinophil chemotactic factor. J Exp Med. 1988;167(5):1737-42.

65. Matthews AN, Friend DS, Zimmermann N, Sarafi MN, Luster AD, Pearlman E, et al. Eotaxin is required for the baseline level of tissue eosinophils. Proc Natl Acad Sci U S A. 1998;95(11):6273-8.

66. Quackenbush EJ, Wershil BK, Aguirre V, Gutierrez-Ramos JC. Eotaxin modulates myelopoiesis and mast cell development from embryonic hematopoietic progenitors. Blood. 1998;92(6):1887-97.

67. Humbles AA, Conroy DM, Marleau S, Rankin SM, Palframan RT, Proudfoot AE, et al. Kinetics of eotaxin generation and its relationship to eosinophil accumulation in allergic airways disease: analysis in a guinea pig model in vivo. J Exp Med. 1997;186(4):601-12.

68. Palframan RT, Collins PD, Williams TJ, Rankin SM. Eotaxin induces a rapid release of eosinophils and their progenitors from the bone marrow. Blood. 1998;91(7):2240-8.

69. Mould AW, Ramsay AJ, Matthaei KI, Young IG, Rothenberg ME, Foster PS. The effect of IL-5 and eotaxin expression in the lung on eosinophil trafficking and degranulation and the induction of bronchial hyperreactivity. Journal of immunology. 2000;164(4):2142-50.

70. Openshaw PJ, Chiu C. Protective and dysregulated T cell immunity in RSV infection. Current opinion in virology. 2013;3(4):468-74.

71. Han Y, Guo Q, Zhang M, Chen Z, Cao X. CD69+ CD4+ CD25- T cells, a new subset of regulatory T cells, suppress T cell proliferation through membrane-bound TGF-beta 1. Journal of immunology. 2009;182(1):111-20.

72. Ziegler SF, Ramsdell F, Alderson MR. The activation antigen CD69. Stem Cells. 1994;12(5):456-65.

73. Schoenberger SP. CD69 guides CD4+ T cells to the seat of memory. Proc Natl Acad Sci U S A. 2012;109(22):8358-9.

74. Rosenberg HF, Dyer KD, Foster PS. Eosinophils: changing perspectives in health and disease. Nat Rev Immunol. 2013;13(1):9-22.

75. Denburg JA, Sehmi R, Upham J. Regulation of IL-5 receptor on eosinophil progenitors in allergic inflammation: role of retinoic acid. International archives of allergy and immunology. 2001;124(1-3):246-8.

76. Liu LY, Sedgwick JB, Bates ME, Vrtis RF, Gern JE, Kita H, et al. Decreased expression of membrane IL-5 receptor alpha on human eosinophils: II. IL-5 down-modulates its receptor via a proteinase-mediated process. Journal of immunology. 2002;169(11):6459-66.

77. Koike M, Takatsu K. IL-5 and its receptor: which role do they play in the immune response? International archives of allergy and immunology. 1994;104(1):1-9.

78. Yoshimura C, Yamaguchi M, Iikura M, Izumi S, Kudo K, Nagase H, et al. Activation markers of human basophils: CD69 expression is strongly and preferentially induced by IL-3. J Allergy Clin Immunol. 2002;109(5):817-23.

79. Stone KD, Prussin C, Metcalfe DD. IgE, mast cells, basophils, and eosinophils. J Allergy Clin Immunol. 2010;125(2 Suppl 2):S73-80.

80. Groskreutz DJ, Monick MM, Yarovinsky TO, Powers LS, Quelle DE, Varga SM, et al. Respiratory syncytial virus decreases p53 protein to prolong survival of airway epithelial cells. Journal of immunology. 2007;179(5):2741-7.

81. Dunn EF, Connor JH. Dominant inhibition of Akt/protein kinase B signaling by the matrix protein of a negative-strand RNA virus. J Virol. 2011;85(1):422-31.

82. McCann KL, Imani F. Transforming growth factor beta enhances respiratory syncytial virus replication and tumor necrosis factor alpha induction in human epithelial cells. J Virol. 2007;81(6):2880-6.

83. Gibbs JD, Ornoff DM, Igo HA, Zeng JY, Imani F. Cell cycle arrest by transforming growth factor beta1 enhances replication of respiratory syncytial virus in lung epithelial cells. J Virol. 2009;83(23):12424-31.

84. Bakre A, Wu W, Hiscox J, Spann K, Teng MN, Tripp RA. Human respiratory syncytial virus non-structural protein NS1 modifies miR-24 expression via transforming growth factor-beta. J Gen Virol. 2015;96(11):3179-91.

85. Amanatidou V, Apostolakis S, Spandidos DA. Genetic diversity of the host and severe respiratory syncytial virus-induced lower respiratory tract infection. The Pediatric infectious disease journal. 2009;28(2):135-40.

86. Seminario MC, Gleich GJ. The role of eosinophils in the pathogenesis of asthma. Current opinion in immunology. 1994;6(6):860-4.

87. Wardlaw AJ, Dunnette S, Gleich GJ, Collins JV, Kay AB. Eosinophils and mast cells in bronchoalveolar lavage in subjects with mild asthma. Relationship to bronchial hyperreactivity. Am Rev Respir Dis. 1988;137(1):62-9.

88. Ohashi Y, Motojima S, Fukuda T, Makino S. Airway hyperresponsiveness, increased intracellular spaces of bronchial epithelium, and increased infiltration of eosinophils and lymphocytes in bronchial mucosa in asthma. Am Rev Respir Dis. 1992;145(6):1469-76.

89. Gleich GJ, Flavahan NA, Fujisawa T, Vanhoutte PM. The eosinophil as a mediator of damage to respiratory epithelium: a model for bronchial hyperreactivity. J Allergy Clin Immunol. 1988;81(5 Pt 1):776-81.

90. De Monchy JG, Kauffman HF, Venge P, Koeter GH, Jansen HM, Sluiter HJ, et al. Bronchoalveolar eosinophilia during allergen-induced late asthmatic reactions. Am Rev Respir Dis. 1985;131(3):373-6.

91. Kumar M, Ahmad T, Sharma A, Mabalirajan U, Kulshreshtha A, Agrawal A, et al. Let-7 microRNA-mediated regulation of IL-13 and allergic airway inflammation. J Allergy Clin Immunol. 2011;128(5):1077-85 e1-10.

92. Lee ST, Chu K, Jung KH, Kim JH, Huh JY, Yoon H, et al. miR-206 regulates brain-derived neurotrophic factor in Alzheimer disease model. Ann Neurol. 2012;72(2):269-77.

93. Trang P, Medina PP, Wiggins JF, Ruffino L, Kelnar K, Omotola M, et al. Regression of murine lung tumors by the let-7 microRNA. Oncogene. 2010;29(11):1580-7.

94. Esquela-Kerscher A, Trang P, Wiggins JF, Patrawala L, Cheng A, Ford L, et al. The let-7 microRNA reduces tumor growth in mouse models of lung cancer. Cell Cycle. 2008;7(6):759-64.

95. Cooray S. The pivotal role of phosphatidylinositol 3-kinase-Akt signal transduction in virus survival. J Gen Virol. 2004;85(Pt 5):1065-76.

96. Guo H, Zhou T, Jiang D, Cuconati A, Xiao GH, Block TM, et al. Regulation of hepatitis B virus replication by the phosphatidylinositol 3-kinase-akt signal transduction pathway. J Virol. 2007;81(18):10072-80.

97. Ji WT, Liu HJ. PI3K-Akt signaling and viral infection. Recent Pat Biotechnol. 2008;2(3):218-26.

Tables and figures

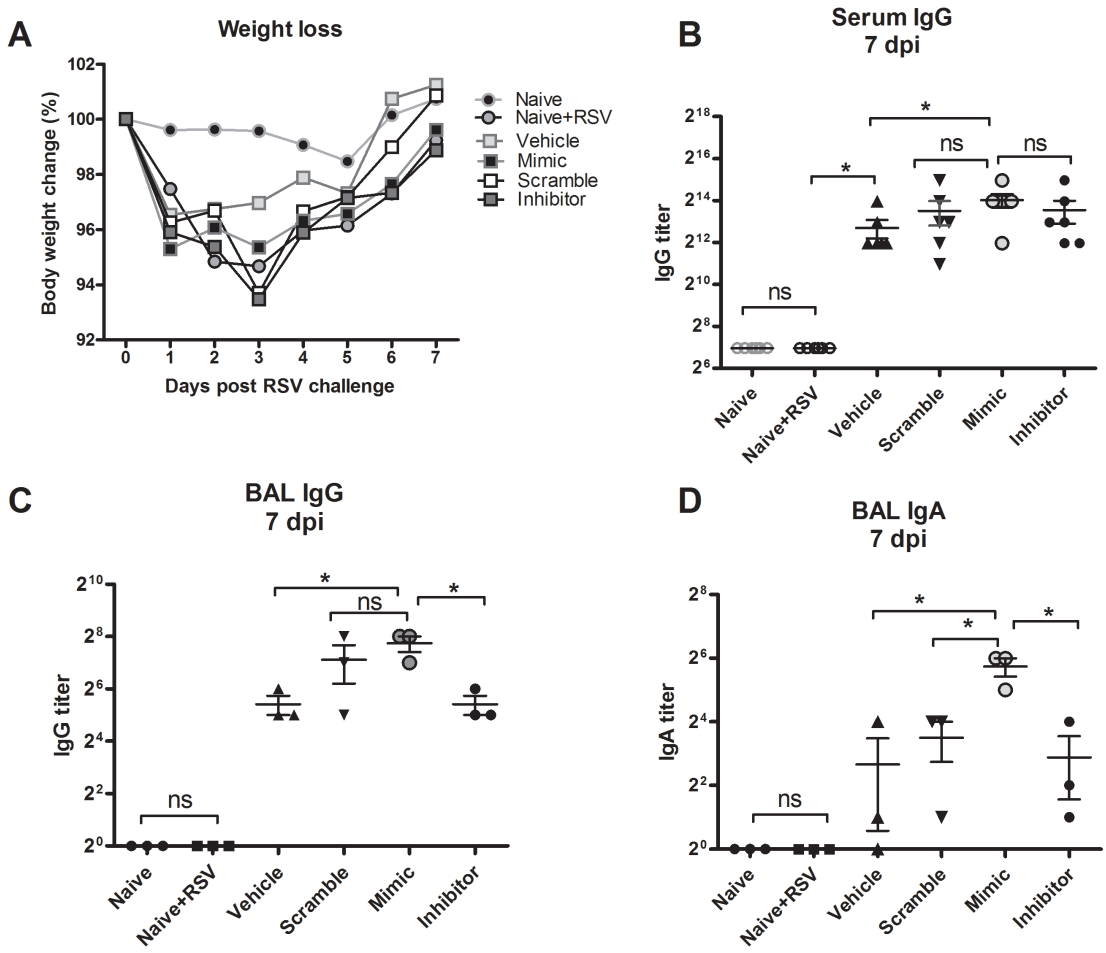

Fig. 6.1: Body weight loss and RSV-specific antibody response. (A) Animals were weighed daily and percentage of weight loss calculated based on day 0 (n=6 mice/group). **(B)** Sera were obtained from blood taken 7 days post-challenge and RSV A2-specific IgG levels were determined by indirect ELISA (n=6 mice/group) BAL supernatant were obtained from mice (n=3/group) and **(C)** RSV A2-specific IgG levels and **(D)** RSV A2-specific IgA levels were determined by indirect ELISA. All data is representative of three independent experiments. Error bars represent the SEM and results were considered significant with a P value ≤ 0.05 (*) as determined by One-way ANOVA and Bonferroni's test.

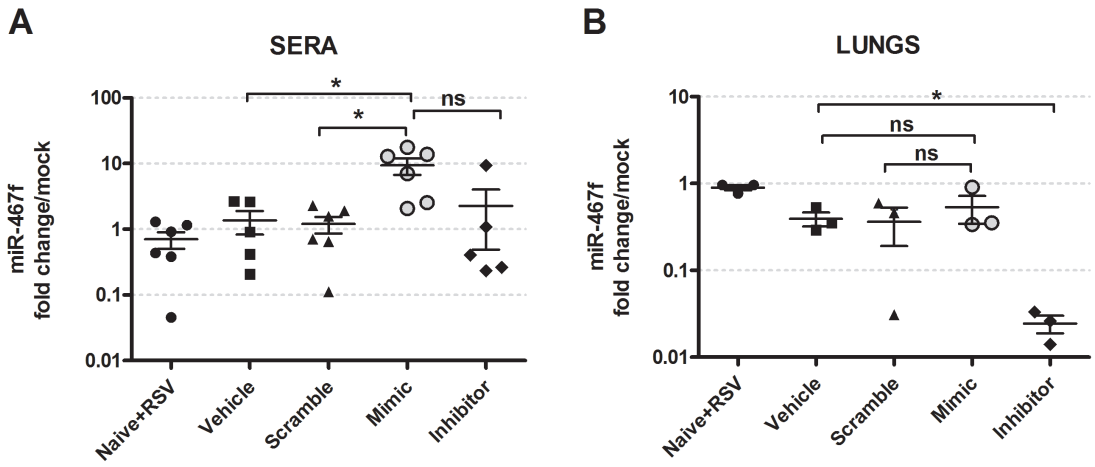

Fig. 6.2: MiR-467f expression levels in the sera and lungs of mice following virus challenge. Groups of BALB/c mice were vaccinated using a prime-boost regimen with FI-RSV A2 diluted in PBS on days -42 and -21. On day -1 mice received a single treatment of either vehicle, miRNA scramble control, miR-467f mimic, or miR-467f inhibitor via i.n. delivery. Control mice (naive and naïve+RSV) did not receive any treatment. 24h post treatment all mice received $1x10^6$ PFU of RSV A2 via i.n. delivery or control mice (naïve) received no virus. Total RNA isolation was performed on **(A)** sera from total blood (n=5-6 mice/group) and **(B)** lung homogenates (n=3 mice/group) and examined for miR-467f expression levels using RT-qPCR. MiR-467f expression levels were normalized by **(A)** RNU6 expression or **(B)** 18S rRNA gene expression. Values are represented as expression over mock (naïve mice). All data is representative of three independent experiments. Error bars represent the SEM and results were considered significant with a P value ≤ 0.05 (*) as determined by One-way ANOVA and Bonferroni's test.

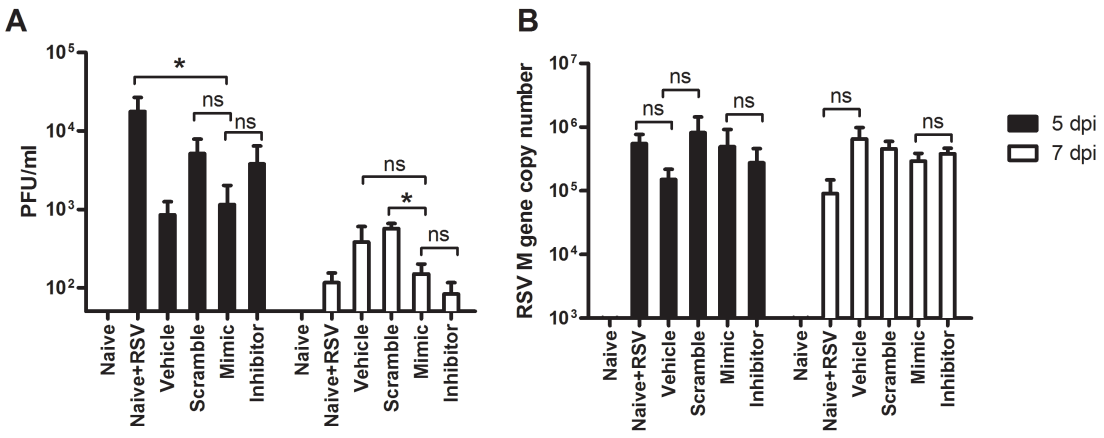

Fig. 6.3: Lung viral titers following virus challenge. Groups of BALB/c mice were vaccinated using a prime-boost regimen with FI-RSV A2 diluted in PBS on days -42 and -21. On day -1 mice received a single treatment of either vehicle, miRNA scramble control, miR-467f mimic, or miR-467f inhibitor via i.n. delivery. Control mice (naive and naïve+RSV) did not receive any treatment. On day 0, mice received $1x10^6$ PFU of RSV A2 via i.n. delivery and control mice (naïve) received no virus. Lung virus titers were determined 5 days post-challenge or 7 days post-challenge by **(A)** plaque assay (n=3 mice/group) and **(B)** RSV A2 M gene copy number using RT-qPCR (n=6-8 mice/group). The data are presented as PFU/ml of lung homogenate. All data is representative of three independent experiments. Error bars represent the SEM and results were considered significant with a P value ≤ 0.05 (*), ns= no significant, as determined by Two-way ANOVA and Bonferroni's test.

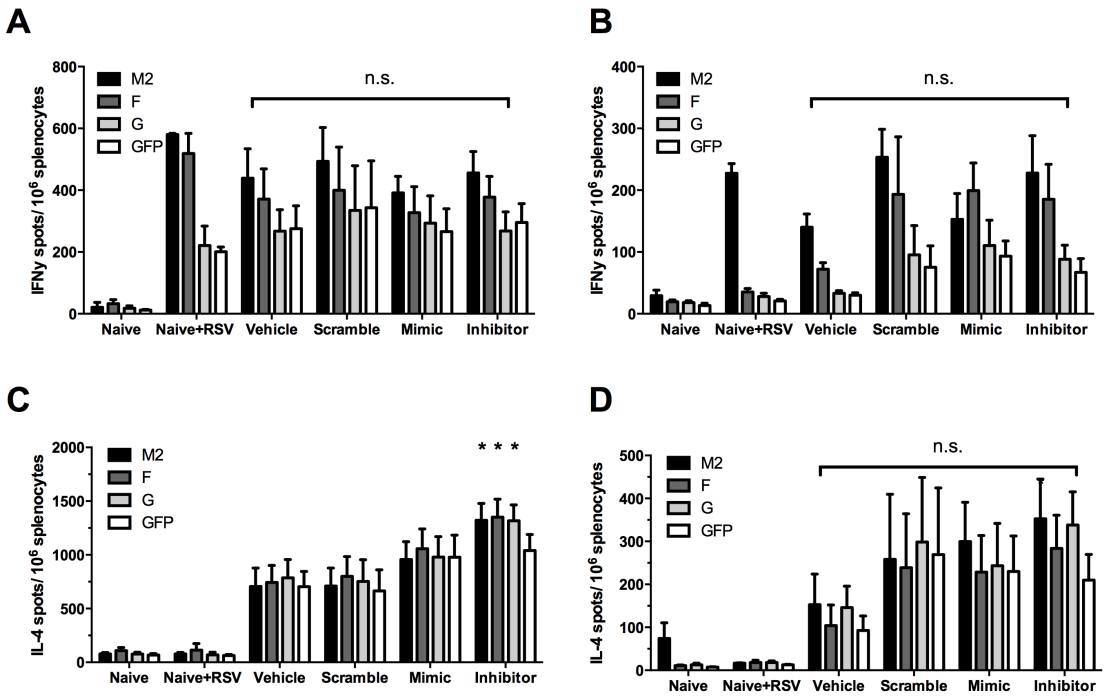
A
B
C
D
M2
F
G
GFP
n.s.
* * *
IFNγ spots/ 10^6 splenocytes
IL-4 spots/ 10^6 splenocytes
Naive
Naive+RSV
Vehicle
Scramble
Mimic
Inhibitor

Fig. 6.4: Frequency of RSV-specific IFNγ and IL-4 secreting cells after virus challenge. Groups of BALB/c mice were vaccinated using a prime-boost regimen with FI-RSV A2 diluted in PBS on days -42 and -21. On day -1 mice received a single treatment of either vehicle, miRNA scramble control, miR-467f mimic, or miR-467f inhibitor via i.n. delivery. 24h post treatment all mice received $1x10^6$ PFU of RSV A2 via i.n. delivery or control mice (naïve) received no virus. The number of $M2_{82-90}$-specific, F_{51-66}-specific, $G_{183-198}$-specific, and GFP-specific (irrelevant peptide control) IL-4 and IFNγ producing splenocytes were determined by ELISPOT in cells harvested at 5 or 7 days post-challenge. **(A)** IFNγ producing splenocytes at 5 days post-challenge, **(B)** IFNγ producing splenocytes at 7 days post-challenge, **(C)** IL-4 producing splenocytes at 5 days post-challenge and **(D)** IL-4 producing splenocytes at 7 days post-challenge. The data are presented as cytokine spots/10^6 splenocytes. Asterisks (*) represent a p-value significant compared to the Vehicle group. All data is representative of three independent experiments. Error bars represent the SEM from n=6-8 mice/group and results were considered significant with a P value ≤ 0.05 (*) as determined by One-way ANOVA and Bonferroni's test.

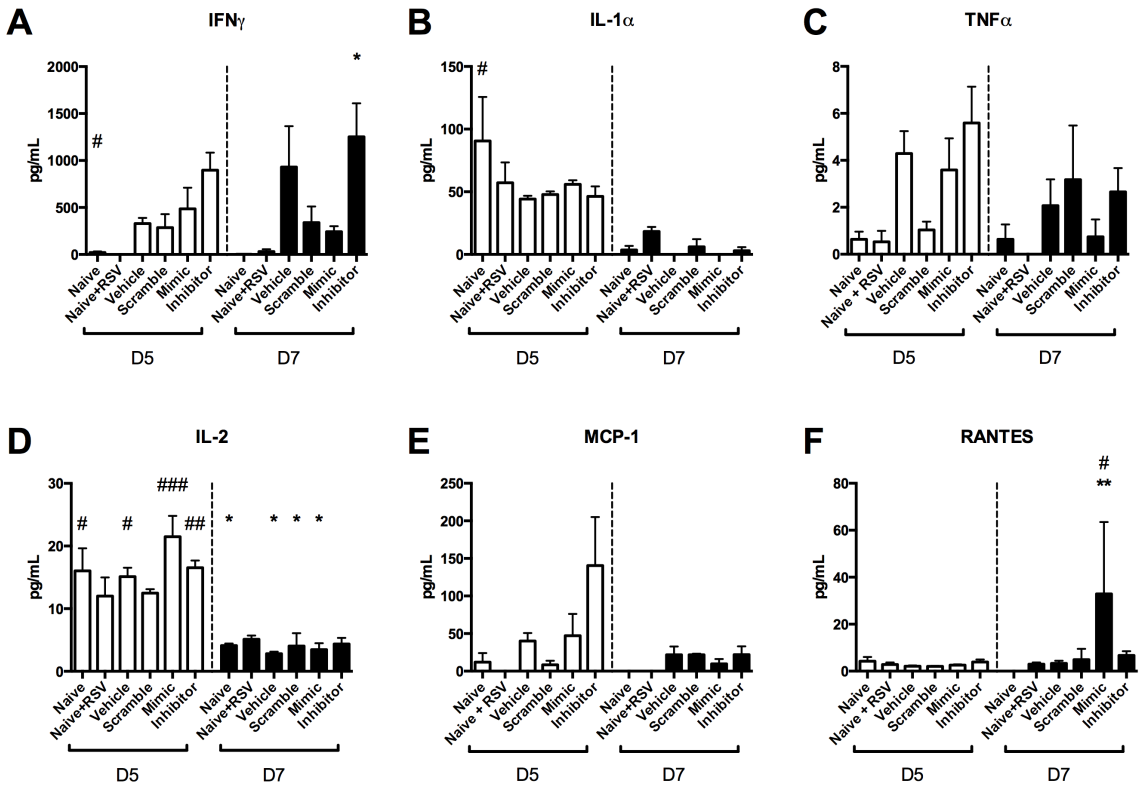
A
IFNγ
pg/mL
2000
1500
1000
500
0
#
*
Naive
Naive+RSV
Vehicle
Scramble
Mimic
Inhibitor
D5
D7
B
IL-1α
150
100
50
C
TNFα
8
6
4
2
D
IL-2
30
20
10
###
##
E
MCP-1
250
200
150
F
RANTES
80
60
40
**

Fig. 6.5: Differential Th1-type cytokine and chemokine expression patterns amongst treatment groups at 5 days and 7 days post-challenge. The level of **(A)** IFN-γ, **(B)** IL-1α, **(C)** TNFα, **(D)** IL-2, **(E)** MCP-1, and **(F)** RANTES were measured in BAL supernatant by Luminex assay, and the data are presented as picograms of cytokine/ mL of BAL supernatant at 5 days post-challenge (n=6-8/group) and 7 days post-challenge (n=3/group). Asterisks (*) represent a p-value significant compared to the vehicle group at 5 days post-challenge and hashtags (#) represent a p-value significant compared to the vehicle group at 7 days post-challenge. All data is representative of three independent experiments. Error bars represent the SEM and results were considered significant with a P value ≤0.05 (*/#), ≤0.01 (**/##) and ≤0.001 (***/###) as determined by One-way ANOVA and Bonferroni's test.

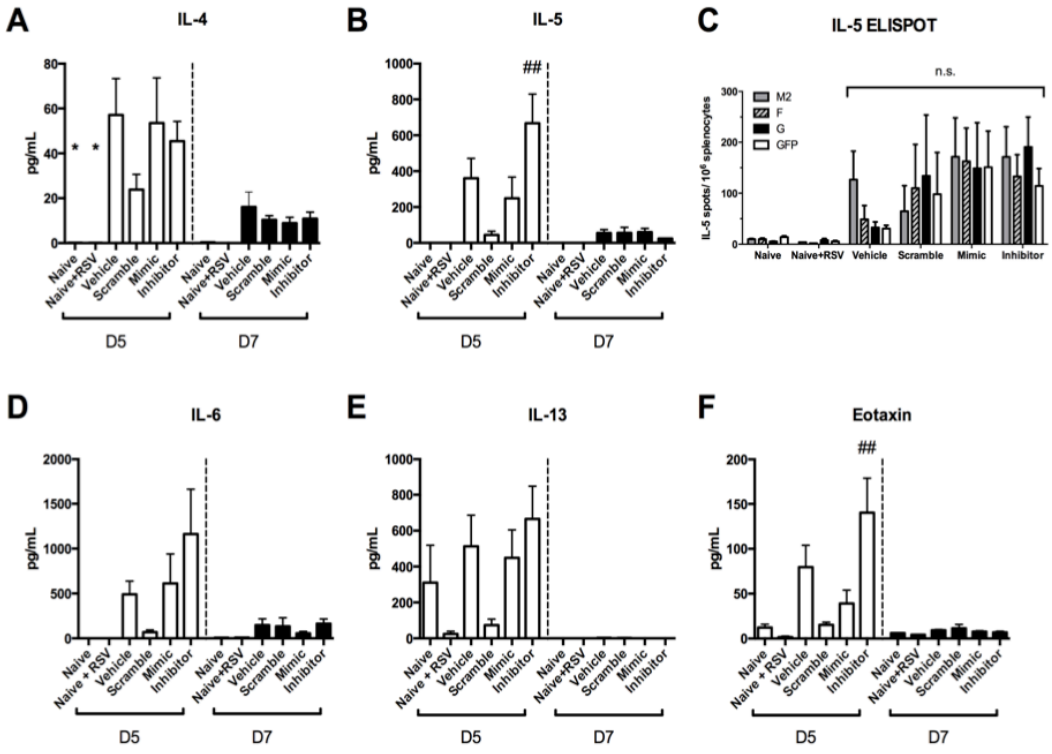
A
IL-4
pg/mL
Naive
Naive+RSV
Vehicle
Scramble
Mimic
Inhibitor
D5
D7
B
IL-5
##
C
IL-5 ELISPOT
n.s.
M2
F
G
GFP
IL-5 spots/ 10^6 splenocytes
D
IL-6
E
IL-13
F
Eotaxin

Fig. 6.6: Differential Th2-type cytokine and chemokine expression patterns amongst treatment groups at 5 days and 7 days post-challenge. The level of **(A)** IL-4, **(B)** IL-5, **(D)** IL-6, **(E)** IL-13, and **(F)** Eotaxin were measured in BAL supernatant by Luminex assay, and the data are presented as picograms of cytokine/ mL of BAL supernatant at 5 days post-challenge (n=6-8/group) and 7 days post-challenge (n=3/group). **(C)** The number of $M2_{82-90}$-specific, F_{51-66}-specific, $G_{183-198}$-sepcific, and GFP-specific (irrelevant peptide control) IL-5 producing splenocytes was determined by ELISPOT in cells harvested at 7 days post-challenge. Asterisks (*) represent a p-value significant compared to the vehicle group at 5 days post-challenge and hashtags (#) represent a p-value significant compared to the vehicle group at 7 days post-challenge. All data is representative of three independent experiments. Error bars represent the SEM and results were considered significant with a P value ≤ 0.05 (*/#) and ≤ 0.01 (**/##) as determined by One-way ANOVA and Bonferroni's test.

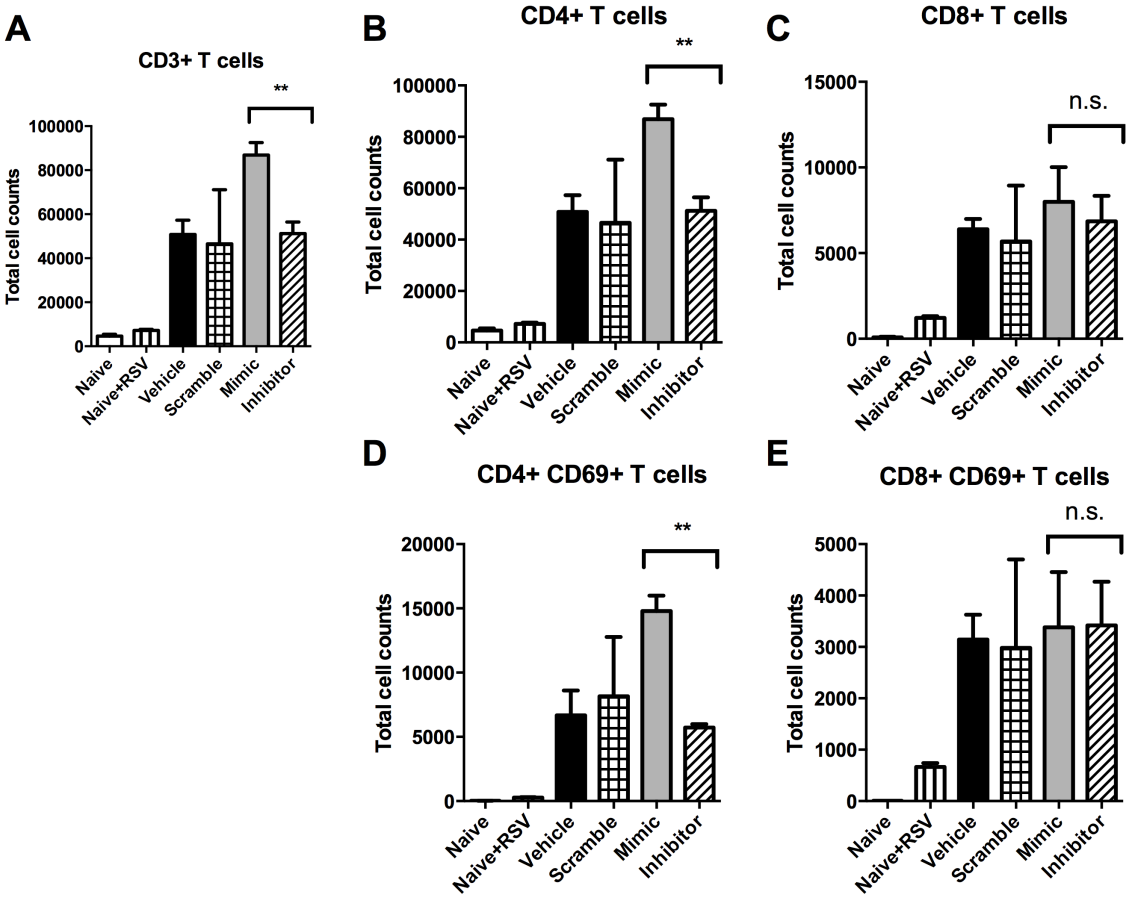
A
CD3+ T cells
Total cell counts
100000
80000
60000
40000
20000
0
**
Naive
Naive+RSV
Vehicle
Scramble
Mimic
Inhibitor
B
CD4+ T cells
Total cell counts
100000
80000
60000
40000
20000
0
**
Naive
Naive+RSV
Vehicle
Scramble
Mimic
Inhibitor
C
CD8+ T cells
Total cell counts
15000
10000
5000
0
n.s.
Naive
Naive+RSV
Vehicle
Scramble
Mimic
Inhibitor
D
CD4+ CD69+ T cells
Total cell counts
20000
15000
10000
5000
0
**
Naive
Naive+RSV
Vehicle
Scramble
Mimic
Inhibitor
E
CD8+ CD69+ T cells
Total cell counts
5000
4000
3000
2000
1000
0
n.s.
Naive
Naive+RSV
Vehicle
Scramble
Mimic
Inhibitor

Fig. 6.7: Treatment with miR-467f mimic is associated with enhancement of the pulmonary $CD4^+$ T cell response. Groups of BALB/c mice were vaccinated using a prime-boost regimen with FI-RSV A2 diluted in PBS on days 0 and 21. Three weeks after the boost vaccination mice received a single treatment of vehicle, miRNA scramble control, miR-467f mimic, or miR-467f inhibitor via I.N. delivery. Control mice (naive and naïve+RSV) did not receive any treatment. 24h post treatment all mice received $1x10^6$ PFU of RSV A2 via I.N. delivery or control mice (naïve) received no virus. **(A)** T cell ($CD3^+$), **(B)** $CD4^+$ T cell ($CD3^+CD4^+$), **(C)** $CD8^+$ T cell ($CD3^+CD8^+$), **(D)** $CD4^+$ $CD69^+$ T cell, and **(E)** $CD8^+$ $CD69^+$ T cell infiltration was determined at 7 days post-challenge by flow cytometry. All data is representative of three independent experiments. Asterisks (*) represent a p-value significant for the miR-467f mimic as compared to the miR-467f inhibitor. Error bars represent the SEM and results were considered significant with a P value ≤ 0.05 (*) and ≤ 0.01 (**) as determined by a Student's t-test.

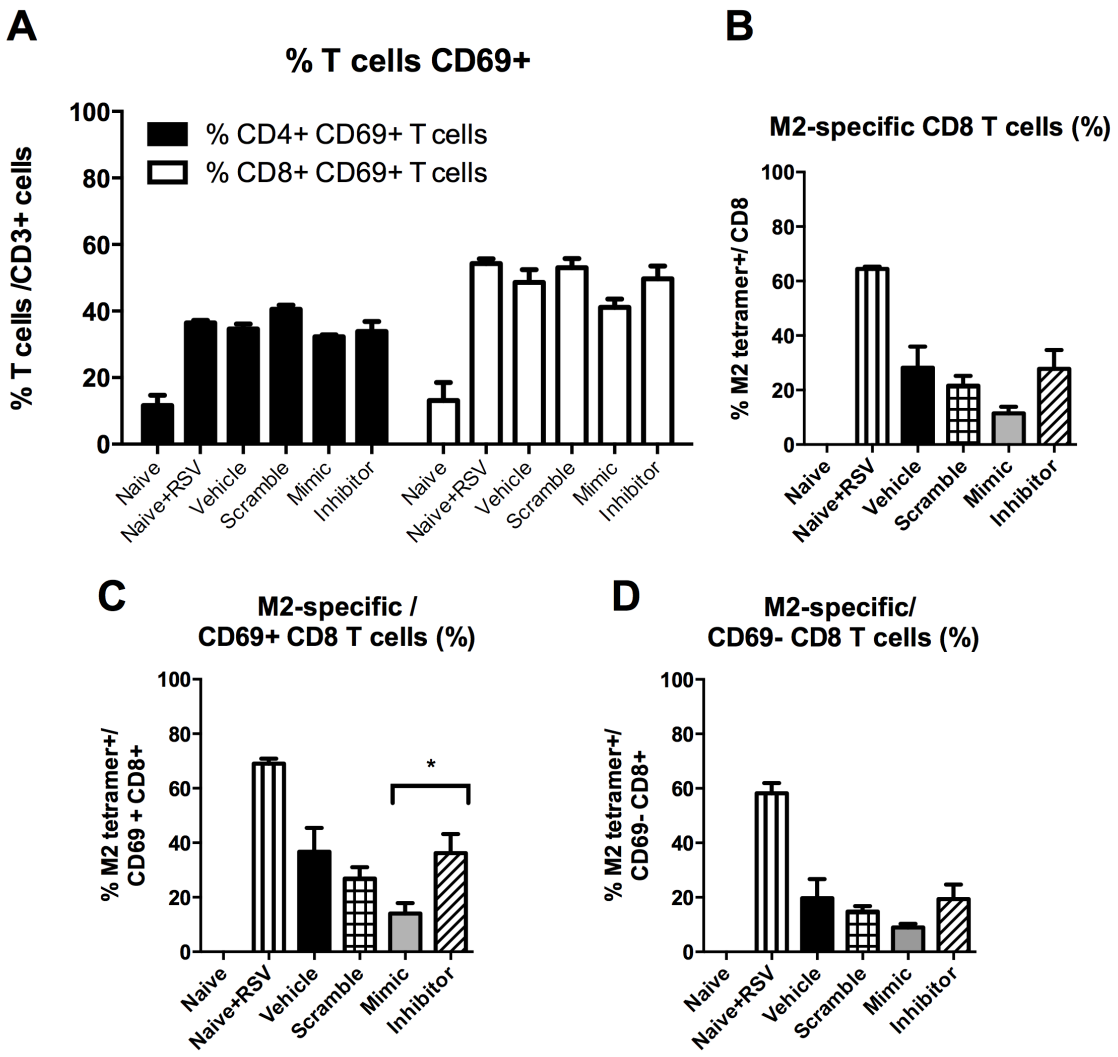
A
% T cells CD69+
% T cells /CD3+ cells
% CD4+ CD69+ T cells
% CD8+ CD69+ T cells
100
80
60
40
20
0
Naive
Naive+RSV
Vehicle
Scramble
Mimic
Inhibitor
B
M2-specific CD8 T cells (%)
% M2 tetramer+/ CD8
C
M2-specific /
CD69+ CD8 T cells (%)
% M2 tetramer+/
CD69 + CD8+
*
D
M2-specific/
CD69- CD8 T cells (%)
% M2 tetramer+/
CD69- CD8+

Fig. 6.8: Treatment with miR-467f mimic reduces the pulmonary M2-specific $CD8^+$ T cell response. Groups of BALB/c mice were vaccinated using a prime-boost regimen with FI-RSV A2 diluted in PBS on days 0 and 21. Three weeks after the boost vaccination mice received a single treatment of either vehicle, miRNA scramble control, miR-467f mimic, or miR-467f inhibitor via I.N. delivery. Control mice (naive and naïve+RSV) did not receive any treatment. 24h post treatment all mice received $1x10^6$ PFU of RSV A2 via I.N. delivery or control mice (naïve) received no virus. **(A)** percentage of $CD69^+$ T cell, **(B)** percentage of M2-specific $CD8^+$ T cell, **(C)** percentage of M2-specific $CD69^+$ $CD8^+$ T cell, **(D)** percentage of M2-specific $CD69^-$ $CD8^+$ T cell infiltration was determined at 7 days post-challenge by flow cytometry. All data is representative of three independent experiments. Asterisks (*) represent a p-value significant for the miR-467f mimic as compared to the miR-467f inhibitor. Error bars represent the SEM and results were considered significant with a P value ≤ 0.05 (*) as determined by a Student's t-test.

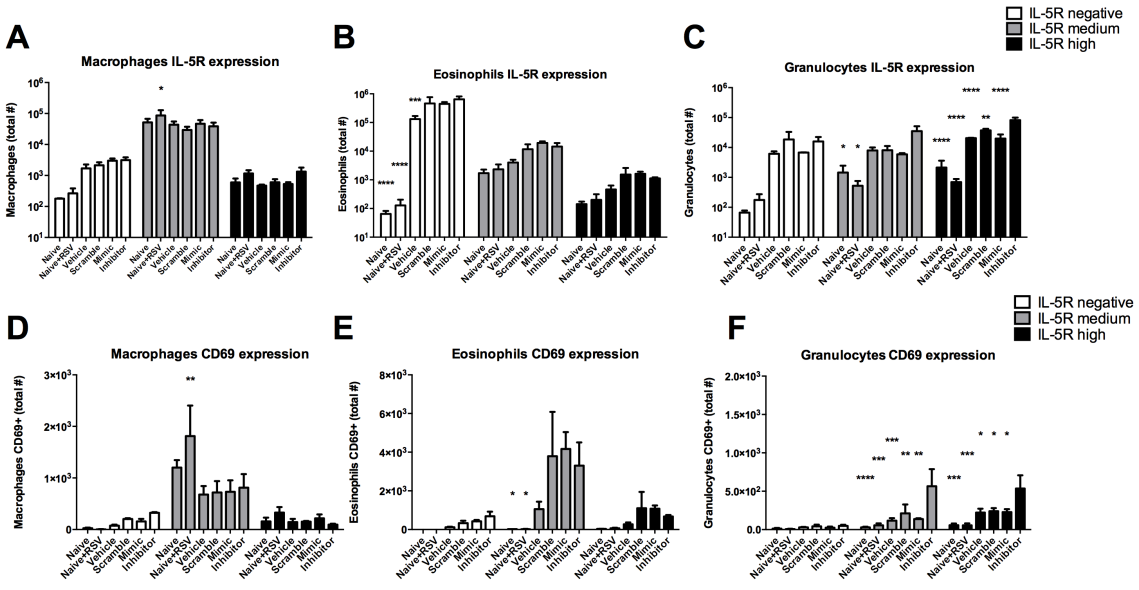
A
Macrophages IL-5R expression
Macrophages (total #)
B
Eosinophils IL-5R expression
Eosinophils (total #)
C
Granulocytes IL-5R expression
Granulocytes (total #)
IL-5R negative
IL-5R medium
IL-5R high
Naive
Naive+RSV
Vehicle
Scramble
Mimic
Inhibitor
D
Macrophages CD69 expression
Macrophages CD69+ (total #)
E
Eosinophils CD69 expression
Eosinophils CD69+ (total #)
F
Granulocytes CD69 expression
Granulocytes CD69+ (total #)

Fig. 6.9: Treatment with miR-467f inhibitor affects pulmonary infiltration of granulocyte cells. Groups of BALB/c mice were vaccinated using a prime-boost regimen with FI-RSV A2 diluted in PBS on days 0 and 21. Three weeks after the boost vaccination mice received a single treatment of vehicle, miRNA scramble control, miR-467f mimic, or miR-467f inhibitor via I.N. delivery. Control mice (naive and naïve+RSV) did not receive any treatment. 24h post treatment all mice received $1x10^6$ PFU of RSV A2 via I.N. delivery or control mice (naïve) received no virus. **(A)** Macrophage, **(B)** eosinophil, **(C)** granulocyte, **(D)** $CD69^+$ macrophage, **(E)** $CD69^+$ eosinophil, **(F)** $CD69^+$ granulocyte cell infiltration by IL-$5R^{neg}$, IL-$5R^{med}$ and IL-$5R^{hi}$ expression was determined at 7 days post-challenge by flow cytometry. All data is representative of three independent experiments. Asterisks (*) represent a p-value significant as compared to the miR-467f inhibitor. Error bars represent the SEM and results were considered significant with a P value ≤0.05 (*), ≤0.01 (**), ≤0.001 (***), and ≤0.001 (****) as determined by a Two-way ANOVA and Bonferroni's test.

Gene	Name	Prediction Score	Pathway
Pten	Phosphatase and tensin homolog	0.974	PI3K-Akt signaling pathway
Apc	Adenomatous polyposis coli	0.973	Wnt signaling pathway
Ncoa2	Nuclear receptor coactivator 2	0.972	Adipogensis and Androgen receptor signaling pathway
Slc1a2	Solute carrier family 1 member 2	0.951	Neurotransmitter Release Cycle
Chp1	Chromodomain protein 1	0.918	Histone acetyltransferase activity and methylated histone binding
Klf6	Krueppel-like factor 6	0.908	Adipogenesis and TGFβ signaling pathway
Ppard	Peroxisome proliferator-activated receptor	0.879	Adipogensis, Wnt signaling pathway, and signaling by GPCR
Cbx5	Chromobox protein homolog 5	0.850	Hemostasis and Chromatin Regulation / Acetylation
Cdkn1b	Cyclin-dependent kinase inhibitor 1B	0.847	PI3K-Akt signaling pathway
Rbm25	RNA-binding protein 25	0.831	mRNA splicing

Table 1: The top 10 functionally relevant gene targets and associated major signal transduction pathways of miR-467f. Predicted gene targets for miR-467f were identified by DIANA TarBase v7.0 based on the criteria of experimentally validated genes and successful binding of miR-467f to the 3'UTR of these chosen gene targets. Important pathways associated with these gene targets were identified through GeneCards®: Human Genome Database.

Supplemental information

Group	Vaccine	Route	Treatment	Route	Challenge
Naïve	-	-	-	-	-
Naïve + RSV	-	-	-	-	$1x10^6$ PFU of RSV A2
Vehicle	FI-RSV A2	i.m.	Vehicle	i.n.	$1x10^6$ PFU of RSV A2
Scramble	FI-RSV A2	i.m.	miRNA Scramble	i.n.	$1x10^6$ PFU of RSV A2
Mimic	FI-RSV A2	i.m.	miR-467f Mimic	i.n.	$1x10^6$ PFU of RSV A2
Inhibitor	FI-RSV A2	i.m.	miR-467f Inhibitor	i.n.	$1x10^6$ PFU of RSV A2

Fig. S6.1: Vaccination and miRNA treatment schedule for *in vivo* BALB/c studies. 6 to 8 mice per group were vaccinated twice with FI-RSV A2 using a prime-boost regimen. Control mice (naïve and naïve+RSV) received no vaccinations. Three weeks after the boost vaccination mice received a single treatment of either vehicle, miRNA scramble control, miR-467f mimic, or miR-467f inhibitor via I.N. delivery. Control mice (naive and naïve+RSV) did not receive any treatment. 24h post treatment all mice received $1x10^6$ PFU of RSV A2 via I.N. delivery or control mice (naïve) received no virus. All mice were sacrificed at either day 5 or day 7 post-challenge with RSV A2.

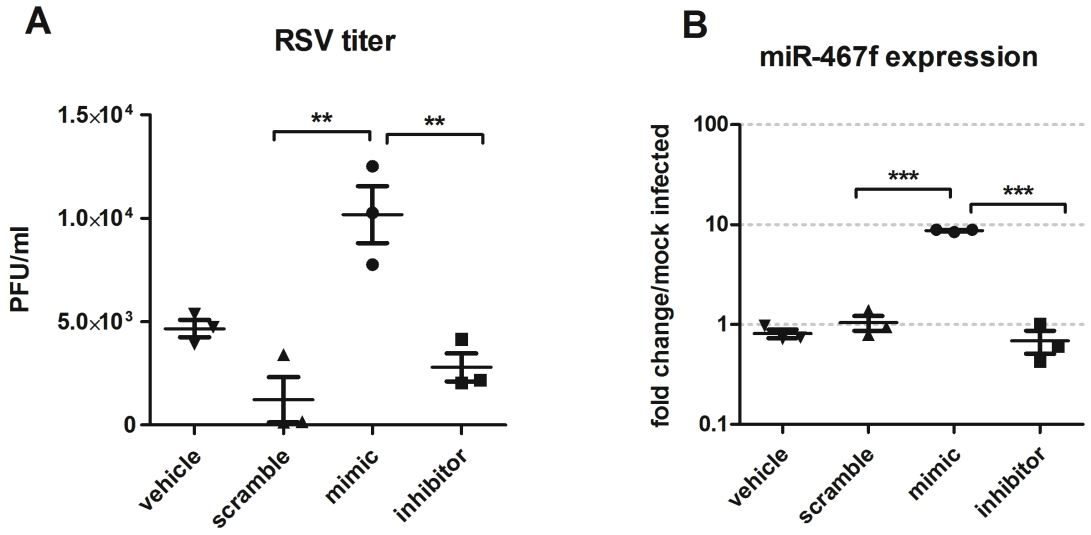

Fig. S6.2: MLE-15 cells were transfected with miR scramble, miR-467f mimic, miR-467f inhibitor, or transfection reagent control. Cells were transfected for 48h prior to RSV A2 infection at MOI=0.5. **(A)** Viral titers were determined at 48 hpi by plaque assay. **(B)** MiR-467f expression levels were determined at 48 hpi by RT-qPCR and normalized by 18S rRNA gene expression. Values are represented as expression over mock infected. All data is representative of three independent experiments performed in triplicate. Asterisks (*) represent a p-value significant compared to the scramble group. Error bars represent the SEM and results were considered significant with a P value ≤0.05 (*), ≤0.01 (**) and ≤0.001 (***) as determined by One-way ANOVA and Bonferroni's test.

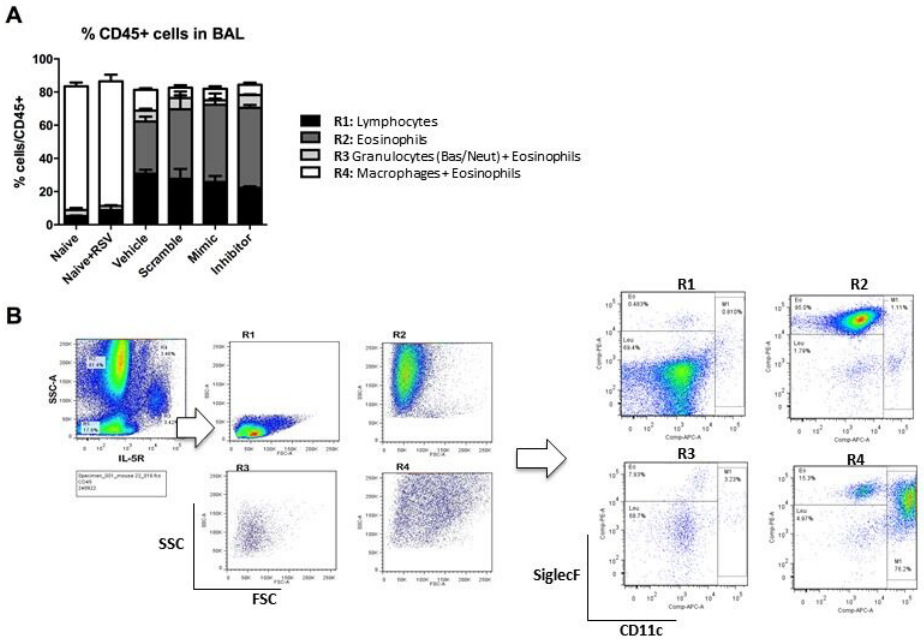

Figure S6.3: Percentage of CD45+ cell types in BAL. Groups of BALB/c mice were vaccinated using a prime-boost regimen with FI-RSV A2 diluted in PBS on days -42 and -21. Three weeks after the boost vaccination mice received a single treatment of vehicle, miRNA scramble control, miR-467f mimic, or miR-467f inhibitor via I.N. delivery. Control mice (naive and naïve+RSV) did not receive any treatment. 24h post treatment all mice received $1x10^6$ PFU of RSV A2 via I.N. delivery or control mice (naïve) received no virus. BAL samples were collected from all mice at day 7 post-challenge. **(A)** Four populations of cell types were identified in the BAL (R1-R4) and gating strategies are shown in **(B)**. All data is representative of three independent experiments and Error bars represent the SEM from n=3 mice per group.

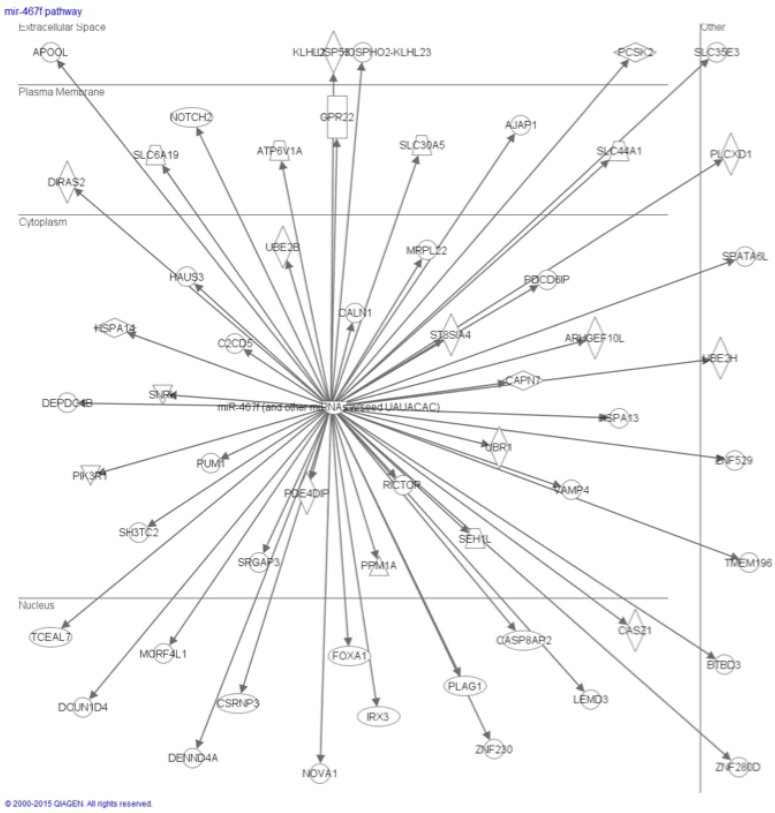

Figure S6.4: Ingenuity Pathway Analysis (IPA) of miR-467f gene targets distributed by cellular compartment. 56 gene targets were identified for miR-467f by pathway analysis using IPA (Qiagen).

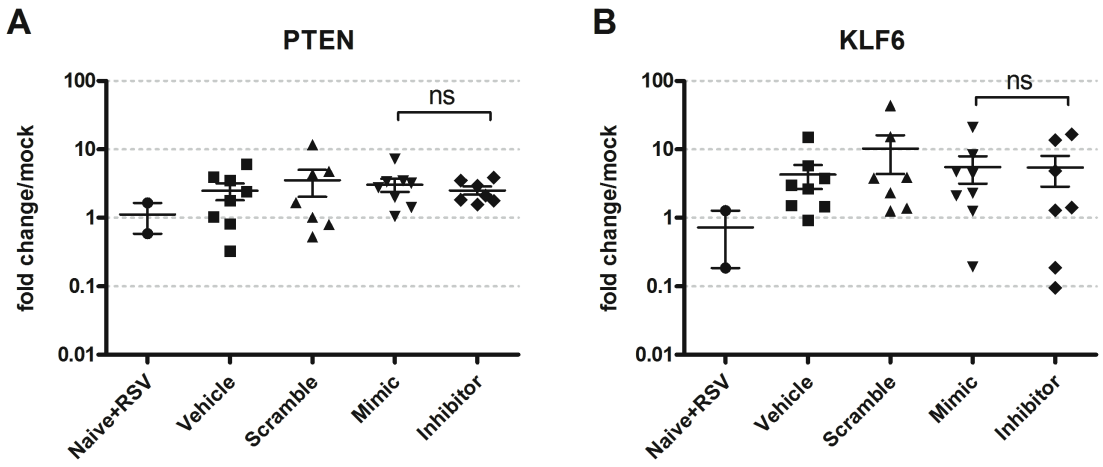

Figure S5: **PTEN and KLF6 expression levels in the lungs of mice following virus challenge.** Groups of BALB/c mice were vaccinated using a prime-boost regimen with FI-RSV A2 diluted in PBS on days -42 and -21. On day -1 mice received a single treatment of either vehicle, miRNA scramble control, miR-467f mimic, or miR-467f inhibitor via I.N. delivery. Control mice (naive and naïve+RSV) did not receive any treatment. 24h post treatment all mice received $1x10^6$ PFU of RSV A2 via I.N. delivery or control mice (naïve) received no virus. Lungs were harvested and homogenized from all mice at day 5 post-challenge. Total RNA isolation was performed on lung homogenates (n=6-8 mice/group) and examined for **(A)** PTEN expression levels and **(B)** KLF6 expression levels using RT-qPCR. PTEN and KLF6 expression levels were normalized by 18S rRNA gene expression. Values are represented as expression over mock (naïve mice). All data is representative of two independent experiments. Error bars represent the SEM and results were considered not significant with a $P > 0.05$ (ns) as determined by a student's t-test.

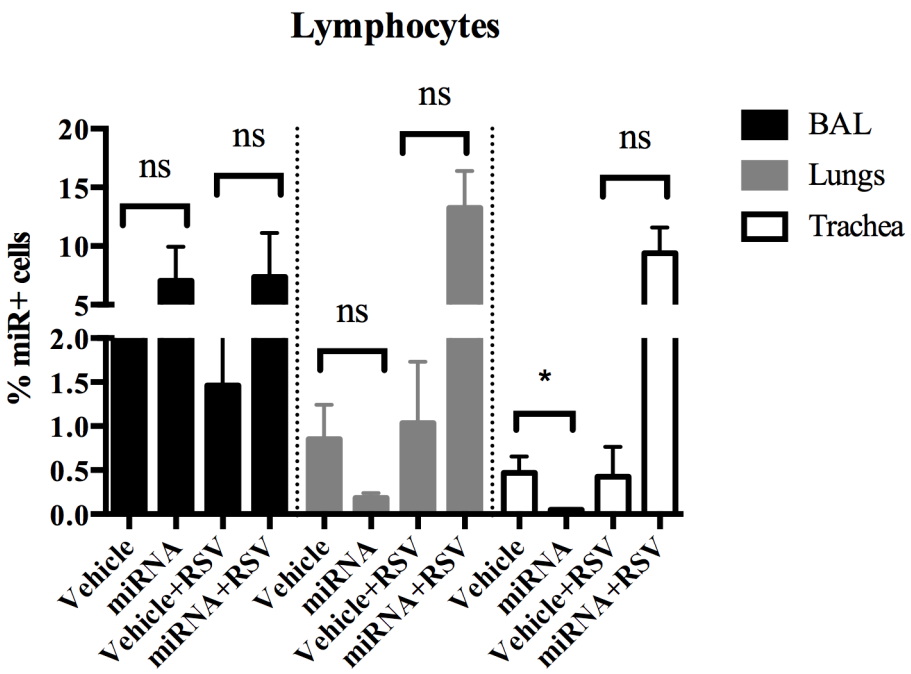
Lymphocytes
% miR+ cells
20
15
10
5
2.0
1.5
1.0
0.5
0.0
ns
ns
ns
ns
ns
*
BAL
Lungs
Trachea
Vehicle
miRNA
Vehicle+RSV
miRNA+RSV
Vehicle
miRNA
Vehicle+RSV
miRNA+RSV
Vehicle
miRNA
Vehicle+RSV
miRNA+RSV

Fig. S6.6: Percentage of miRNA positive lymphocytes in the respiratory tract pre- and post-infection with RSV. Dy547-labeled miRNA mimic transfection control (GE Dharmacon) was resuspended in Opti-MEM (ThermoFisher), then 5μl of DharmaFECT1 (GE Dharmacon) was added, mixed gently and incubated for 20 minutes at room temperature. Female 6-8 week old BALB/c mice were i.n. administered either 5 nmol of miRNA or 50 μl of vehicle (transfection reagent control). 24h post-treatment, a subset of mice treated with either miRNA or vehicle were sacrificed and BAL, lungs, and trachea were harvested. The additional mice were i.n. challenged with 10^6 PFU of RSV A2 in PBS, at 3 days post-infection (4 days post-treatment) the mice were sacrificed and BAL, lungs, and trachea were harvested. The percentage of $miRNA^+$ cells in the BAL (black), lungs (grey), and trachea (white) was determined by flow cytometry. For flow cytometry analysis, cell suspensions were incubated in FACS staining buffer and blocked with FcγIII/II receptor antibody, and subsequently stained with optimized concentrations of anti-mouse antibodies obtained from BD bioscience: APC-conjugated MHC class I H-2Kd tetramer complexes bearing the peptide SYIGSINNI (Beckman Coulter) representing the immunodominant epitope of the RSV M2-1 protein (RSV-specific cells), PerCP-Cy5.5-conjugated anti-CD45 (30-F11) ($CD45^+$ cells), and Dy547-labeled miRNA was visualized using Cy3 channel ($miRNA^+$ cells). Values are represented as percentage of $miRNA^+$ cells/$CD45^+$ cells. All data is representative of three independent experiments and n=4 mice/group. Error bars represent the SEM and results were considered significant with a P value ≤ 0.05 (*) and ns= no significant as determined by One-way ANOVA and Bonferroni's test.

CHAPTER 7

CONCLUSIONS

Respiratory syncytial virus (RSV) infection occurs in the majority of children during infancy, and by 2 years of age over 80% of children have been infected (1, 2). In addition, 2-3% of infants with RSV infection are admitted to the hospital, presenting clinically with bronchiolitis or pneumonia (1, 2). In addition, RSV infection does not confer long-term protection, as reinfections occur throughout life, which poses a substantial disease risk in elderly individuals and immunocompromised patients (3, 4). Despite more than 50 years of research there are no licensed vaccines to prevent RSV infection, and prophylaxis treatment is limited to passive immunization with palivizumab, a humanized anti-F monoclonal antibody (4). Palivizumab is expensive, and its use is limited to high-risk infants and young children (4). Current therapeutic options for RSV are limitied, and treatment is primarily supportive care; bronchodilators and inhaled and systemic corticosteroids have been shown as minimally effective (4-6).

Given that the high burden of RSV disease, it warrants substantial effort to develop a safe and efficacious vaccine. The first clinical trial using a formalin-inactivated RSV (FI-RSV) vaccine resulted in disastrous outcomes in young patients upon RSV infection; of which, many patients developed enhanced pulmonary disease and required hospitalized, and 2 deaths occurred (4, 7, 8). Efforts to develop an effective RSV vaccine have led to extensive investigation of the immune response to RSV; however, the

development of vaccine enhanced disease remains a critical concern in the development of a safe and efficacious RSV vaccine. Recent studies also suggest that there is an association between RSV-induced bronchiolitis and asthma within the first decade of life (2). Therefore, despite the considerable progress made in our understanding of several aspects of respiratory viral infections, further investigation needs to be done to understand the pathogenesis of FI-RSV and establish immune correlates of protection from RSV, as well as elucidate molecular mechanisms governing early virus-host interactions during the RSV infection process.

More recently, microRNAs (miRNAs) have emereged as gene expression regulators with the potential to modulate airway inflammation and lung diseases (9-11). miRNAs comprise a class of highly conserved noncoding single-stranded RNA molecules, approximately 18-25 nt in length (9). Their biological functions include modulation of the innate (11-16) and adaptive (17-22) immune response as well as other nonimmuniological cell functions (9, 23-25). In addition, the scope of biological function is wide, ranging from the regulation of cell differentiation and proliferation to influencing apoptosis (9). The long-term goal of this research project was to evaluate miRNA expression profiles as biomarkers for determing vaccine protection and disease outcomes for RSV infection. The specific hypothesis was that an alteration in the expression of host miRNAs implicated in chronic inflammatory diseases of the lung could be utilized as biomarker for disease outcome and vaccine-enhanced disease upon subsequent RSV infection. In addition, better knowledge of miRNA regulation may be a valuable target for novel approaches to prevent and treat inflammatory diseases of the lung.

Specific Aim 1: To determine the pattern and tempo of miRNA expression profiles in an *in vivo* BALB/c mouse model post-vaccination/pre-RSV challenge and post-vaccination/post-RSV challenge. In Chapter 3, we found that RSV infection and vaccination induced expression of nine host miRNAs that showed unique expression profiles in the lung compared to naïve mice. Specifically, miRNAs previously implicated in asthma and airway hyperresponsiveness were differentially expressed in response to vaccine candidates and live RSV vaccination that prime for protection and enhanced disease following RSV challenge. In addition, the differential expression of these lung miRNA profiles among the vaccine candidates appeared to correlate with other immune correlates (Th2-type immune response and cytokine production) and markers of disease severity (lung viral load and pulmonary inflammation). In addition, we identified six miRNAs in the lungs of BALB/c mice (miR-21, miR-145, miR-146b, miR-155, let-7d, and let-7f) that showed unique expression patterns in correlation with specific vaccine adjuvants, which shows that adjuvants alone produce characteristic miRNA profiles. To our knowledge, this is the first report of miRNA expression profiles of RSV vaccine candidates and vaccine adjuvants. These findings provide proof-of-principle for the utilization of miRNAs as potential biomarkers of vaccine efficacy, and may be important in forwarding RSV vaccine development.

In chapter 4, a miRNA PCR array was used to screen 84 miRNAs implicated in the activation and differentiation of T cells and B cells; briefly, sera was collected from BALB/c mice vaccinated with model vaccines (GA2-MP, FI-RSV, RSV CP52) and evaluated for miRNA expression levels at various time points post vaccination/pre-challenge and post-/vaccination/post-challenge with RSV at 10^6 PFU. We identified 50

unique miRNAs post-prime vaccination, 75 unique miRNAs post-boost vaccination, and 50 unique miRNAs post-challenge with RSV that were differentially expressed among the model vaccines. In addition, array analysis showed that each vaccine induced vaccine- and temporal-specific miRNA expression patterns, and that vaccination and subsequent RSV infection caused a group of common and distinct differentially expressed miRNAs. The model vaccines were also evaluated for immune correlates and clinical markers of disease severity to link known vaccine-induced immunological responses to miRNA expression profiles, thereby demonstrating their potential use as novel biomarkers for RSV vaccine safety and efficacy.

Specific Aim 2: To develop an *in vitro* model to characterize miRNAs expressed by lung epithelial cells in response to RSV antigens and vaccines. As demonstrated in Chapter 5, we identified key differences in cellular and exosome miR-associated expression patterns in MLE-15 and CALU3 cells infected with live RSV and uvRSV. In addition, these studies demonstrate that exosomes preferentially incorporate specific miRNAs as their cargo during RSV infection, as shown by the upregulated exosome-derived miRNA-associated expression patterns of miR-126, miR-155, let-7d, and let-7f. Intracellular miRNA expression was also evaluated using a novel P19 protein-based immunostaining technique, both RSV-infected and uninfected lung epithelial cells (MLE-15 cells) induced miRNA expression by 8 hpi, and miRNA induction was detected at both 24 and 48 hpi as well. Taken together, these studies identified common miRNAs that may have a major role in the innate response mounted against RSV, and perhaps other respiratory pathogens and lung injuries.

Specific Aim 3: To utilize bioinformatic tools to identify functionally relevant gene targets of particular miRNAs. In chapter 6, the role of miR-467f was evaluated regarding cellular and humoral immune responses to FI-RSV vaccination and subsequent RSV infection using gain- and loss- of function studies. To investigate the biological role of miR-467f, we identified 56 predicted host gene targets for miR-467f using Ingenuity Pathway Analysis (IPA) software. The top 10 functionally relevant gene targets were identified using DIANA TarBase v7.0, and 11 major signal transduction pathways were found to be associated with these gene targets. Of these major signaling transduction pathways both PI3K-Akt signaling and TGFβ signaling have been previously implicated in various aspects of RSV infection. This data demonstrates that further studies are needed to elucidate the mechanism of action by which miR-467f influences the adaptive immune response to FI-RSV induced enhanced disease.

Specific Aim 4: To develop RNA interference (RNAi) approaches to target the expression of miRNA biomarkers of interest. Chapter 6 focused on evaluating the potential immunomodulatory role of intranasal delivery of exogenous miR-467f mimic and miR-467f inhibitor in mice using FI-RSV vaccination as a model of vaccine enhanced disease. In addition, we examine features of the antiviral effect, host immune response, histopathology, and *in vivo* tracking of miR-467f treatment. These studies utilized *in vivo* tracking of exogenous miRNA delivery using a Dy547-labeled miRNA, and we found that the miRNA was present in lymphocytes ($CD45^+$) cells obtained from the BAL, lungs, and trachea of mice at 24 hours pre- and 3 days post-infection with RSV. We demonstrated that miR-467f promoted antibody responses and CD4+ T cell recruitment to the lungs of RSV-challenged mice, without affecting RSV replication *in*

vivo; where as, inhibition of miR-467f enhances expression of proinflammatory cytokines (i.e. IL-5 and eotaxin) that results in recruitment of IL-5R^{med} and IL-5R^{hi} granulocytes and enhanced lung pathogenesis. Therefore, the miR-467f inhibitor appears to further exacerbate the Th2-type response previously reported in FI-RSV induced enhanced disease.

Taken together, this work establishes that miRNAs are intimately involved in the cellular and adaptive immune response and intracellular mechanisms controlling RSV replication and disease pathogenesis, and can be measured as parameters of disease severity and manipulated for therapeutic purposes. These studies identified common miRNAs whose expression altered in response to inflammatory responses; therefore, commonalities in the changing expression of specific miRNAs suggest that these miRNAs may have a critical role in vaccine-induced immune responses and the innate response to RSV infection. In conclusion, these findings may offer promising biomarkers for vaccine development and novel targets for developing new therapies against RSV infection. Furthermore, with the emergence of miRNAs across many disease platforms, these studies provide innovations that facilitate detection of miRNAs, as well as techniques that allow for their characterization in biofluids, tissue samples, and exosomal vesicles. In addition, a better understanding of the influence of miRNAs on RSV disease pathogenesis provides a valuable contribution to the research field, in terms of applying this knowledge across species.

References

1. Inchley CS, Sonerud T, Fjaerli HO, Nakstad B. Nasal mucosal microRNA expression in children with respiratory syncytial virus infection. BMC Infect Dis. 2015;15:150.
2. Mohapatra SS, Boyapalle S. Epidemiologic, experimental, and clinical links between respiratory syncytial virus infection and asthma. Clin Microbiol Rev. 2008;21(3):495-504.
3. PATH Vaccine Resource Library. Respiratory syncytial virus (RSV) 2016 [Available from: http://www.path.org/vaccineresources/rsv.php.
4. Haynes LM. Progress and challenges in RSV prophylaxis and vaccine development. J Infect Dis. 2013;208 Suppl 3:S177-83.
5. Fernandes RM, Hartling L. Glucocorticoids for acute viral bronchiolitis in infants and young children. Jama. 2014;311(1):87-8.
6. Kellner JD, Ohlsson A, Gadomski AM, Wang EE. Bronchodilators for bronchiolitis. Cochrane Database Syst Rev. 2000(2):CD001266.
7. Connors M, Giese NA, Kulkarni AB, Firestone CY, Morse HC, 3rd, Murphy BR. Enhanced pulmonary histopathology induced by respiratory syncytial virus (RSV) challenge of formalin-inactivated RSV-immunized BALB/c mice is abrogated by depletion of interleukin-4 (IL-4) and IL-10. J Virol. 1994;68(8):5321-5.
8. Connors M, Kulkarni AB, Firestone CY, Holmes KL, Morse HC, 3rd, Sotnikov AV, et al. Pulmonary histopathology induced by respiratory syncytial virus (RSV) challenge of formalin-inactivated RSV-immunized BALB/c mice is abrogated by depletion of CD4+ T cells. J Virol. 1992;66(12):7444-51.

9. Globinska A, Pawelczyk M, Kowalski ML. MicroRNAs and the immune response to respiratory virus infections. Expert review of clinical immunology. 2014;10(7):963-71.

10. Foster PS, Plank M, Collison A, Tay HL, Kaiko GE, Li J, et al. The emerging role of microRNAs in regulating immune and inflammatory responses in the lung. Immunol Rev. 2013;253(1):198-215.

11. Oglesby IK, McElvaney NG, Greene CM. MicroRNAs in inflammatory lung disease--master regulators or target practice? Respiratory research. 2010;11:148.

12. Taganov KD, Boldin MP, Chang KJ, Baltimore D. NF-kappaB-dependent induction of microRNA miR-146, an inhibitor targeted to signaling proteins of innate immune responses. Proc Natl Acad Sci U S A. 2006;103(33):12481-6.

13. Sonkoly E, Pivarcsi A. Advances in microRNAs: implications for immunity and inflammatory diseases. J Cell Mol Med. 2009;13(1):24-38.

14. Zhou T, Garcia JG, Zhang W. Integrating microRNAs into a system biology approach to acute lung injury. Transl Res. 2011;157(4):180-90.

15. Nahid MA, Pauley KM, Satoh M, Chan EK. miR-146a is critical for endotoxin-induced tolerance: IMPLICATION IN INNATE IMMUNITY. J Biol Chem. 2009;284(50):34590-9.

16. Bazzoni F, Rossato M, Fabbri M, Gaudiosi D, Mirolo M, Mori L, et al. Induction and regulatory function of miR-9 in human monocytes and neutrophils exposed to proinflammatory signals. Proc Natl Acad Sci U S A. 2009;106(13):5282-7.

17. Anglicheau D, Muthukumar T, Suthanthiran M. MicroRNAs: small RNAs with big effects. Transplantation. 2010;90(2):105-12.

18. Sonkoly E, Stahle M, Pivarcsi A. MicroRNAs and immunity: novel players in the regulation of normal immune function and inflammation. Semin Cancer Biol. 2008;18(2):131-40.

19. Li QJ, Chau J, Ebert PJ, Sylvester G, Min H, Liu G, et al. miR-181a is an intrinsic modulator of T cell sensitivity and selection. Cell. 2007;129(1):147-61.

20. Allantaz F, Cheng DT, Bergauer T, Ravindran P, Rossier MF, Ebeling M, et al. Expression profiling of human immune cell subsets identifies miRNA-mRNA regulatory relationships correlated with cell type specific expression. PLoS One. 2012;7(1):e29979.

21. Curtale G, Citarella F, Carissimi C, Goldoni M, Carucci N, Fulci V, et al. An emerging player in the adaptive immune response: microRNA-146a is a modulator of IL-2 expression and activation-induced cell death in T lymphocytes. Blood. 2010;115(2):265-73.

22. Tsai CY, Allie SR, Zhang W, Usherwood EJ. MicroRNA miR-155 affects antiviral effector and effector Memory CD8 T cell differentiation. J Virol. 2013;87(4):2348-51.

23. Bueno MJ, Malumbres M. MicroRNAs and the cell cycle. Biochimica et Biophysica Acta (BBA) - Molecular Basis of Disease. 2011;1812(5):592-601.

24. Chen D, Farwell MA, Zhang B. MicroRNA as a new player in the cell cycle. J Cell Physiol. 2010;225(2):296-301.

25. Zhou JY, Ma WL, Liang S, Zeng Y, Shi R, Yu HL, et al. Analysis of microRNA expression profiles during the cell cycle in synchronized HeLa cells. BMB Rep. 2009;42(9):593-8.